EUR 4074 e
Part I

EUROPEAN ATOMIC ENERGY COMMUNITY - EURATOM

MECHANICAL PROPERTIES OF AL-AL_2O_3 COMPOSITES

Part I : SAP-ISML

by

D.J. BOERMAN, M. GRIN and M. VEAUX

1969

Joint Nuclear Research Center
Ispra Establishment - Italy

Metallurgy and Ceramics

This report is on sale at the addresses listed on cover page 4

at the price of FF 31.—	FB 310.—	DM 24.80	Lit. 3 870	Fl. 22.30

When ordering, please quote the EUR number and the title, which are indicated on the cover of each report.

Printed by Guyot, s.a.
Brussels, April 1969

EUR 4074 e
Part I

MECHANICAL PROPERTIES OF AL-AL_2O_3 COMPOSITES
PART I : SAP-ISML by D.J. BOERMAN, M. GRIN and M. VEAUX

European Atomic Energy Community - EURATOM
Joint Nuclear Research Center - Ispra Establishment (Italy)
Metallurgy and Ceramics
Luxembourg, April 1969 - 232 Pages - 119 Figures - FB 310

This report treats principally the mechanical properties (till 600 °C) of the four SAP-grades (Sintered Aluminium Powder) fabricated by ISML (Istituto Sperimentale Metalli Leggeri, Novara - Italy).

Most of the results, described in this report, were realised between 1960 and 1967 in three research centers : JRC-Ispra, ISML, Novara, and Battelle Institut, Frankfurt.

The first chapter describes in short the fabrication process of the semi-finished products (bars and tubes) and finished products (canning tubes and pressure tubes).

The second chapter deals with the mechanical properties of the SAP-alloys in general. Essentially the chapter consists of :

— talks with results of tension-, compression-, creep- and fatigue tests at various temperatures;

— diagram with the mechanical properties as a function of temperature or percentage of aluminium oxide.

The third chapter describes the experimental conditions and some physical properties of SAP.

EUR 4074 e
Part I

EUROPEAN ATOMIC ENERGY COMMUNITY - EURATOM

MECHANICAL PROPERTIES OF AL-AL_2O_3 COMPOSITES

Part I : SAP-ISML

by

D.J. BOERMAN, M. GRIN and M. VEAUX

1969

Joint Nuclear Research Center
Ispra Establishment - Italy

Metallurgy and Ceramics

ABSTRACT

This report treats principally the mechanical properties (till 600 °C) of the four SAP-grades (Sintered Aluminium Powder) fabricated by ISML (Istituto Sperimentale Metalli Leggeri, Novara - Italy).

Most of the results, described in this report, were realised between 1960 and 1967 in three research centers : JRC-Ispra, ISML, Novara, and Battelle Institut, Frankfurt.

The first chapter describes in short the fabrication process of the semi-finished products (bars and tubes) and finished products (canning tubes and pressure tubes).

The second chapter deals with the mechanical properties of the SAP-alloys in general. Essentially the chapter consists of :

— talks with results of tension-, compression-, creep- and fatigue tests at various temperatures;
— diagram with the mechanical properties as a function of temperature or percentage of aluminium oxide.

The third chapter describes the experimental conditions and some physical properties of SAP.

KEYWORDS

MECHANICAL PROPERTIES
SAP
FABRICATION
TESTING
TEMPERATURE

TABLE OF CONTENTS

Page

INTRODUCTION

Under the Orgel Program, Euratom envisaged the possibility of using aluminium alumina composites (Sintered Aluminium Product) for cladding fuel elements (temperature 450°C) and for pressure tubes (temperature 450°C and pressure 20 atm.).

The most important work done on such products with the aim of making them suitable for use in the nuclear field was carried out either under contracts, specially with the ISML (Istituto Sperimentale dei Metalli Leggeri, NOVARA, Italy), and in the laboratories of Euratom's Joint Research Center at Ispra, Italy, especially in the Metallurgy and Ceramics Division.

The research program at ISML was sponsored by Mr. D. GUALANDI (ISML) and Mr. P. JEHENSON (Euratom) (Ref. 1 to 23).

1. MANUFACTURING PROCESS

1.1 Improvement of the Starting Powders (Ref. 22)

The SAP powders used were commercial products which were manufactured by AIAG* up to 1962, after which they were further developed by the West German firm of Eckart-Werke.

1.1.1 SAP Powders Produced by AIAG

The SAP powders of the following grades

SAP 960	about 4 wt.% Al_2O_3
SAP 930	" 7 " "
SAP 895	" 10-11 " "
SAP 865	" 13-14 " "

were obtained from 99.5% pure aluminium powders which had undergone fairly lengthy milling at room temperature in a dry oxidizing atmosphere in the presence of stearic acid (Refs. 46-59). Work carried out on several tons of these powders showed that the aluminium oxide content of a specific grade

---

* Aluminium-Industrie AG (Alusuisse)

may differ between extreme limits of ± 1 wt.% of Al_2O_3 from the theoretical percentage for the grade.

The results of two analyses carried out on two batches are given below (wt.%):-

Material	% Al_2O_3	% Fe	% Si	% Zn
SAP 930	7.50	0.27	0.12	0.02
SAP 895	10.40	0.27	0.11	0.01

The grain size is generally between 50 and 150 microns. The grains have irregular round shapes and are of spongy aspect (Illustration 1).

The work carried out in 1960-62 on these AIAG commercial powders indicated that it was necessary to obtain better defined powders, especially with regard to the homogeneity of the product (% Al_2O_3) and the uniformity of dispersion of the Al_2O_3 particles in the aluminium matrix.

1.1.2 <u>SAP Powders Produced by Eckart-Werke</u>

The powders were developed by the West German firm in accordance with the basic manufacturing procedures established by AIAG. They are heavy powders the oxide content of which is mainly due to natural oxidation during the milling of the aluminium powder at room temperature. The original aluminium is nuclear aluminium of the order of 99.85% purity.

The aluminium oxide content must be as follows:

SAP 930	6.5 - 7.5	wt.% Al_2O_3
SAP 895	10 - 11	wt.% Al_2O_3

The results of two analyses carried out on two batches are given below (wt.%):-

Material	% Al_2O_3	% Fe	% Si	% Zn	% C
SAP 930	7.25	0.07	0.05	0.01	0.20
SAP 895	10.35	0.08	0.06	0.01	0.25

1.2 Cold-compression and Vacuum Treatment (Ref. 22, Ill. 2)

Commercial products exposed to high temperatures (500-600°C) for several hours showed surface blisters and internal micro-cracks, and consequently insufficient structural stability for nuclear uses (Ref. 36). This serious drawback was due to the high residual gas content (mainly hydrogen) of the finished products. While the lowering of the hydrogen content is of fundamental importance, a study has been in progress since 1960 aimed at eliminating this gas by vacuum treatment. The treatment selected, described in patent No. 13.532, registered in Italy on 30 May 1961, has the following main features:

- cold-compression of the powders at about 20 kg/mm^2 before heating in the vacuum furnace;
- treatment in the 590-620°C range for a period of 20-24 hr;
- vacuum between 10^{-4} and 10^{-5} mm Hg.

The extruded products contain only a small amount of residual gas, the quantity of which seems to be a function of the oxide content.

Material	Gas content ppm
SAP ISML 4% Al_2O_3	1-3
SAP ISML 7% "	2-5
SAP ISML 10% "	3-6
SAP ISML 14% "	4-8

Illustration 1 Structural aspect of $Al-Al_2O_3$ powders grade 960

Etching HF 0.5%

Magnification 500 x

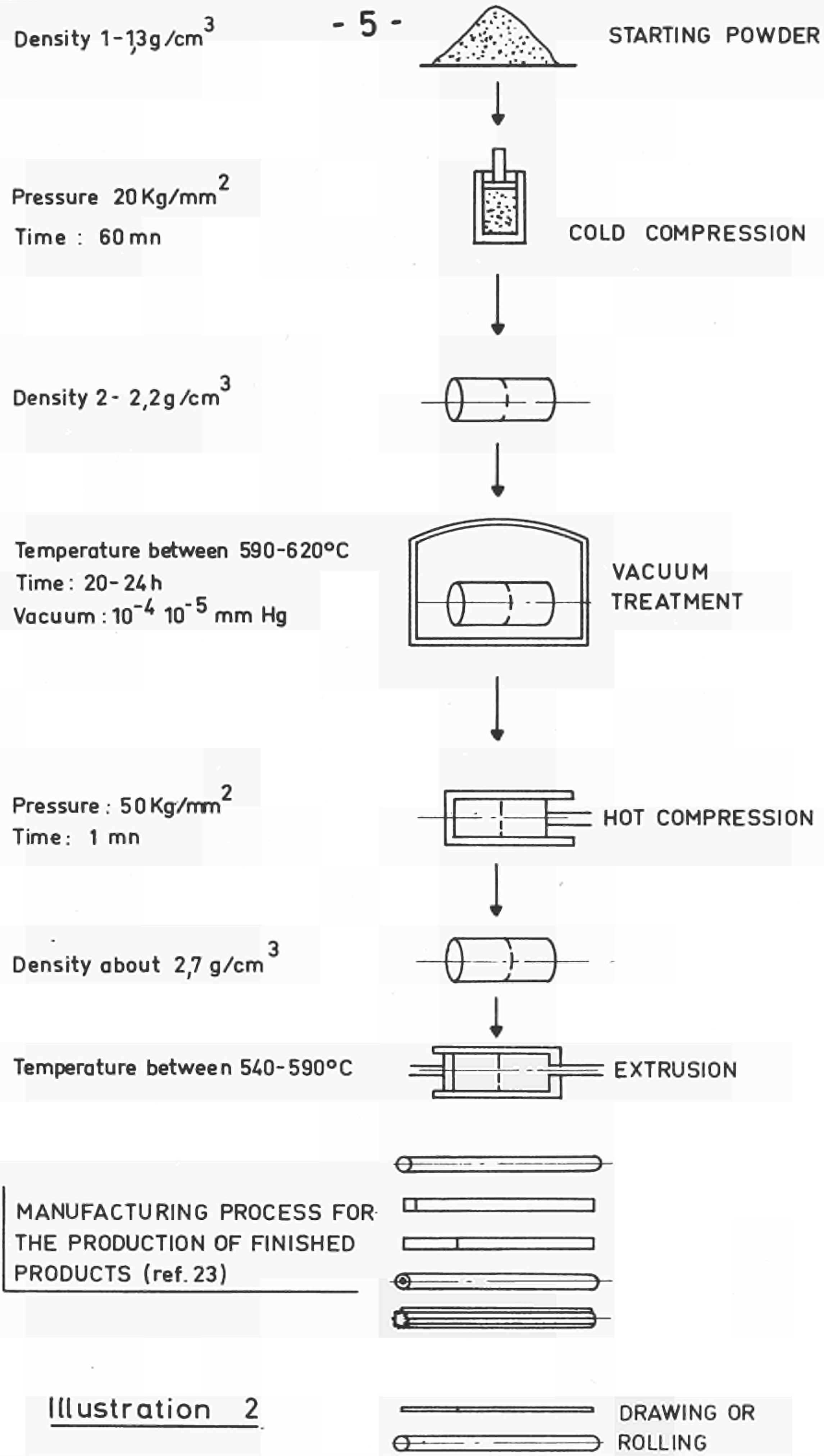

MANUFACTURING PROCESS FOR THE PRODUCTION OF FINISHED PRODUCTS (ref. 23)

Illustration 2

extrusion direction

Illustration 3 Longitudinal microstructure of bars of SAP ISML 7%

Magnification 500 x 2

Etching HF 0.5%

1.3 Hot-compression and Extrusion (Ref. 23, Ill. 2)

1.3.1 Hot-compression

After the vacuum treatment the billet, wrapped in an aluminium foil, is immediately inserted in the container of the press and subjected to a specific pressure of 50 kg/mm^2 for 30 min.

The process is carried out with a 250 t press for billets 80 mm in diameter and with one of 500 t for billets 110 mm in diameter. At the end of the process, the density of the product is of the order of 2.7 g/cm^3. The crust is then removed and the billet pickled.

1.3.2 Extrusion

The compacted billets (diameter 110 or 80 mm) are preheated at a temperature of between 540 and 590°C for 3 hr. The temperature of the extrusion container is about 330°C. The process is carried out on one of the three presses, the characteristics of which are given below:-

Max. force tons	Diameter of starting billet (mm)	Utilization
250	80	smooth tubes rods
500	80 110	finned tubes rods
2700	250	pressure tube

The extrusion velocity varies between 8 m/sec (pressure tube) and 16 to 20 m/sec (rods and finned tubes). In order to obtain rods and tubes, a double extrusion is usually carried out.

The extruded product constitutes the starting material for the rolling and cold drawing processes, which followed in some cases by heat treatment, lead to the finished products.

Illustration 4 Electron micrograph of a bar of SAP-ISML 7% Al_2O_3
Electron microscope magnification x 8,000
Total magnification x 20,000

1.3.3 Structure of the Extruded Product

The extruded product seems to have a very fine dispersion of Al_2O_3 particles inside the aluminium matrix. The dimension of the particles is between 0.02 and 0.1 micron and the interparticle distance is of the order of 0.1 to 0.2 micron (see Illustrations 3 and 4).

1.3.4 Definition of the Extrusion Ratio

Any time extruded products (rods, thick-walled tubes, finned tubes) are handled, the strictest definition we can give is the following:-

$$E' = \frac{A_1}{A_2}$$

A_1: section of the container
A_2: section of the die

However, in current practice another relation which gives quite reliable results is used:

$$E = \frac{S_1}{S_2}$$

S_1: section of the container
S_2: section of the extruded product

It is the latter relation which will be taken into consideration in our study.

1.3.5 Influence of the Extrusion Ratio on the Mechanical Properties

It is interesting to note that the value E is not sufficient to characterize the state of deformation of the material. For example, a finned tube or a round rod extruded at the same extrusion ratio will not give an equivalent strain hardening and consequently the mechanical properties will not be comparable. For instance, the final extrusion ratio for rods Ø 9.5 and for finned tubes are approximately the same (comprised between 70 and 80). However, the longitudinal strength of finned tubes is 18% higher (see Section 3.4.2 and Histograms Fig. 117).

In order to examine this influence in the simple case of rods, we performed tensile tests at 20 and 450°C on rods of SAP ISML 7% and 10% of various extrusion ratios respectively prepared from the same batch of powder. The characteristics of the material are listed in the table below:-

$\%Al_2O_3$	Bar Ø (mm)	Extrusion ratio	Batch No. (extrusion)	Batch No. (powder)
7%	9.5 16 21 23	76 27 14 13	3,504/3 3,448/1 3,447/1&2 3,504/1&2	M 133 M 129 " M 133
10%	9.5 16 21 23	76 27 14 13	3,240/1 3,239-3,240/2 3,237-3,238 3,234-3,235-3,236	M 4041

For the 9.5 mm Ø bar, the test specimen was as represented on Fig. 3, but for the others, the cross section was greater in order to maintain constant the ratio

$$R = \frac{\text{specimen cross section}}{\text{bar cross section}} = 0.18$$

However, for all specimens, the ratio $\frac{\text{length}}{\text{diameter}} = 7.5$ was maintained, constant (see Section 3.1.1.1.1 and Fig. 1.2.3).

The results obtained show that the extrusion ratio influences only the values of elongation at breaking point (e_{pb}).

1.4 Drawing (Ref. 23)

This procedure has mainly been used for the fabrication of smooth tubes and pressure tubes. The deformation ratio as a percentage, obtained either by drawing or by rolling without intermediate annealing, is given by the following relation:

$$H = \frac{S - s}{s} \times 100$$

H : ratio of cold-deformation in %
S : initial section of the material
s : final section of the material

1.5 Rolling (Ref. 23)

The starting material consists of plates of 50 x 12 mm or 30 x 2.5 mm. These are either directly cold-rolled or partly hot-rolled ($40 < H < 70\%$) and then finished at room temperature.

1.5.1 Hot-rolling

The extruded rough shapes are first preheated to 530°C for 24 hr and then rolled transverse to the extrusion direction until a deformation ratio of 50% is obtained, and then parallel to the extrusion direction until a ratio of 70% is reached.

1.5.2 Cold-rolling

This is carried out either directly on the extruded material or on materials that have already undergone hot-rolling deformation. The table below gives the deformation ratios obtained by the two methods:

Deformation ratio values (%)		
%Al_2O_3	hot-rolling	extrusion
4	73	-
7	37	32
10	19	20
14	10	8

Before cold-rolling, an annealing treatment of 2 hr at 530°C is necessary. In the case of SAP ISML 4 and 7% deformation ratios of 99% are obtained.

1.6 Fabrication of Rods (Ref. 23)

Up to the end of 1965 (batch No. 2500) the starting billet (hot-compacted) had a diameter of 78.5 mm. The results of the mechanical tests on rods presented in this document concern only the extruded materials made from billets 78.5 mm in diameter.

Characteristics of the first extrusion

diameter of container: 80 mm
dimension of starting billet: 78.5 x 140 mm
diameter of billet obtained: 58 mm
extrusion ratio: E = 1.9
extrusion rate: 1.3 m/min
temperature: 568°C

Afterwards the second extrusion is carried out directly on the final diameter of the rod with the same temperature conditions. The extrusion ratios relating to the various diameters of rods extruded from compacts of O.D. 80 mm are given in the following table.

1st Extrusion		2nd Extrusion		Final Extrusion ratio
Diameter (mm)	Extrusion ratio	Diameter (mm)	Extrusion ratio	
58	1.9	23	6.8	13
		21	8.2	14
		16	14	26.6
		12	25	47.5
		9.5	40	76

1.7 Fabrication of Cladding Tubes (Ref. 23)

The smooth tubes are fabricated by extrusion followed by cold-drawing, the finned tubes by extrusion only.

1.7.1 Smooth Tubes

Since the mechanical tests were only carried out on tubes 13.1 x 14.7mm in diameter we can limit ourselves to indicating the fabrication conditions of smooth tubes of these dimensions only.

1.7.1.1 Extrusion

The starting material is a cylindrical hollow billet through which a lubricated, slightly conical mandrel is passed which is of the same diameter as the internal diameter of the tube after extrusion (extrusion by free floating mandrel).

In the case considered here, the extruded tube has diameters of 16 and 14 mm (E = 59). The extrusion temperature is 571°C and the velocity is between 16 and 20 m/min.

1.7.1.2 Cold-drawing

The cold-drawing characteristics for the tubes concerned are given below:-

	diameter of die (mm)	diameter of mandrel (mm)	wall thickness of tube (mm)
1st step	15.0	13.4	0.8
2nd step	14.7	13.1	0.8

ratio of final cold-deformation : H = 25%
cold-drawing rate : 12 m/min

1.7.2 Finned tubes (Ref. 23)

The extrusion is carried out in two steps on a 500 t press at a temperature of 575°C starting from a hot-compacted billet 110 mm in diameter. The first extrusion gives a billet either 80 mm in (E = 2) diameter of 60 mm (E = 4). The extrusion rate is 1.3 m/min. Afterwards a central hole with a diameter equal to the final internal diameter of the hole is drilled. A second extrusion at rates between 16 and 20 m/min results in the desired profile. The extrusion ratios are between 17 and 20. The method is the same as that applied for extruding smooth tubes (free floating mandrel). The fins may be straight or helicoidal.

1.8 Fabrication of Pressure Tubes

These are tubes of large diameter (about 100 mm). As in the case of smooth tubes, they are first extruded and then cold-drawn.

1.8.1 Extrusion

The process is carried out at a temperature of 570°C on a 2700 t press followed by annealing for 2 hr at 540°C. The extrusion rate is of the order of 8 m/min. The dimensional characteristics are listed in the table below:

dimension of the extruded tube

	before extrusion		after extrusion	
	ID mm	OD mm	ID mm	OD mm
1st extrusion	98	250	97	198
2nd extrusion	97	198	96	102

At the end of the process the extruded tube is annealed for 2 hr at 540°C.

1.8.2 Cold-drawing

The cold-drawing is carried out in two steps; after each step annealing for 2 hr at 540°C is necessary. The dimensional characteristics are given below:-

dimension of the drawn tube

	before cold-drawing		after cold-drawing	
	ID mm	OD mm	ID mm	OD mm
1st step	96	102	94.05	100.4
2nd step	94.05	100.4	92.2	98.4

2. STUDY OF THE MATERIAL

2.1 Research Laboratories

Euratom has undertaken studies on the improvement of this material in the laboratories of the Ispra Joint Research Center and has concluded contracts with several companies.

With the Italian firm of Montecatini, it has drawn up two contracts: a research contract to be carried out in the laboratories of the Istituto Sperimentale dei Metalli Leggeri (ISML), Novara, and a contract for the production of bars, cladding tubes and pressure tubes on a semi-industrial scale.

A research contract concerning creep tests has also been concluded with the Battelle Institute, Frankfurt, Germany.

Some other results, reported here, were obtained by the Danish Atomic Energy Commission at its Risö research establishment. Other tests were conducted by the Civilian Atomic Power Department of the Canadian General Electric Company Ltd. (Peterborough, Ontario) and reprinted in the AECL publications (Atomic Energy of Canada Ltd., Chalk River, Ontario).

2.2 Presentation of Results

The main results will be presented in the form of diagrams whenever possible; the experimental conditions, the comments and some complementary results in tabular form will be found with all the references in an appendix at the end of the report.

2.2.1 Denomination of Material

The material is characterized by its percentage number (4, 7,10 or 14% principally). This refers to the nominal percentage of Al_2O_3 by weight in the aluminium matrix. Often the real weight percentage differs by at least $\pm$ 1 wt.% of Al_2O_3. The results refer only to SAP produced in standard conditions (see Section 1). In addition, all the results concern SAP manufactured by ISML, which is named SAP ISML in order to distinguish it from, for example:

SAP AIAG
FRITTOXAL (TLH)
APM alloys, etc.

The material is also given a batch number at the beginning of the fabrication process. The batch numbers are allocated chronologically, so this number indicates the fabrication period. The principal fabrication characteristics for a given batch number are collected in tables published in the quarterly progress reports of ISML, Novara.

Table 1 gives a list of the batch numbers for the specific quarterly progress reports and for the various types of powders used.

Table 1

Fabrication Data of the Various Batches of SAP

No. of Batch	Date of fabrication	Ref.	Type of powder employed			
			4% ↓	7% ↓	10% ↓	14% ↓
1	1 - 5 - 1960	...1				
82	30 - 7 - 1960	...2				
128	31 - 10 - 1960	...3				
173	15 - 2 - 1961	...4				
251	15 - 5 - 1961	...5				
347	31 - 7 - 1961	...6	AIAG			
441	30 - 11 - 1961	...7				
555	28 - 2 - 1962	...8				
734	31 - 5 - 1962	...9				
851	30 - 9 - 1962	..10				
926	31 - 12 - 1962	..11		Eckart-Werke and AIAG		
1137	30 - 4 - 1963	..12				
1241	31 - 8 - 1963	..13				
1344	31 - 12 - 1963	..14	AIAG	Eckart-Werke		AIAG
1636	30 - 6 - 1964	..15				
1831	31 - 10 - 1964	..16				
1939	31 - 12 - 1964	..17				
2209	30 - 4 - 1965	..18				
2353	31 - 8 - 1965	..19				
2483	31 - 12 - 1965	..20				
2680	30 - 4 - 1966	..21				
3172	31 - 8 - 1966	..21A				
3440	31 - 12 - 1966	..21B				
3740	30 - 4 - 1967	..21C				
3827	31 - 8 - 1967					
			↑ 4%	↑ 7%	↑ 10%	↑ 14%

2.2.2 Presentation of Diagrams

Normally metric units were used, but whenever the references employed British units, both are reported. As far as possible standard scales were adopted for the different graphs in order to facilitate comparison. The dimensions of specimens often influence the results, so they were given. For every cumulative diagram, reference is made to the figure numbers in the original individual diagrams and their respective document reference numbers.

The general scheme of presentation of the results will be the following:

- a table and a figure (Table 2 and Illustration 5) show all the symbols and terms used in English, French and German to characterize the mechanical properties in tensile and compression testing.

- seven tables summarize the main mechanical properties of the four grades of SAP for bars, smooth tubes and finned tubes (Tables 3 to 9).

- an index of all the measured mechanical and physical properties of SAP with reference to the corresponding figures (Tables 10 and 11).

- the figures gathered according to the type of test:

Semi-finished products

- Mechanical properties
  - Tensile tests
  - Compression tests
  - Creep tests
  - Relaxation tests
  - Impact strength tests
  - Hardness tests
  - Fatigue tests
  - Evolution of rod production
- Physical properties

Finished products

Various mechanical tests like tensile tests, compression tests, burst tests and fatigue burst tests.

SYMBOLS

Table 2

Symbol	Definition	Unit	English	French	German
P_{pr}		kg	Proportional elastic load	charge à la limite de proportionnalité	Kraft an der Proportionalitätsgrenze
$P_{0.2}$		kg	0.2 offset yield load	charge à la limite élastique à 0,2%	Kraft an der 0,2 Streckgrenze
P_u		kg	upper load	charge maximum	Maximum-Kraft
A_o		mm^2	original gauge cross-section	section originale	originaler Querschnitt
L_{pu}		mm	plastic uniform elongation	allongement plastique réparti	plastische Gleichmass-verlängerung
L_{pb}		mm	plastic elongation at breaking point	allongement plastique à la rupture	plastische Verlängerung beim Bruch
L_o		mm	original gauge length	base de mesure	originale Messlänge
S_{pr}	P_{pr}/A_o	kg/mm^2	engineering proportional elastic limit	contrainte à la limite de proportionnalité	technologische Proportionalitätsgrenze
$S_{0.2}$	$P_{0.2}/A_o$	kg/mm^2	engineering 0.2 offset yield stress	limite élastique à 0,2%	technologische 0,2 Streckgrenze
S_u	P_u / A_o	kg/mm^2	engineering maximum tensile stress	contrainte maximum	technologische Zugfestigkeit
e_{pu}	$\frac{\Delta L_{pu}}{L_o} \times 100$	%	engineering plastic uniform strain	allongement plastique (unitaire) réparti	technologische plastische Gleichmassdehnung
e_{pb}	$\frac{\Delta L_{pb}}{L_o} \times 100$	%	engineering plastic strain at breaking point	allongement plastique unitaire à la rupture	technologische plastische Bruchdehnung
E	$\frac{S}{e}$	kg/mm^2	Young's Modulus of elasticity	module élastique (module d'Young)	Elastizitätsmodul

ILLUSTRATION 5

GENERAL FORM
OF TENSION AND COMPRESSION CURVES
AND SYMBOLS EMPLOYED

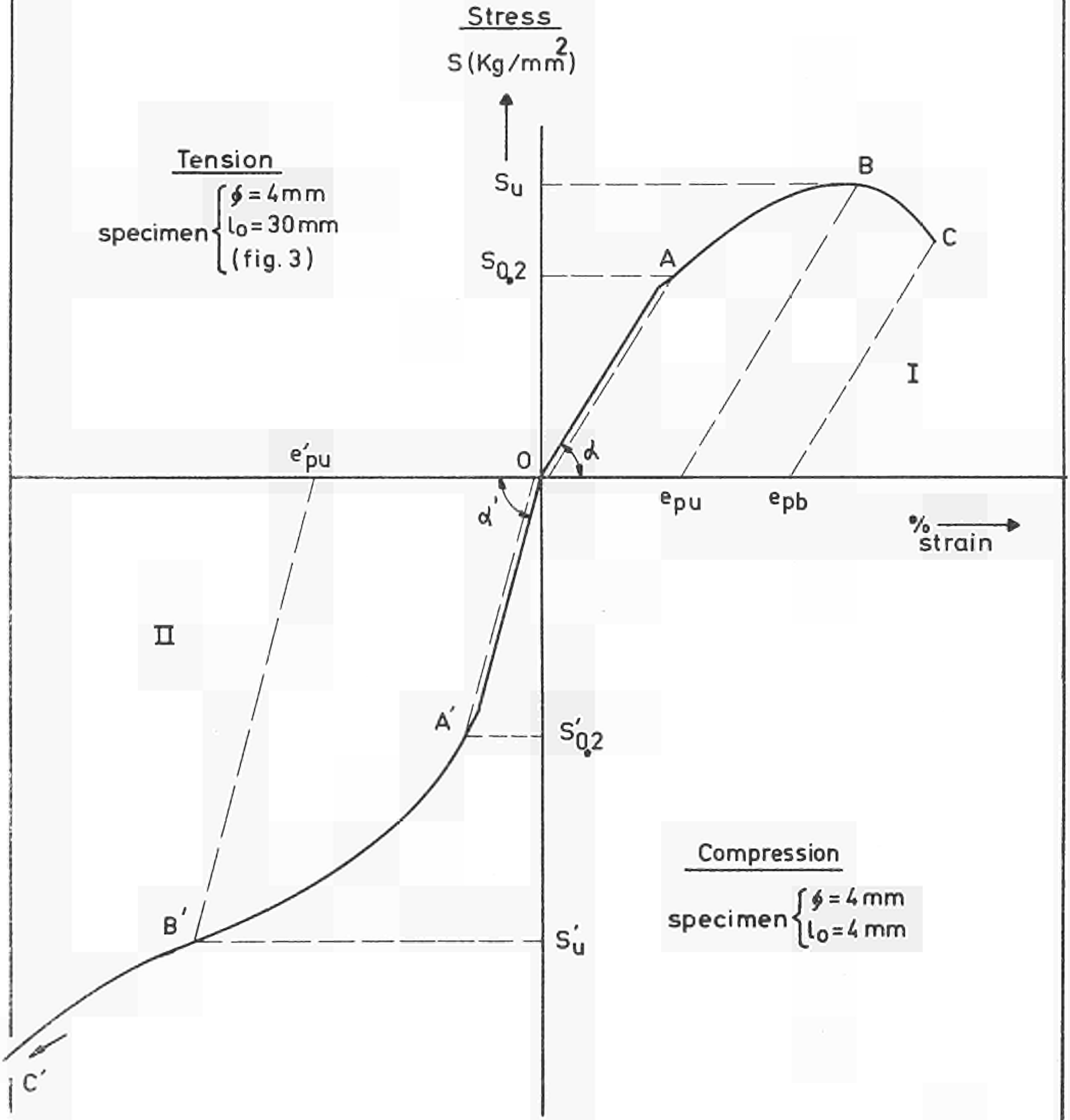

SUMMARY OF THE MAIN MECHANICAL PROPERTIES

MAIN MECHANICAL PROPERTIES

Type of Material	Table
bars SAP 4%	3
bars SAP 7%	4
bars SAP 10%	5
bars SAP 14%	6
smooth tubes SAP 4%	7
smooth tubes SAP 7%	8
finned tubes SAP 7%	9

Table 3

Main mechanical properties of SAP ISML 4%

Type of test	Room temperature properties				High temperature properties										References of Figures
Tensile	S_u (kg/mm^2)	$S_{0.2}$ (kg/mm^2)	e_{pu} (%)	e_{pb} (%)	Test temperature °C	S_u (kg/mm^2)	$S_{0.2}$ (kg/mm^2)	e_{pu} (%)	e_{pb} (%)	Test temperature °C	S_u (kg/mm^2)	$S_{0.2}$ (kg/mm^2)	e_{pu} (%)	e_{pb} (%)	11-12 (Eur) 20-22-25-28 (ISML)
test (1)	20.0 24.5	13.2 18	9.6 12.2	19.8 25.8	400	5.9 6.5	4.5 6.2	0.6 0.7	2.5 11.0	450	5.0 6.1	4.0 6.0	0.6 0.8	4.3 9.6	32-33 (AECL) 34 (Risö)
Compression tests	34.8 32.8	21.2 19.6	16.0 15.3		400	7.8	6.2	9.0		450	6.7	6.0	6.7		35-36-37
Creep tests (Maximum admissible stress for 10,000 hrs life).						Max. stress (kg/mm^2)		Elongation at rupture (%)			Max. stress (kg/mm^2)		Elongation at rupture (%)		40
					400	4.3				460	3.2 ± 0.1		$0.5 \pm {}^{0.1}_{0.2}$		55-56
					426	3.1									60
Fatigue limit in rotating bending	Maximum stress (kg/mm^2)					Maximum stress (kg/mm^2)									75
	8.5				400	4.8									
Young's Modulus (kg/mm^2)	7,200				400	4,400 ± 200				450	4,100 ± 100				93

(1) 6 to 15 specimens for each temperature

Main Mechanical Properties of SAP ISML 7%

Table 4

Type of test	Room temperature properties				High temperature properties										References of Figures
Tensile	S_u (kg/mm^2)	$S_{0.2}$ (kg/mm^2)	e_{pu} (%)	e_{pb} (%)	Test temperature °C	S_u (kg/mm^2)	$S_{0.2}$ (kg/mm^2)	e_{pu} (%)	e_{pb} (%)	Test temperature °C.	S_u (kg/mm^2)	$S_{0.2}$ (kg/mm^2)	e_{pu} (%)	e_{pb} (%)	13-14 (EUR) 20-22-25-28 (ISML)
tests(1)	20.0 25.5	14.3 20.4	7.9 12.7	15.0 23.2	400	8.3 9.0	7.8 8.1	0.7 0.8	1.8 6.3	450	7.5 7.8	7.0 7.6	0.4 0.6	3.5 6.4	34 (Risö)
Compression tests	40.3 40.0	22.7 22.0	20.8 18.7		400	9.4	8.3	5.7		450	8.2	7.2	5.3		35-36-37
Creep tests (Maximum admissible stress for 10,000 hrs. life).						Max. stress (kg/mm^2)		Elongation at rupture (%)			Max. stress (kg/mm^2)		Elongation at rupture (%)		41-42 43-44
					400	5.8				460	4.5 ± 0.2		0.6 $^{+0.8}_{-0.3}$		55-57-58
					420	5 ± 0.3									60
Fatigue limit in rotating bending	Maximum stress (kg/mm^2)					Maximum stress (kg/mm									
	7.5				400	6									76
Young's Modulus (kg/mm^2)	7,200				400	5,000 $^{+50}_{-0}$				450	4,700 ± 50				93

(1) 5 to 10 specimens for each temperature

Main Mechanical Properties of SAP ISML 10%

Table 5

Type of test	Room temperature properties				High temperature properties										References of Figures
Tensile tests(1)	S_u (kg/mm^2)	$S_{0.2}$ (kg/mm^2)	e_{pu} (%)	e_{pb} (%)	Test temperature °C	S_u (kg/mm^2)	$S_{0.2}$ (kg/mm^2)	e_{pu} (%)	e_{pb} (%)	Test temperature °C	S_u (kg/mm^2)	$S_{0.2}$ (kg/mm^2)	e_{pu} (%)	e_{pb} (%)	15-16 (Eur)
	29.8 30.8	21.5 24.8	6.9 8.2	12.0 18.0	400	11.0 12.5	9.4 12.0	0.3 0.4	1.0 3.8	450	9.5 10.0	8.0 9.9	0.3 0.6	2.6 5.2	20-22-25-28 (ISML) 34 (Risö)
Compression tests	47.6 46.4	28.6 26.7	21.3 21.0		400	11.6	10.3	7.7		450	10.1	8.9	6.0		35-36-37
Creep tests (Maximum admissible stress for 10,000 hrs life).						Max. stress (kg/mm^2)		Elongation at rupture (%)			Max. stress (kg/mm^2)		Elongation at rupture (%)		
					400	6.8				460	5.9				45
					426	6.2									60
Fatigue limit in rotating bending	Maximum stress (kg/mm^2)					Maximum stress (kg/mm^2)									77
	9.5				400	5.8									
Young's Modulus (kg/mm^2)	7,500				400	5,150 ± 150				450	4,850				93

(1) 6 to 11 specimens for each temperature

Main Mechanical Properties of SAP ISML 14%

Table 6

Type of test	Room temperature properties				High temperature properties										References of Figures
Tensile	S_u (kg/mm^2)	$S_{0.2}$ (kg/mm^2)	e_{pu} (%)	e_{pb} (%)	Test temperature °C	S_u (kg/mm^2)	$S_{0.2}$ (kg/mm^2)	e_{pu} (%)	e_{pb} (%)	Test temperature °C	S_u (kg/mm^2)	$S_{0.2}$ (kg/mm^2)	e_{pu} (%)	e_{pb} (%)	17-18 (Eur) 20-22-25-28
Tests(1)	36.0 37.7	26.0 30.7	6.6 7.0	8.0 12.0	400	14.0 14.5	12.0 14.3	0.3 0.5	0.8 2.3	450	11.8 13.0	10.5 12.6	0.3 0.4	1.0 2.6	(ISML) 34 (Risö)
Compression tests	57.2 47.6	34.7 33.6	21.3 19.0		400	14.2	12.3	5.0		450	12.3	11.2	4.3		35-36-37
Creep tests (Maximum admissible stress for 10,000 hrs. life).						Max. stress (kg/mm^2)		Elongation at rupture (%)			Maximum stress (kg/mm^2)		Elongation at rupture (%)		
					400	7.5				450	7.1				46
Fatigue limit in rotating bending	Maximum stress (kg/mm^2)					Maximum stress (kg/mm^2)									
	12				400	7									78
Young's Modulus (kg/mm^2)	7,700				400	5,300 ± 50				450	5,100 ± 50				93

(1) 4 to 6 specimens for each temperature.

Main Mechanical Properties of Smooth Tubes in SAP ISML 4%

Table 7

Type of test	Mechanical and thermal treatment	Room temperature properties			High temperature properties				Reference figures
		S_u (kg/mm^2)	$S_{0.2}$ (kg/mm^2)	e_{pb} (%)	Test temperature °C	S_u (kg/mm^2)	$S_{0.2}$ (kg/mm^2)	e_{pb} (%)	
Tensile test	Extruded then annealed	22,5		14	450	6.0	4.5	5±1	105
	Extruded, Cold-drawn, then annealed	25	22.3	8	450	5.0	4.0	5±1	106 107
Creep under internal gas pressure	Annealed					Maximum stress (kg/mm^2) for a life of 2,000 hrs.			108 109
					400	3.1			
					450	1.9 ± 0.6			

Table 8

Main mechanical properties of smooth tubes in SAP ISML 7%

Type of test	Mechanical and thermal treatment of the material	Room temperature properties			High temperature properties				References of figures
		S_u (kg/mm^2)	$S_{0.2}$ (kg/mm^2)	e_{pb} (%)	Test temperature °C	S_u (kg/mm^2)	$S_{0.2}$ (kg/mm^2)	e_{pb} (%)	
Tensile Test	Extruded then annealed	27.3	14.5	10	450	8.7	6.5	3±0.8	105
	Extruded, Cold-drawn then annealed	30	22	5	450	6.8	4.5	3±0.8	106 107
Creep under internal gas pressure	Annealed					Maximum stress for a life of 1,000 hrs.			
					400	4.1			110
					450	3.5			
	Cold-drawn				400	4.4			111
	Cold-drawn then annealed				400	3.2			

Main high temperature mechanical properties of finned tubes in SAP ISML 7%

Table 9

Type of test	Test temperature °C	Rupture stress (kg/mm^2)			Elongation at rupture (%)			References of Sections and Figures
		Min. value	Mean value	Max. value	Min. value	Mean value	Max. value	
Tensile tests	450	6.8	9	10.8	1	3.2	5	Fig. 112
Compression tests	450	6.9	7	7.4	0.16 (1)	0.26 (1)	0.39 (1)	Sect. 3.3.2
Burst test (tangential stress)	460	5.1	5.6	6.0				Sect. 3.3.2
Burst test on tubes with internal artificial defects (15% wall thickness)	460	5.0	5.3	5.55				Sect. 3.3.2 Fig. 118
Fatigue tests with internal gas pressure (with and without internal defects)	460	4.1 (2)	4.3 (2)	4.45 (2)				Sect. 3.3.2 Fig. 119
Creep tests in compression	460		≈4 (3)					Sect. 3.3.2

(1) In this case, the elongation corresponds to e_{pu}.

(2) For a life to rupture of 5,000 cycles.

(3) For a life to rupture of about 5.000 hours.

INDEX OF FIGURES

Table 10 Index of Figures Mechanical Properties of Semi-finished Products

Type of test	Figures as a function of temperature for each grade of SAP				Figures as a function of oxide content	
	SAP 4%	SAP 7%	SAP 10%	SAP 14%	Room temp.	High temp.
Tensile	11-12-29 30-32-33 19-20-21-22 23-24-25	13-14 19-20-21 22-23-24-25	15-16 19-20-21 22-23-24-25	17-18 19-20-21-22 23-24-25	10-28-34 26-27	10-28-34 26-27
Compression	35-36-37	35-36-37	35-36-37	35-36-37		
Creep	40-52-55-56 48-49-50-51-60 61	41-42-43-44 53-57-58 47-48-49-50 51-60-61	45 48-49-50-51-60	46 48-49-50-51		
Relaxation		64-65a-66 65	65			
Impact	68	68				
Hardness	69a-72-70a-71-73	69a-70a-70b-71-73	69a-70a-71-73	70a-70b-71-73	69-70	
Fatigue	75-82-79	76-83-79	77-84-79	78-85-79		
Evolution of rod production	86-87	88-89-90-91 86-87	86-87	86-87		

NB: Underlined numbers refer to cumulative figures.

Table 11 Index of Figures

Physical properties of semi-finished products

Property or Test	Figures as a function of temperature for each grade of SAP				Figures as a function of oxide content	
	SAP 4%	SAP 7%	SAP 10%	SAP 14%	Room temp.	High temp.
Young's Modulus	93	93	93	93	92	
Coefficient of thermal expansion					94	94
Electrical resistivity	96-97	96-97	96-97	96-97	95	98
Thermal conductivity	99-100-101	99-100-101	99-100-101	99-100-101		102 - 103
Density					104 - 104A	

Mechanical properties of finished products

Property or Test	SAP 4%	SAP 7%	SAP 10%	SAP 14%	Room temp.	High temp.
Tensile tests on smooth tubes					105-106-107	105-106-107
Creep tests with internal gas pressure on smooth tubes	108-109-115	110-111-116				
Tensile tests on finned tubes		112-113-114 117				

NB: Underlined numbers refer to cumulative figures.

FIGURES

2.2.7 Captions of Figures

SEMI-FINISHED PRODUCTS

Tensile Tests

Fig.	
1 and 2	Influence of the gauge length on the engineering plastic elongation at breaking point during tensile test.
3	Euratom tensile specimen (TR1)
4	ISML tensile specimen
5	Influence of the extrusion ratio on the elongation e_{pb}
6	Influence of test duration on the mechanical properties
7,8,9 9A,9B,9C	Influence of the crosshead speed on the mechanical properties
10	The elastic limit of SAP ISML at 20° and 400°C obtained through different methods
11	Tensile tests on SAP 4% Stress S = f(T)
12	Tensile tests on SAP 4% Strain e = f(T)
13	Tensile tests on SAP 7% Stress S = f(T)
14	Tensile tests on SAP 7% Strain e = f(T)
15	Tensile tests on SAP 10% Stress S = f(T)
16	Tensile tests on SAP 10% Strain e = f(T)
17	Tensile tests on SAP 14% Stress S = f(T)
18	Tensile tests on SAP 14% Strain e = f(T)
19	Cumulative Euratom results Stress S_u = f(T)
20	Cumulative ISML results Stress S_u = f(T)
21	Cumulative Euratom results Stress $S_{0.2}$ = f(T)
22	Cumulative ISML results Stress $S_{0.2}$ = f(T)
23	Cumulative Euratom results Strain e_{pu} = f(T)
24	Cumulative Euratom results Strain e_{pb} = f(T)
25	Cumulative ISML results Strain e_{pb} = f(T)
26	Cumulative results Stress S_u & $S_{0.2}$ = f(%Al_2O_3)
27	Cumulative results Strain e_{pb} & e_{pu} = f(%Al_2O_3)

Compression Tests

Creep Tests

Relaxation Tests

Fig.

Impact Strength Tests

Hardness

Fatigue Tests

SEMI - FINISHED PRODUCTS

TENSILE TESTS

INFLUENCE OF THE SPECIMEN GAUGE LENGTH ON THE VALUES OF PLASTIC STRAIN (ISML Results on SAP ISML 10 %) Ref. 14-22

Fig. 1

$e_{pb} = f(T)$ on cylindrical specimens

Name of Specimens	(x= length/diamet)	Length (mm)
A 1,5	1,5	10
A 3	3	20
A 5	5	35
A 10	10	70

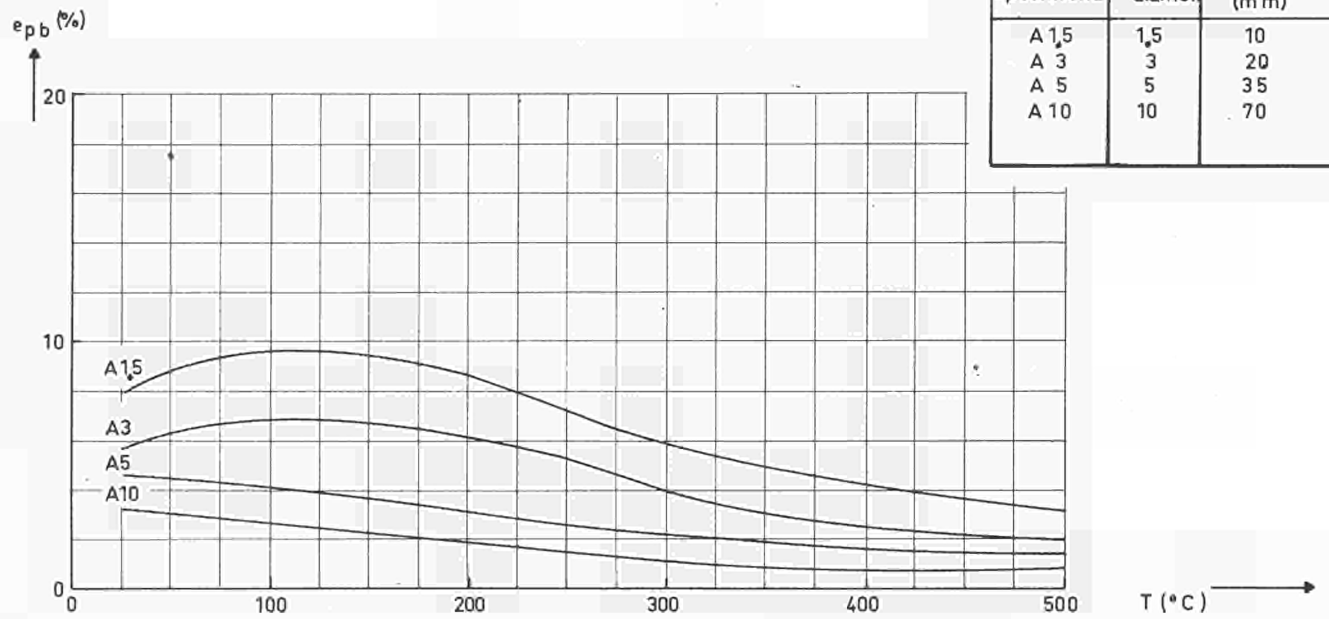

INFLUENCE OF THE SPECIMEN GAUGE LENGTH ON THE VALUES OF PLASTIC STRAIN (ISML Results on SAP ISML 7% and 10%) Ref. 14-22

Fig. 2

$e_{pb} = f(Ax)$ on cylindrical specimens

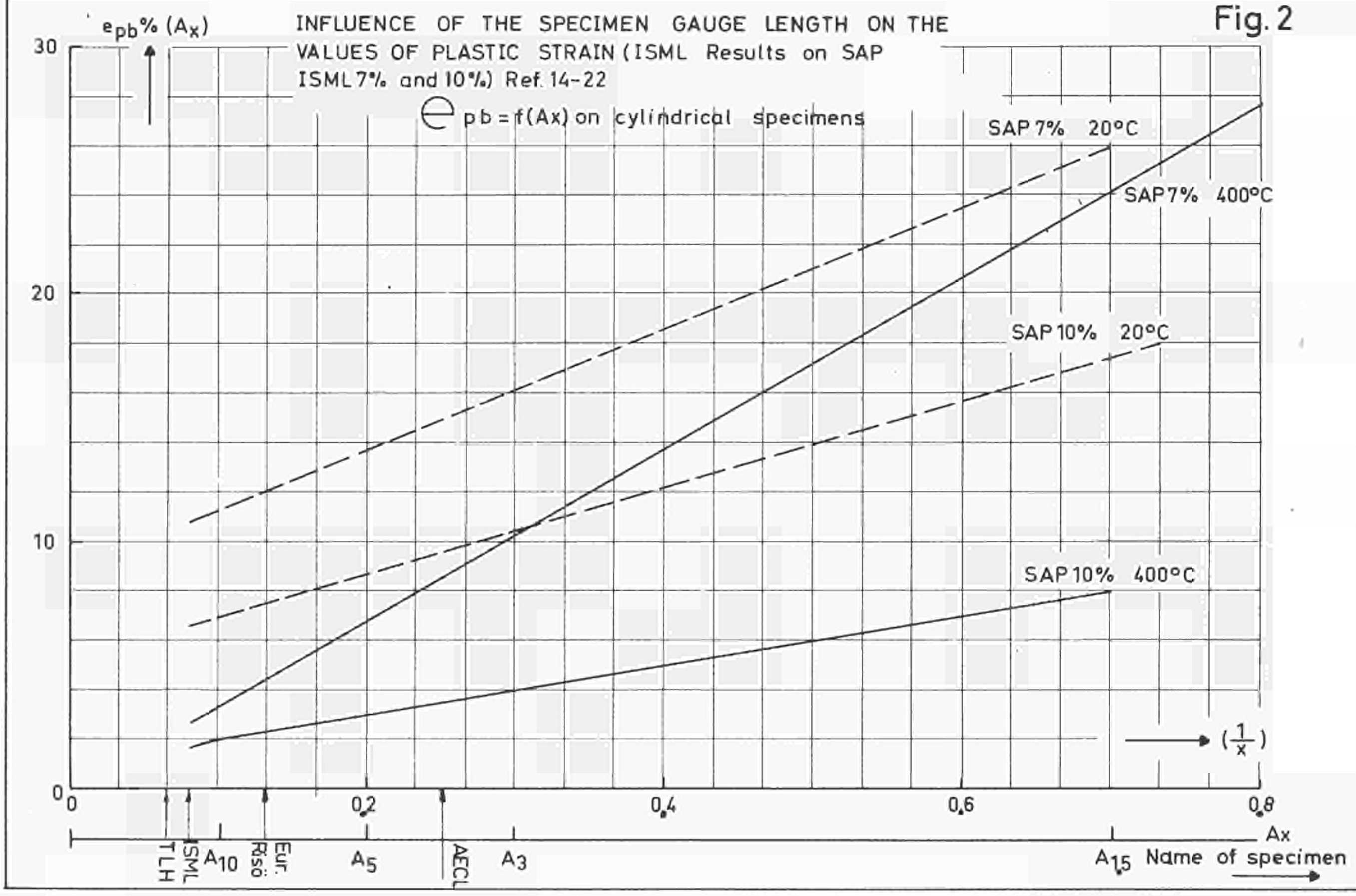

EURATOM TENSILE SPECIMEN TR 1
(gauge length = 7.5 X Diameter)

Fig. 3

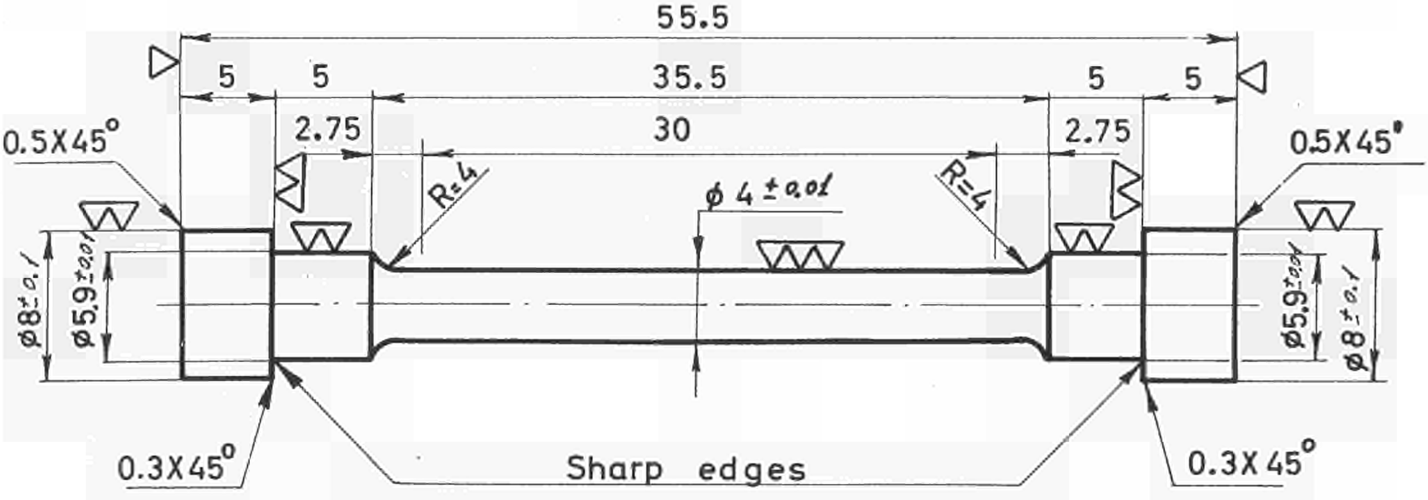

ISML TENSILE SPECIMEN
(Gauge length =11.4 Diameter)
Ref. ISML drawing PDc 13/1

Fig. 4

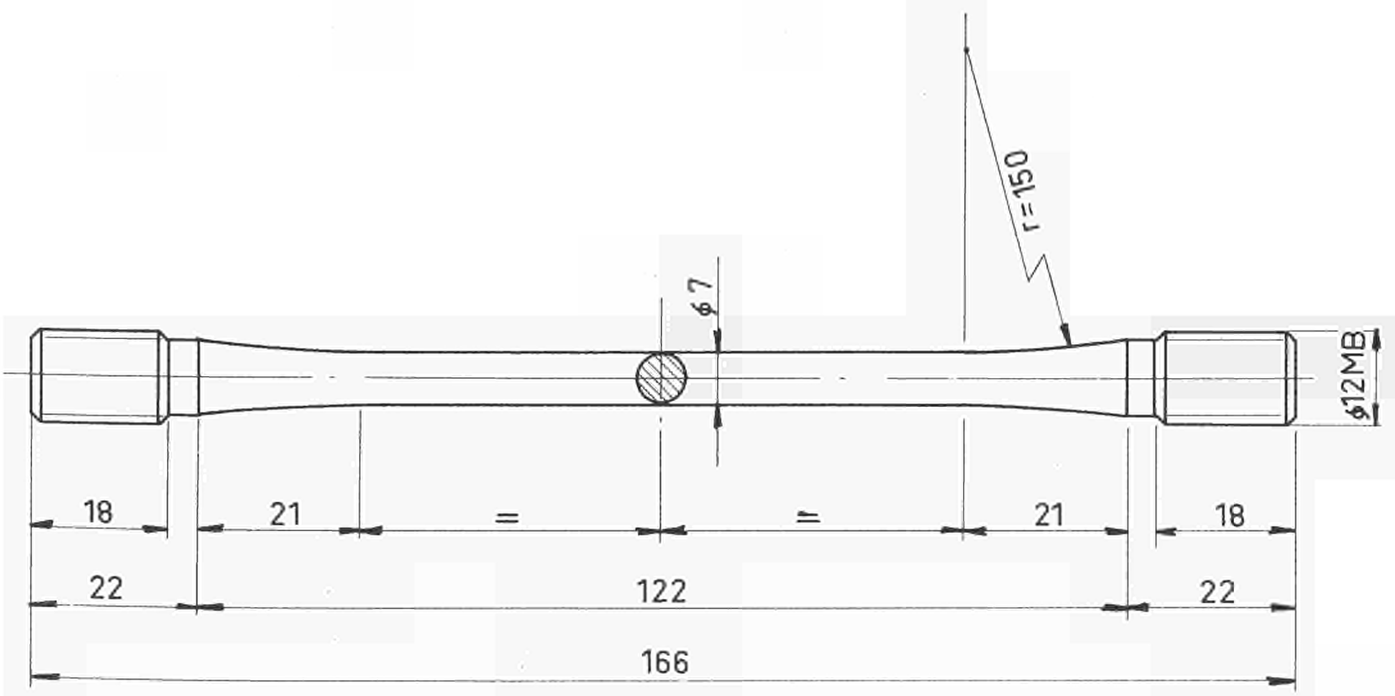

Influence of the extrusion ratio on the elongation e_{pb} (Tensile test)
(Euratom results - Specimen Fig 3)

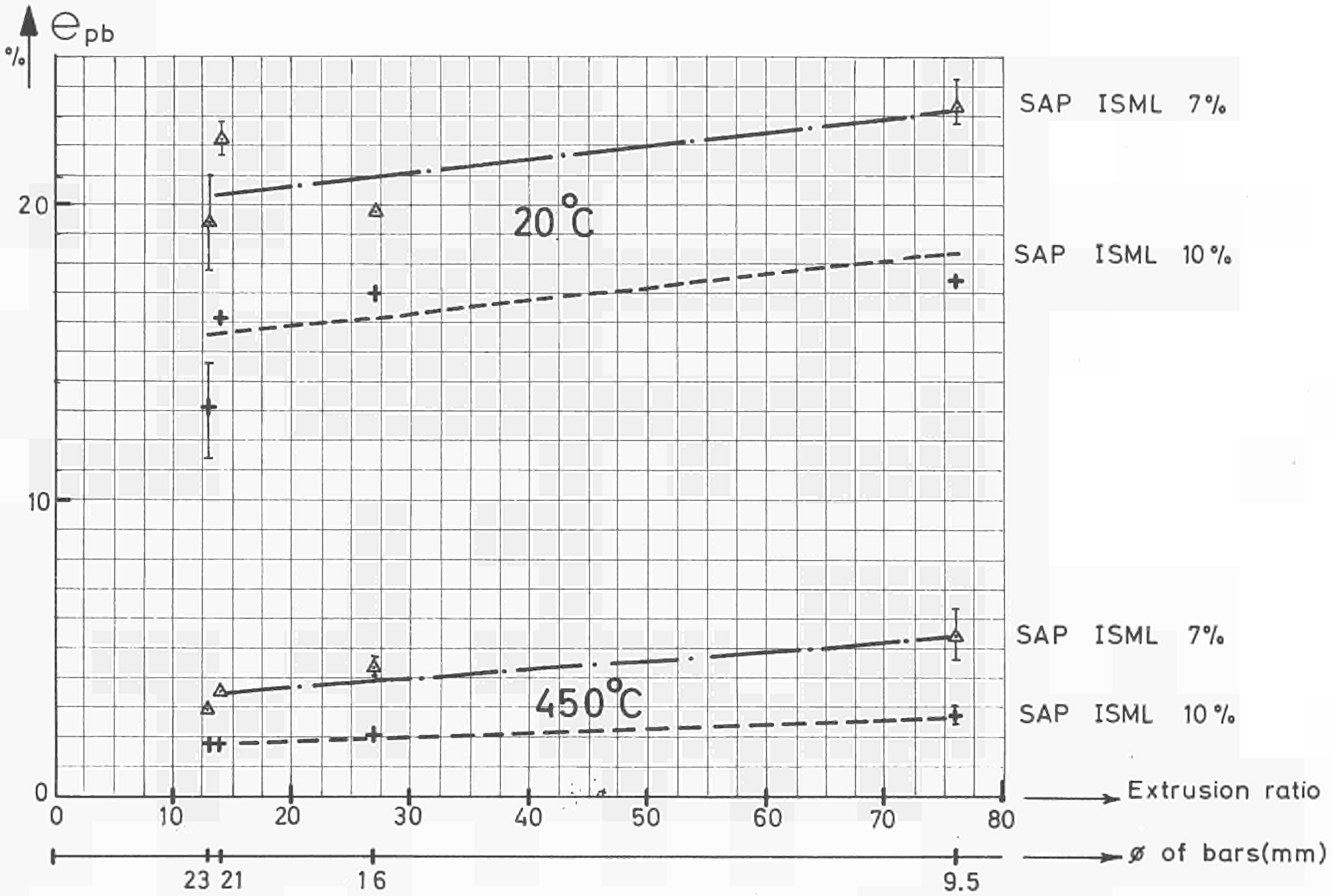

Fig 5

Fig. 6

INFLUENCE OF THE TEST DURATION ON THE MECHANICAL PROPERTIES OF SAP ISML 7 %

(Euratom and ISML results)

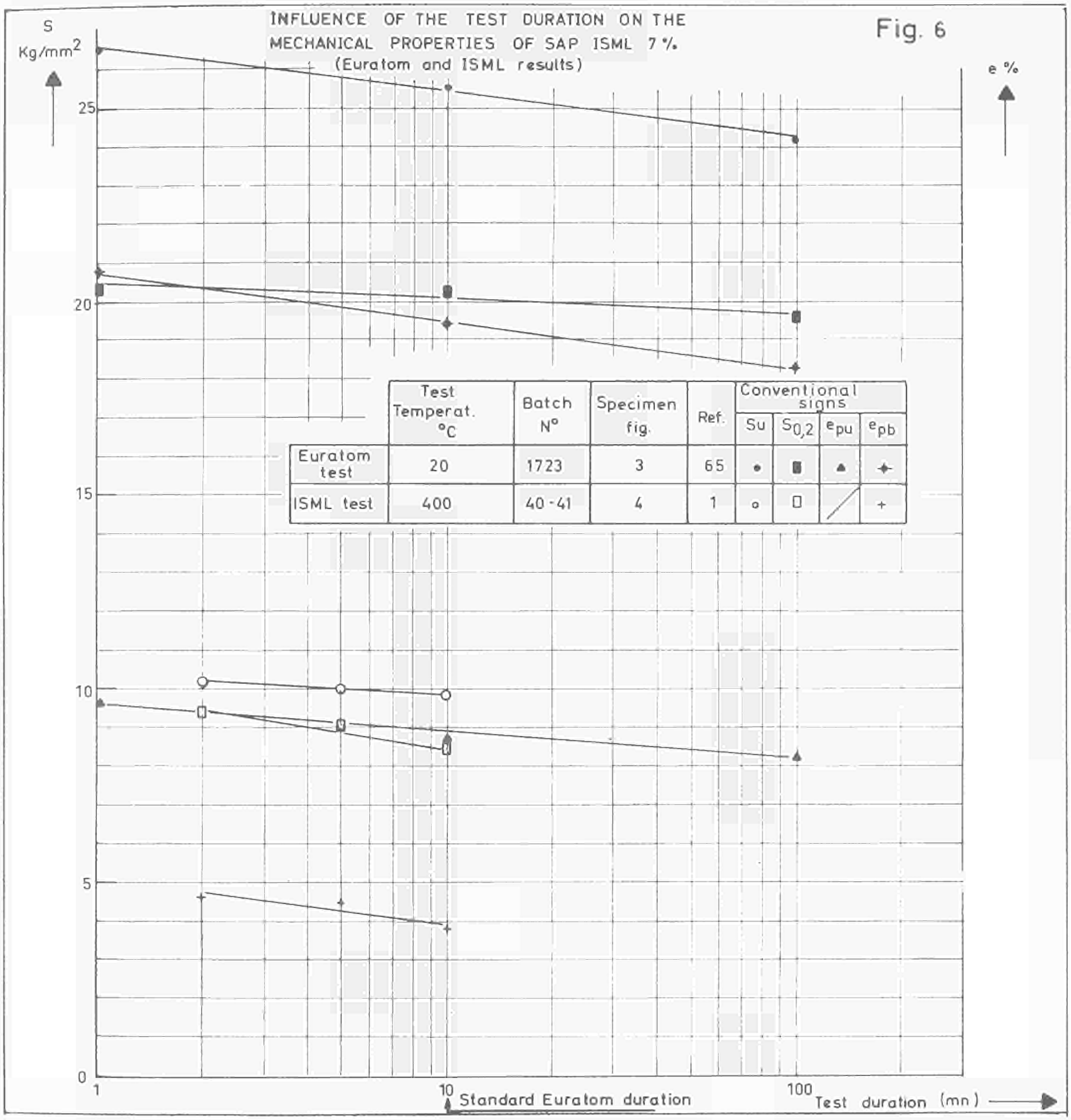

	Test Temperat. °C	Batch N°	Specimen fig.	Ref.	Conventional signs: Su	$S_{0,2}$	e_{pu}	e_{pb}
Euratom test	20	1723	3	65	●	■	▲	✦
ISML test	400	40-41	4	1	○	□	/	+

INFLUENCE OF THE CROSSHEAD SPEED ON THE MECHANICAL PROPERTIES OF SAP ISML 4 %
(Euratom results Ref: 51)

⊙ Su Engineering maximum tensile stress
⊡ $S_{0.2}$ " 0.2 offset yield stress
Specimen Fig 3
Batch N. 828 - 829 (bars Ø 9.5mm)

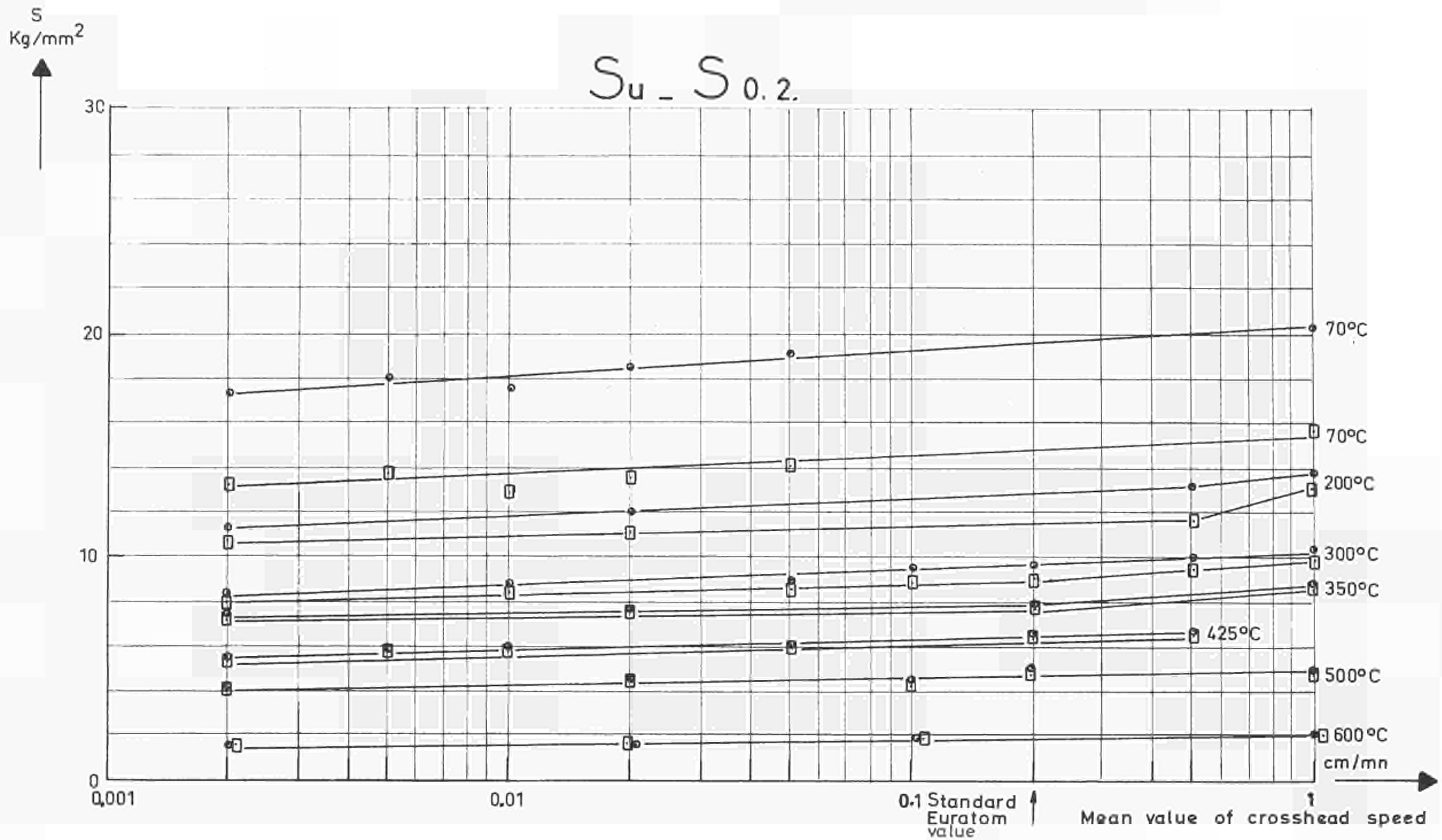

Fig. 7

INFLUENCE OF THE CROSSHEAD SPEED ON THE MECHANICAL PROPERTIES OF SAP ISML 4%
(Euratom results Ref. 51)

+ epb: Engineering plastic strain at breaking point

Specimen Fig3 Batch N. 828 - 829 (bars Ø 9.5mm)

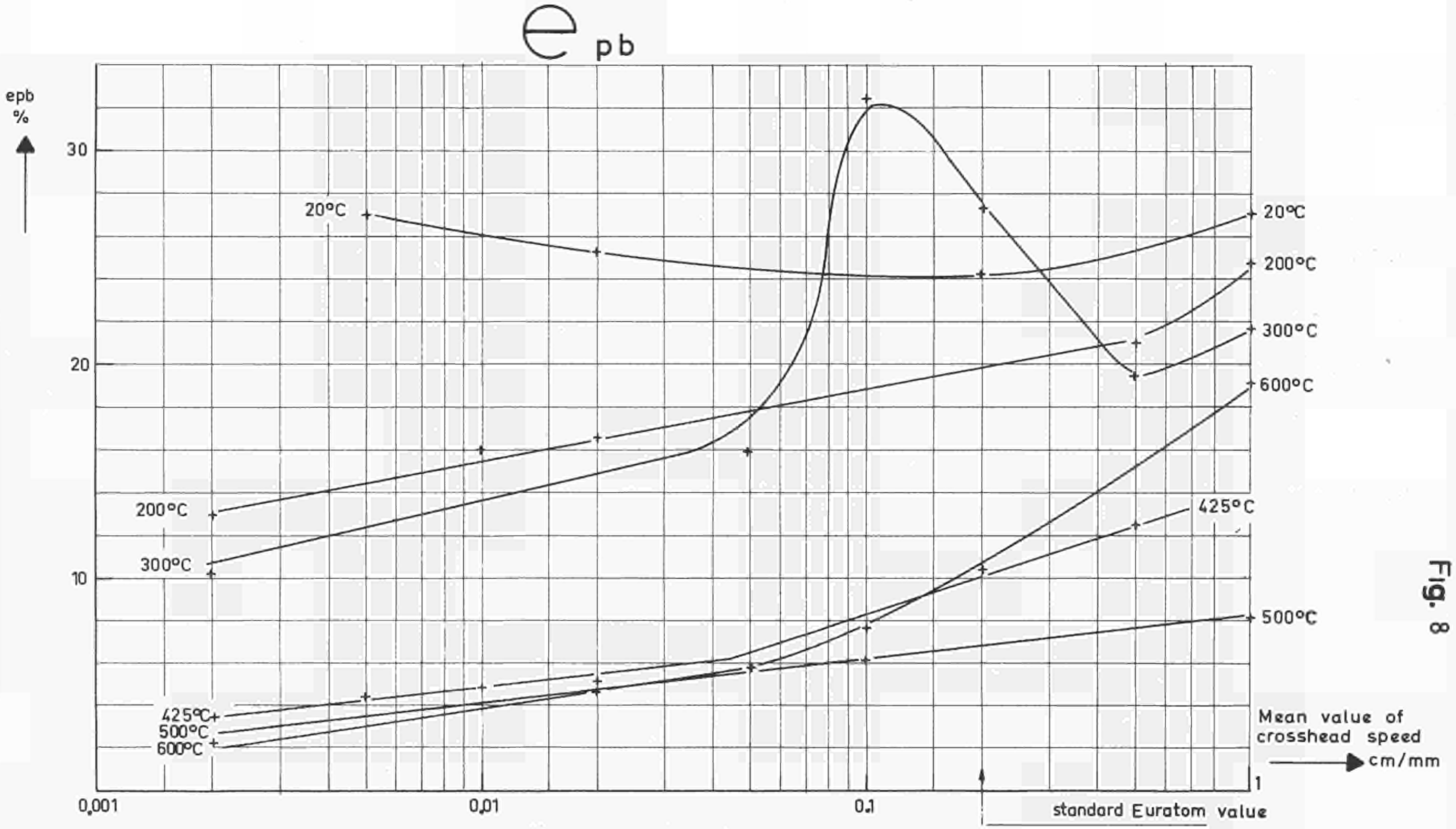

Fig. 8

INFLUENCE OF CROSSHEAD SPEED ON THE MECHANICAL PROPERTIES OF SAP ISML 7%
(Euratom results Ref.51)

⊙ Su Engineering maximum tensile stress
⊡ $S_{0.2}$ " offset yield stress
Specimen Fig 3 Batch N.906-907 (bars Ø 9,5)

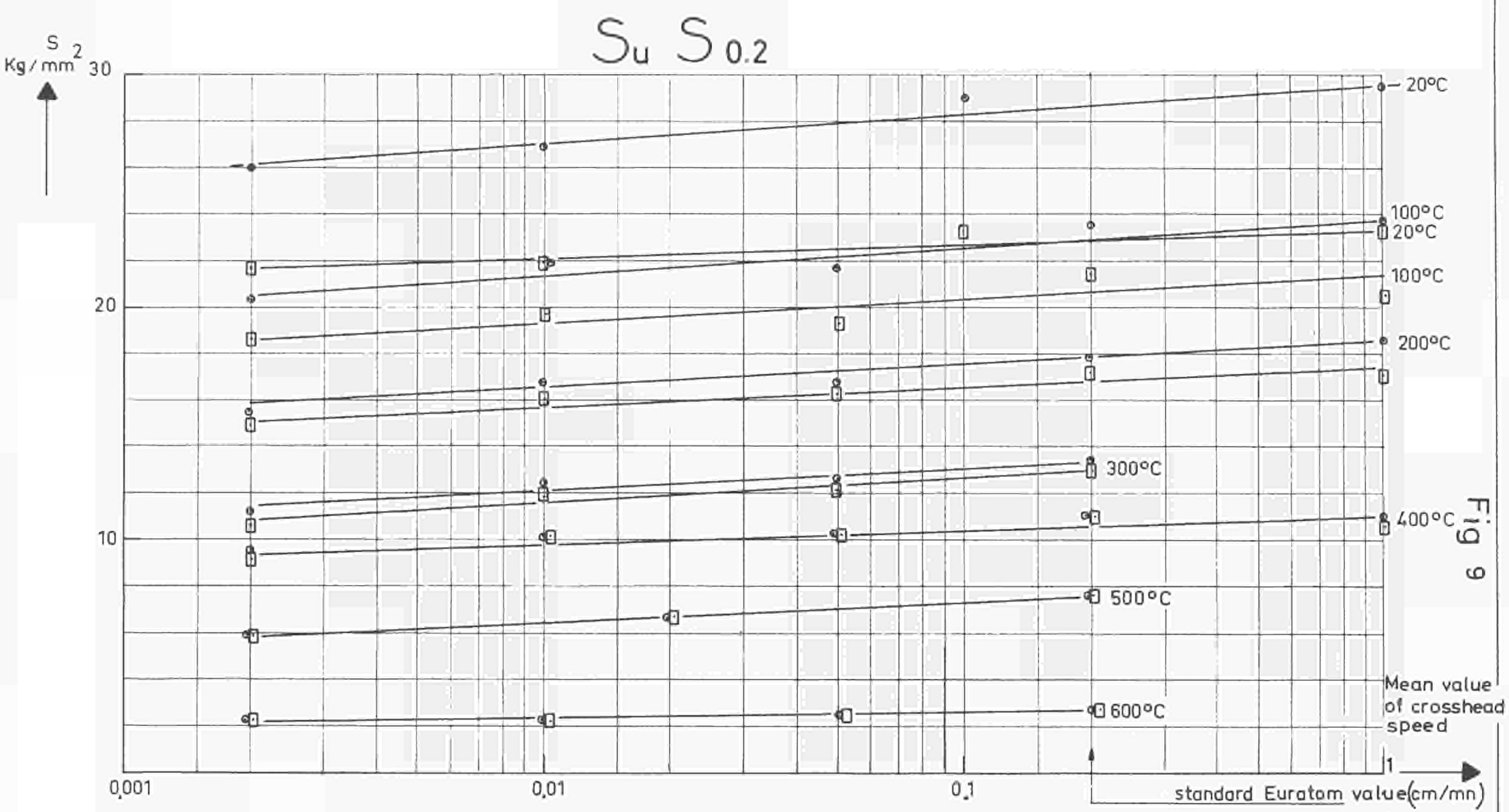

Fig 9

INFLUENCE OF THE CROSSHEAD SPEED ON THE MECHANICAL PROPERTIES OF SAP ISML 7%
(Euratom results. Ref.: 57)

+ e_{pb} Engineering plastic strain at breaking point
Specimen Fig 3 Batch N. 861 (bars Ø 9,5 mm)

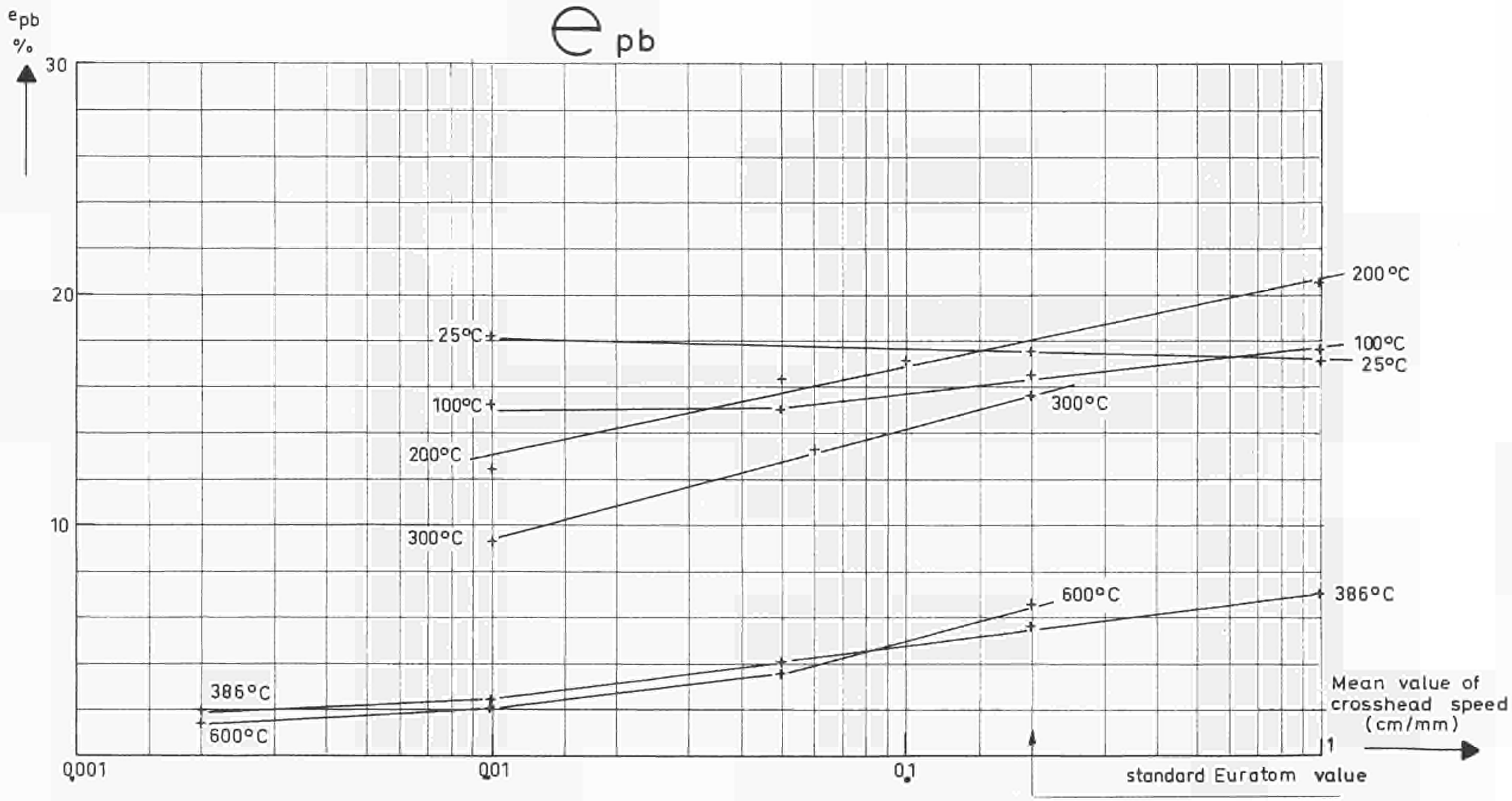

Fig: 9A

INFLUENCE OF THE CROSSHEAD SPEED ON THE MECHANICAL PROPERTIES OF SAP ISML 10%
(Euratom results Ref.51)

⊙ Su Engineering maximum tensile stress
⊡ $S_{0.2}$ " 0.2 offset yield stress
Specimen Fig3 Batch N.1051 (bars Ø 9.5mm)

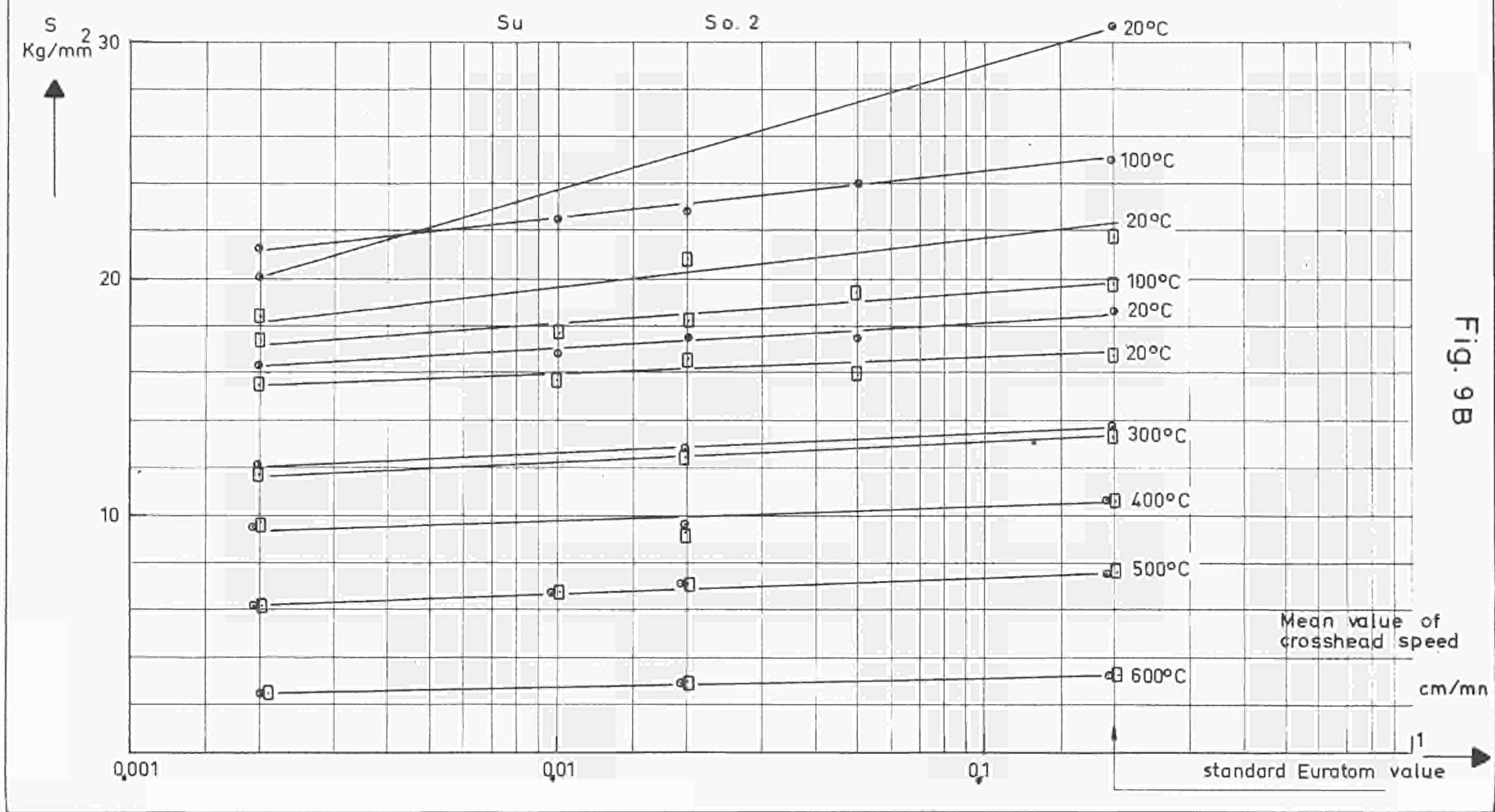

Fig. 9B

INFLUENCE OF THE CROSSHEAD SPEED ON THE MECHANICAL PROPERTIES OF SAP ISML 10%
(Euratom results.Ref51)

+ e_{pb}: Engineering plastic strain at breaking point
Specimen Fig 3 Batch N.1051 (bar Ø 9.5mm)

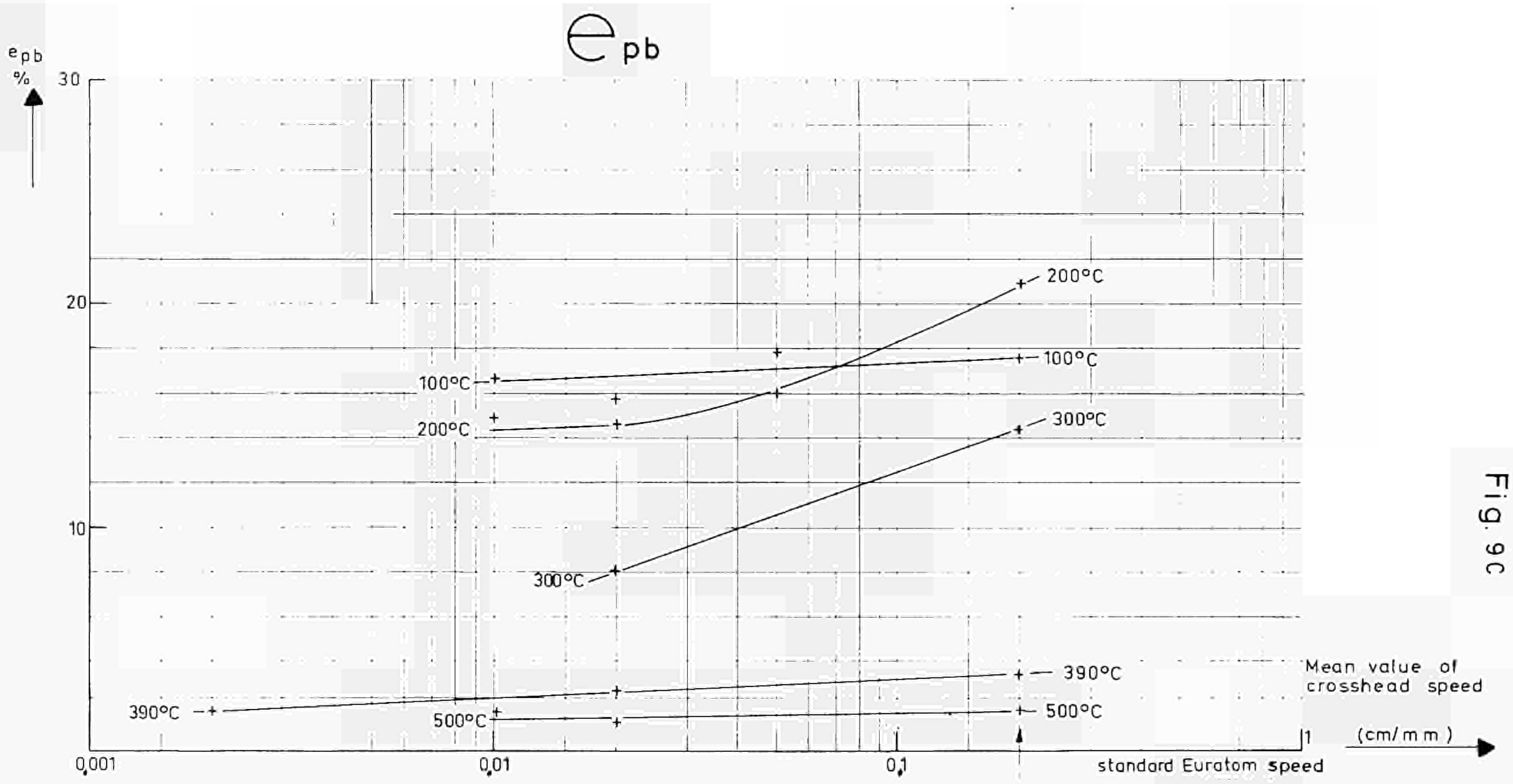

Fig. 9C

THE ELASTIC LIMIT OF S.A.P ISML
OBTAINED THROUGH DIFFERENT METHODS
(ISML and EURATOM RESULTS)

Euratom Tests

Batch No				
% Al_2O_3	4	7	10	14
Batch No	291	300	321	316
ϕbar (mm)	9,5	9,5	16	16

		Batch No			
	% Al_2O_3	4	7	10	14
Euratom Tests	Batch No	289-291	275	280	287-317
	ϕbar mm	9,5	9,5	9,5	9,5
ISML Tests (Ref 5)	Batch No	117	119	124	125
	ϕbar mm	21	21	21	21

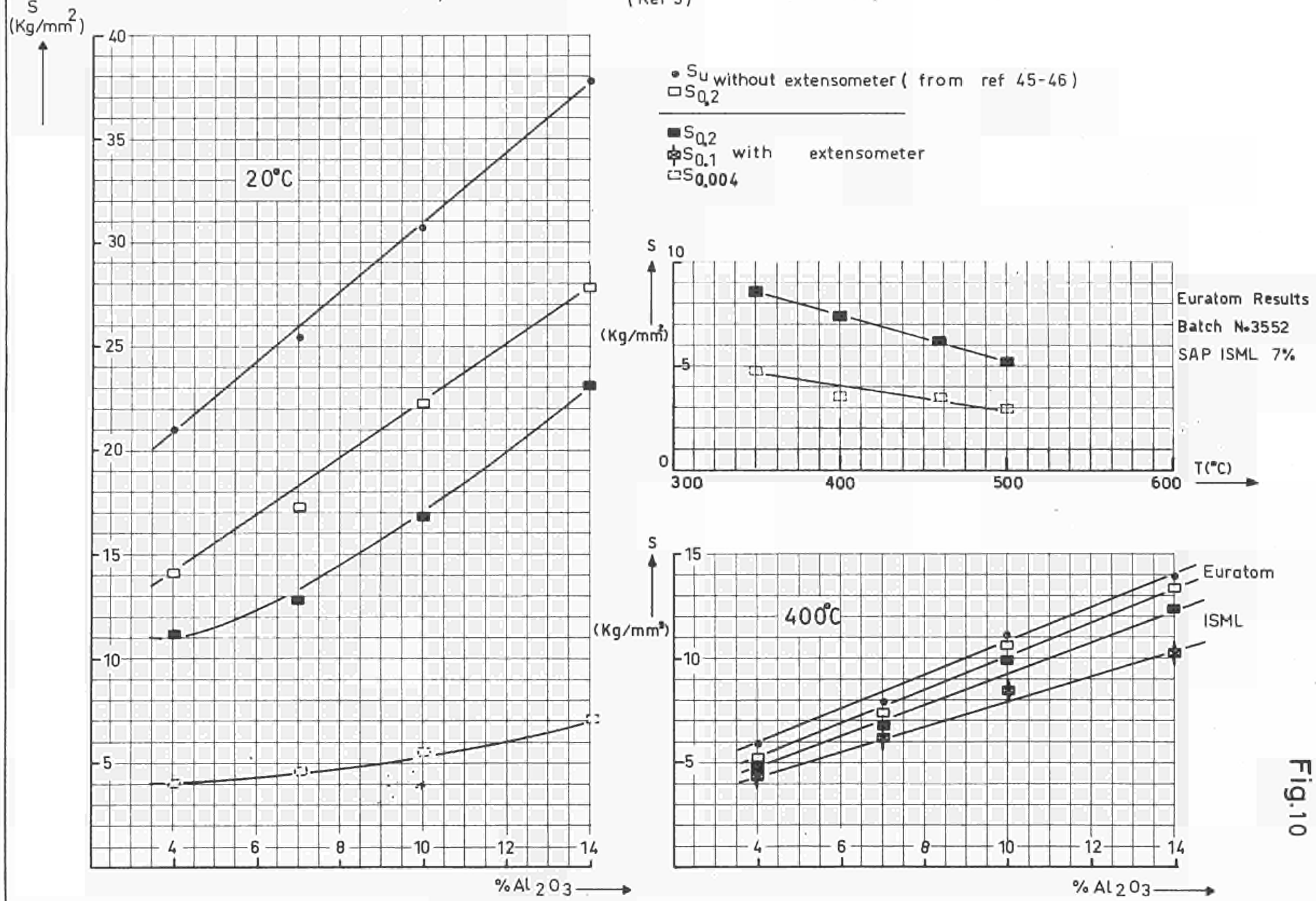

Fig.10

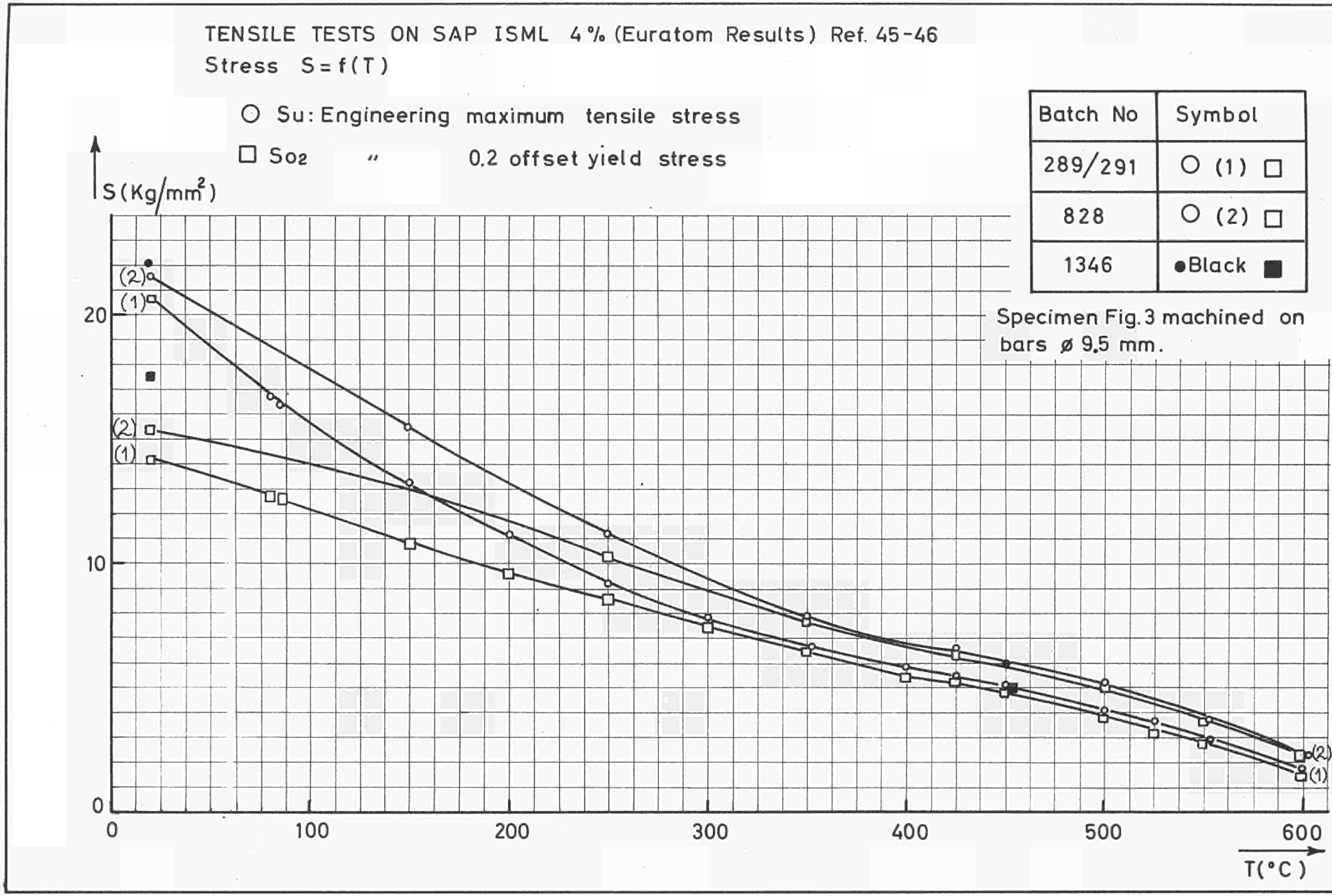

TENSILE TESTS ON SAP ISML 4% (Euratom Results) Ref. 45-46
Stress S = f(T)
○ Su: Engineering maximum tensile stress
□ So2 " 0.2 offset yield stress
S (Kg/mm²)
Batch No | Symbol
289/291 | ○ (1) □
828 | ○ (2) □
1346 | ●Black ■
Specimen Fig. 3 machined on bars ø 9,5 mm.
(2)
(1)
(2)
(1)
20
10
0
0
100
200
300
400
500
600
(2)
(1)
T(°C)

Fig. 11

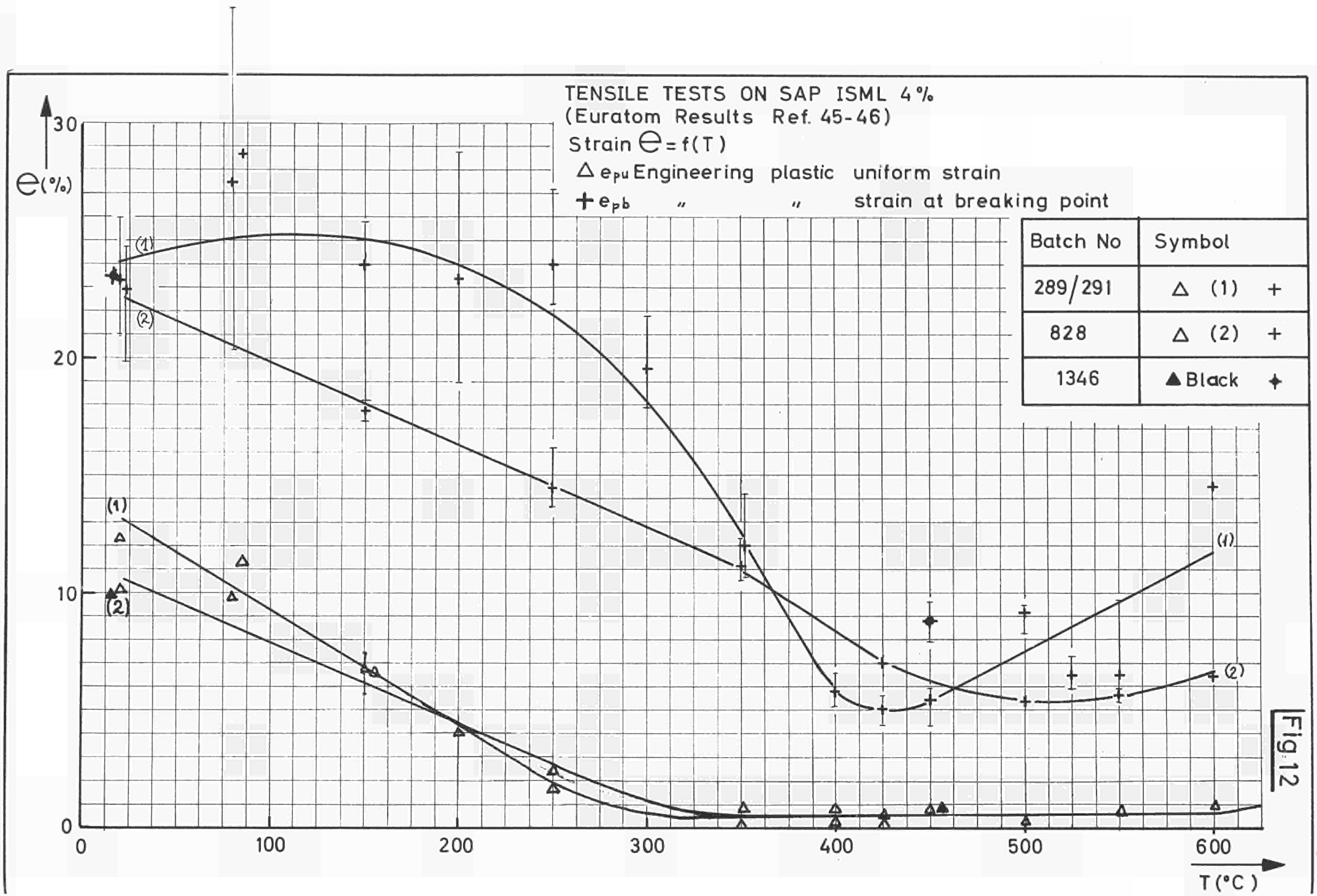

TENSILE TESTS ON SAP ISML 4%
(Euratom Results Ref. 45-46)
Strain e = f(T)
△ epu Engineering plastic uniform strain
+ epb " " strain at breaking point
Batch No
Symbol
289/291
△ (1) +
828
△ (2) +
1346
▲ Black ✚
e(%)
30
20
10
0
100
200
300
400
500
600
T(°C)
(1)
(2)
Fig.12

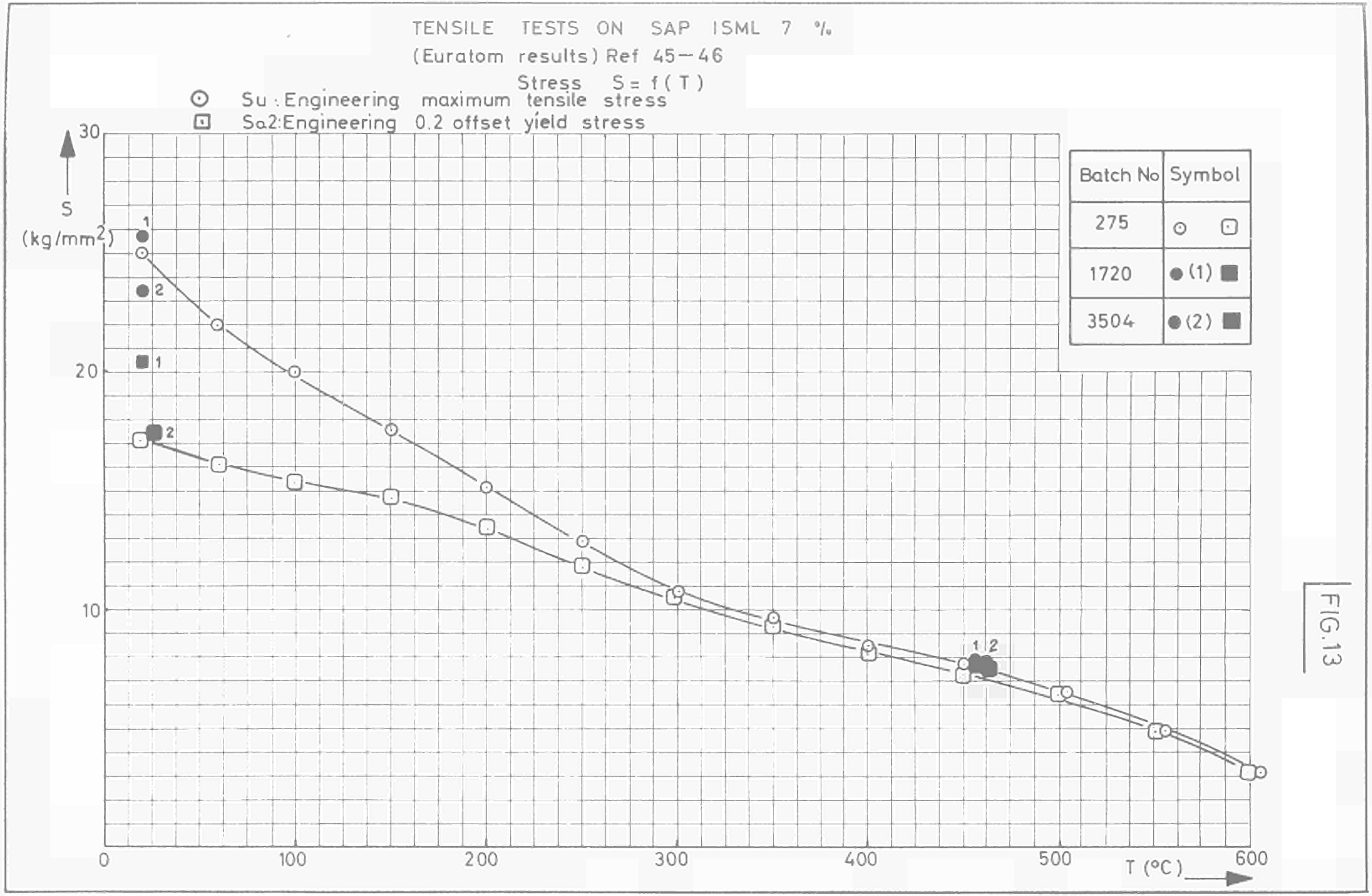
TENSILE TESTS ON SAP ISML 7 %
(Euratom results) Ref 45-46
Stress S = f (T)
Su : Engineering maximum tensile stress
Sο2:Engineering 0.2 offset yield stress
S
(kg/mm2)
30
20
10
0
100
200
300
400
500
600
T (°C)
1
2
1
2
1 2
Batch No
Symbol
275
1720
(1)
3504
(2)

FIG.13

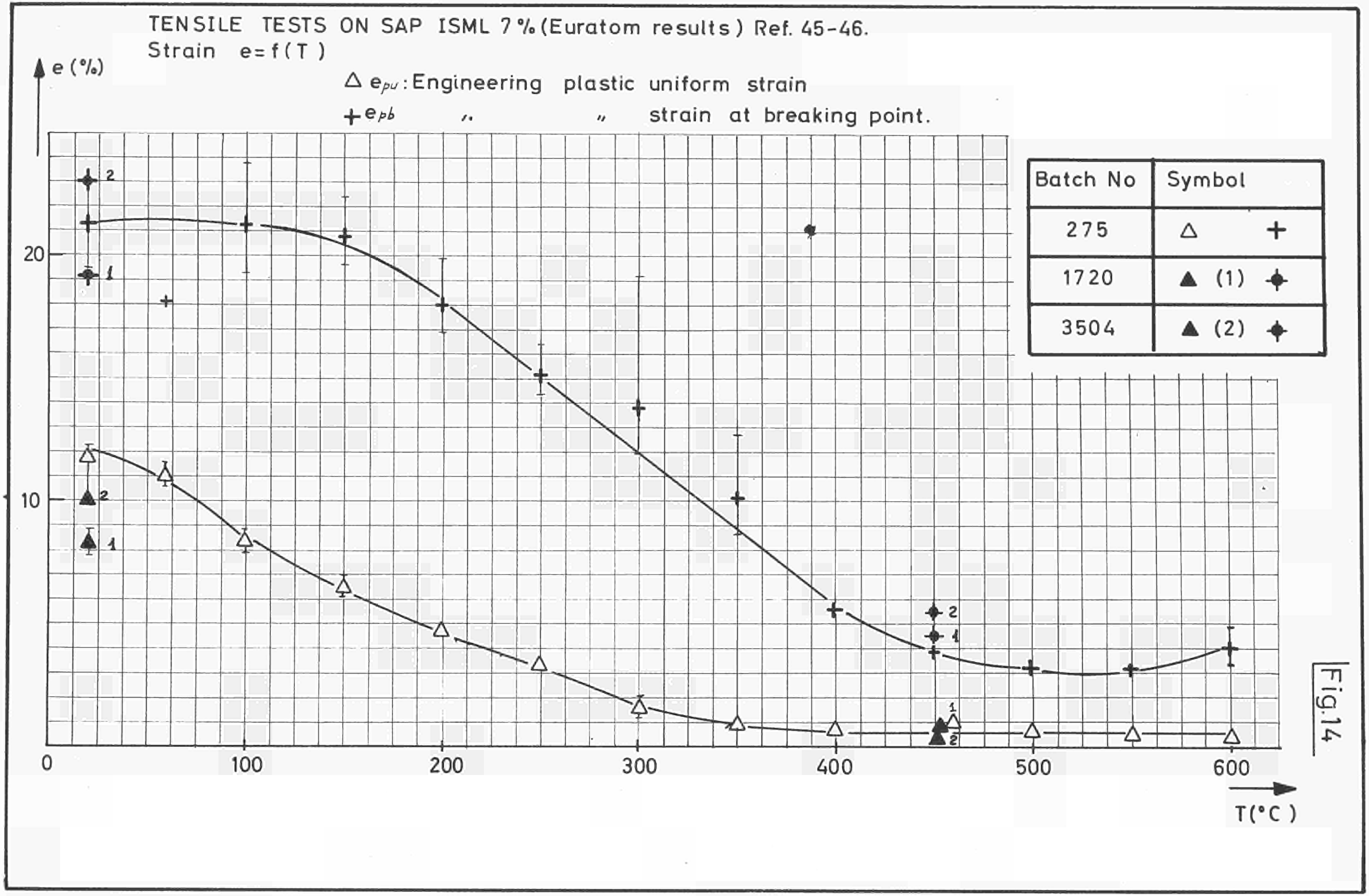

TENSILE TESTS ON SAP ISML 7 % (Euratom results) Ref. 45-46.
Strain e = f (T)
e (%)
△ e_{pu} : Engineering plastic uniform strain
+ e_{pb} " " strain at breaking point.
Batch No
Symbol
275
1720
(1)
3504
(2)
20
10
0
100
200
300
400
500
600
T (°C)

Fig.14

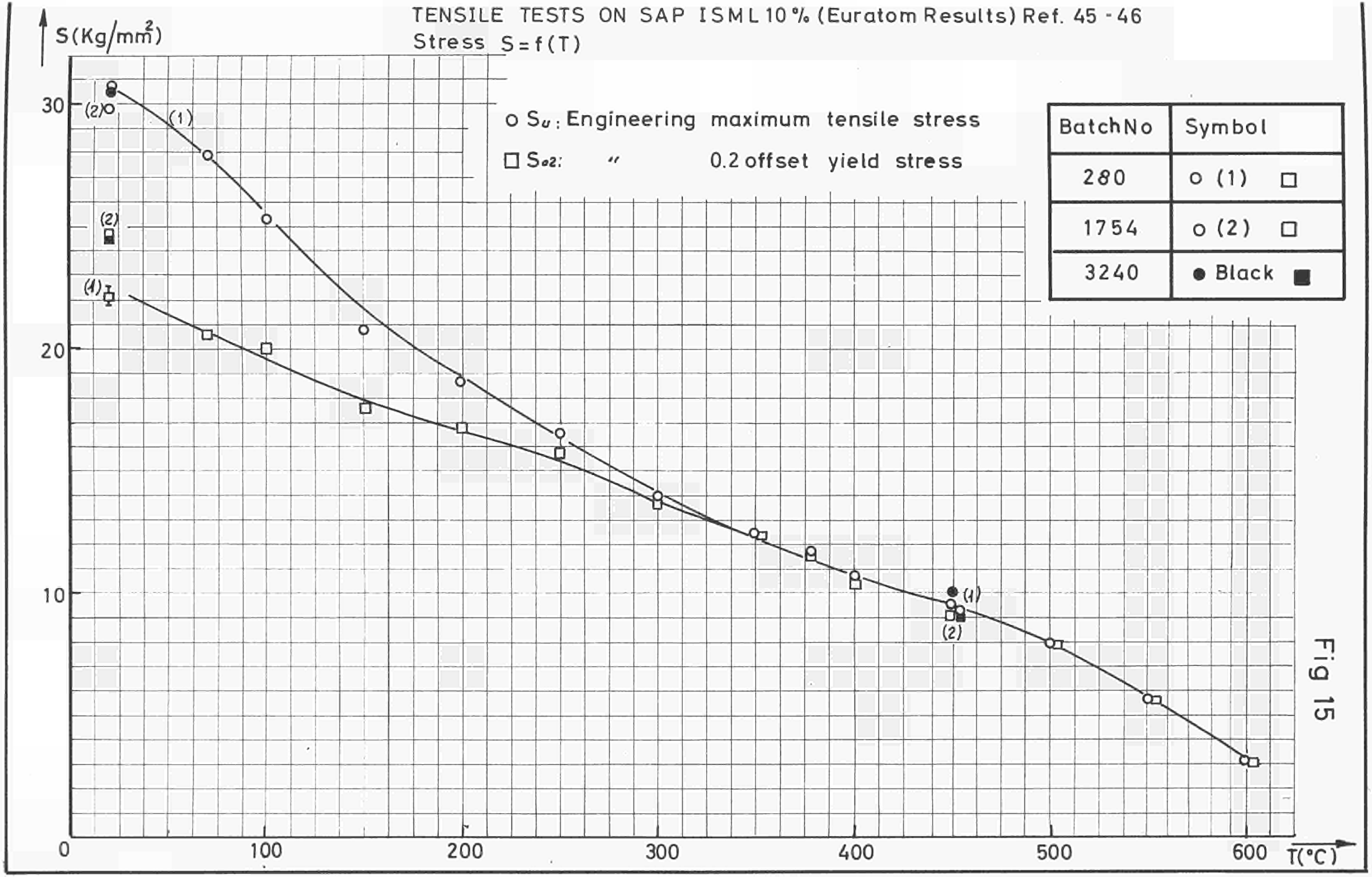
TENSILE TESTS ON SAP ISML 10 % (Euratom Results) Ref. 45 - 46
Stress S = f(T)
S(Kg/mm²)
○ Su : Engineering maximum tensile stress
□ S02: " 0.2 offset yield stress
Batch No | Symbol
280 | ○ (1) □
1754 | ○ (2) □
3240 | ● Black ■
30
20
10
0
100
200
300
400
500
600
T(°C)
(1)
(2)

Fig 15

TENSILE TESTS ON SAP ISML 10 %
(Euratom results) ref 45-46.

Strain e = f(T)

▲ epu: Engineering plastic uniform strain.
+ epb: " " strain at breaking point

Batch No	Symbol
280	▲ (1) +
1754	▲ (2) +
3240	▲ Black +

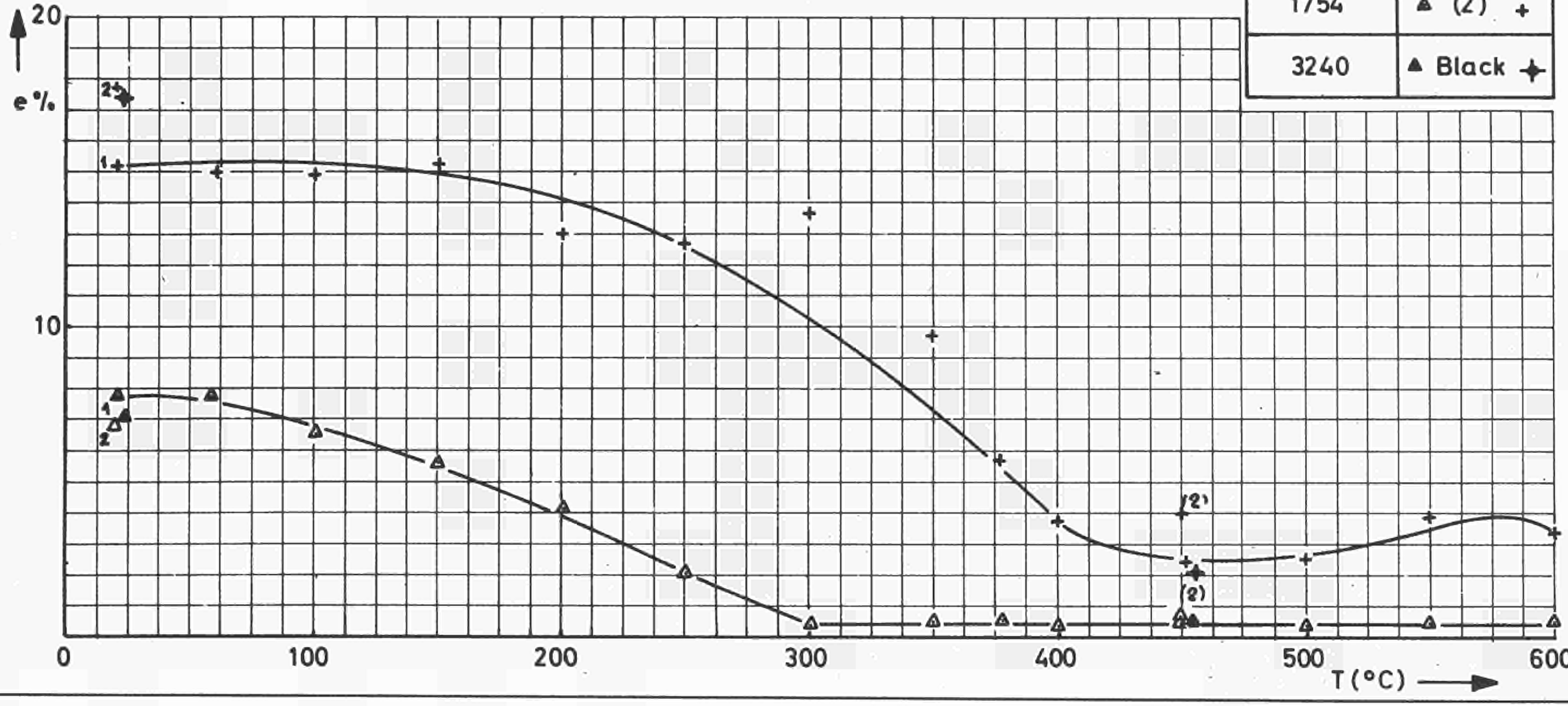

FIG. 16

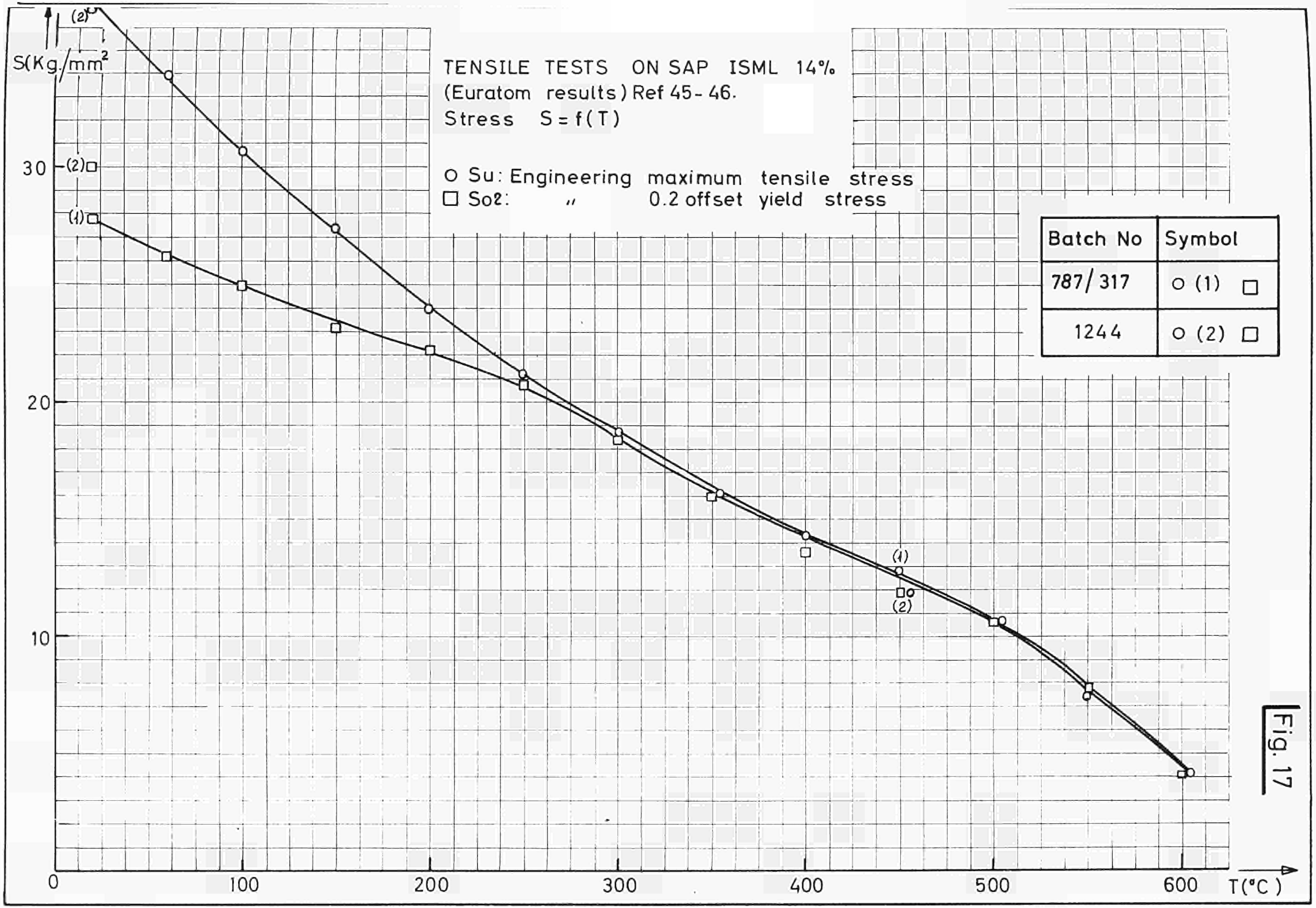

S(Kg./mm²)
TENSILE TESTS ON SAP ISML 14%
(Euratom results) Ref 45-46.
Stress S = f(T)
○ Su: Engineering maximum tensile stress
□ So2: " 0.2 offset yield stress
Batch No | Symbol
787/317 | ○ (1) □
1244 | ○ (2) □
30
20
10
0
100
200
300
400
500
600
T(°C)
(1)
(2)

Fig. 17

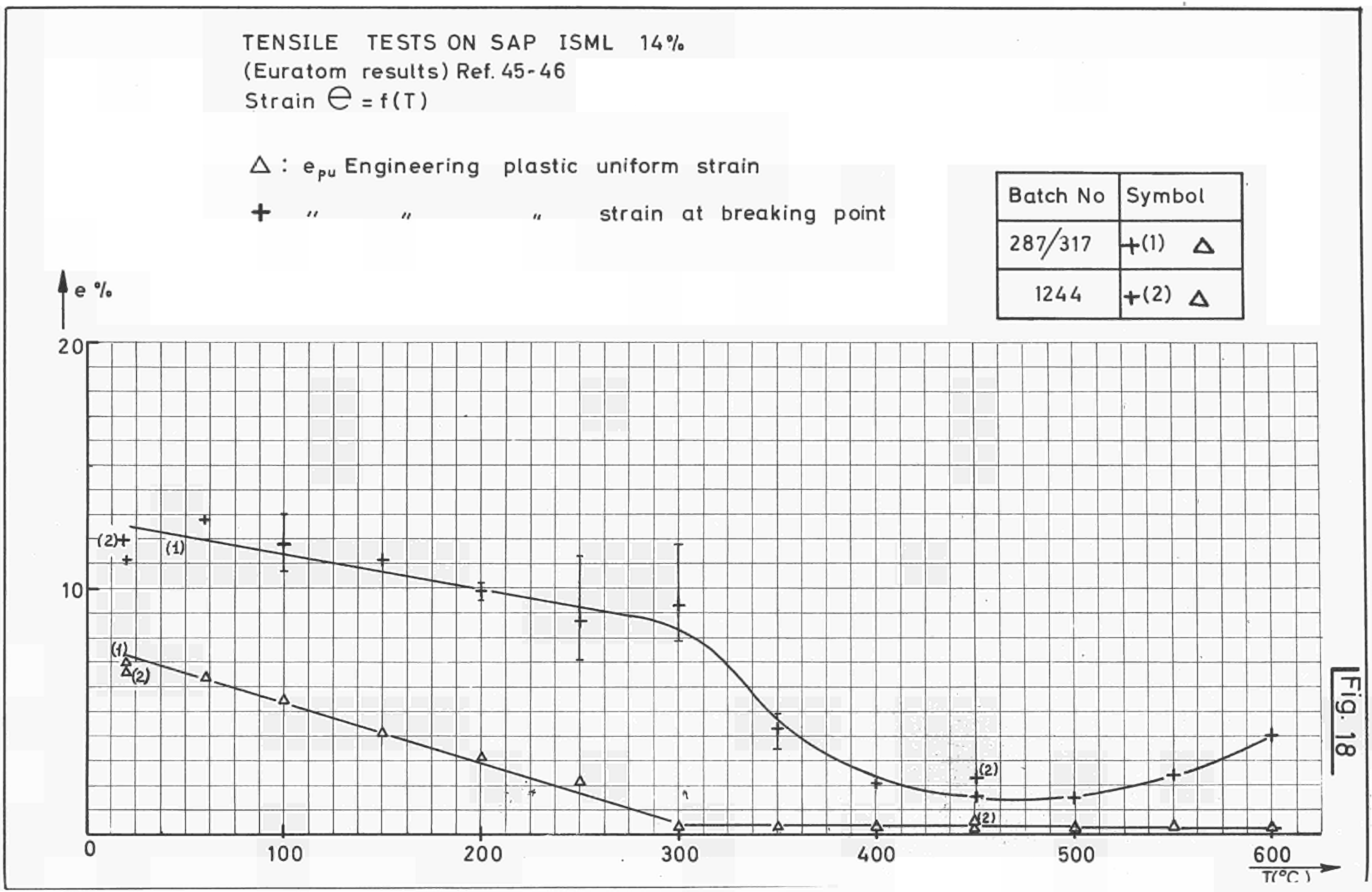
TENSILE TESTS ON SAP ISML 14%
(Euratom results) Ref. 45-46
Strain e = f(T)
△ : e pu Engineering plastic uniform strain
+ " " " strain at breaking point
Batch No | Symbol
287/317 | +(1) △
1244 | +(2) △
e %
20
10
0
100
200
300
400
500
600
T(°C)
(1)
(2)

Fig. 18

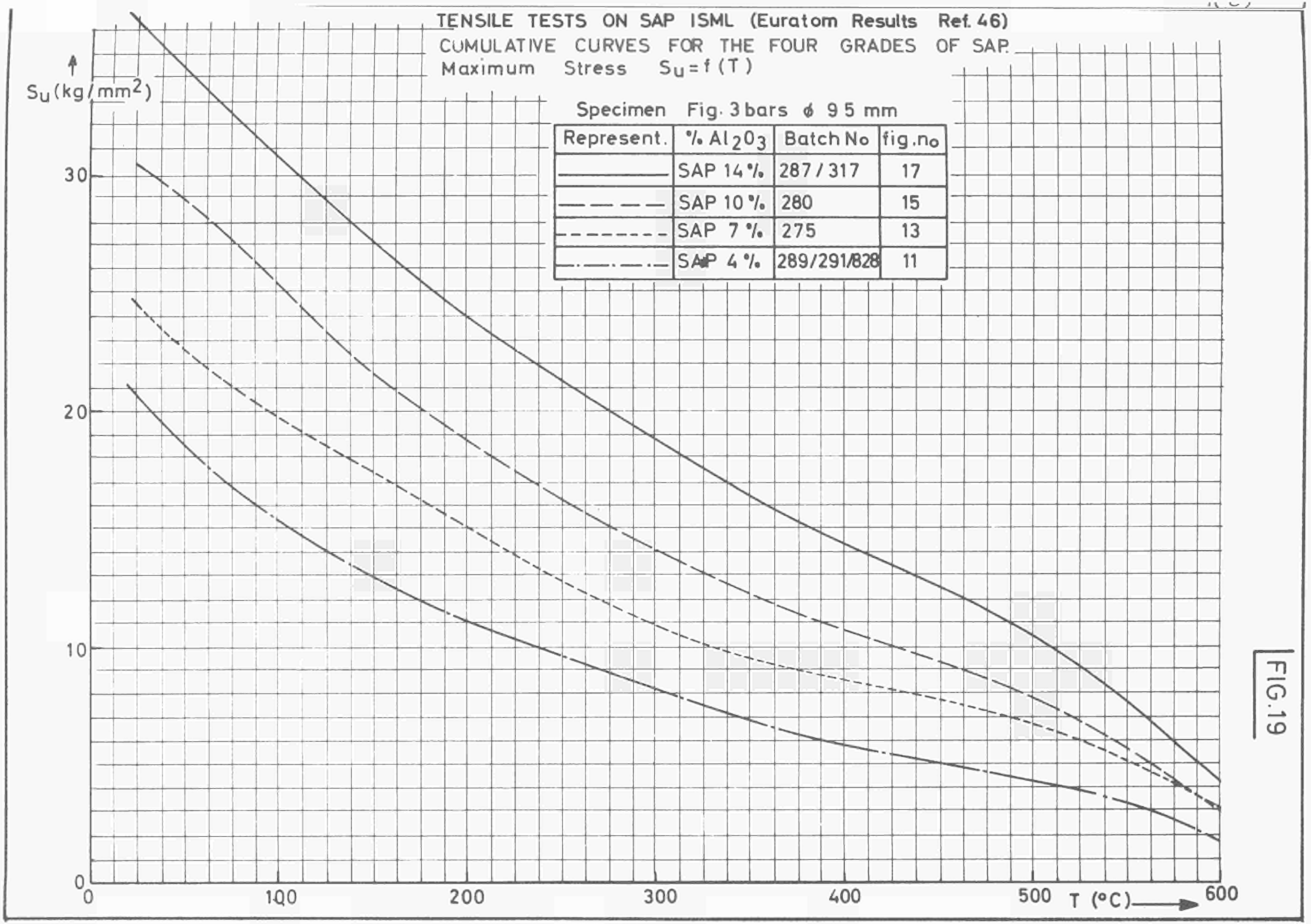
TENSILE TESTS ON SAP ISML (Euratom Results Ref. 46)
CUMULATIVE CURVES FOR THE FOUR GRADES OF SAP
Maximum Stress Su = f (T)
Su (kg/mm2)
Specimen Fig. 3 bars ϕ 9 5 mm
Represent.
% Al2O3
Batch No
fig. no
SAP 14 %
287 / 317
17
SAP 10 %
280
15
SAP 7 %
275
13
SAP 4 %
289/291/828
11
30
20
10
0
0
100
200
300
400
500
600
T (°C)
FIG. 19

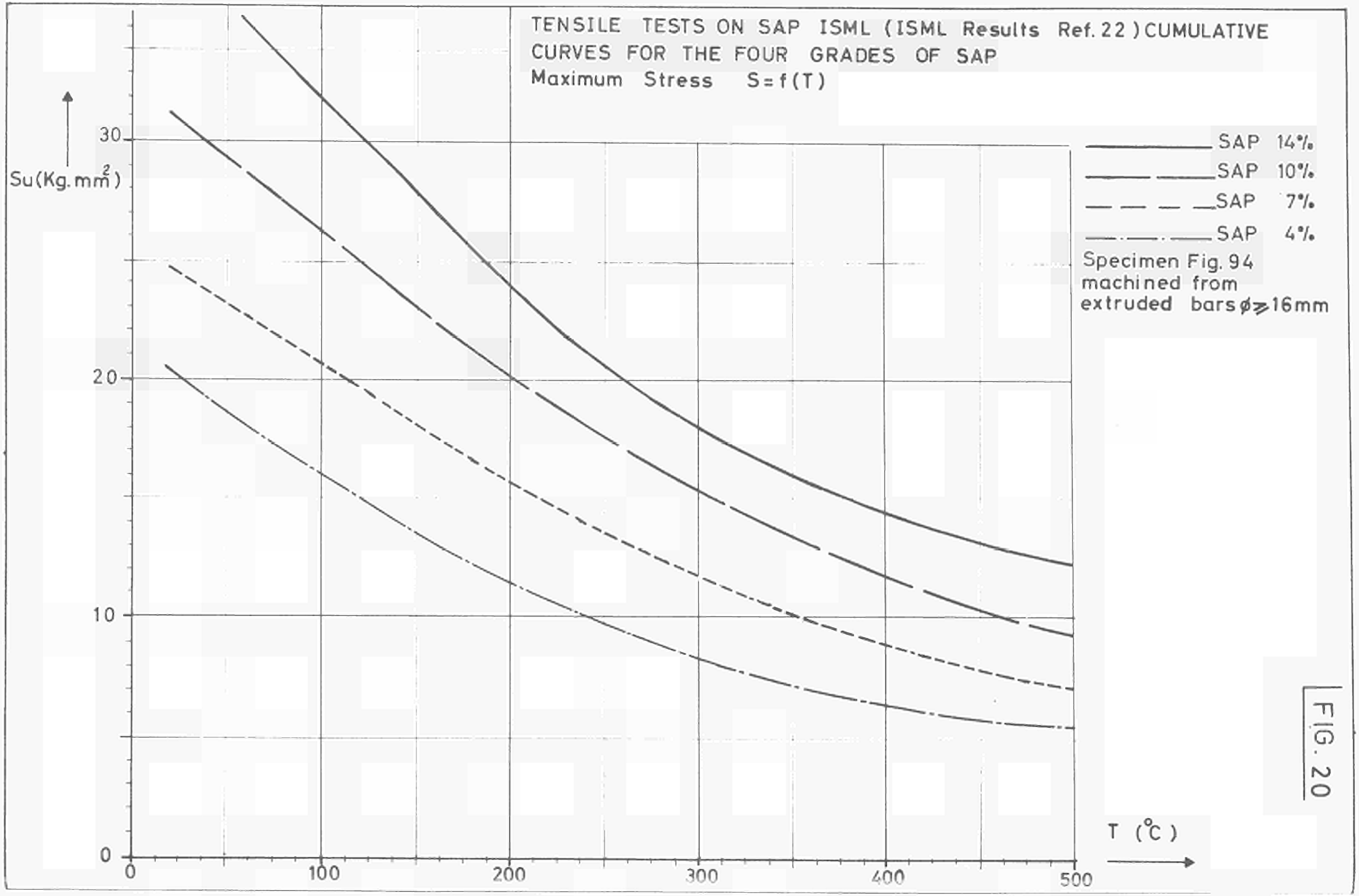

TENSILE TESTS ON SAP ISML (ISML Results Ref. 22) CUMULATIVE CURVES FOR THE FOUR GRADES OF SAP
Maximum Stress S = f(T)
Su(Kg.mm²)
30
20
10
0
0
100
200
300
400
500
T (°C)
SAP 14%
SAP 10%
SAP 7%
SAP 4%
Specimen Fig. 94 machined from extruded bars ø≥16mm

FIG. 20

TENSILE TESTS ON SAP ISML (Euraton Results Ref. 46)
CUMULATIVE CURVES FOR THE FOUR GRADES OF SAP.
Engineering 0.2 offset yield Stress = f(T)

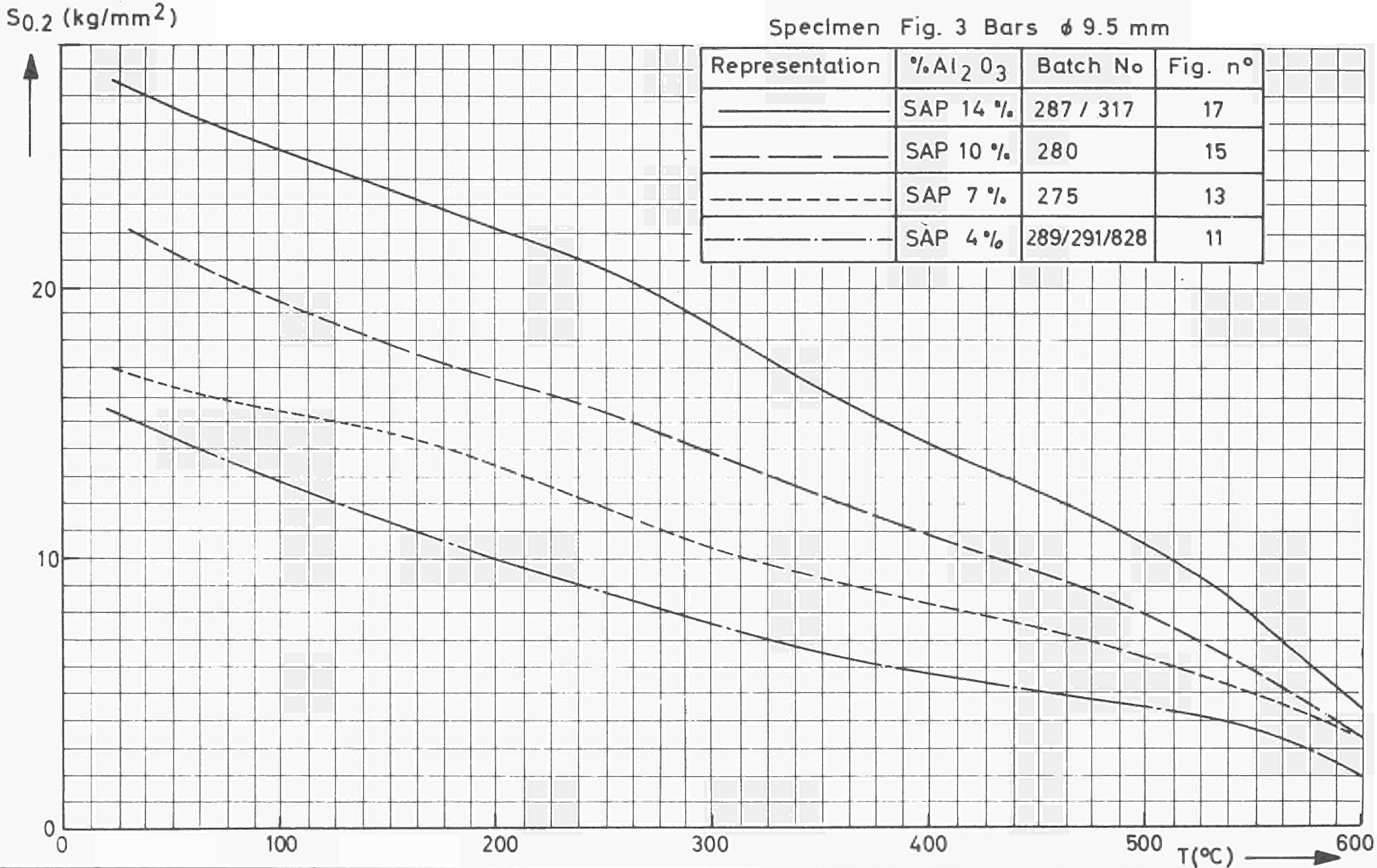

FIG. 21

TENSILE TESTS ON SAP ISML (ISML Results Ref. 22) CUMULATIVE CURVES FOR THE FOUR GRADES OF SAP
Engineering 0.2 offset yield Stress = f (T)

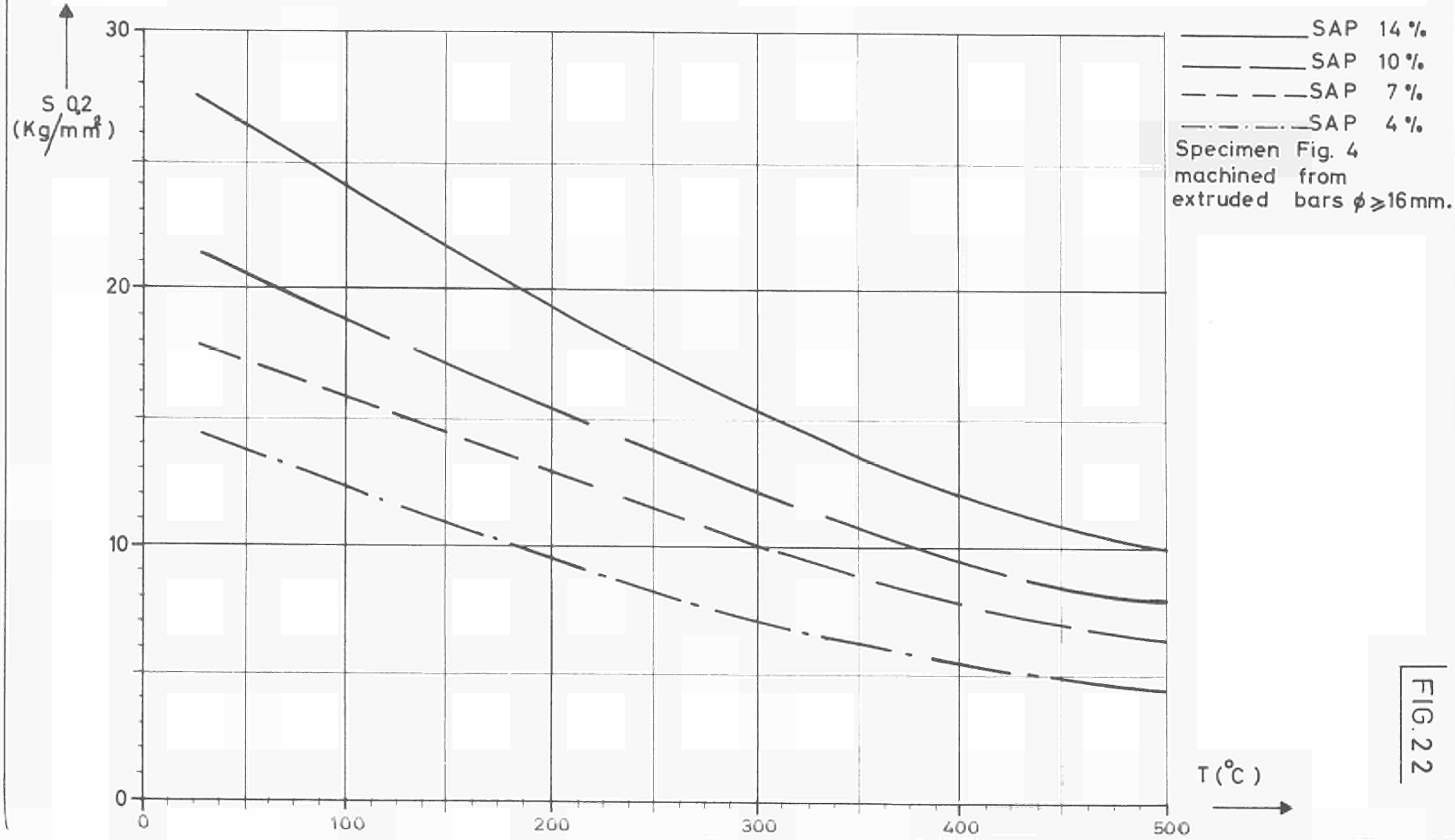

FIG. 22

TENSILE TESTS ON SAP ISML (Euratom Results Ref. 46) CUMULATIVE CURVES FOR THE FOUR GRADES OF SAP — Engineering plastic uniform Strain $e_{pu} = f(T)$_

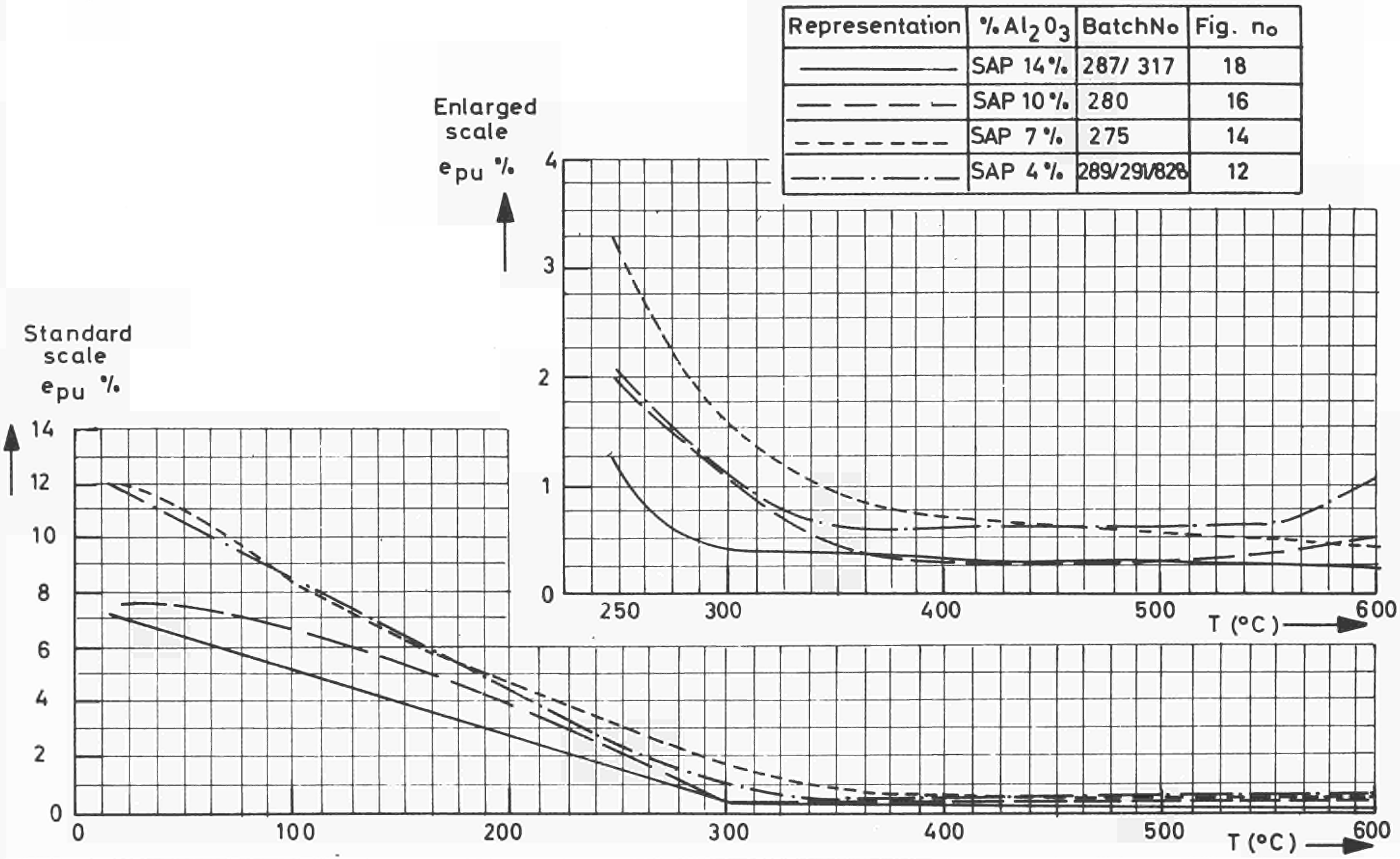

FIG. 23

TENSILE TESTS ON SAP ISML (Euratom Results Ref. 46) CUMULATIVE CURVES FOR THE FOUR GRADES OF SAP Engineering plastic strain at breaking point (e_{pb}) = f (T)

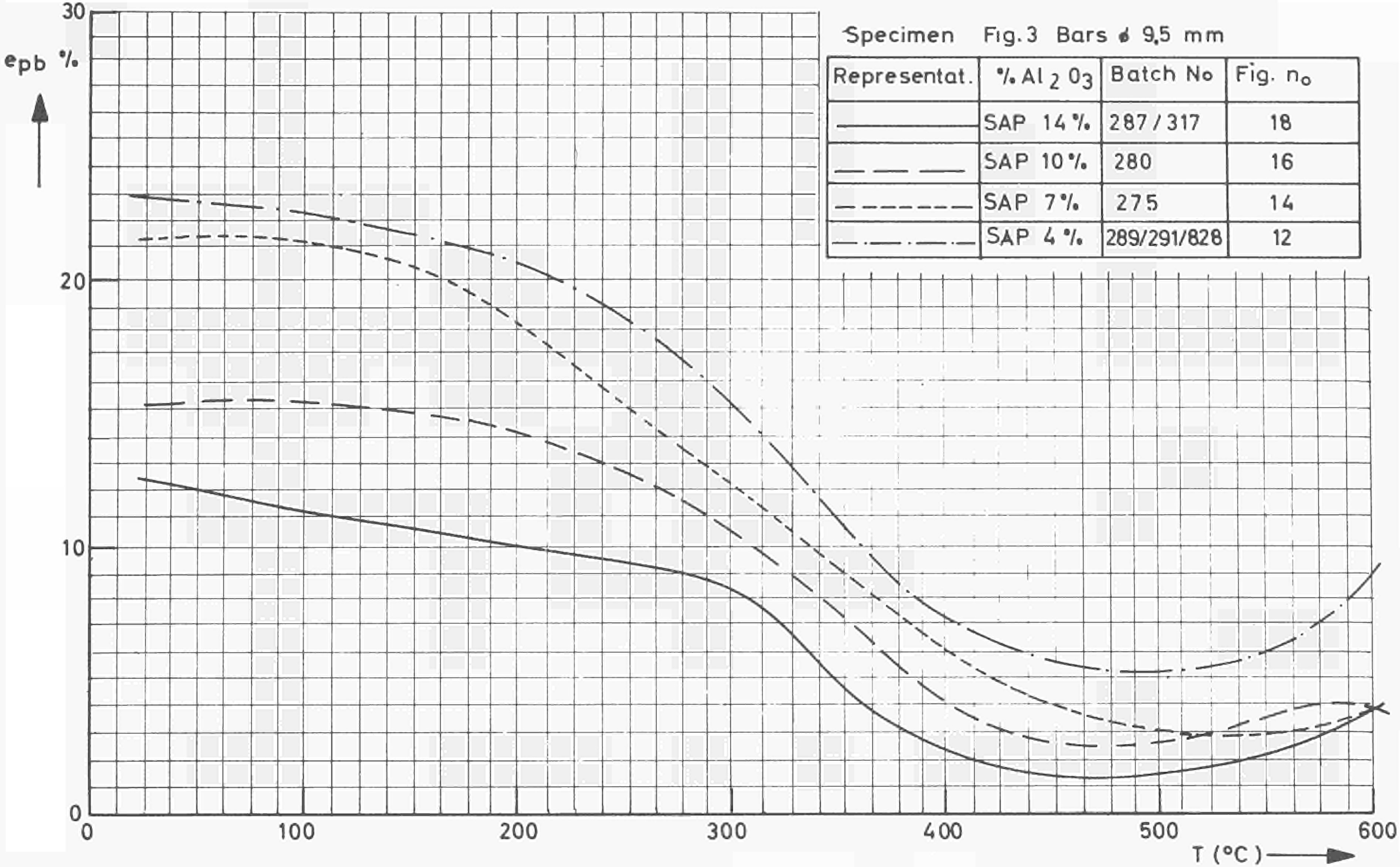

FIG. 24

TENSILE TESTS ON SAP ISML (ISML Results Ref. 22)
CUMULATIVE CURVES FOR THE FOUR GRADES OF SAP
Engineering plastic strain at breaking point $e_{pb} = f(T)$

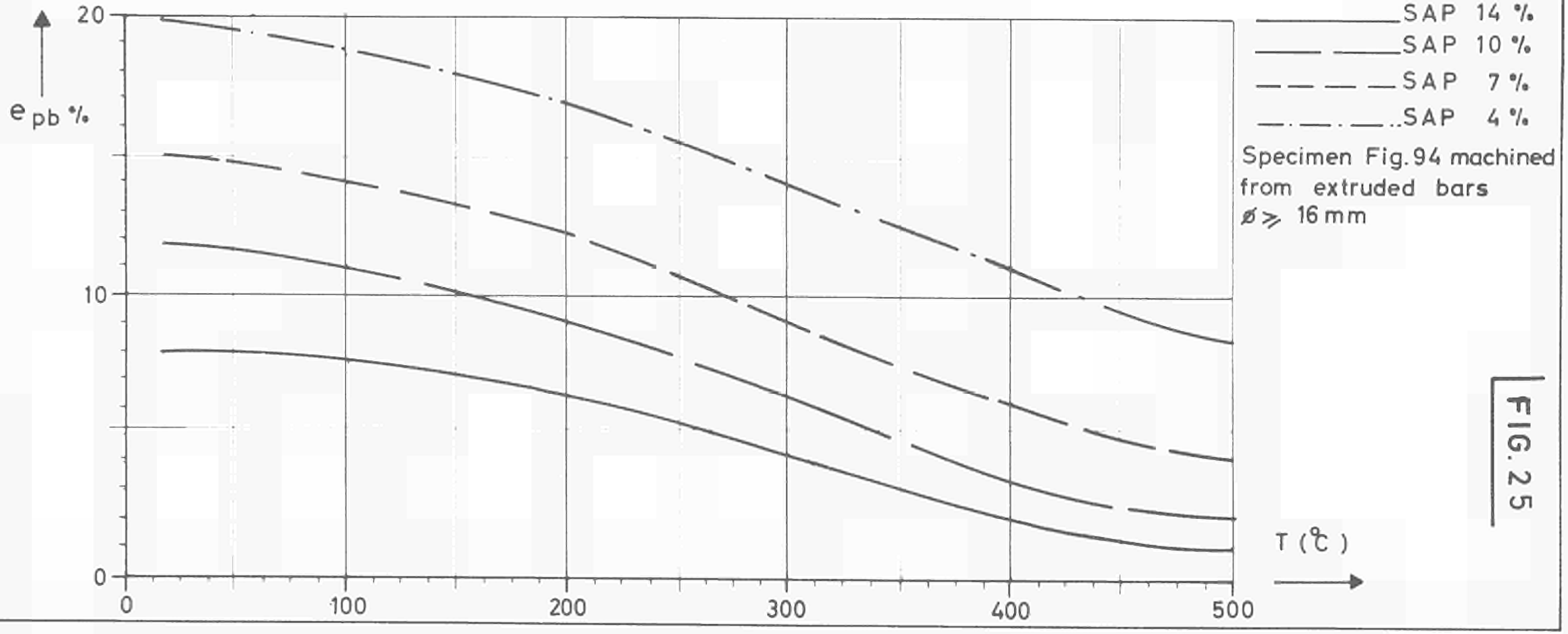

FIG. 25

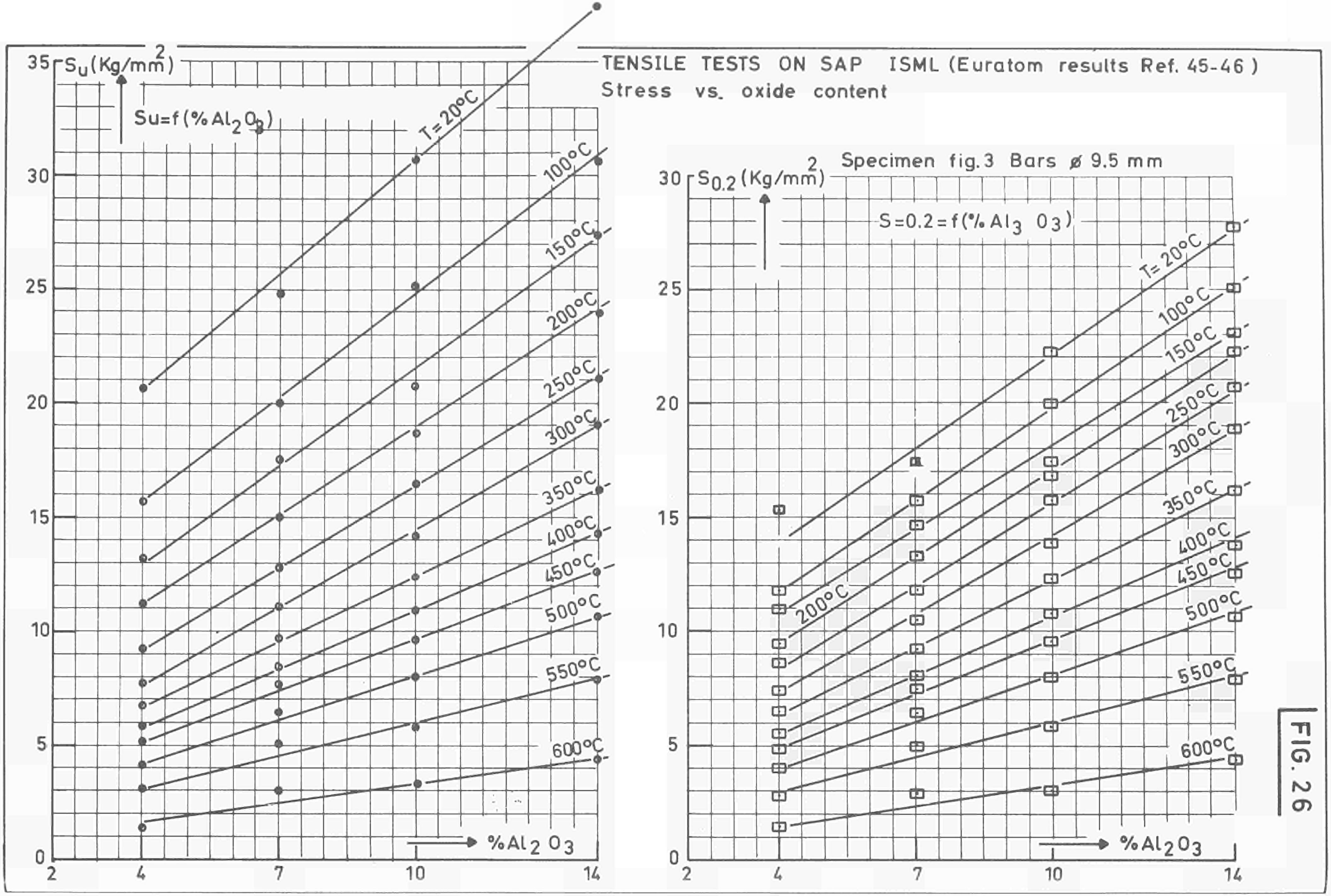
TENSILE TESTS ON SAP ISML (Euratom results Ref. 45-46)
Stress vs. oxide content
Specimen fig.3 Bars ø 9.5 mm
Su (Kg/mm2)
Su=f (%Al2 O3)
T=20°C
100°C
150°C
200°C
250°C
300°C
350°C
400°C
450°C
500°C
550°C
600°C
%Al2 O3
S0.2 (Kg/mm2)
S=0.2=f(%Al3 O3)
35
30
25
20
15
10
5
0
2
4
7
10
14

FIG. 26

TENSILE TESTS ON SAP ISML
(Euratom results Ref. 45-46)
Strain vs oxide content

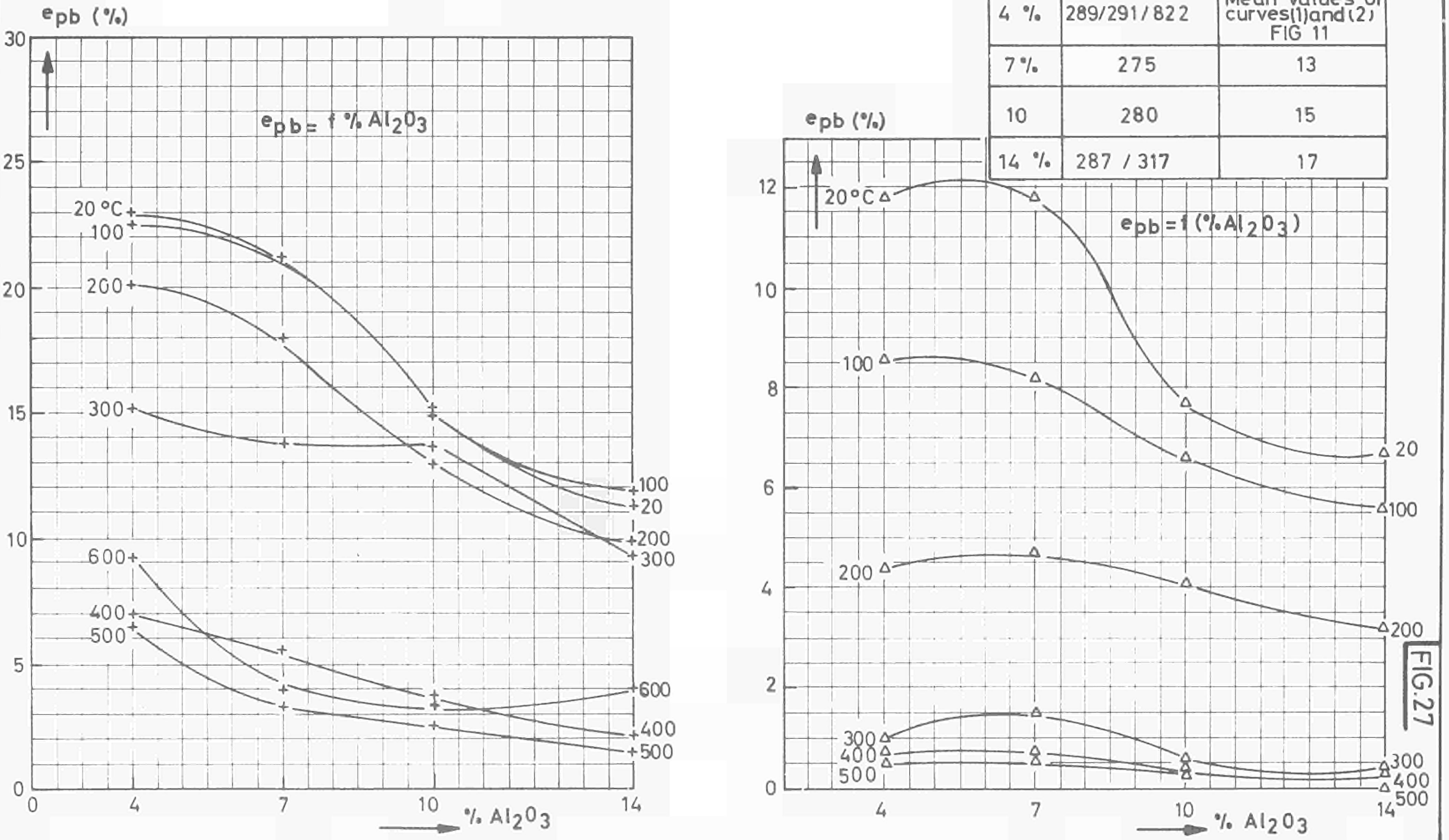

% Al_2O_3	Batch No	From Fig. No
4 %	289/291/822	Mean values of curves (1) and (2) FIG 11
7 %	275	13
10	280	15
14 %	287 / 317	17

FIG. 27

TENSILE TESTS ON SAP ISML (ISML Results Ref. 11)
Tensile properties vs. oxide content
(The values are taken from histograms of Fig. 86-87)

⊙ Su Engineering maximum tensile stress
⊡ $S_{0.2}$ " 0.2 offset yield "
+ e_{pb} " plastic strain at breaking point
Specimen Fig 4 Bars ∅ ≫ 16 mm

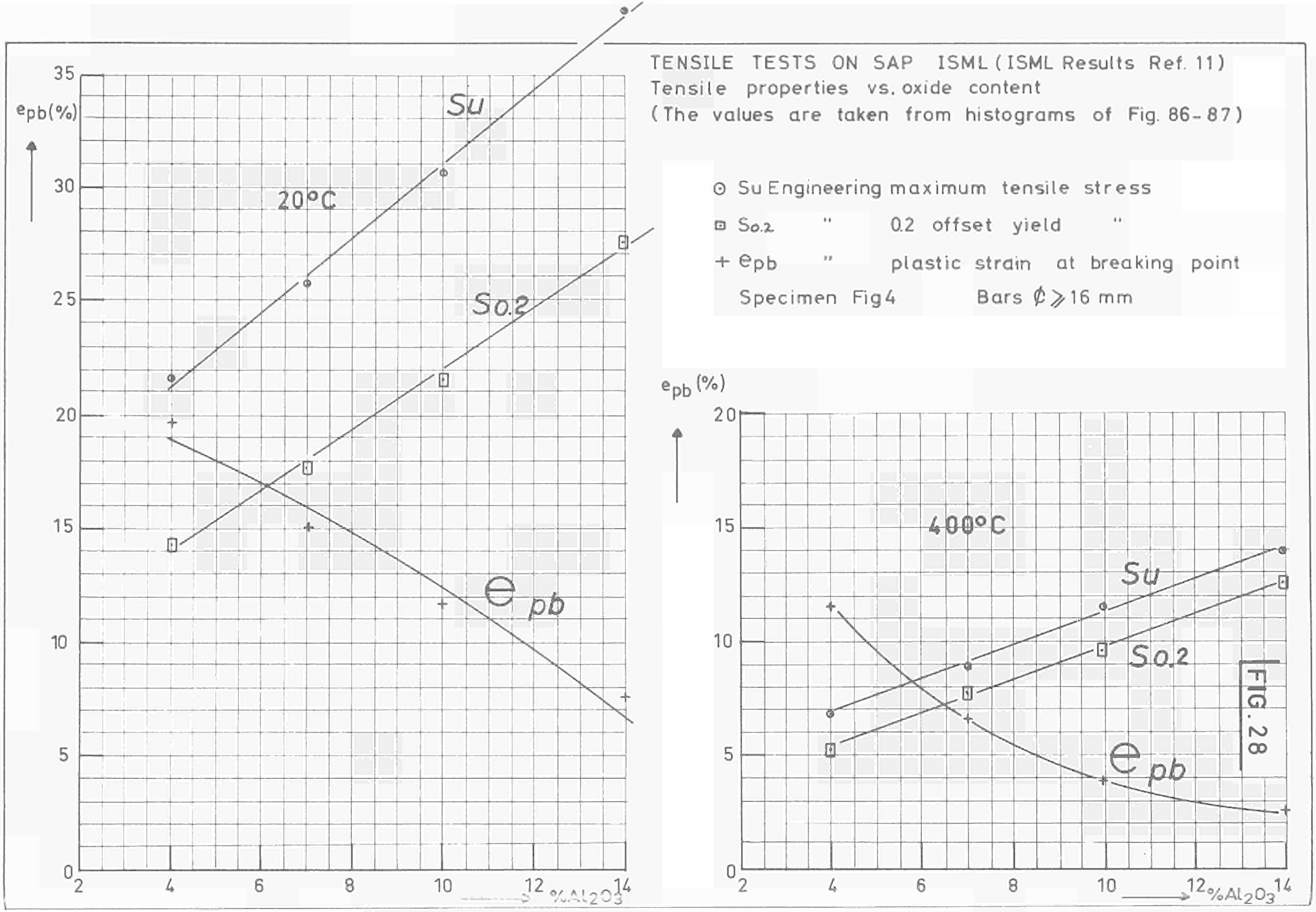

FIG. 28

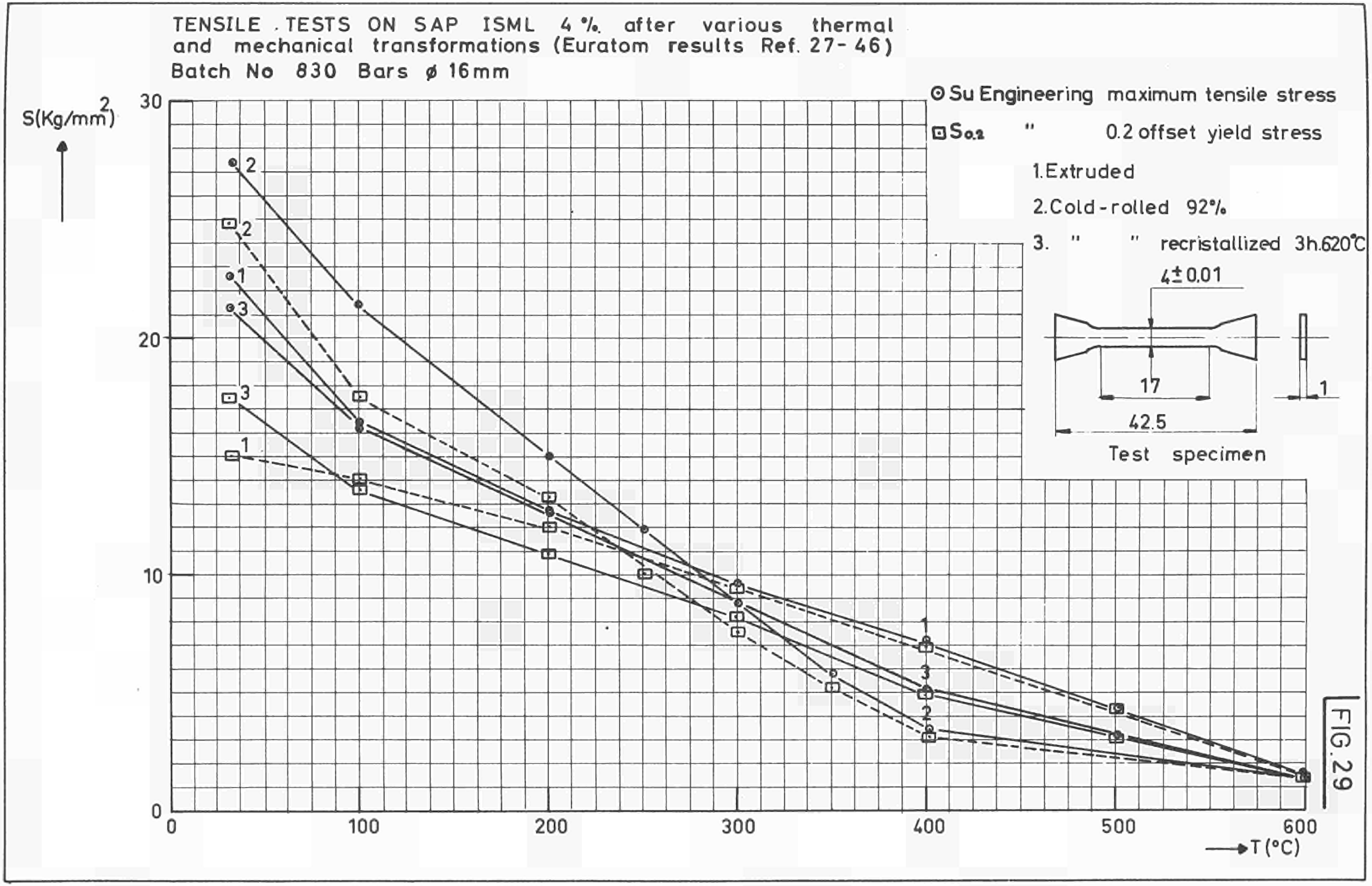
TENSILE . TESTS ON SAP ISML 4 %. after various thermal and mechanical transformations (Euratom results Ref. 27- 46)
Batch No 830 Bars ø 16mm
S(Kg/mm²)
30
20
10
0
0
100
200
300
400
500
600
T (°C)
⊙ Su Engineering maximum tensile stress
⊡ S0.2 " 0.2 offset yield stress
1.Extruded
2.Cold-rolled 92%
3. " " recristallized 3h.620°C
4±0.01
17
1
42.5
Test specimen

FIG. 29

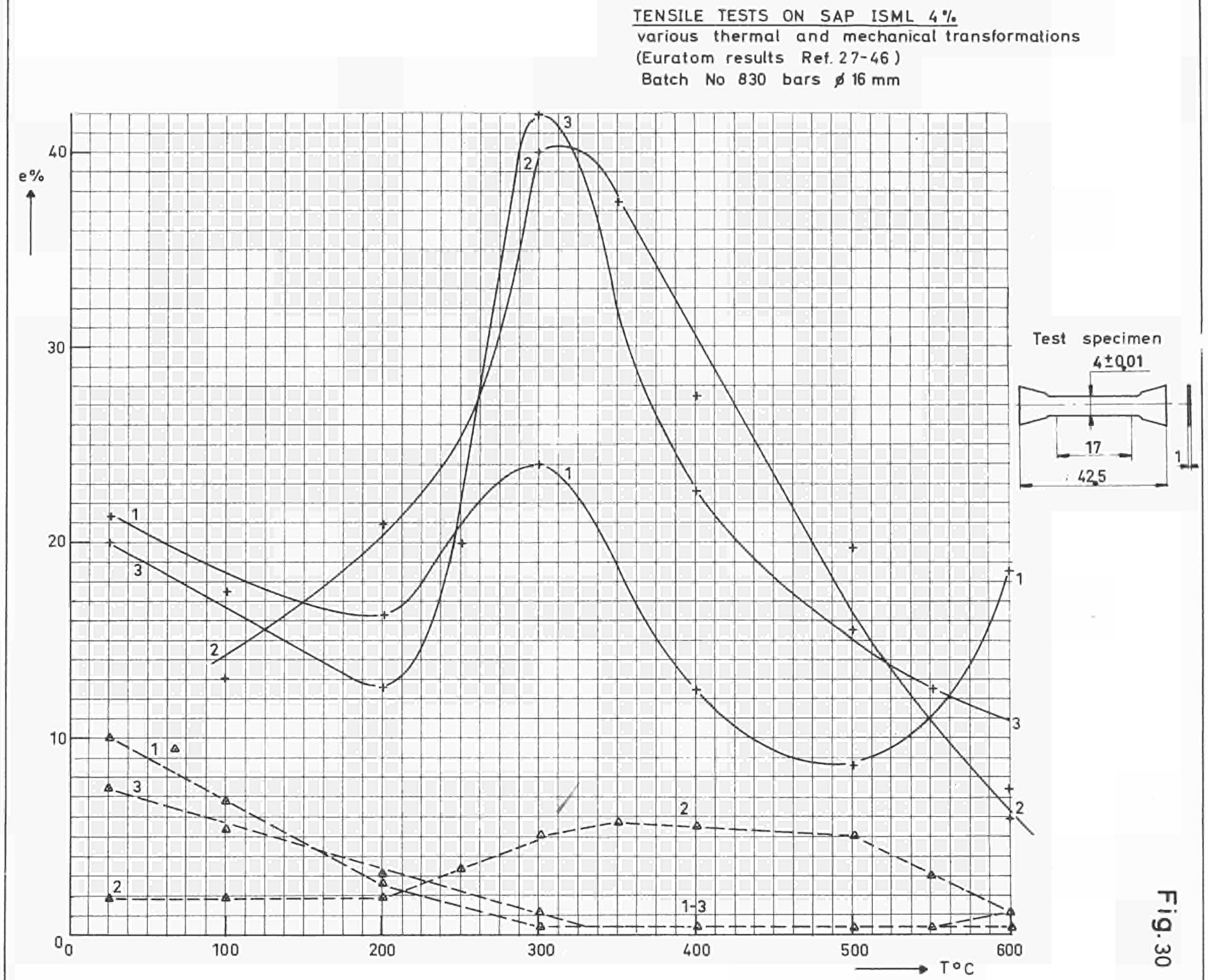
TENSILE TESTS ON SAP ISML 4%
various thermal and mechanical transformations
(Euratom results Ref. 27-46)
Batch No 830 bars ø 16 mm
e%
T°C
Test specimen
4±0.01
17
42.5
0
10
20
30
40
100
200
300
400
500
600
1-3

Fig.30

AECL TENSILE SPECIMEN Ref. 33

(Gauge length = 3.9 X diameter)

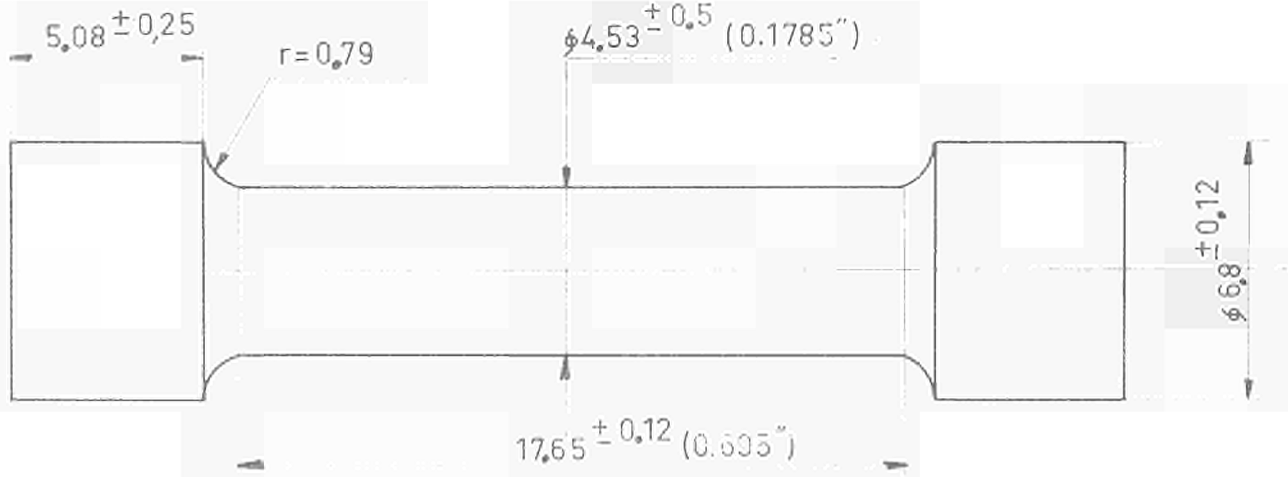

FIG.31

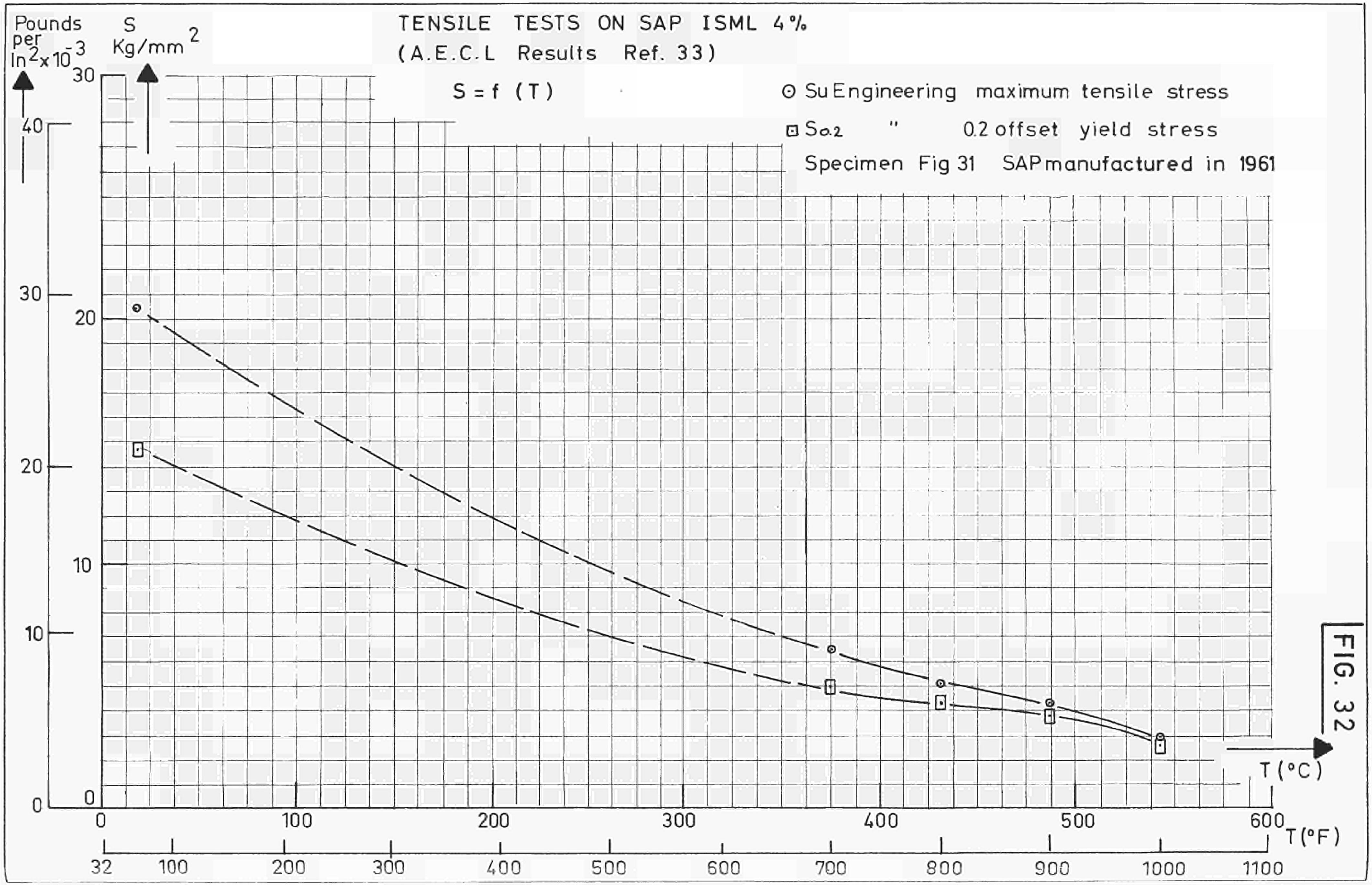

TENSILE TESTS ON SAP ISML 4%
(A.E.C.L Results Ref. 33)
S = f (T)
Su Engineering maximum tensile stress
So.2 " 0.2 offset yield stress
Specimen Fig 31 SAP manufactured in 1961
Pounds per In2 x 10-3
S Kg/mm2
0
10
20
30
40
0
10
20
30
0
100
200
300
400
500
600
T (°C)
32
100
200
300
400
500
600
700
800
900
1000
1100
T (°F)

FIG. 32

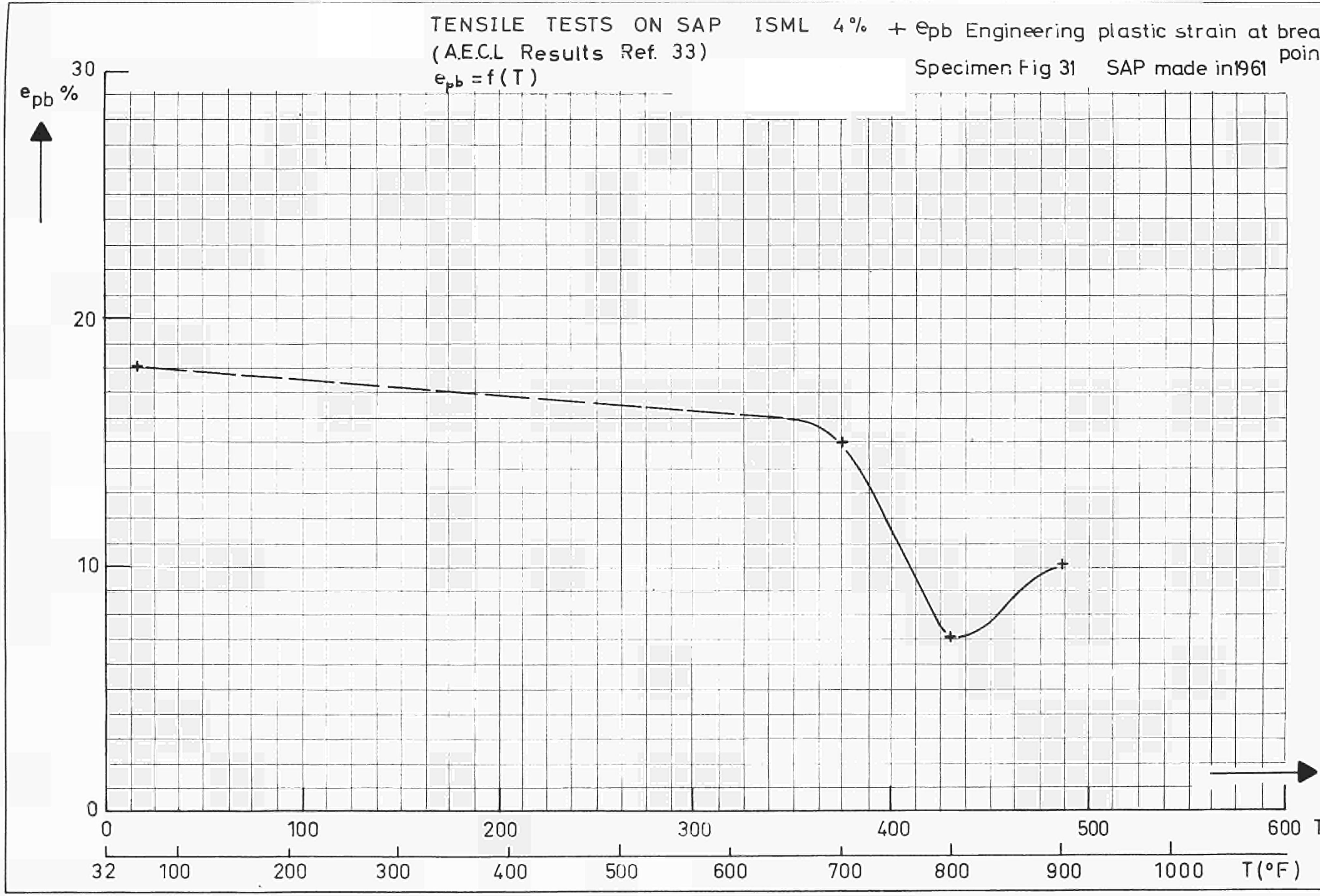

TENSILE TESTS ON SAP ISML 4%
(A.E.C.L Results Ref. 33)
$e_{pb} = f(T)$
+ e_{pb} Engineering plastic strain at breaking point
Specimen Fig 31
SAP made in 1961
e_{pb} %
30
20
10
0
0
100
200
300
400
500
600
T(°C)
32
100
200
300
400
500
600
700
800
900
1000
T(°F)

FIG. 33

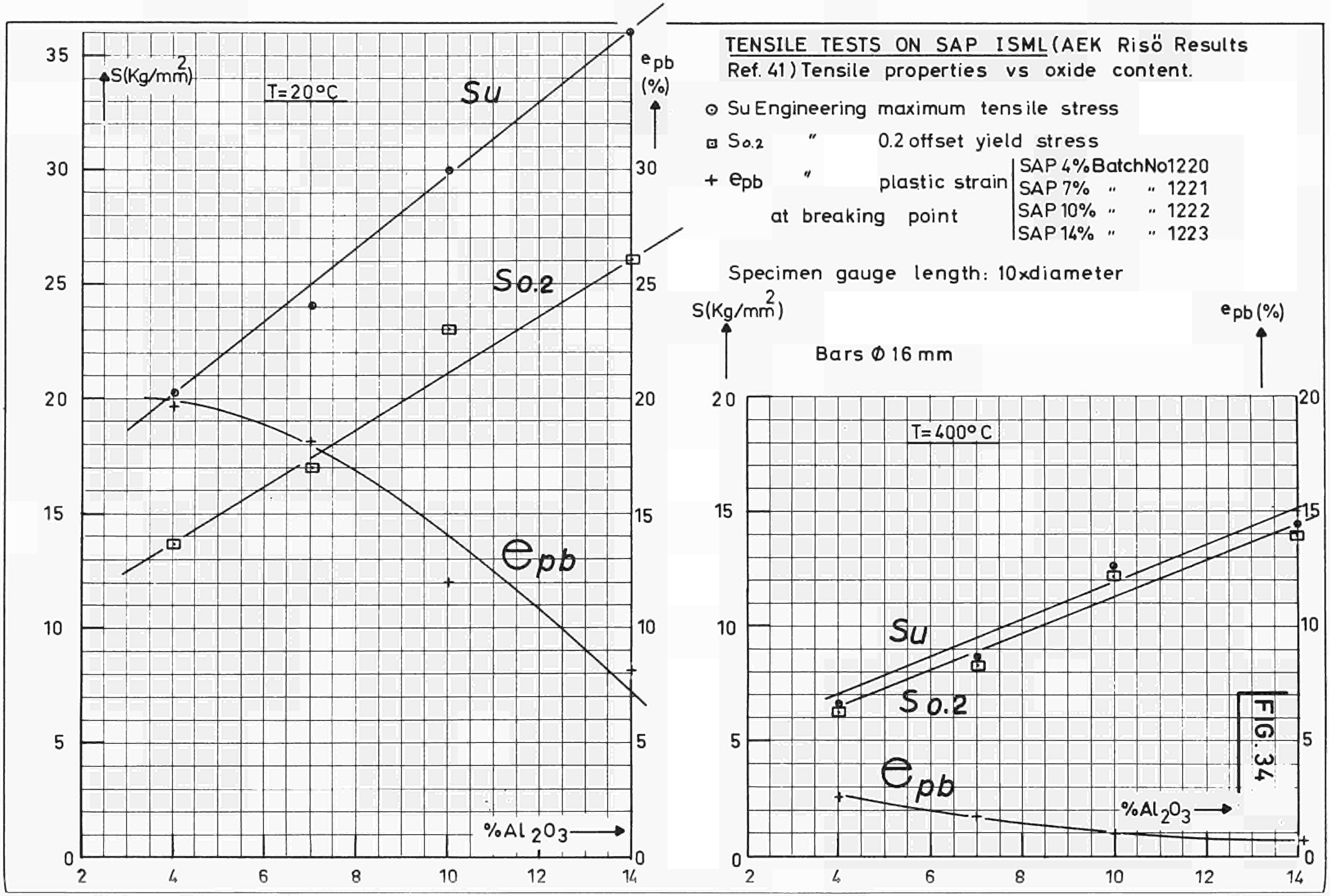
TENSILE TESTS ON SAP ISML (AEK Risö Results
Ref. 41) Tensile properties vs oxide content.
⊙ Su Engineering maximum tensile stress
⊡ So.2 " 0.2 offset yield stress
+ epb " plastic strain at breaking point
SAP 4% Batch No 1220
SAP 7% " " 1221
SAP 10% " " 1222
SAP 14% " " 1223
Specimen gauge length: 10×diameter
Bars Ø 16 mm
S(Kg/mm2)
epb (%)
T=20°C
T=400°C
Su
So.2
epb
%Al2O3

FIG. 34

Fig. 35

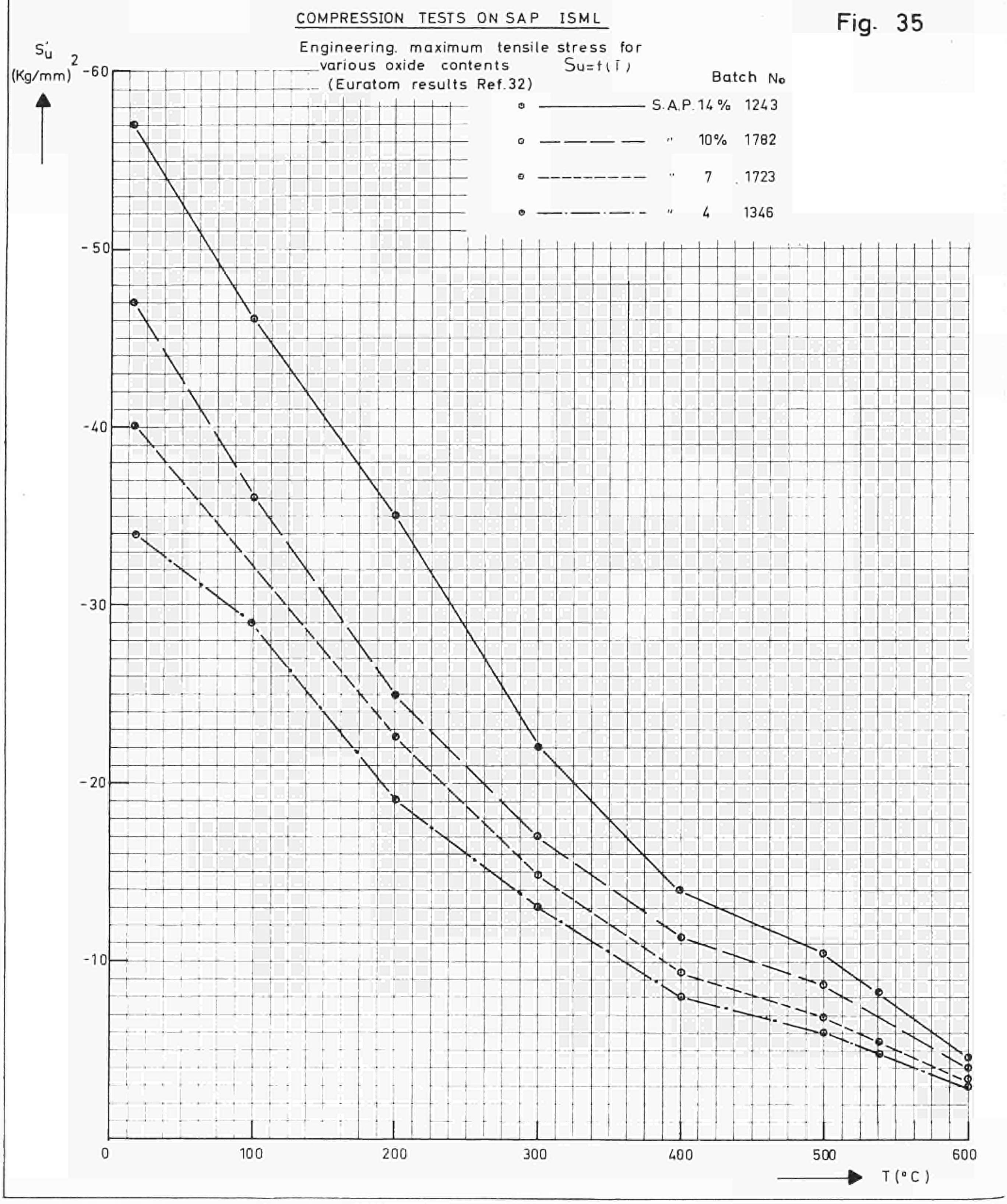

COMPRESSION TESTS ON SAP ISML
Engineering. maximum tensile stress for
various oxide contents Su=f(T)
(Euratom results Ref.32)
Batch No
S.A.P. 14 % 1243
" 10% 1782
" 7 1723
" 4 1346
S'u (Kg/mm)2
-60
-50
-40
-30
-20
-10
0
100
200
300
400
500
600
T (°C)

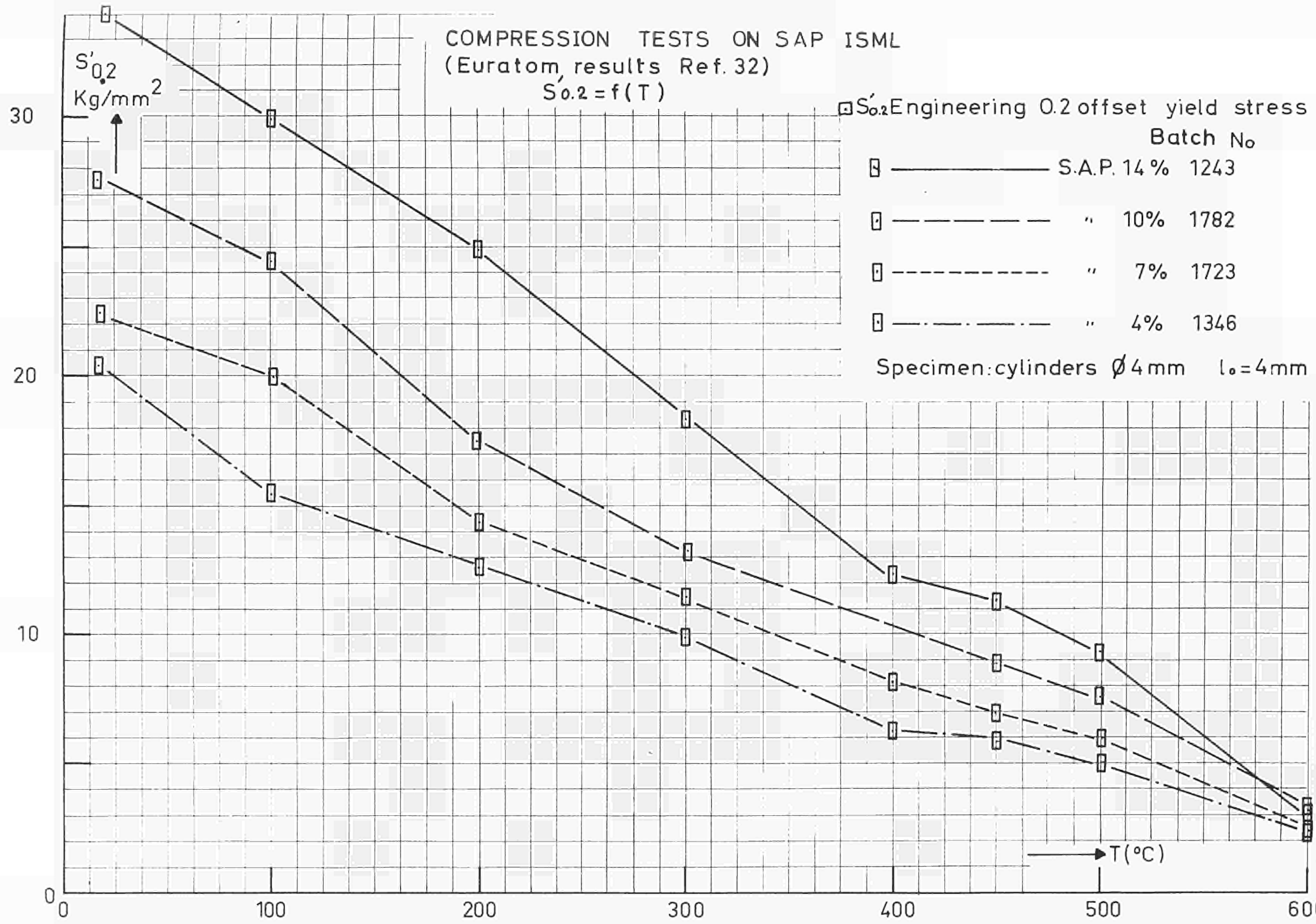
COMPRESSION TESTS ON SAP ISML
(Euratom results Ref. 32)
S'0.2 = f(T)
S'0.2 Kg/mm2
S'0.2 Engineering 0.2 offset yield stress
Batch No
S.A.P. 14 % 1243
" 10% 1782
" 7% 1723
" 4% 1346
Specimen: cylinders Ø 4 mm l0 = 4 mm
T(°C)
0
10
20
30
0
100
200
300
400
500
600

FIG. 36

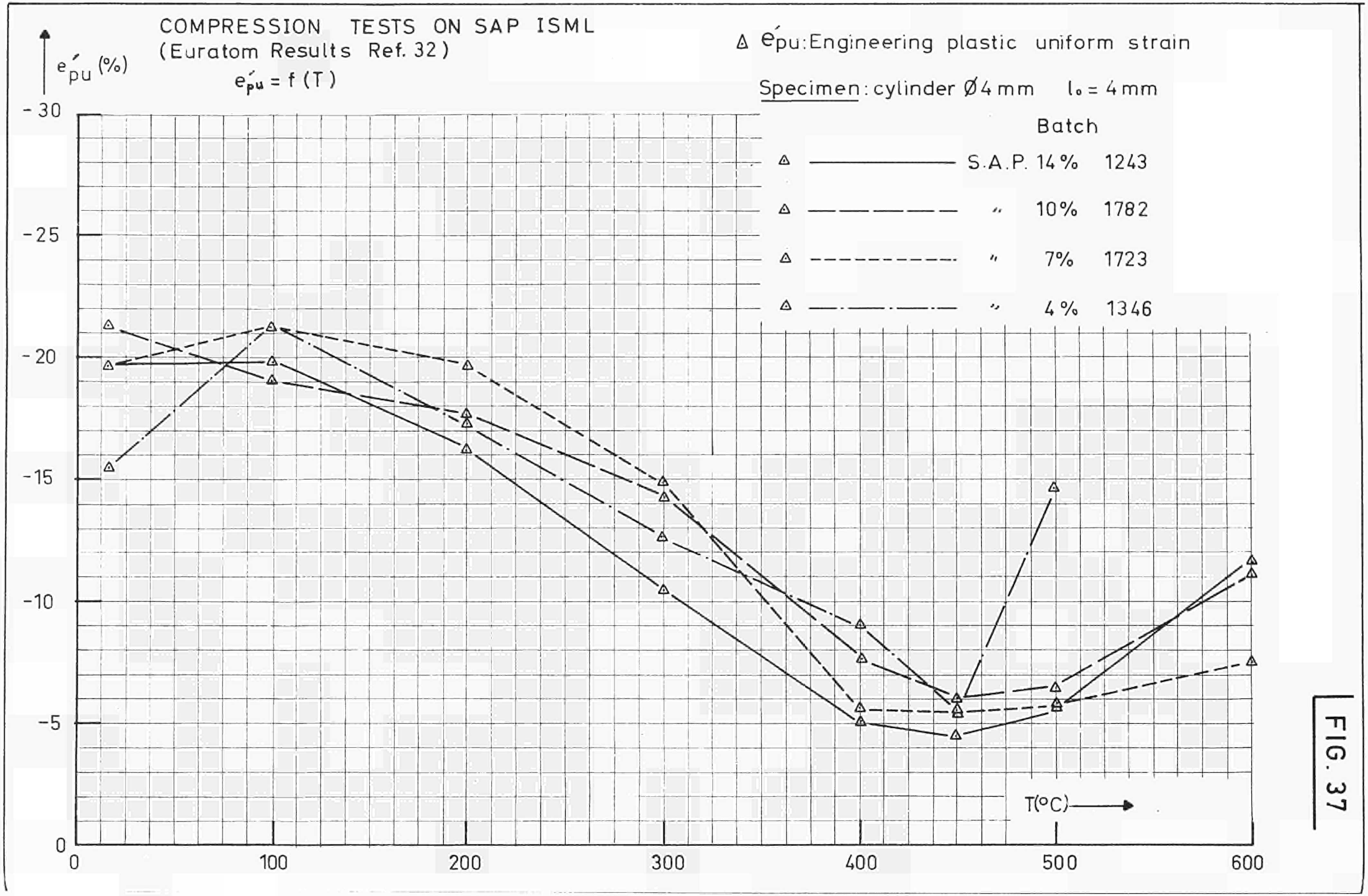

COMPRESSION TESTS ON SAP ISML
(Euratom Results Ref. 32)
$e'_{pu} = f(T)$
e'_{pu} (%)
Δ e'_{pu}: Engineering plastic uniform strain
Specimen: cylinder Ø4 mm l_0 = 4 mm
Batch
S.A.P. 14% 1243
" 10% 1782
" 7% 1723
" 4% 1346
T(°C)
-30
-25
-20
-15
-10
-5
0
100
200
300
400
500
600

FIG. 37

EURATOM CREEP SPECIMEN (FL 2)

Fig. 38

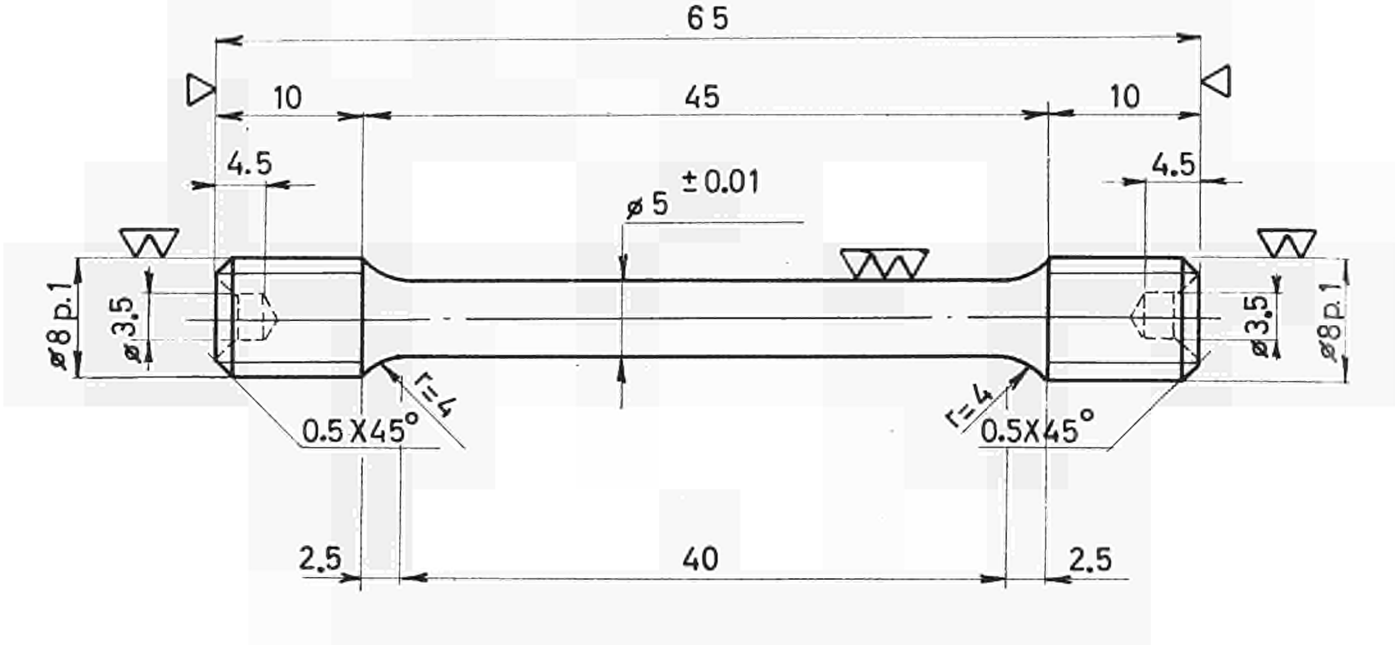

ISML CREEP SPECIMEN (Ref. 9)

Fig. 39

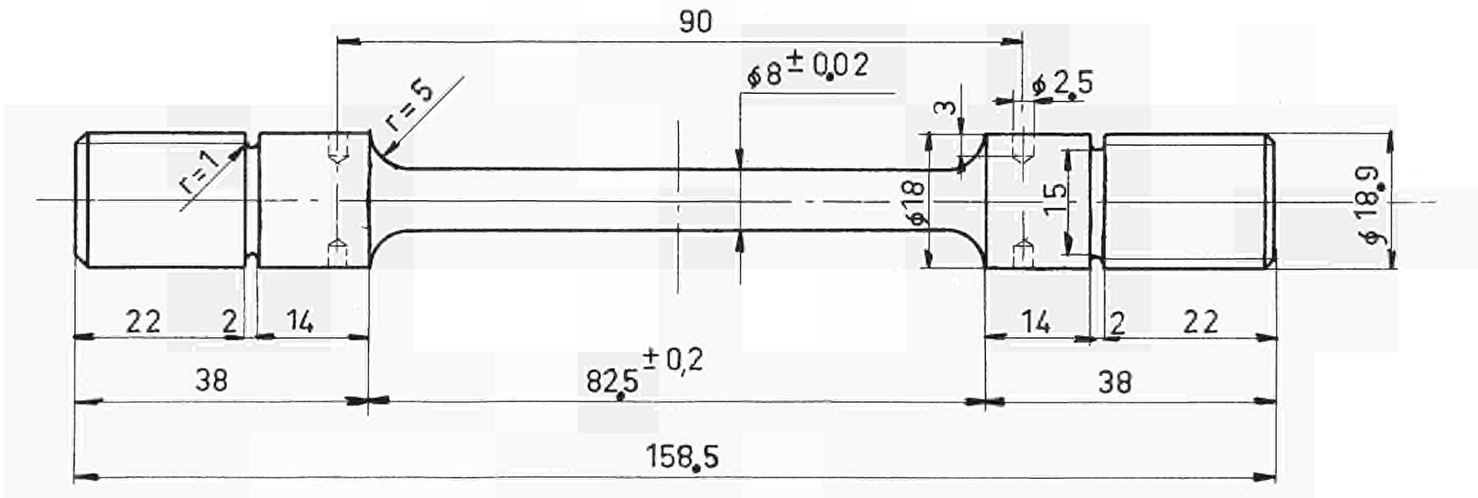

STRESS RUPTURE TESTS AT 400°C AND 460°C ON SAP ISML 4 %
(Euratom and ISML Results)

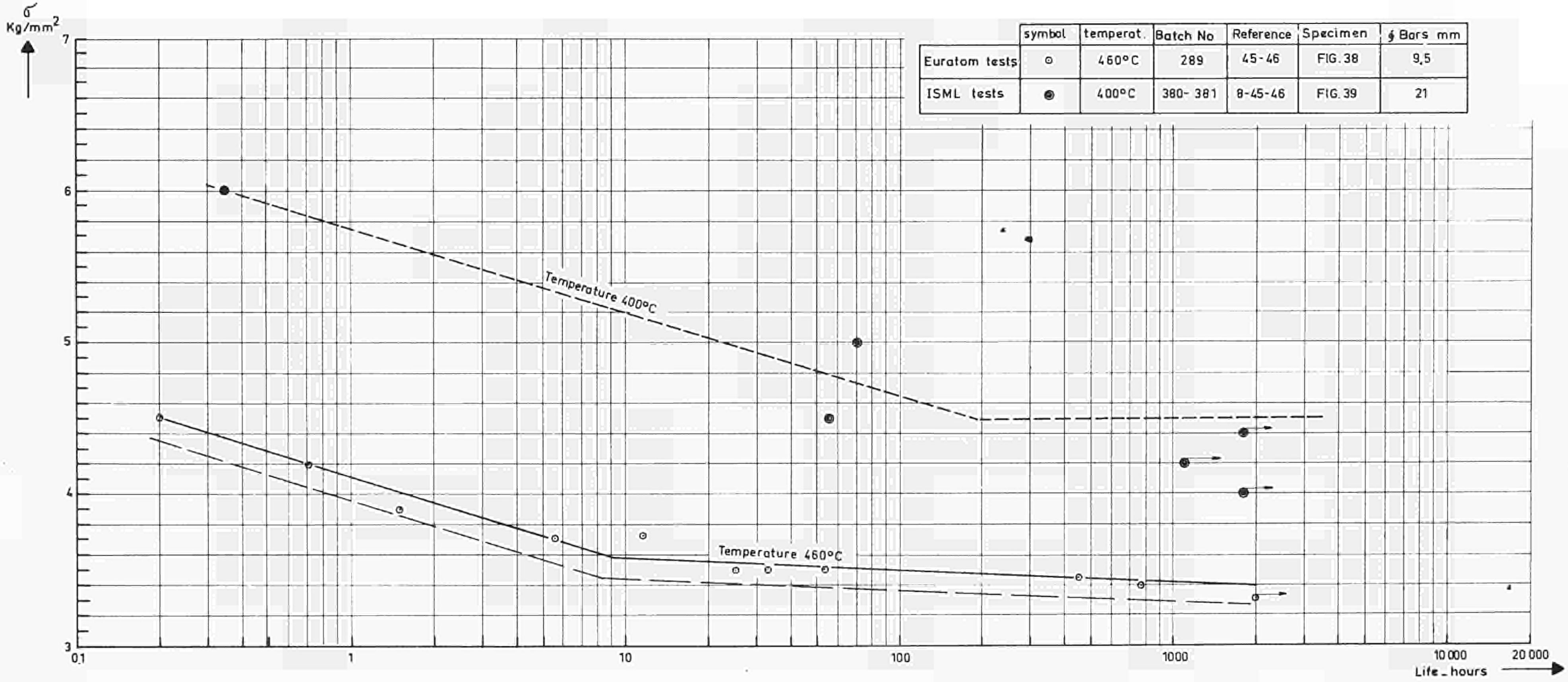

	symbol	temperat.	Batch No	Reference	Specimen	∅ Bars mm
Euratom tests	⊙	460°C	289	45-46	FIG. 38	9,5
ISML tests	◉	400°C	380-381	8-45-46	FIG. 39	21

Fig. 40

STRESS-RUPTURE TESTS on SAP ISML 7% at 400°C and 460°C
(Euratom and ISML results)

	symbol	temperat.	Batch No	REFERENCE	Specimen	ϕ BARS (mm)
Euratom tests	•	460°C	275	45-46	FIG. 38	9,5
ISML tests	●	400°C	393-394	8-45-46	FIG. 39	21

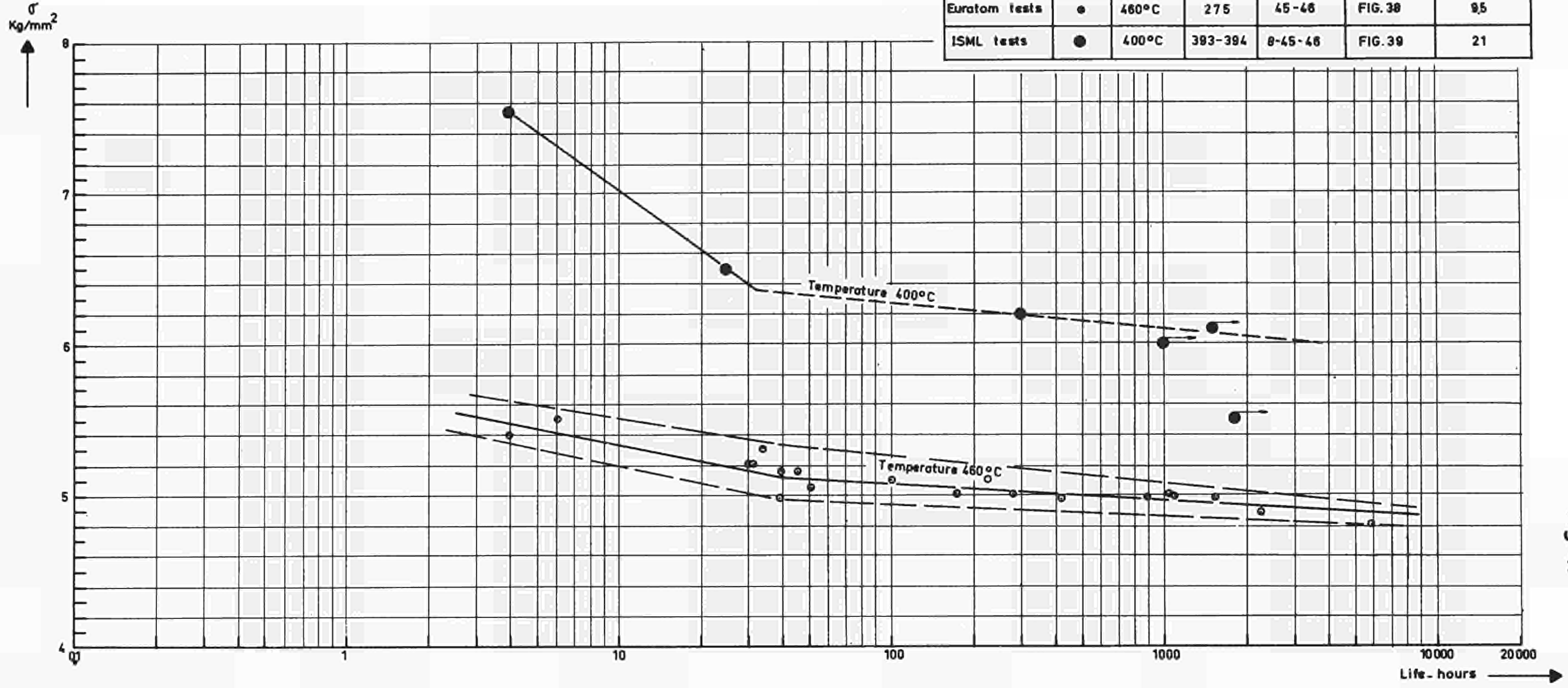

Fig. 41

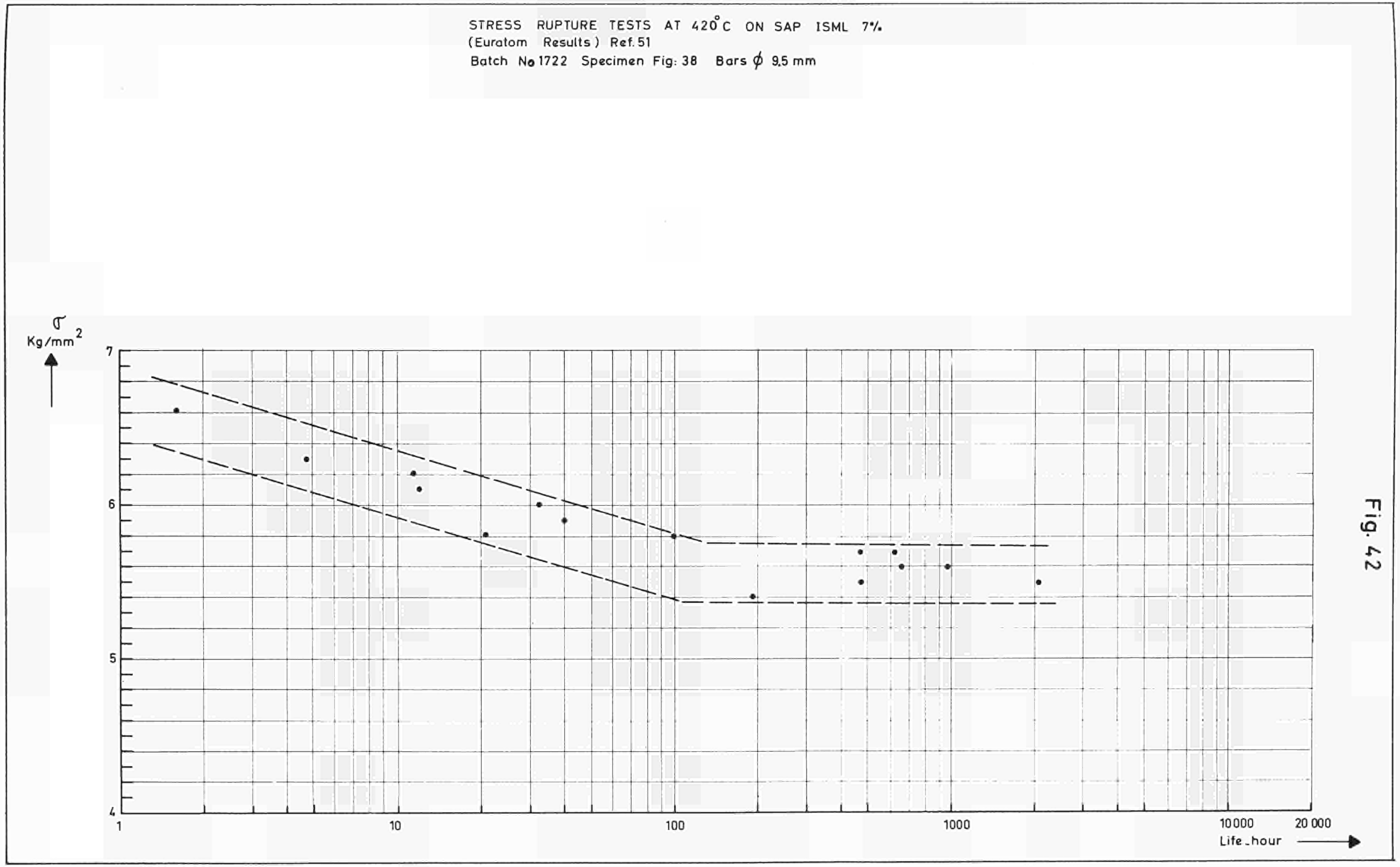

STRESS RUPTURE TESTS AT 420°C ON SAP ISML 7%
(Euratom Results) Ref. 51
Batch No 1722 Specimen Fig: 38 Bars ϕ 9,5 mm
σ
Kg/mm²
7
6
5
4
1
10
100
1000
10000
20 000
Life _ hour

Fig. 42

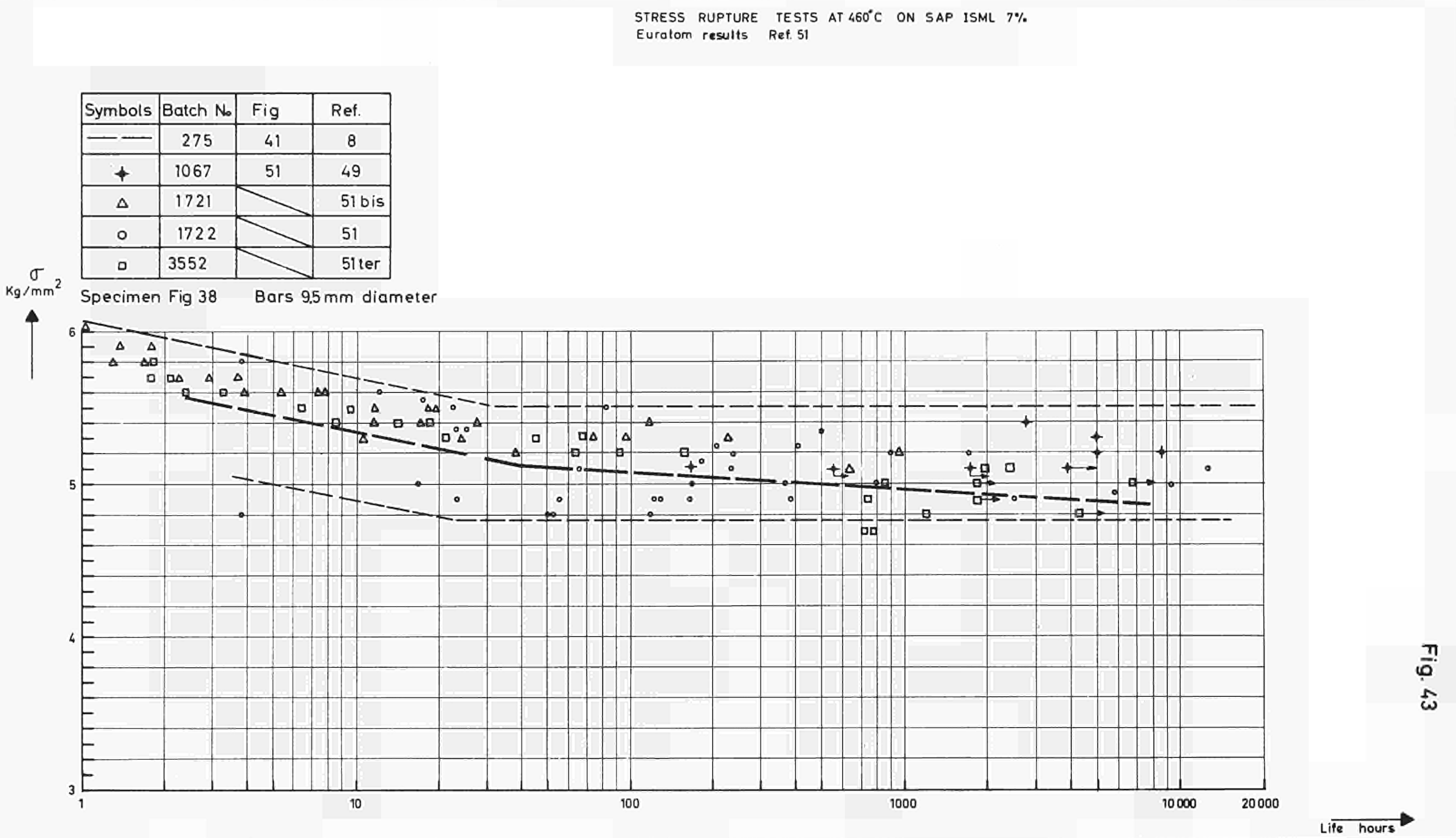

Symbols	Batch No	Fig	Ref.
— —	275	41	8
✦	1067	51	49
△	1721		51 bis
○	1722		51
□	3552		51 ter

Fig. 43

HISTOGRAMS OF ELONGATIONS DURING CREEP TESTS AT 460°C
ON SAP ISML 7 % (Euratom Results Ref. 51) Specimen Fig. 38
Bars ø 9.5 Batch No 1722

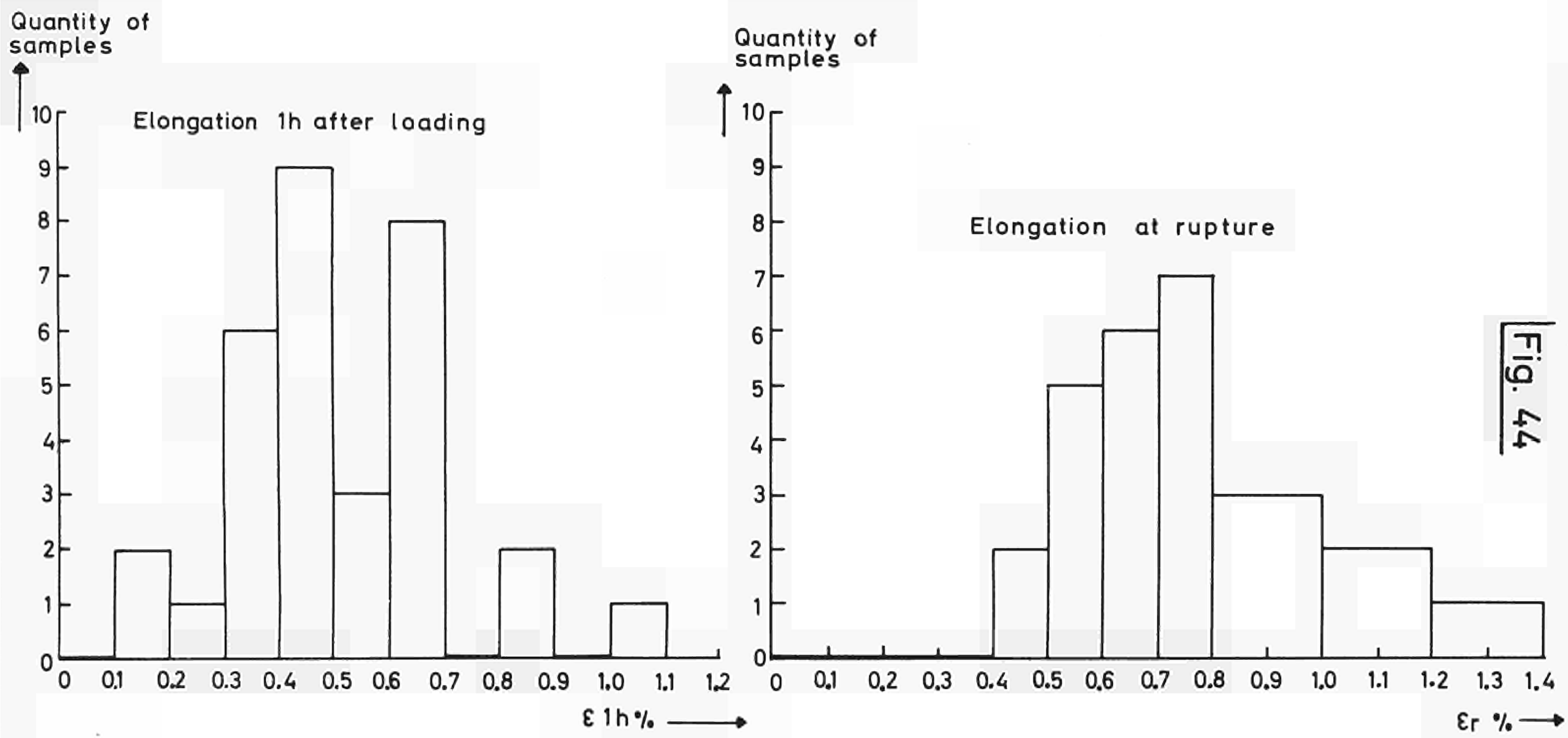

Fig. 44

STRESS RUPTURE TESTS AT 400°C AND 460°C ON SAP ISML 10%
(Euratom and ISML Results)

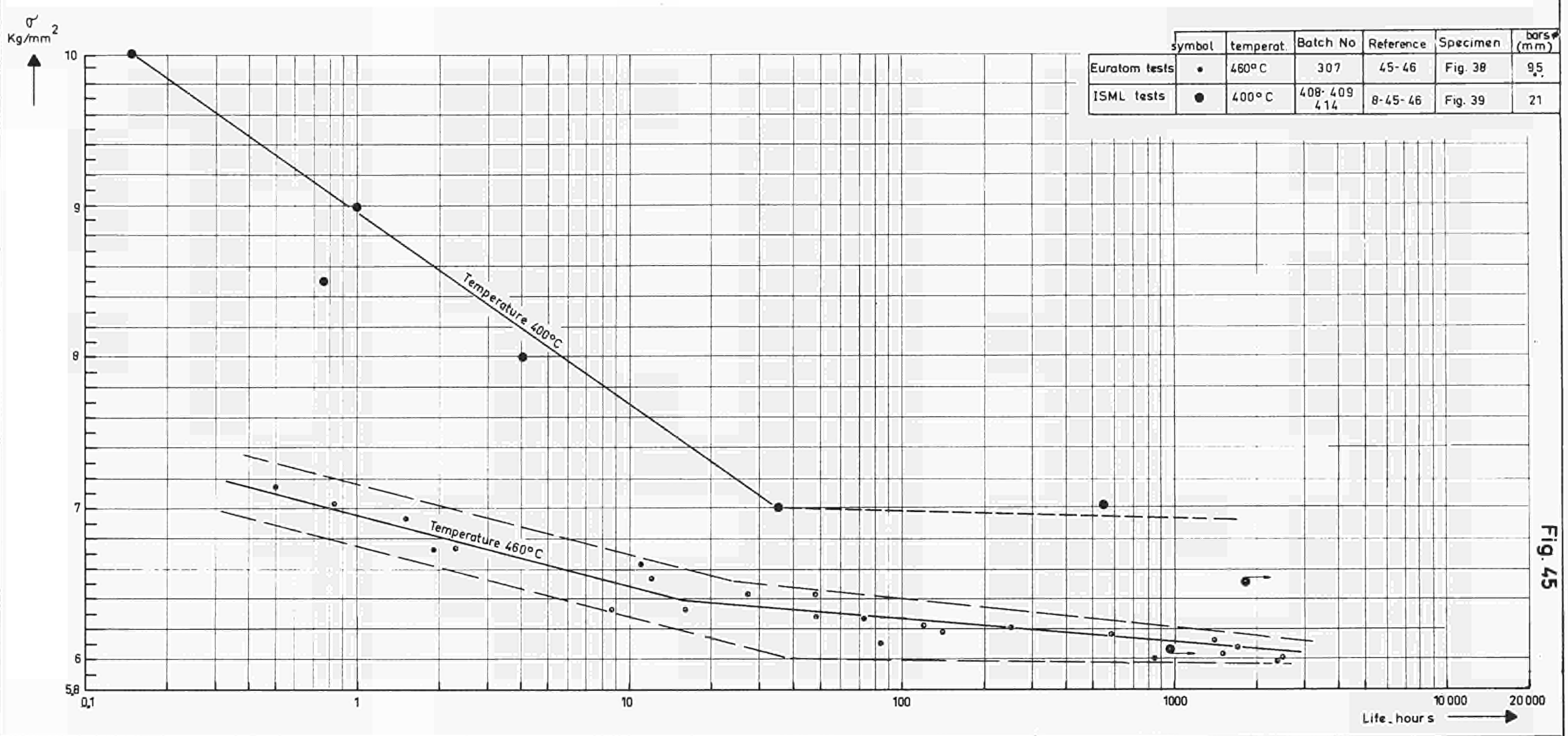

Fig. 45

STRESS RUPTURE TESTS AT 400°C AND 460°C ON SAP ISML 14 %
(Euratom and ISML Results)

	symbol	temperat.	Batch No	Reference	Specimen	bar ø (mm)
Euratom tests	•	460° C	313-314/1	46	Fig. 38	9,5
ISML tests	◎	400° C	415	8-46	Fig. 39	21

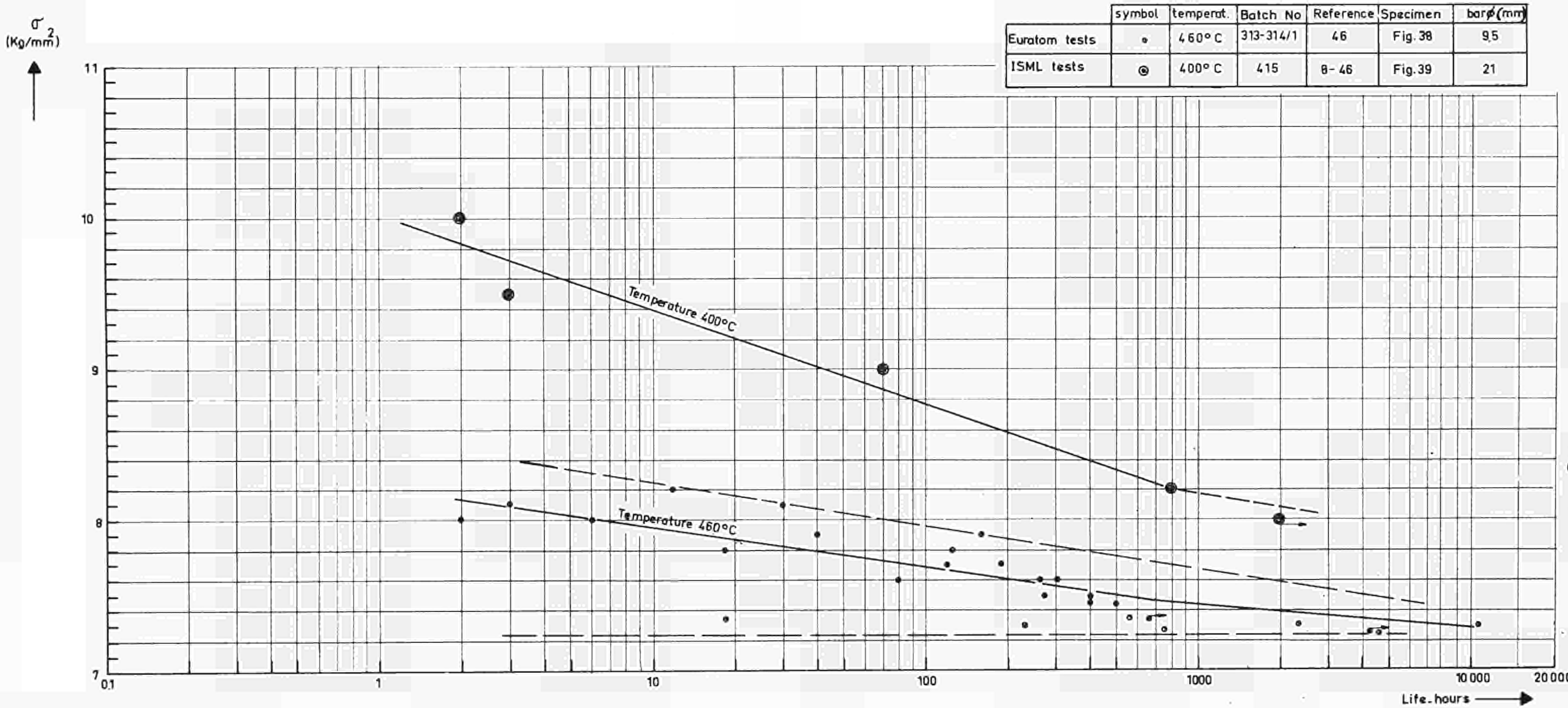

Fig. 46

STRESS RUPTURE TESTS ON SAP 7 %
(Euratom results)
Influence of temperature

Symbol	Batch No	Test temp.	from fig	ref.	∅bars (mm)
solid line	393-394	400	41	8-45-46	21
hatched (/)	1722	420	42	51	9,5
hatched (\)	1067-1722-3552	460	43	51 51bis 51ter	9,5
heavy dashed line	275	460	41	45-46	9,5

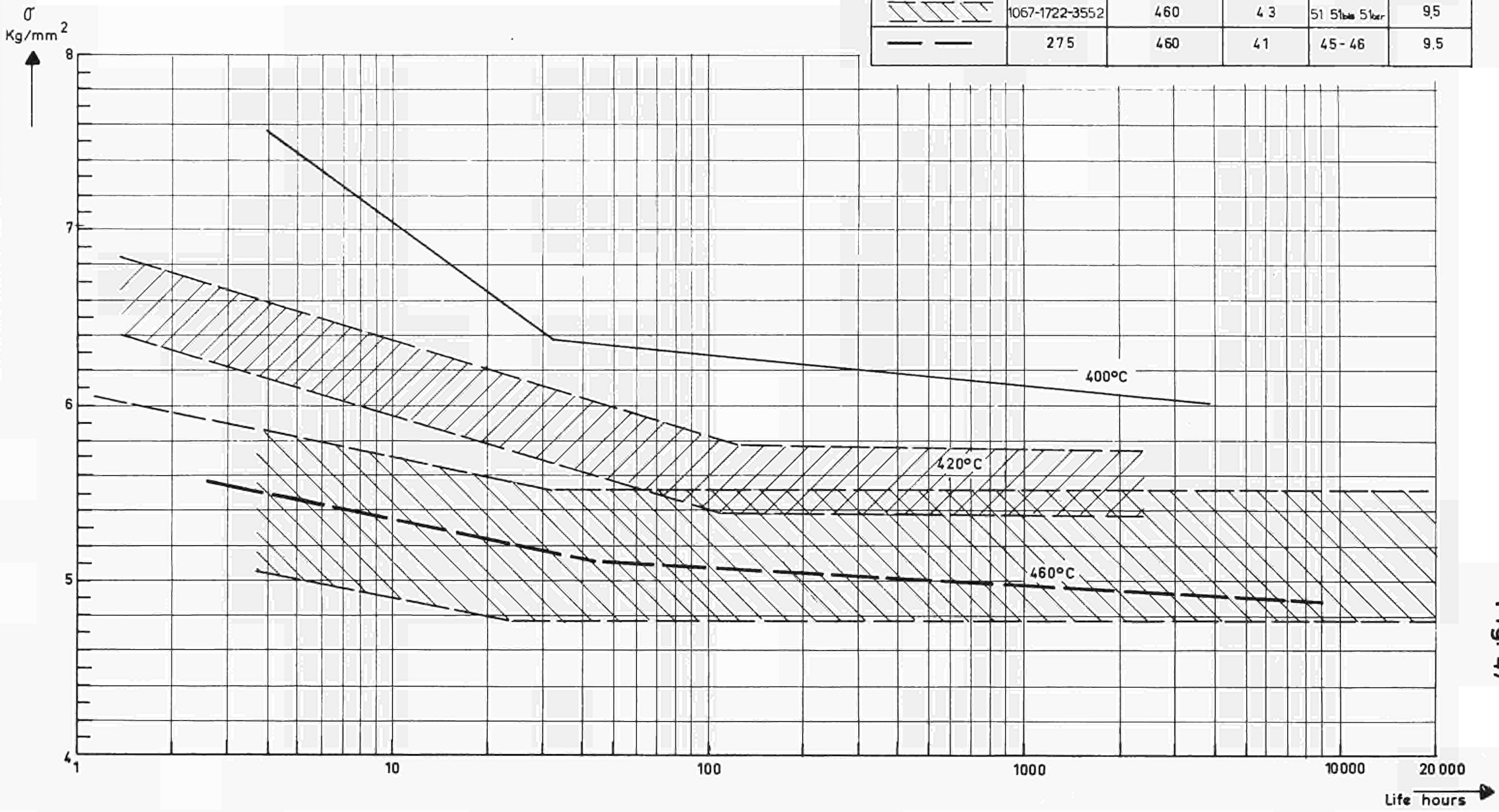

Fig. 47

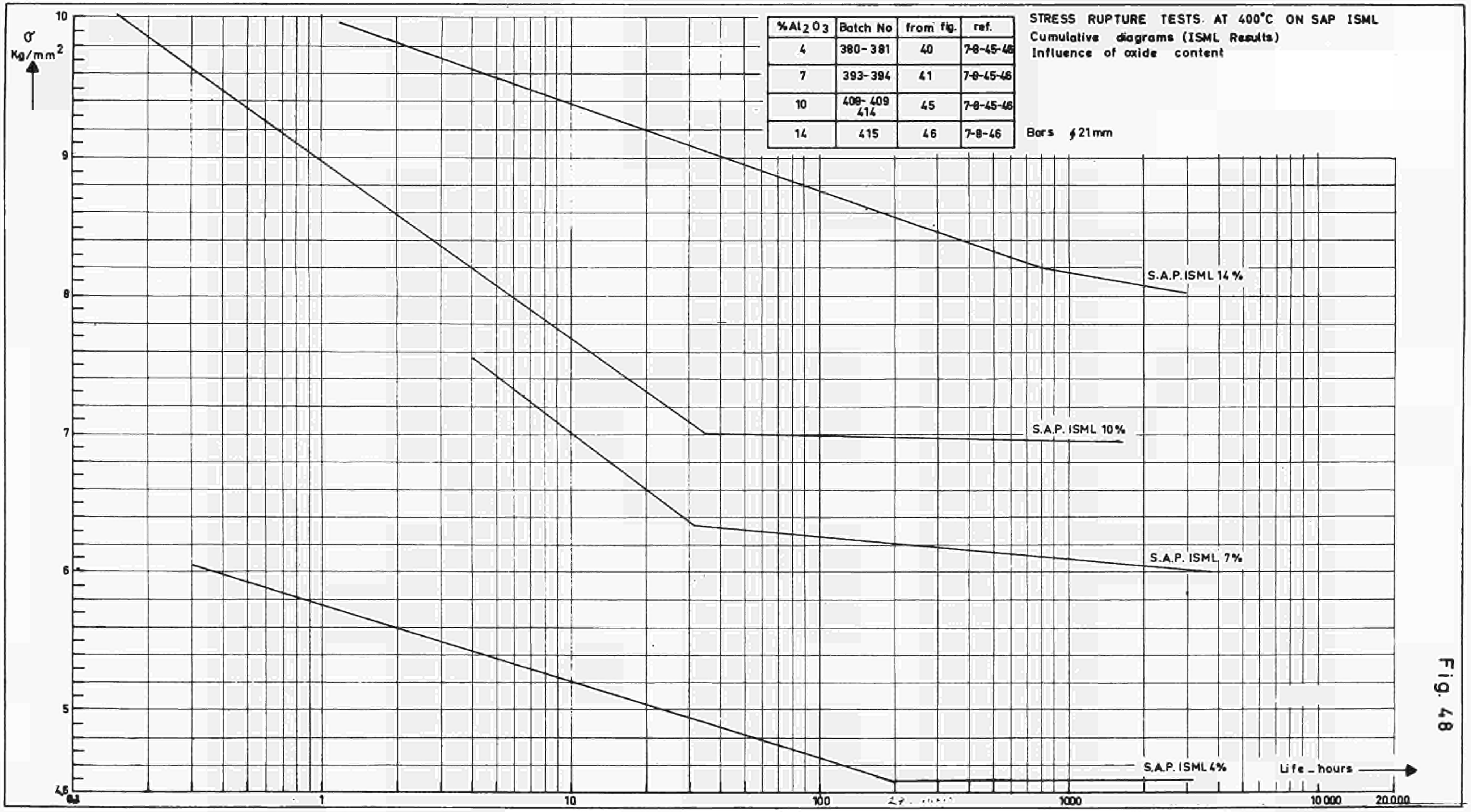

% Al_2O_3	Batch No	from fig.	ref.
4	380-381	40	7-8-45-46
7	393-394	41	7-8-45-46
10	408-409 414	45	7-8-45-46
14	415	46	7-8-46

Fig. 48

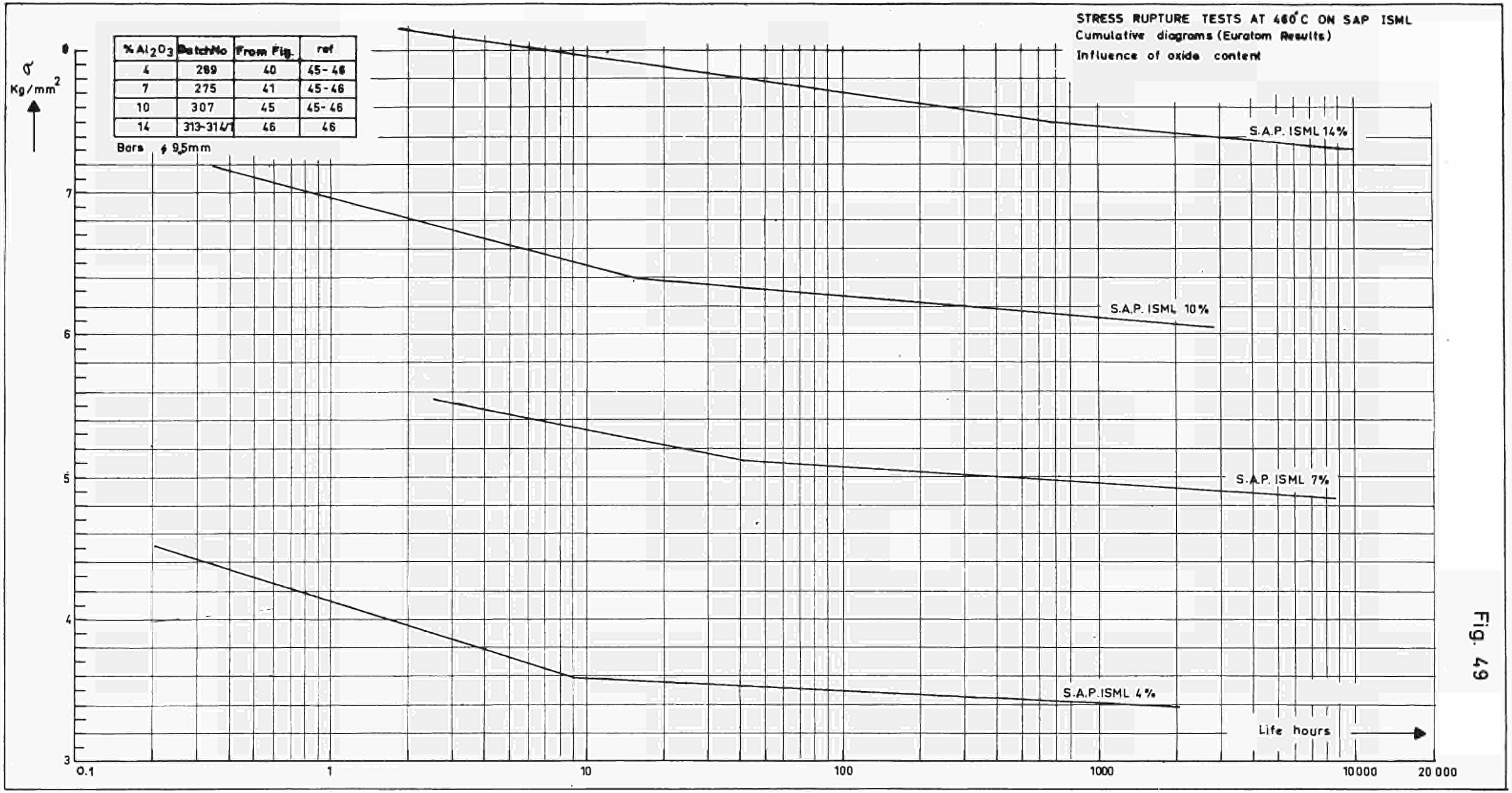
STRESS RUPTURE TESTS AT 460°C ON SAP ISML
Cumulative diagrams (Euratom Results)
Influence of oxide content
% Al2O3 | Batch No | From Fig. | ref
4 | 289 | 40 | 45-46
7 | 275 | 41 | 45-46
10 | 307 | 45 | 45-46
14 | 313-314/T | 46 | 46
Bars ϕ 9,5mm
σ Kg/mm2
S.A.P. ISML 14%
S.A.P. ISML 10%
S.A.P. ISML 7%
S.A.P. ISML 4%
Life hours
8
7
6
5
4
3
0.1
1
10
100
1000
10000
20 000

Fig. 49

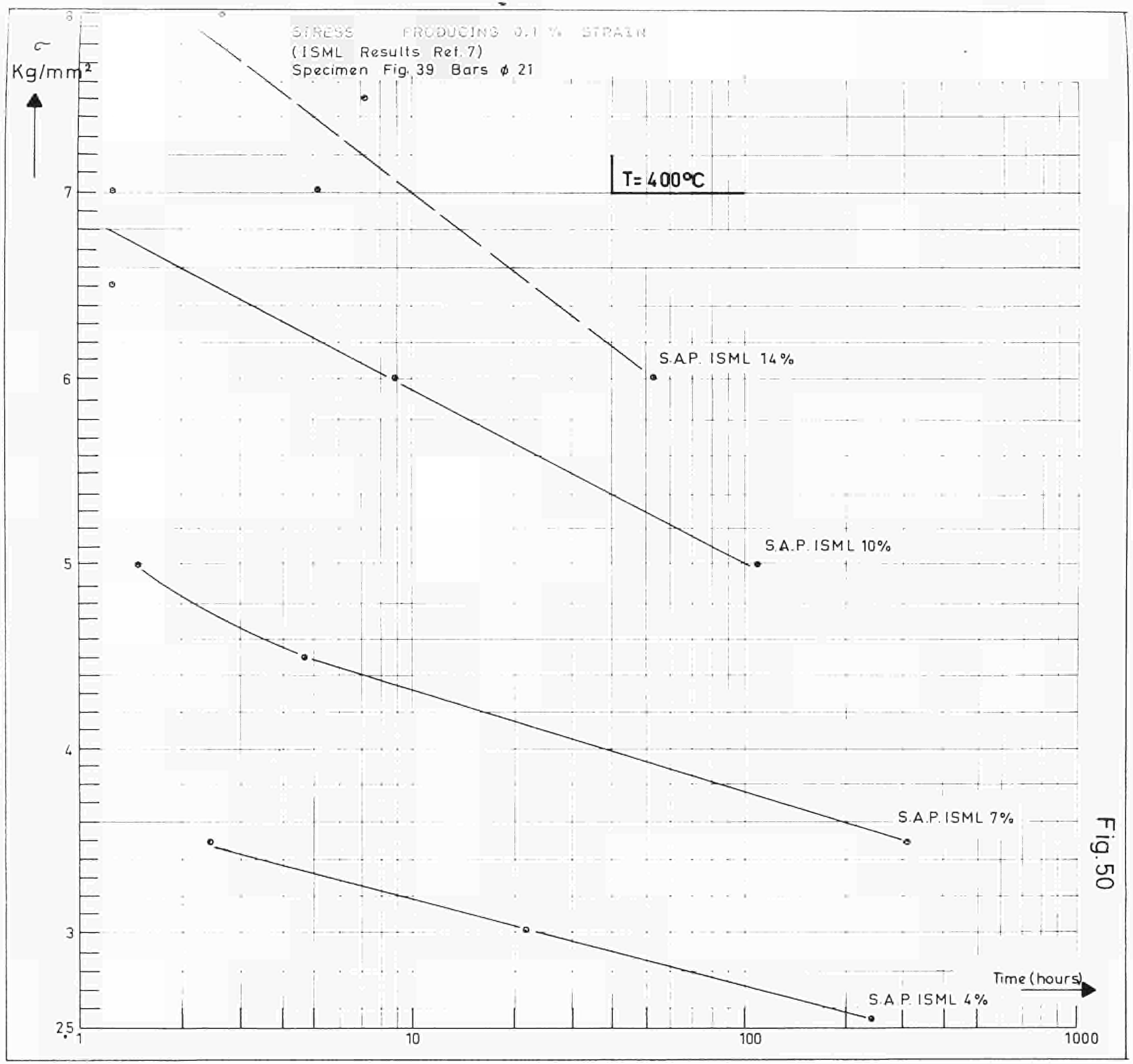

STRESS PRODUCING 0.1 % STRAIN
(ISML Results Ref. 7)
Specimen Fig. 39 Bars ϕ 21
σ Kg/mm²
T= 400°C
S.A.P. ISML 14%
S.A.P. ISML 10%
S.A.P. ISML 7%
S.A.P. ISML 4%
Time (hours)
8
7
6
5
4
3
2.5
1
10
100
1000

Fig. 50

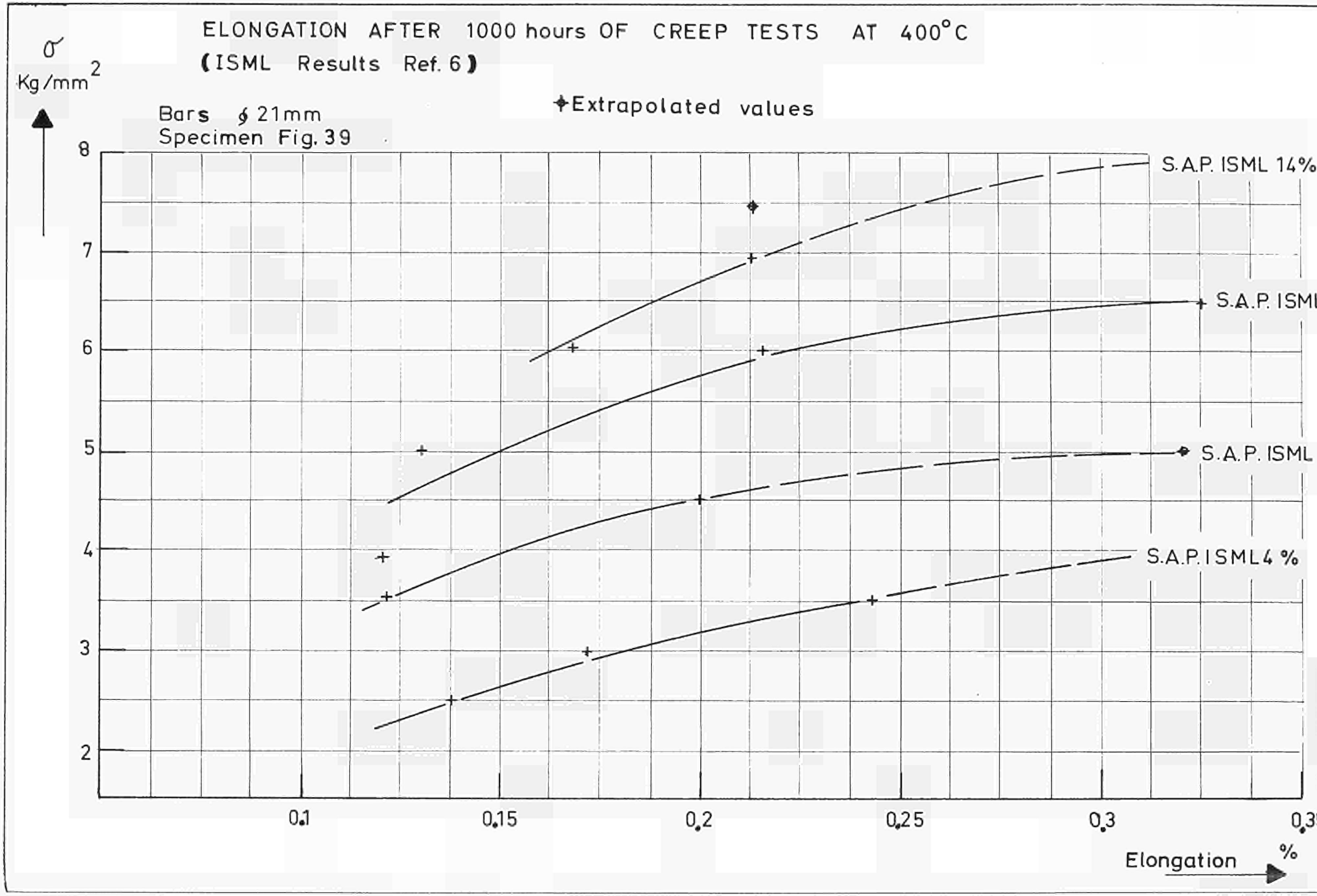
ELONGATION AFTER 1000 hours OF CREEP TESTS AT 400°C
(ISML Results Ref. 6)
σ
Kg/mm2
+ Extrapolated values
Bars ∅ 21mm
Specimen Fig. 39
8
7
6
5
4
3
2
0,1
0,15
0,2
0,25
0,3
0,35
S.A.P. ISML 14%
S.A.P. ISML 10%
S.A.P. ISML 7%
S.A.P. ISML 4%
Elongation
%

FIG. 51

STRESS RUPTURE TESTS AT 460°C ON THERMAL TREATED SAP 4%

(Euratom Results) Ref. 48

Symbol	Thermal treatment	
	Temperature °C	Time (h)
• A	600	23
⊗ B	640	1584
+ C	640	3000
— D	none	none

Specimen Fig. 38 Bars ϕ 95 mm

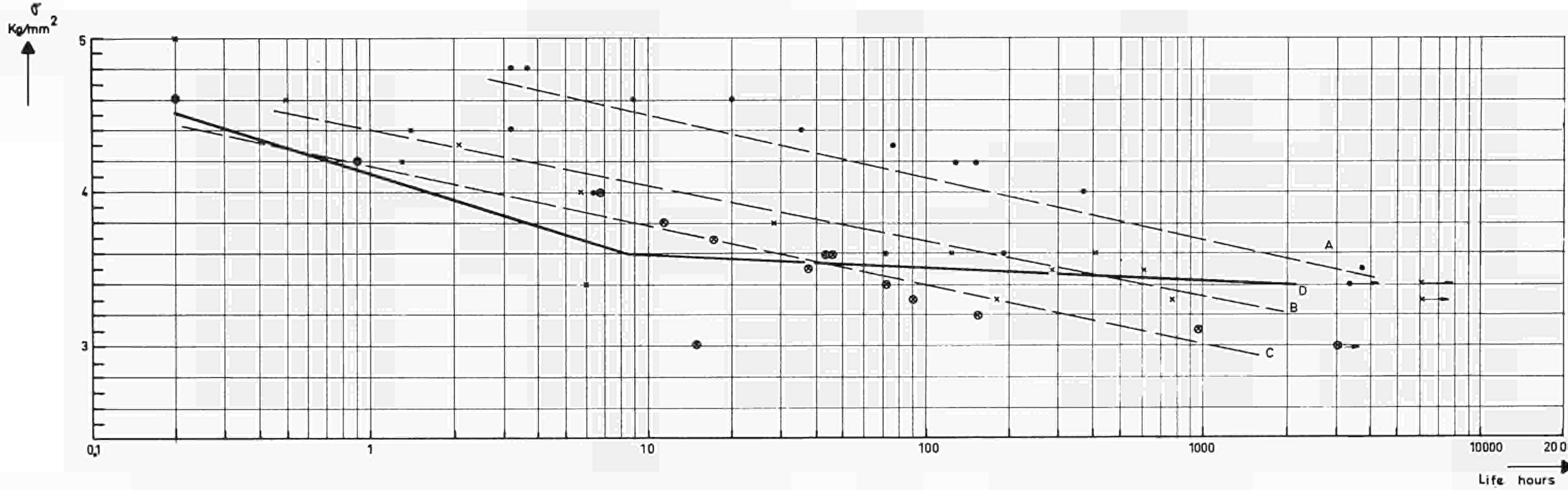

Fig. 52

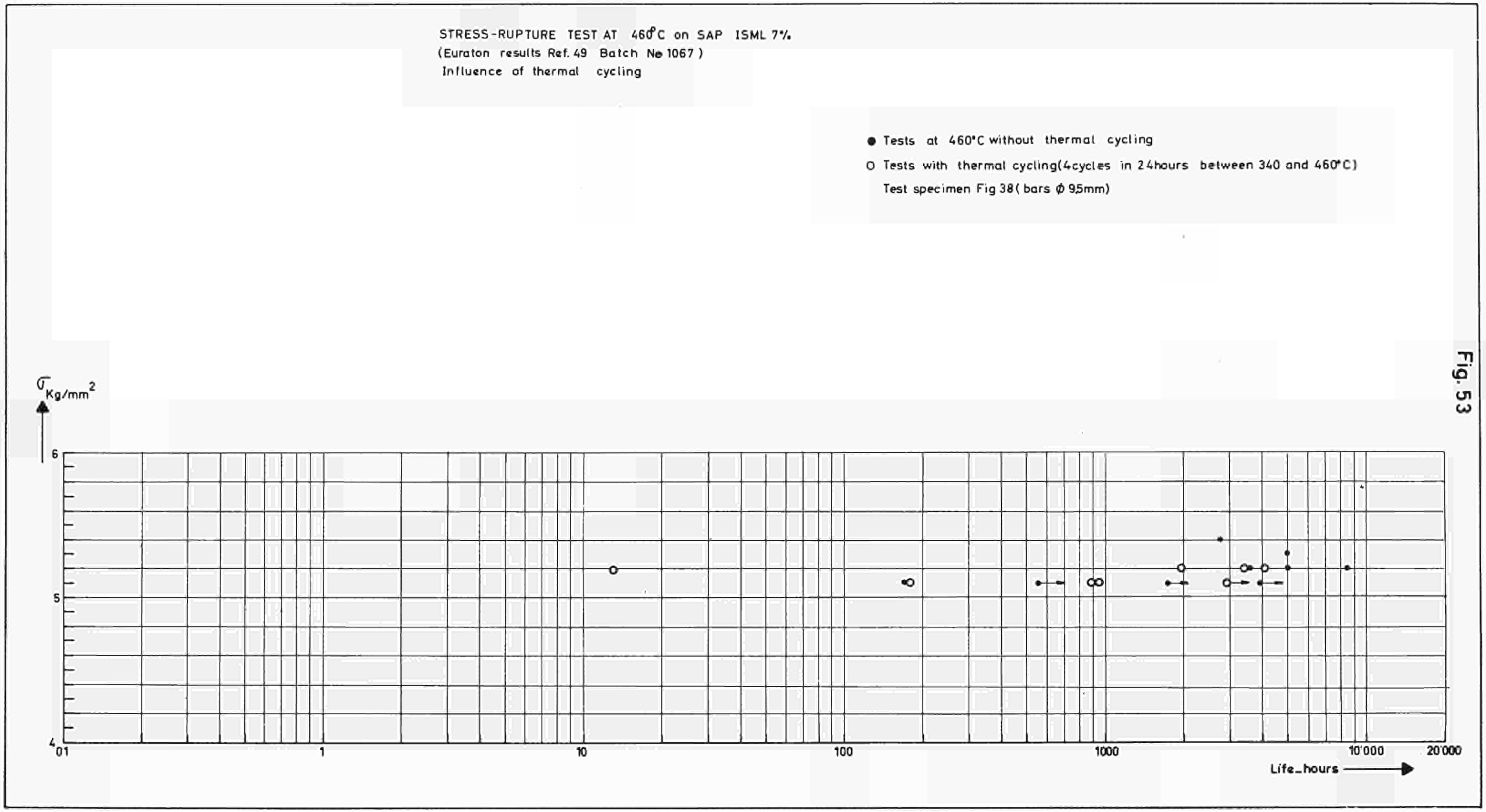
STRESS-RUPTURE TEST AT 460°C on SAP ISML 7%
(Euraton results Ref. 49 Batch No 1067)
Influence of thermal cycling
● Tests at 460°C without thermal cycling
○ Tests with thermal cycling(4cycles in 24hours between 340 and 460°C)
Test specimen Fig 38(bars ϕ 9,5mm)
σ Kg/mm²
6
5
4
01
1
10
100
1000
10'000
20'000
Life_hours

Fig. 53

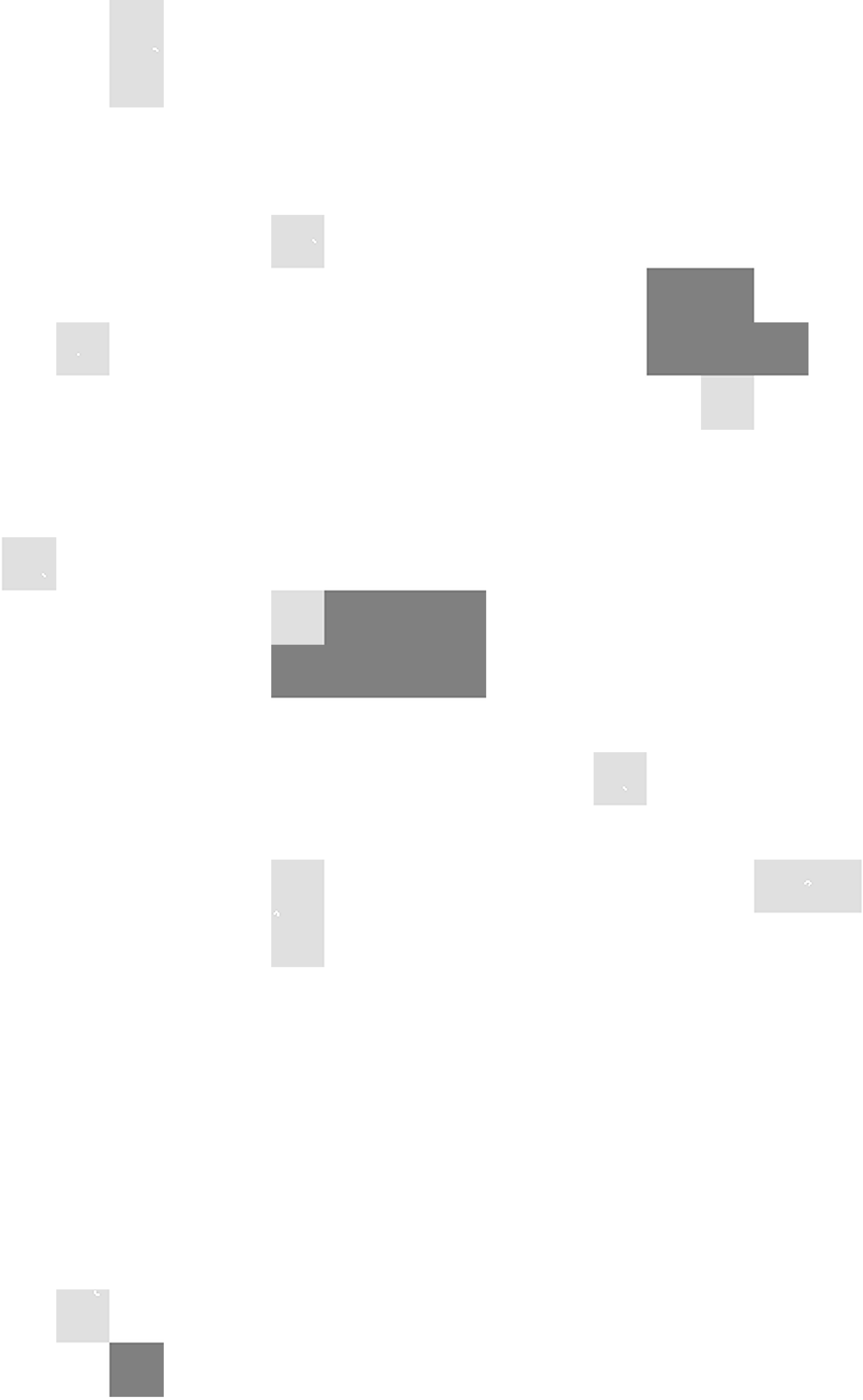

FIG. 54

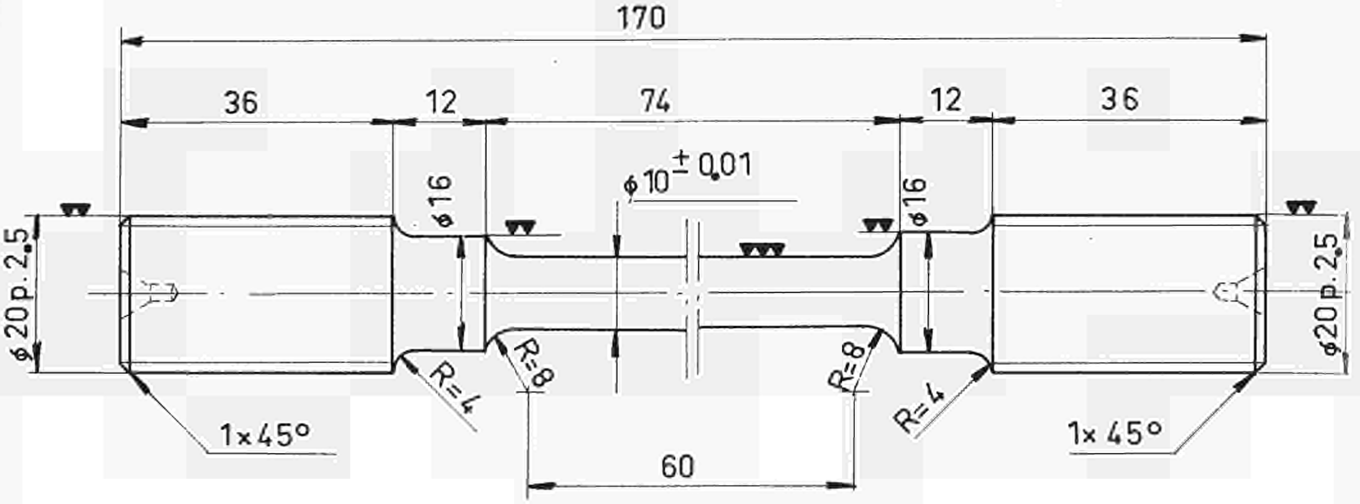

BATTELLE INSTITUTE FRANKFURT CREEP SPECIMEN(FL1)

STRESS RUPTURE TESTS AT 460°C ON SAP ISML 4%
(Battelle Institut Frankfurt Results) Ref. 47

Symbol	Batch N.
●	890
o	645

Specimen Fig 54 Bars ϕ 21 mm

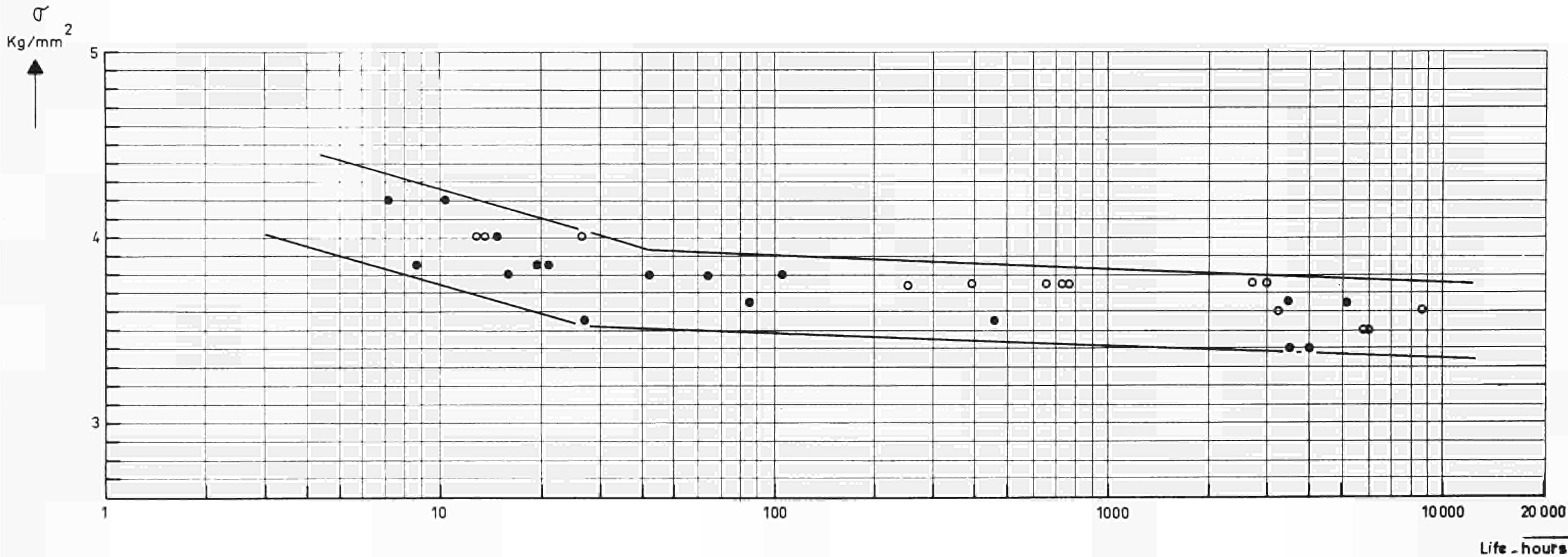

Fig. 55

HISTOGRAMS OF ELONGATIONS DURING CREEP TESTS AT 460 °C ON SAP ISML 4%
(Battelle Institut Frankfurt Results Ref. 47) Specimen Fig. 54 Bars ø 21mm Batch No 645-890

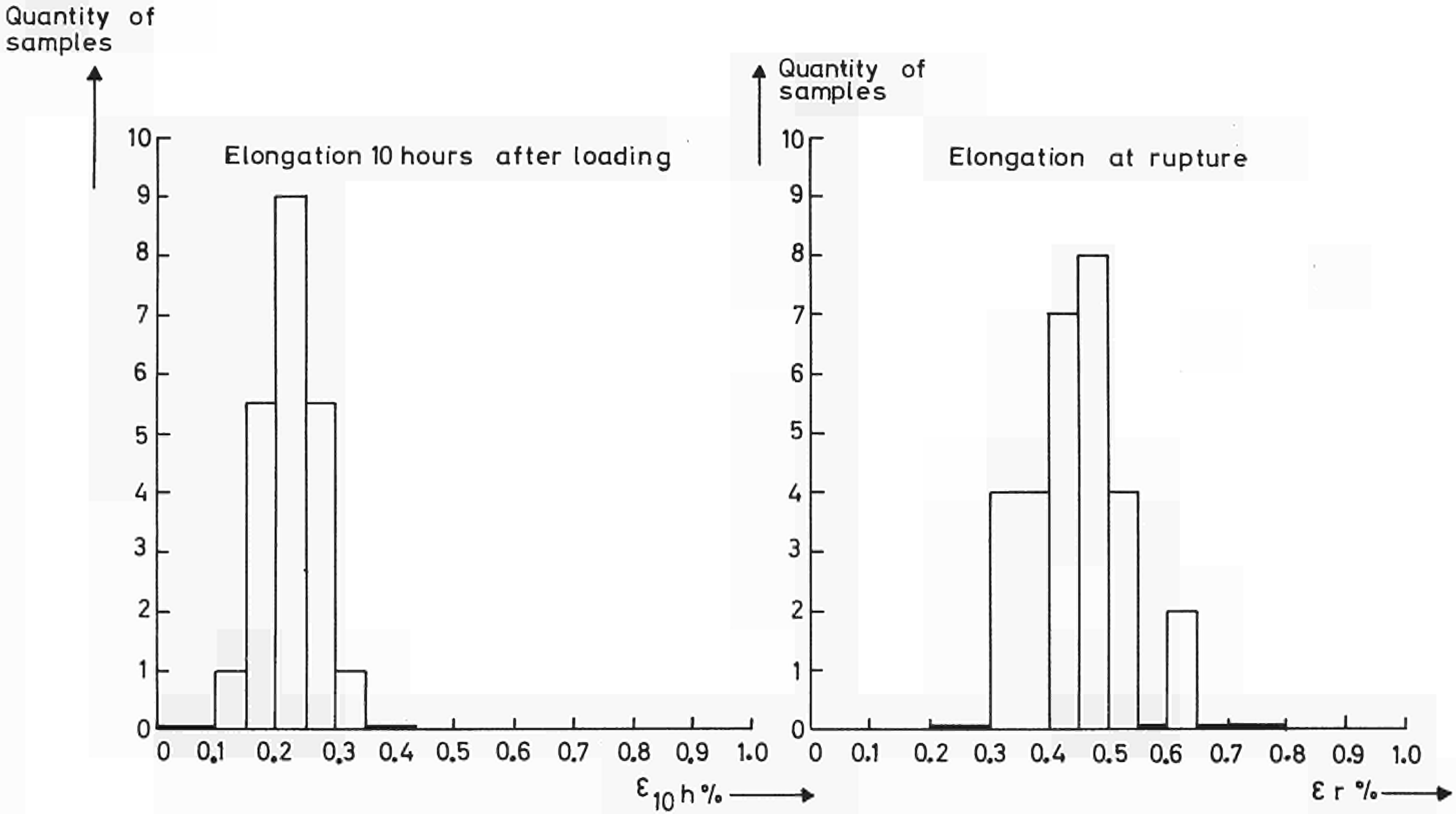

Fig.56

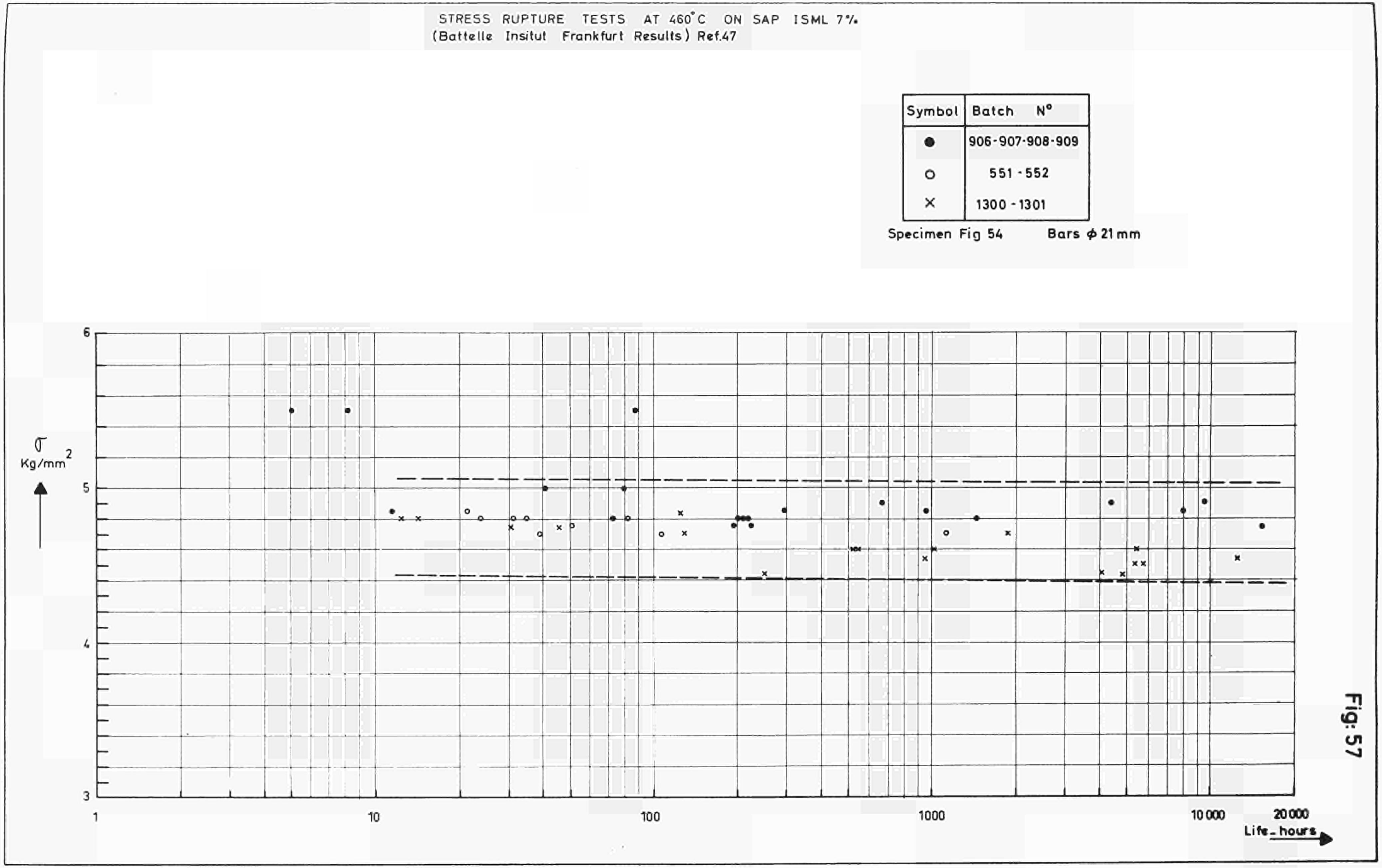

STRESS RUPTURE TESTS AT 460°C ON SAP ISML 7%
(Battelle Insitut Frankfurt Results) Ref.47
Symbol
Batch N°
906-907-908-909
551 - 552
1300 - 1301
Specimen Fig 54
Bars ϕ 21 mm
σ Kg/mm2
6
5
4
3
1
10
100
1000
10 000
20 000
Life_hours

Fig: 57

HISTOGRAMS OF ELONGATIONS DURING CREEP TESTS AT 460°C ON SAP ISML 7 %
(Battelle Institut Frankfurt Results Ref. 47) Specimen Fig. 54 Bars ø 21 mm

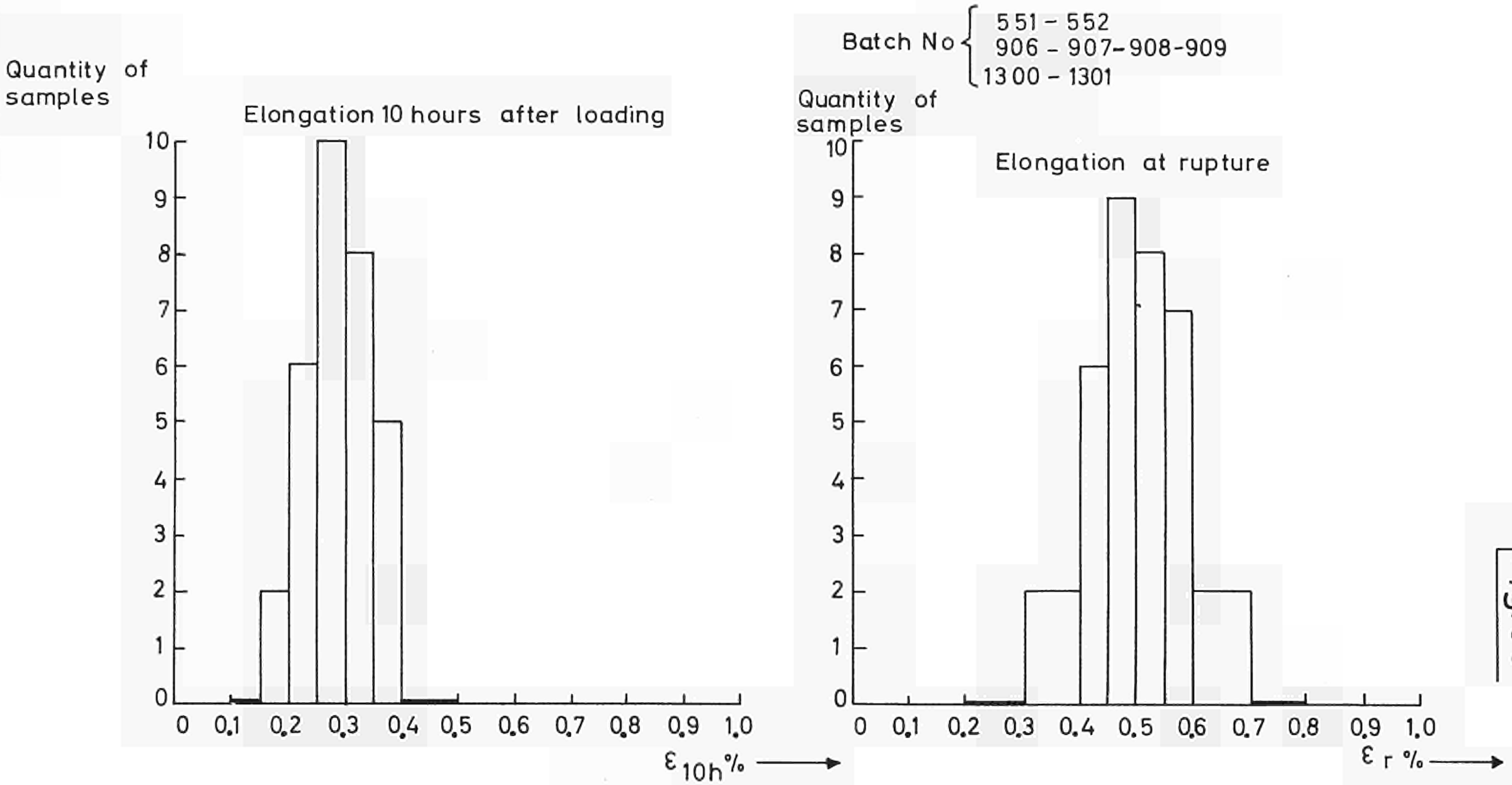

Fig. 58

AECL CREEP SPECIMEN Ref. 33

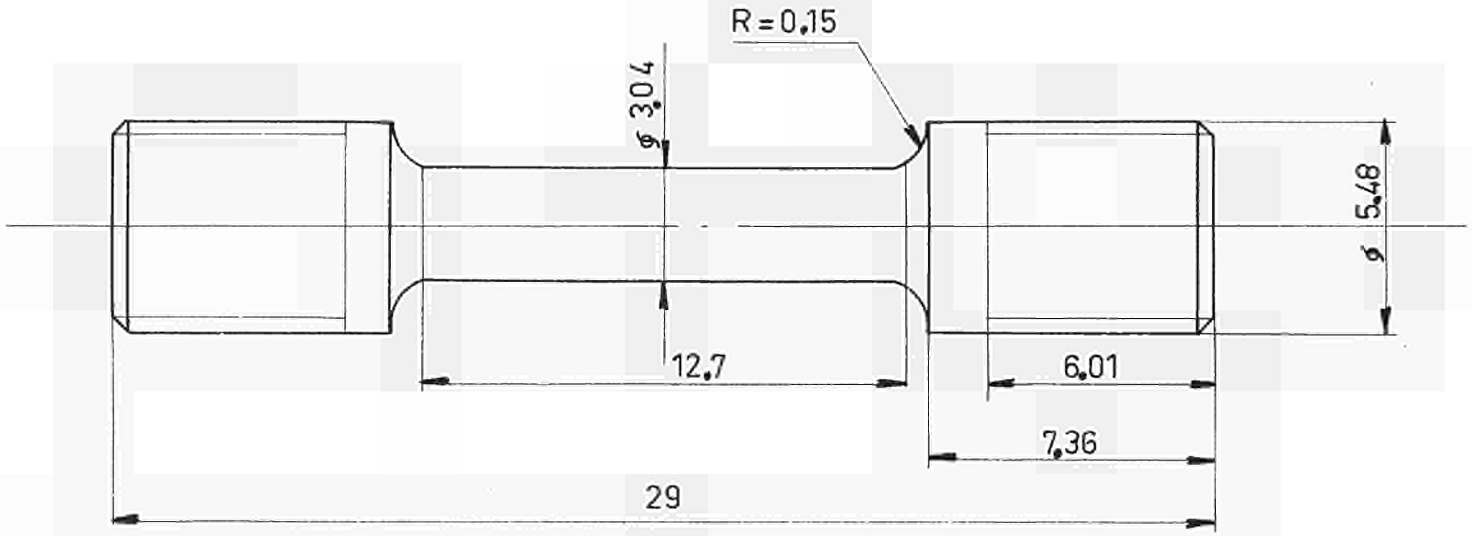

FIG. 59

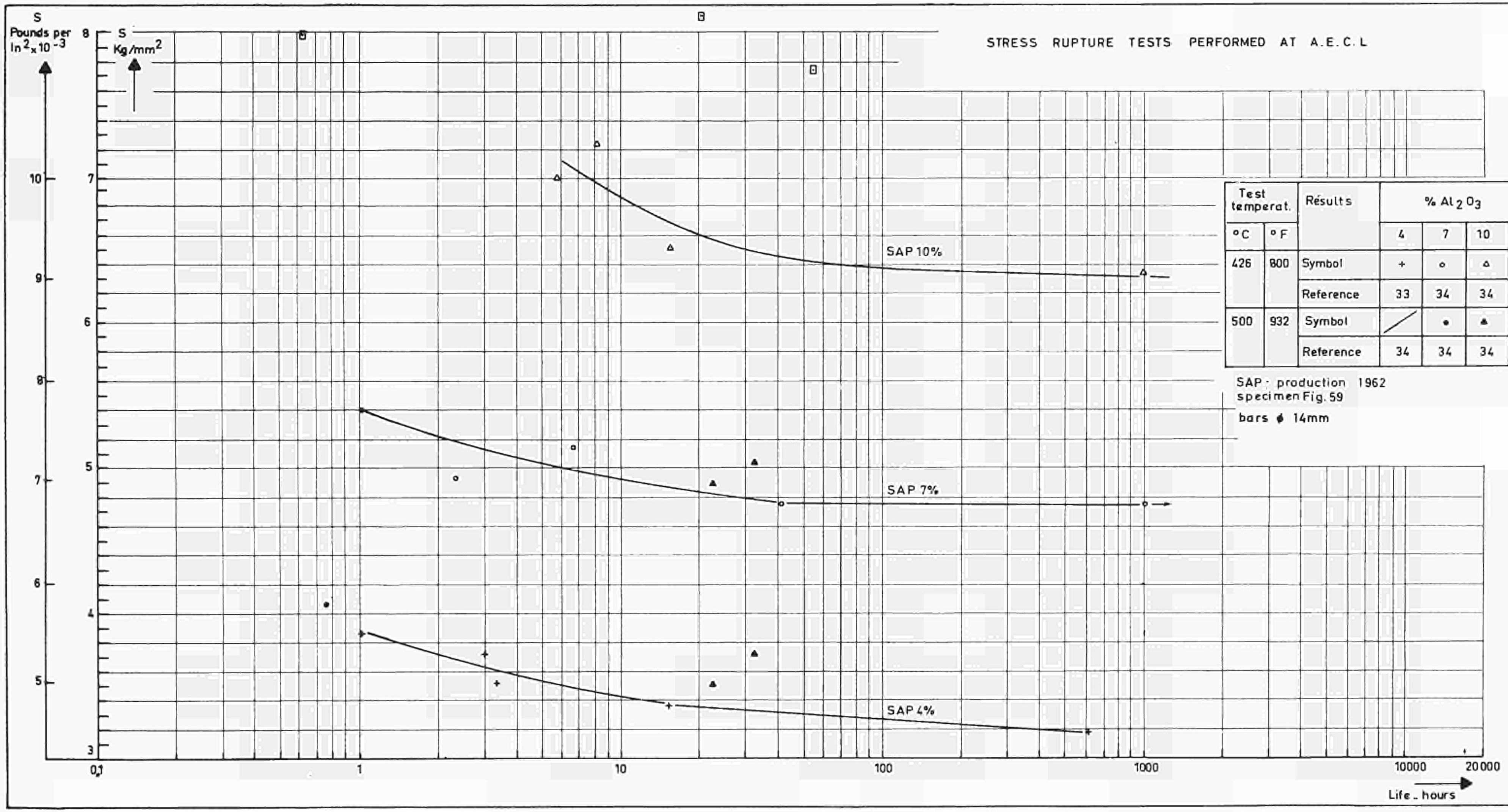
STRESS RUPTURE TESTS PERFORMED AT A.E.C.L
S
Pounds per In 2 x 10 -3
S
Kg/mm2
SAP 10%
SAP 7%
SAP 4%
Test temperat.
°C
°F
Résults
% Al 2 O3
4
7
10
14
426
800
Symbol
Reference
33
34
34
34
500
932
Symbol
Reference
34
34
34
34
SAP - production 1962
specimen Fig. 59
bars ϕ 14mm
0,1
1
10
100
1000
10000
20000
Life - hours

Fig. 60

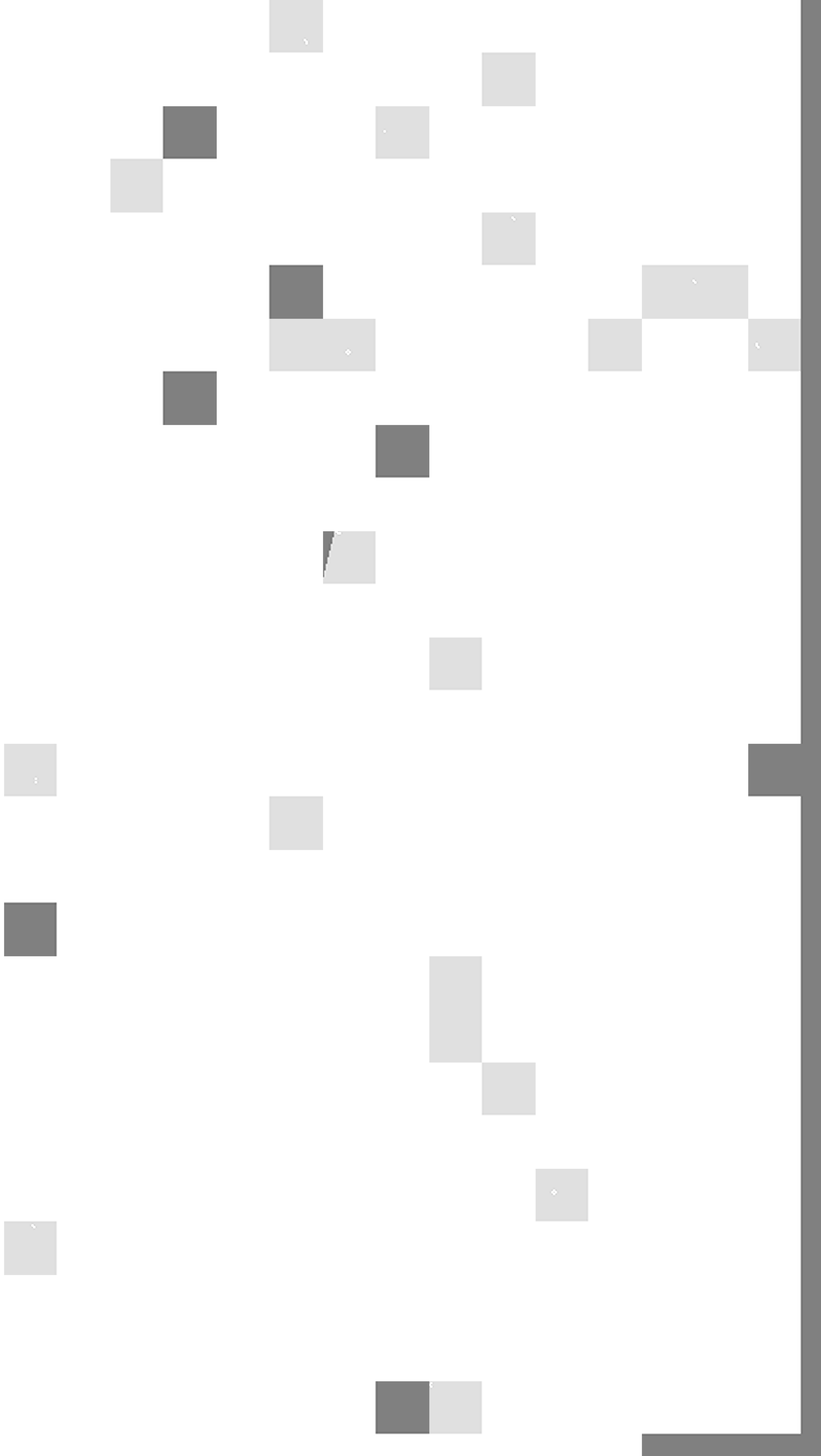

RODS

C [redacted] P

COMPARISON OF RESULTS

FRO[redacted] LA[redacted]ES

STRESS RUPTURE TESTS ON SAP ISML 4% AND 7%

Comparison of results from different laboratories

	$\%Al_2O_3$	Specimen fig.	Batch No	from fig	ref	symbol	∅ barrs mm
EURATOM	4	38	289	40	45-46	— — —	9,5
	7	38	275	41	45-46	——	
	7	38	1067-1721 1722-3552	43	51 51 51		
BATTELLE INSTITUT FRANKFURT	4	54	645 890	55	47		21
	7	54	551 552 906-909 1300-1301	57	47		

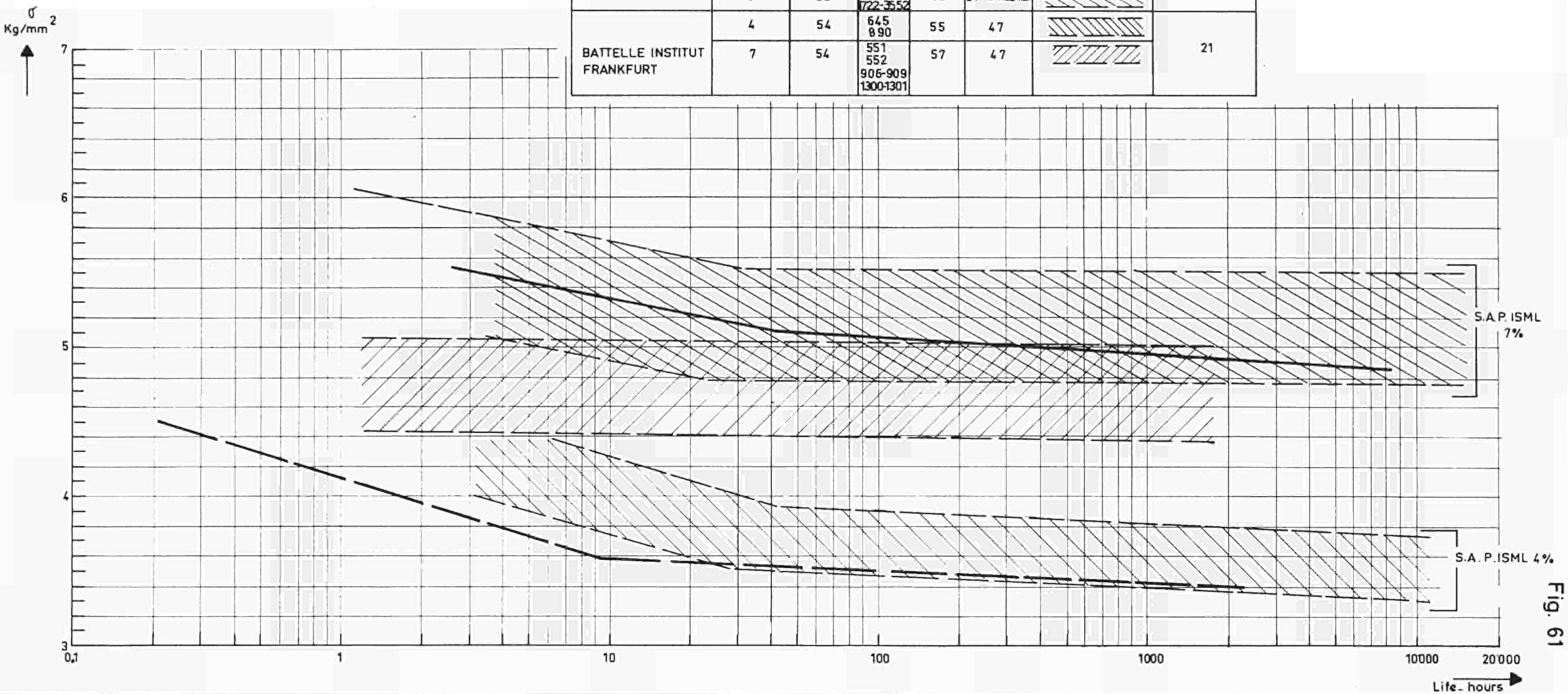

Fig. 61

Fig. 62

ISML RELAXATION SPECIMEN (Ref. ISML Drawing P. Dc 27/1)

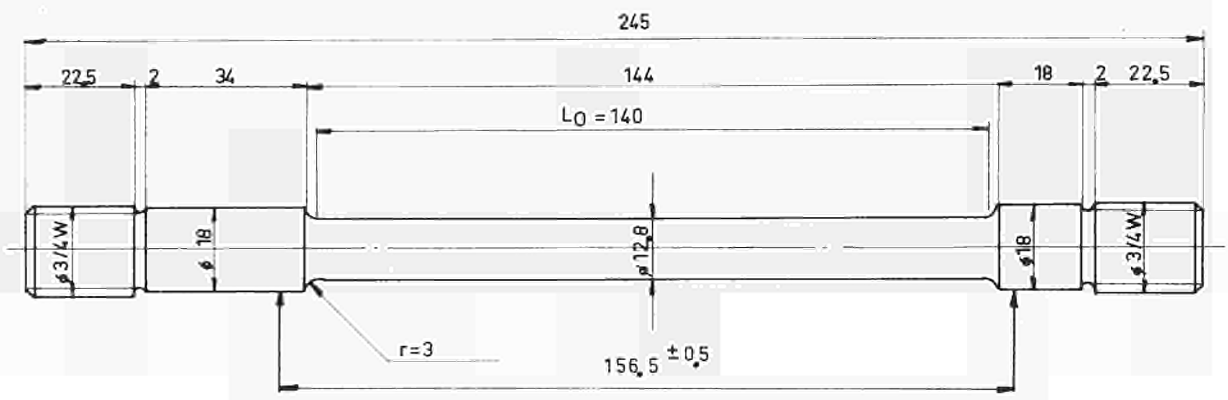

Fig. 63

EURATOM RELAXATION SPECIMEN (Ref. 57)

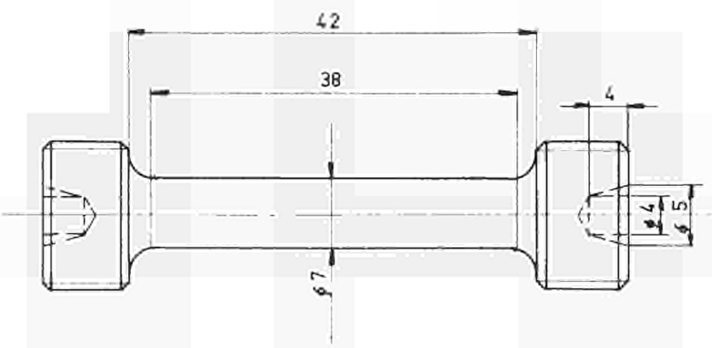

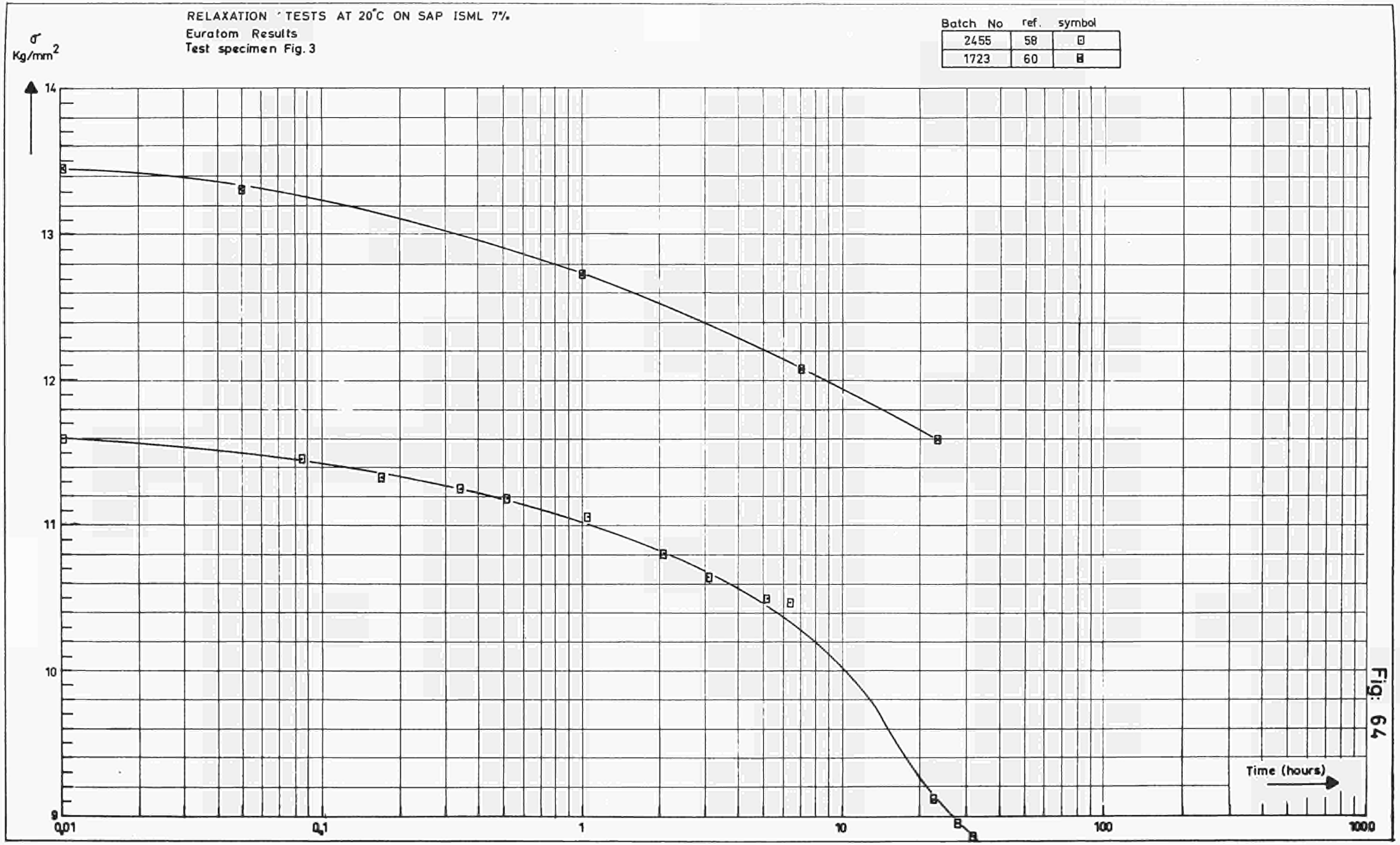
RELAXATION TESTS AT 20°C ON SAP ISML 7%
Euratom Results
Test specimen Fig. 3
σ
Kg/mm2
Batch No
ref.
symbol
2455
58
1723
60
14
13
12
11
10
9
0,01
0,1
1
10
100
1000
Time (hours)

Fig: 64

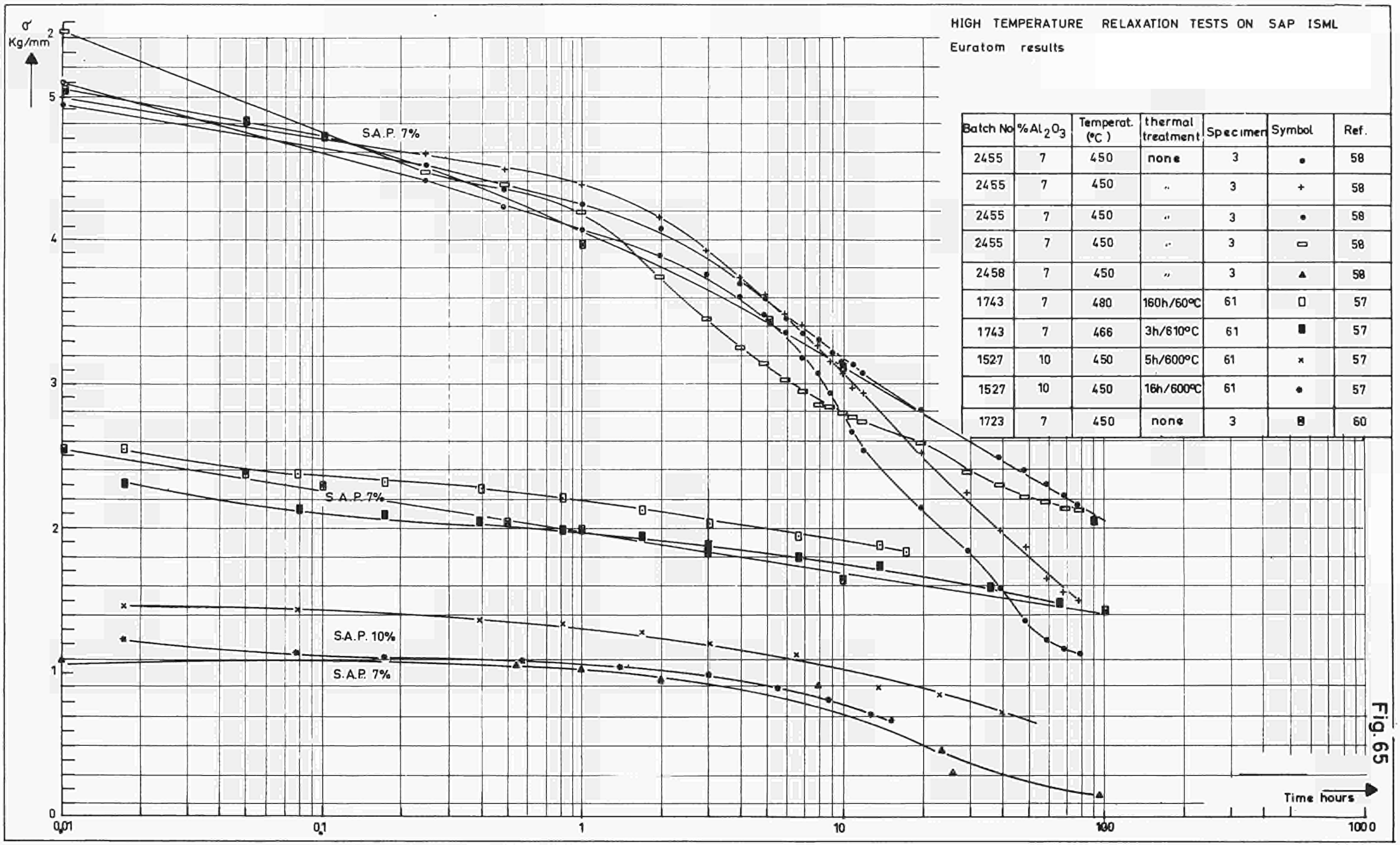

Batch No	%Al_2O_3	Temperat. (°C)	thermal treatment	Specimen	Symbol	Ref.
2455	7	450	none	3	●	58
2455	7	450	"	3	+	58
2455	7	450	"	3	●	58
2455	7	450	"	3	▭	58
2458	7	450	"	3	▲	58
1743	7	480	160h/600°C	61	□	57
1743	7	466	3h/610°C	61	■	57
1527	10	450	5h/600°C	61	×	57
1527	10	450	16h/600°C	61	●	57
1723	7	450	none	3	⊟	60

Fig. 65

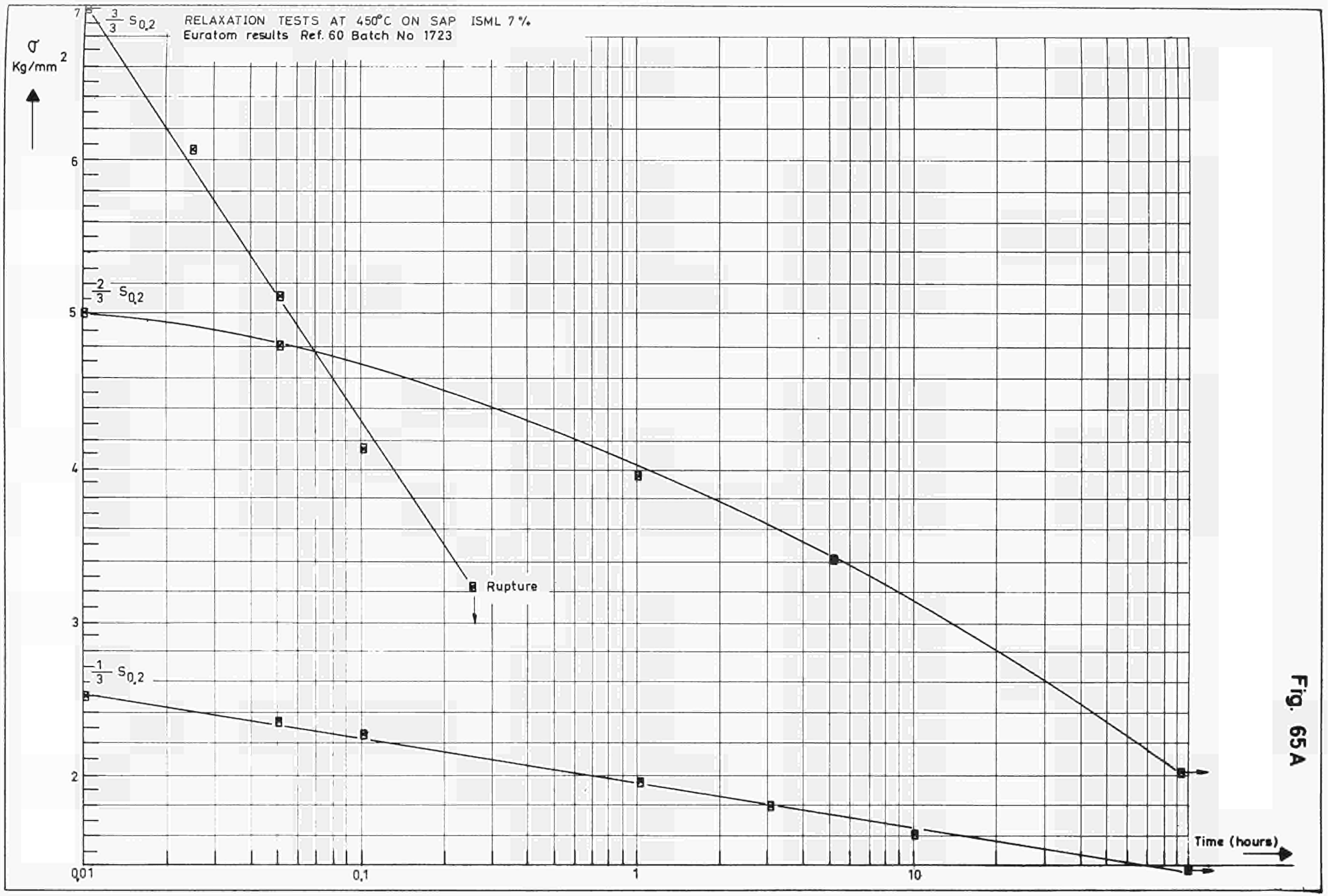

RELAXATION TESTS AT 450°C ON SAP ISML 7 %
Euratom results Ref. 60 Batch No 1723
σ Kg/mm 2
3/3 S0,2
2/3 S0,2
1/3 S0,2
Rupture
Time (hours)
7
6
5
4
3
2
0,01
0,1
1
10

Fig. 65A


RELAXATION TESTS AT 450°C ON SAP ISML 7%
ISML Results Ref 21 Batch N° 2622
Test specimen Fig. 62
Strain (%) | symbol
0,165 | x
0,120 | +
0,120 | •
σ Kg/mm2
5
4
3
2
1
0
0,01
0,1
1
10
100
1000
Time (hours)

Fig. 66

Fig. 67

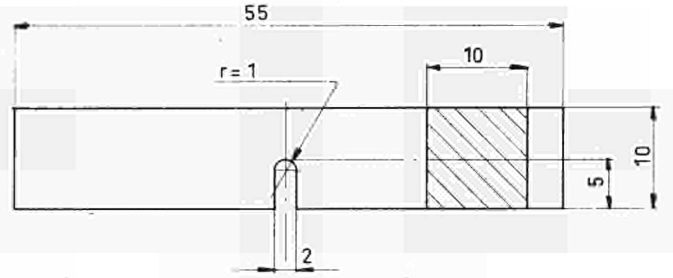

CHARPY SPECIMEN FOR IMPACT STRENGTH TEST

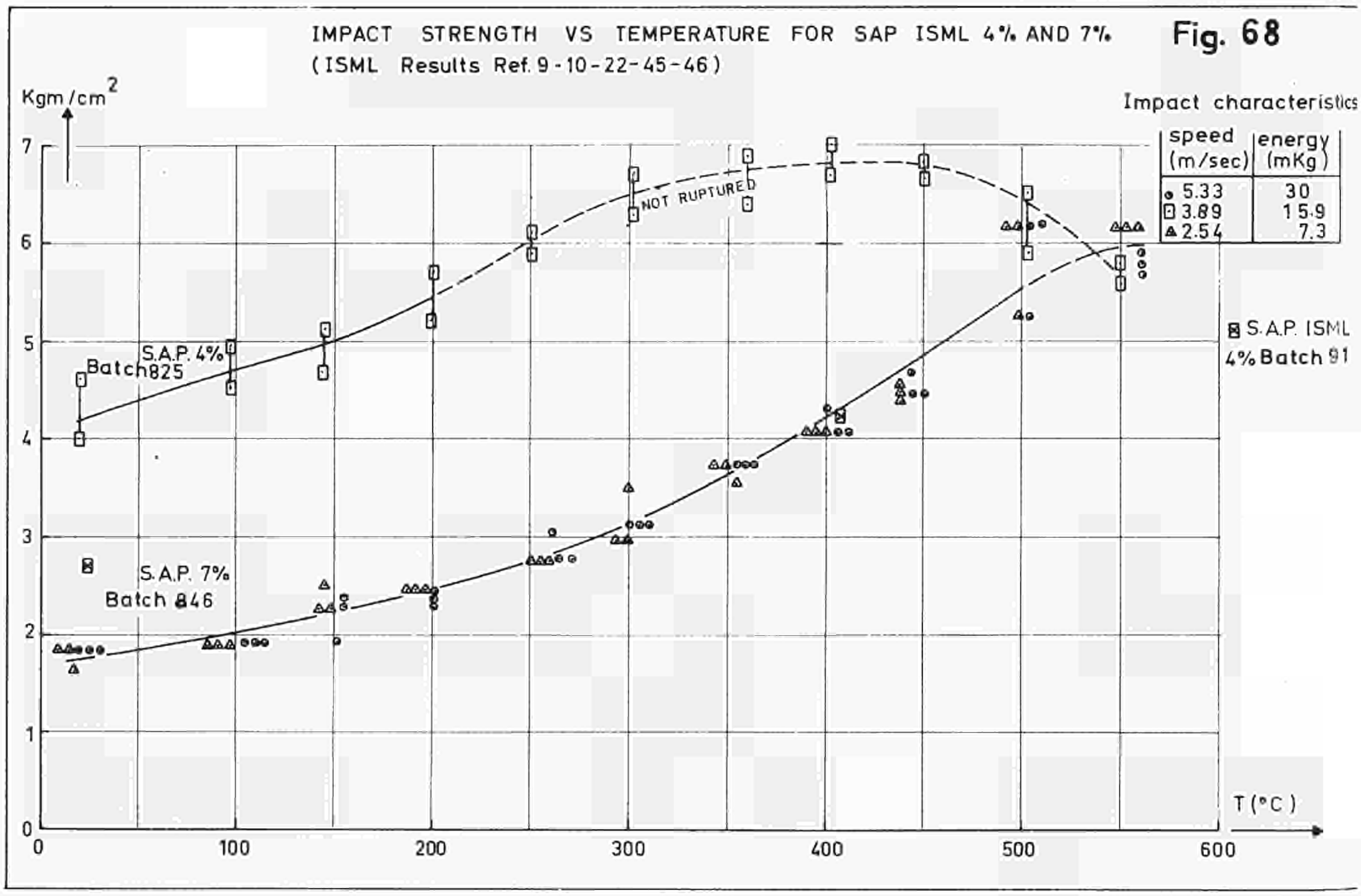

VICKERS MICRO AND MACRO HARDNESS AT 20°C ON SAP ISML AND ALUMINIUM A 5 **Fig. 69**
(Euratom Results Ref. 28) SAP PRODUCED ON MAX 1961

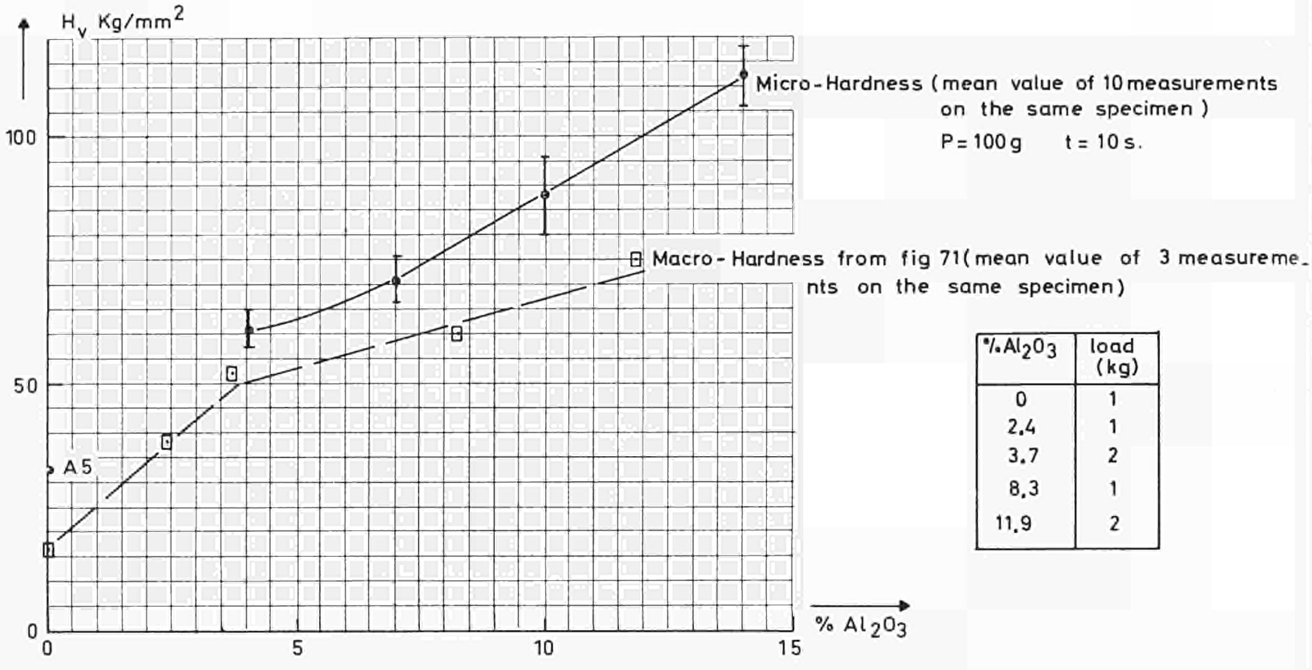

VICKERS MICROHARDNESS OF SAP ISML VS. TEMPERATURE **Fig. 69A**
(Euratom Results Ref. 28 bis)

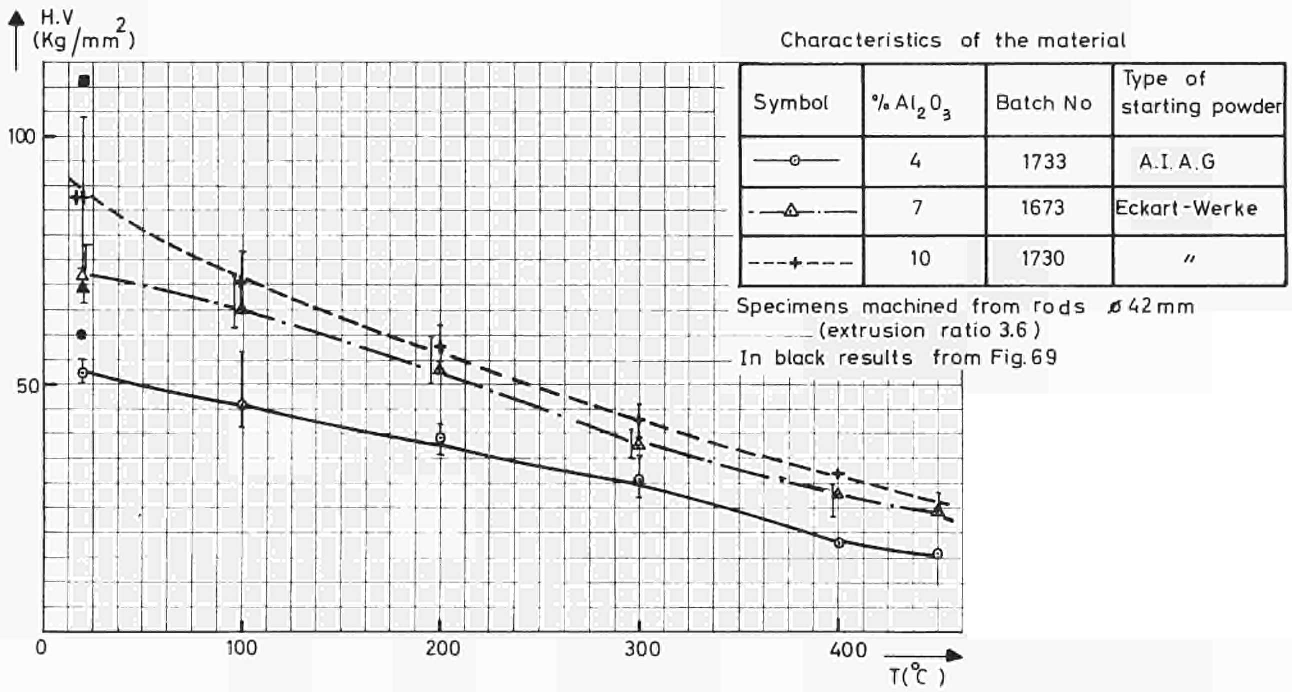

BRINNEL MACRO - HARDNESS AT 20°C ON SAP ISML
(ISML Results Ref. 2-3-4)

Fig. 70

Test condition

ball ϕ 2.5 mm
load 62.5 Kg
time of application : 30 s

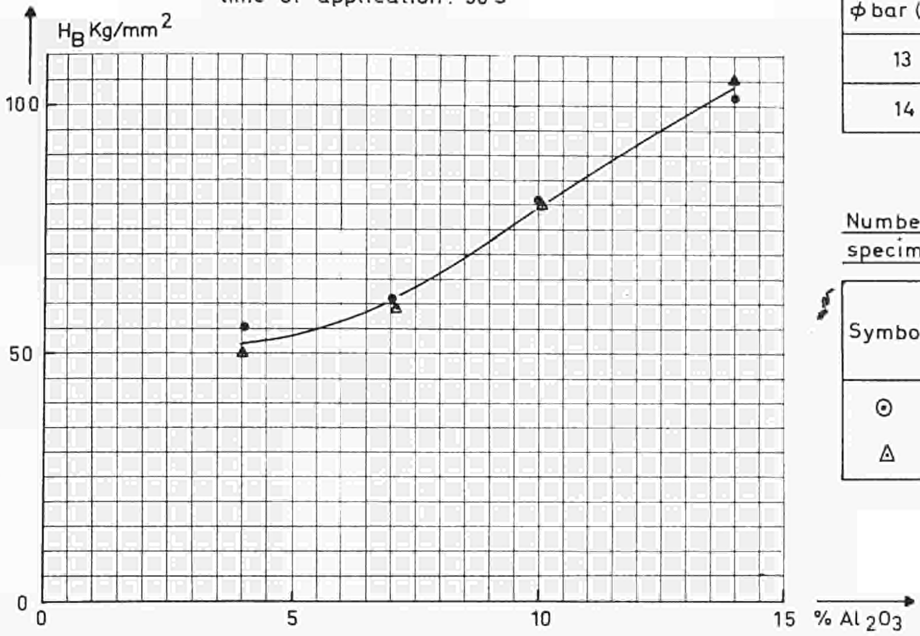

Batch No

	% Al_2O_3			
ϕ bar (mm)	4	7	10	14
13	96 112	95 113	114	115
14	118	121	122	127

Number of measurements on each specimen

Symbol	ϕ bar (mm)	Number of measurements on each specimen
⊙	13	3 to 6
△	14	2

BRINNEL MACRO- HARDNESS OF SAP ISML VS. TEMPERATURE
(Euratom results Ref. 30 bis)
(bars ø 14 to 22mm

Fig. 70 A

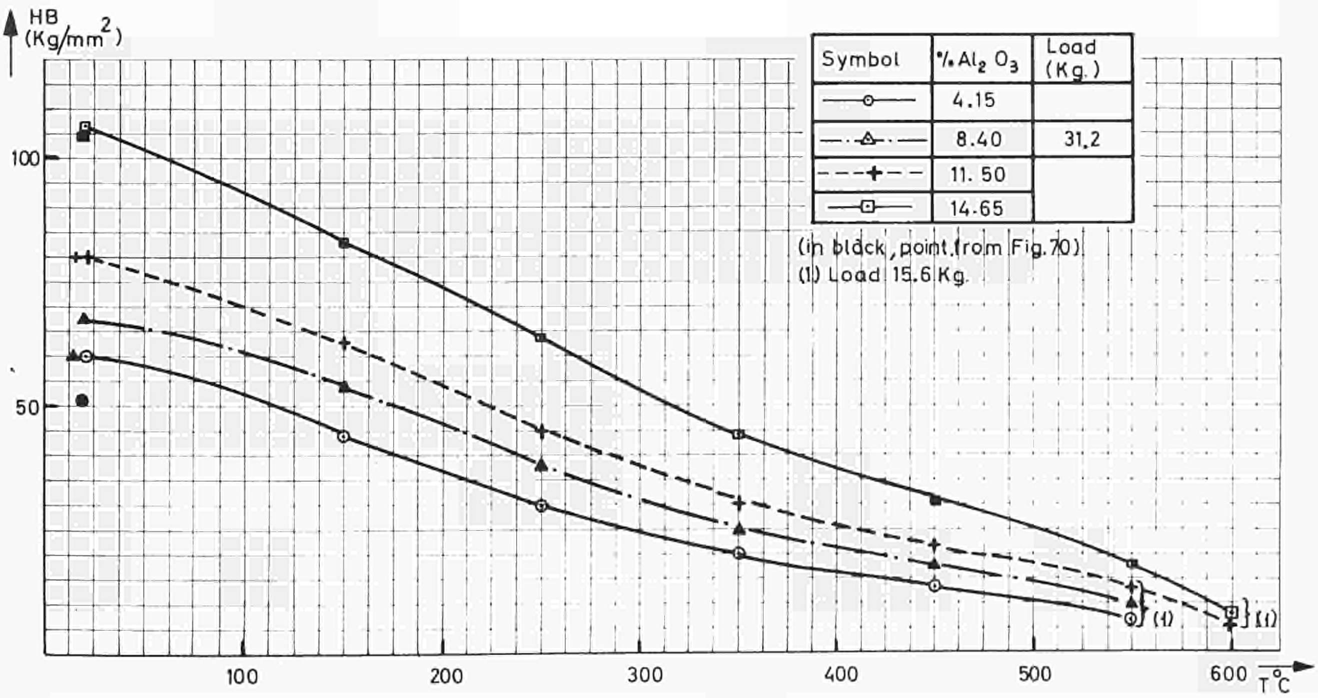

BRINNEL MACRO-HARDNESS OF SAP ISML 7 AND 14% V S. TEMPERATURE
(ISML Results Ref. 21B)

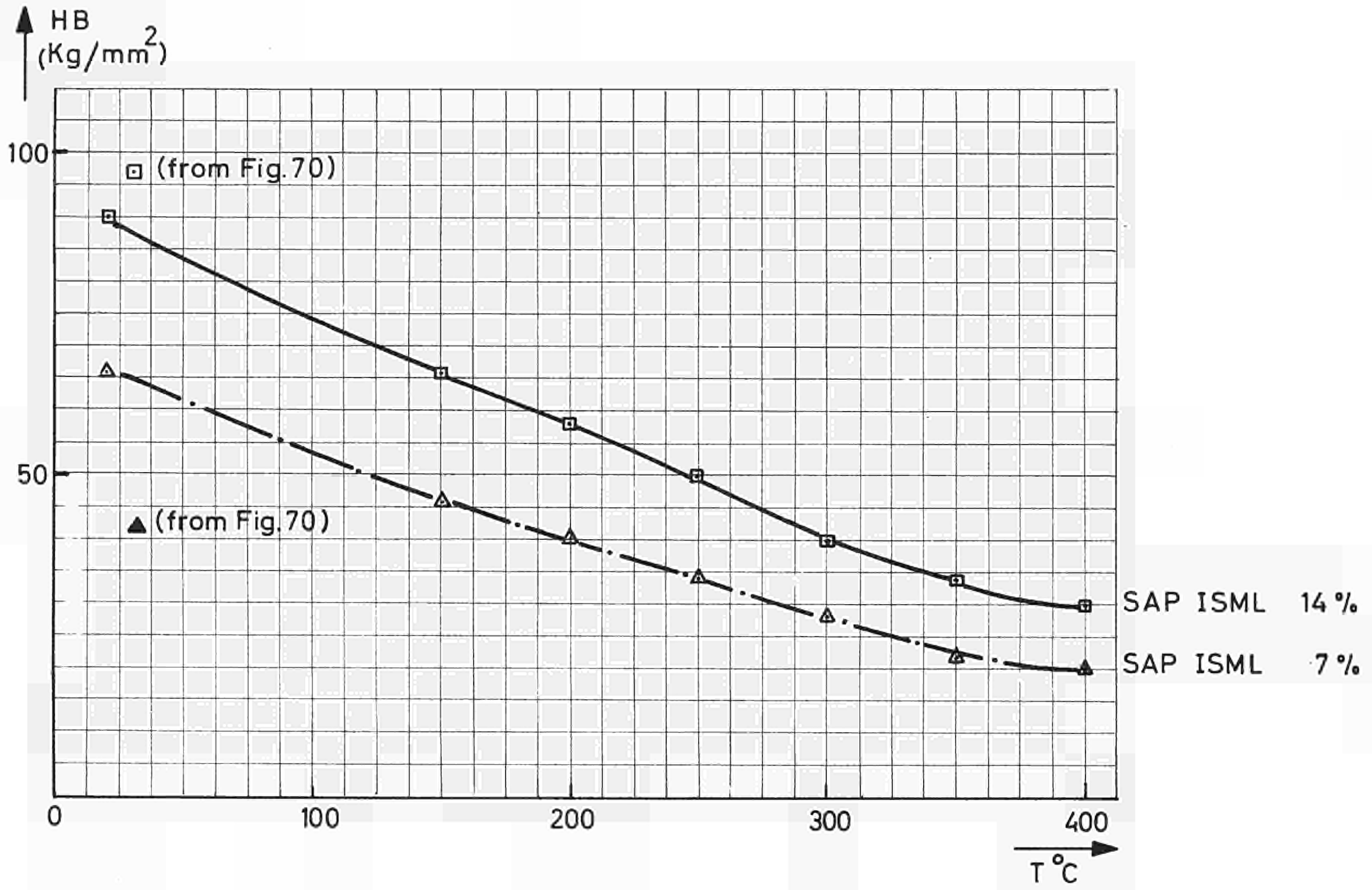

Fig 70 B

VICKER HARDNESS AT 20°C ON SAP ISML VS DEFORMATION RATIO

(Euratom Results Ref.56) Influence of cold deformation

Symbol	% Al_2O_3	Load on the Vickers indenter (Kg.)
○	11.9	2
△	8.3	1
●	3.7	2
▲	2.4	1
+	0	1

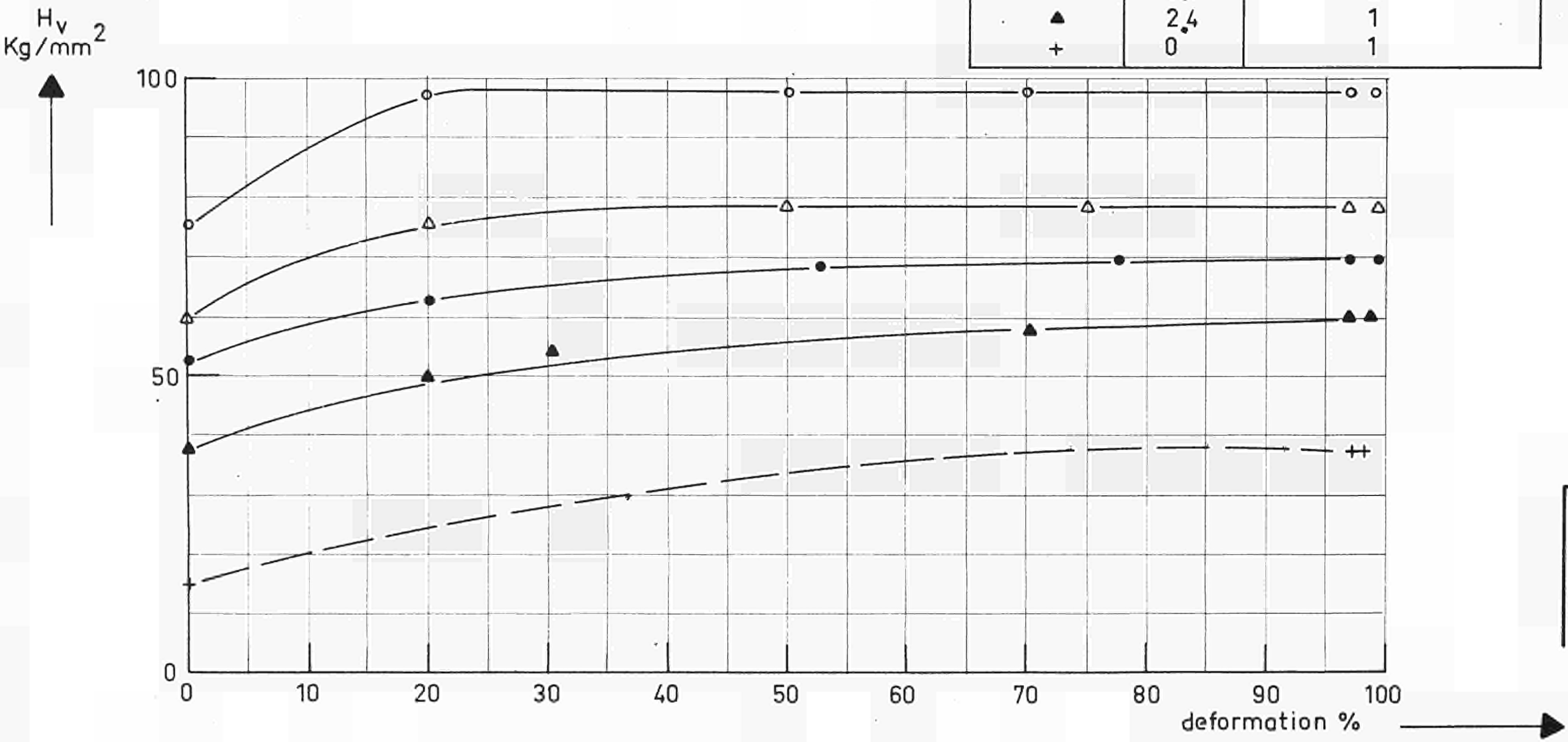

FIG. 71

VICKERS HARDNESS AT 20° C ON SAP ISML AFTER DIFFERENT RATES OF COLD WORK VS. ANNEALING TEMPERATURE (Euratom results Ref. 56)

Symbole	Cold_work
○	95
△	90
●	74
▲	53
+	22
⊙	0

SAP specimens 3.7% Al_2O_3 Cold-rolled.

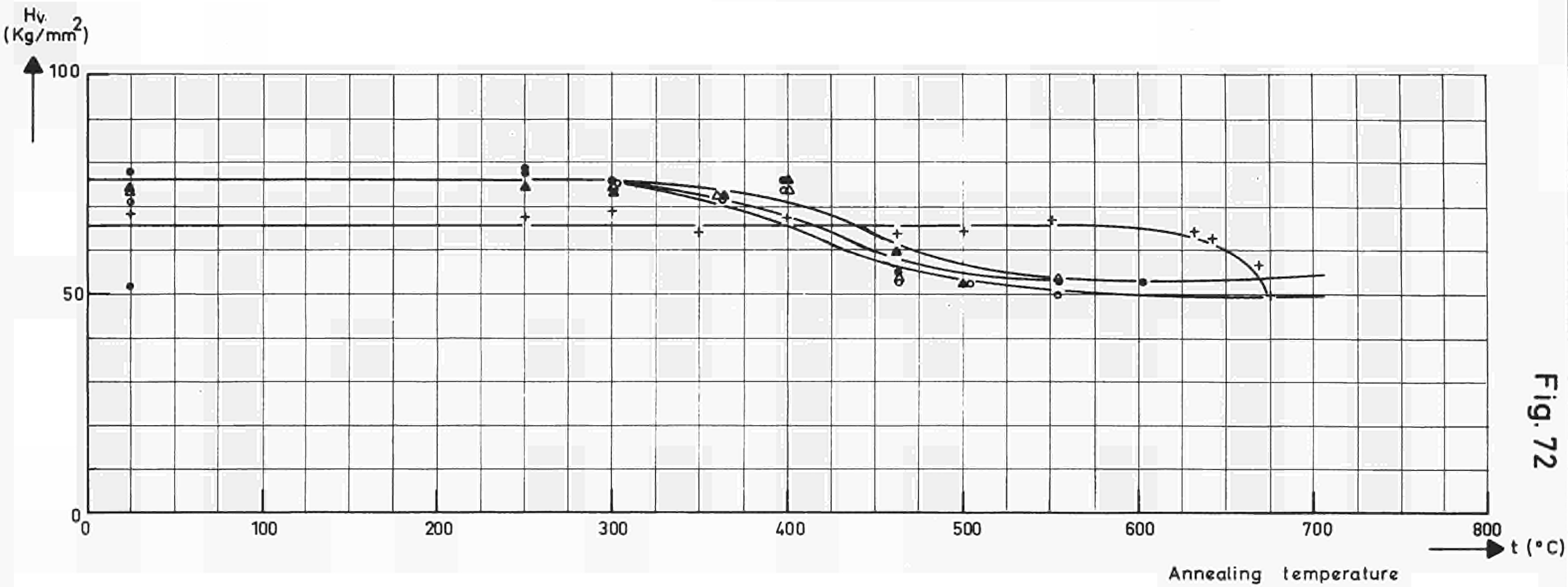

Fig. 72

VICKERS HARDNESS AT 20°C ON COLD WORKED SAP ISML
VS. ANNEALING TEMPERATURE
(Euratom resuls Ref. 56)

Cold rolled S.A.P. (rate 95 %)

Symbole	% Al_2O_3	Load (Kg.)
○	11,9	2
△	8,3	1
●	3,7	2
▲	2,4	1

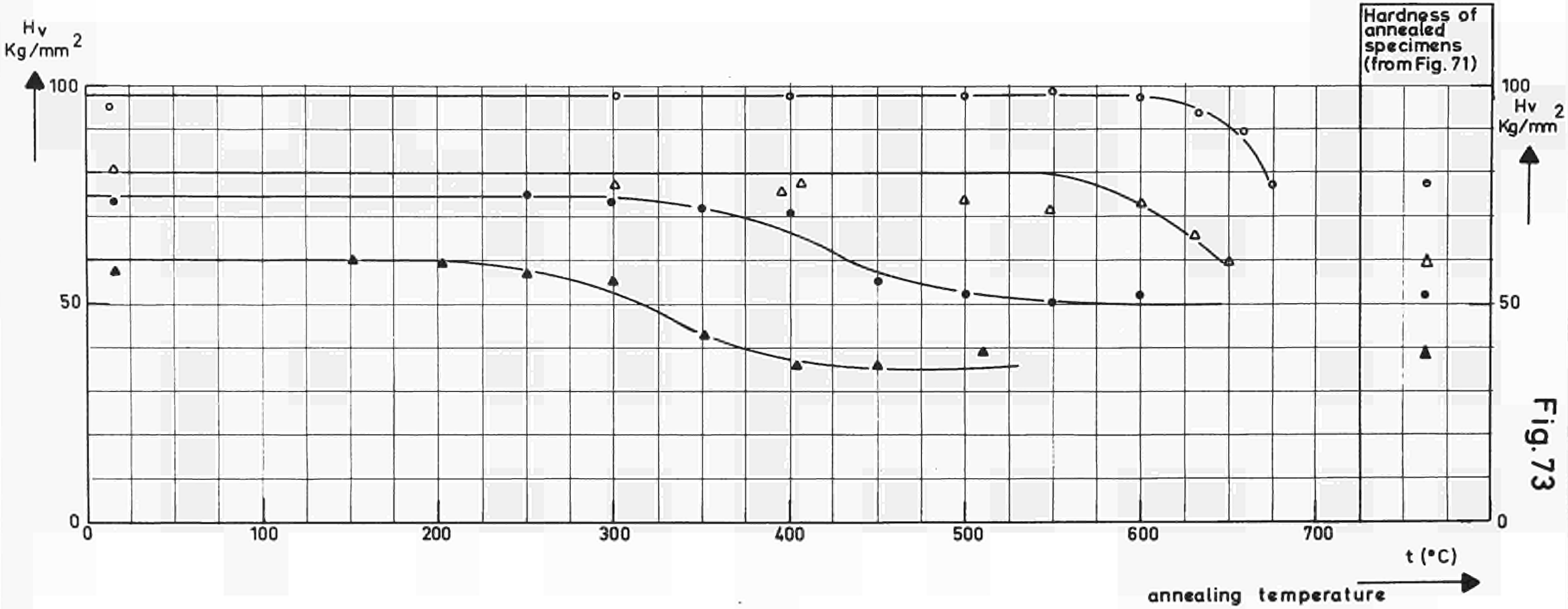

Fig. 73

Fig 74

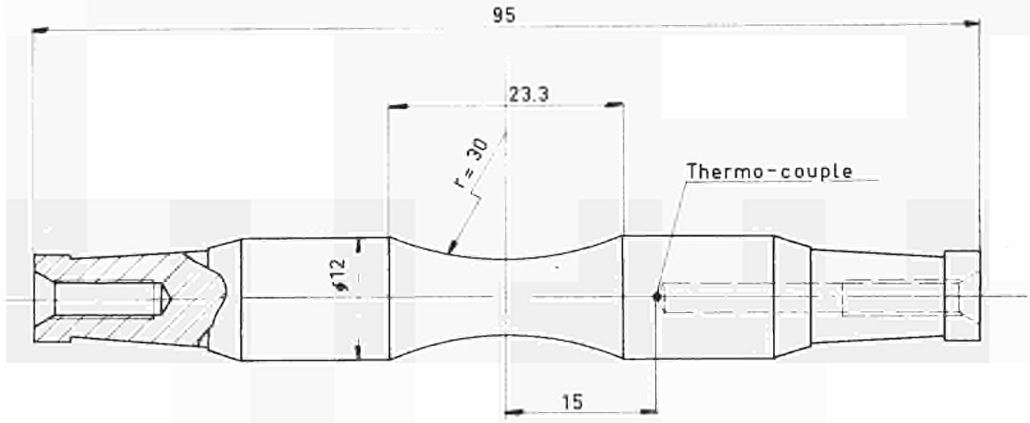

ISML SPECIMEN FOR ROTATING BENDING TESTS AT 20°C AND 400°C (Ref. 8)

Fig. 75

ROTATING BENDING TESTS AT 20°C AND 400°C ON SAP ISML 4%
(ISML Results Ref. 8-4-6)

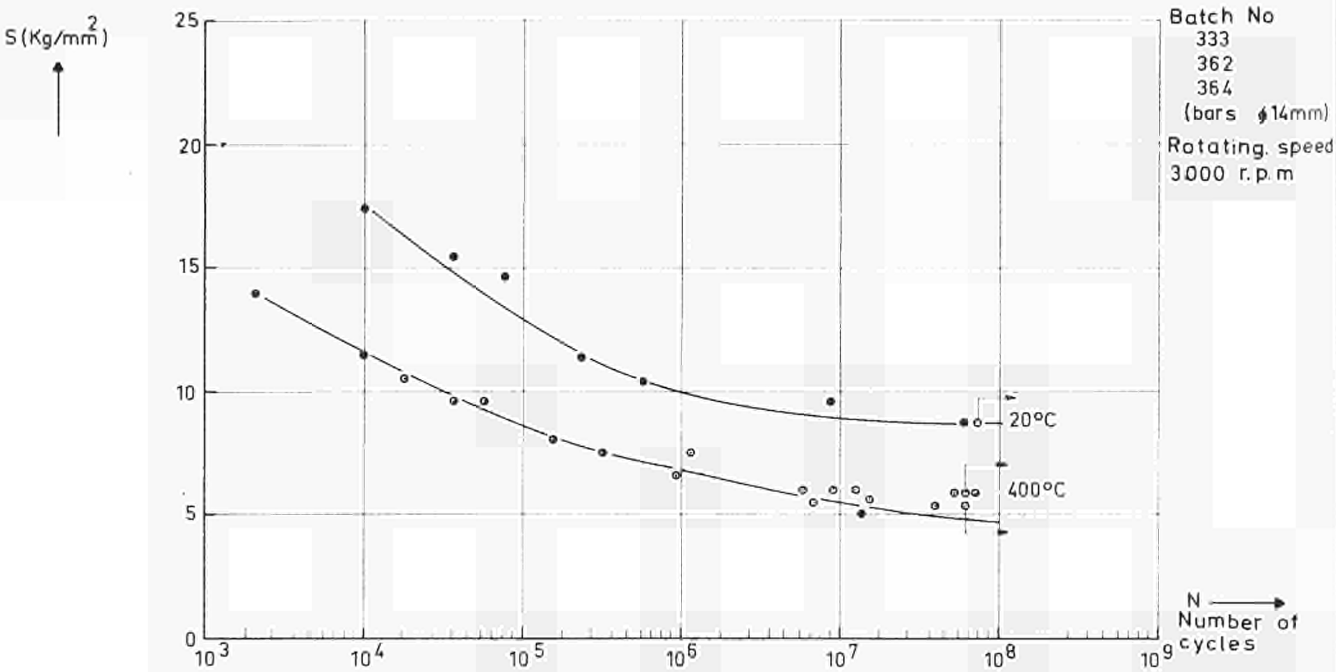

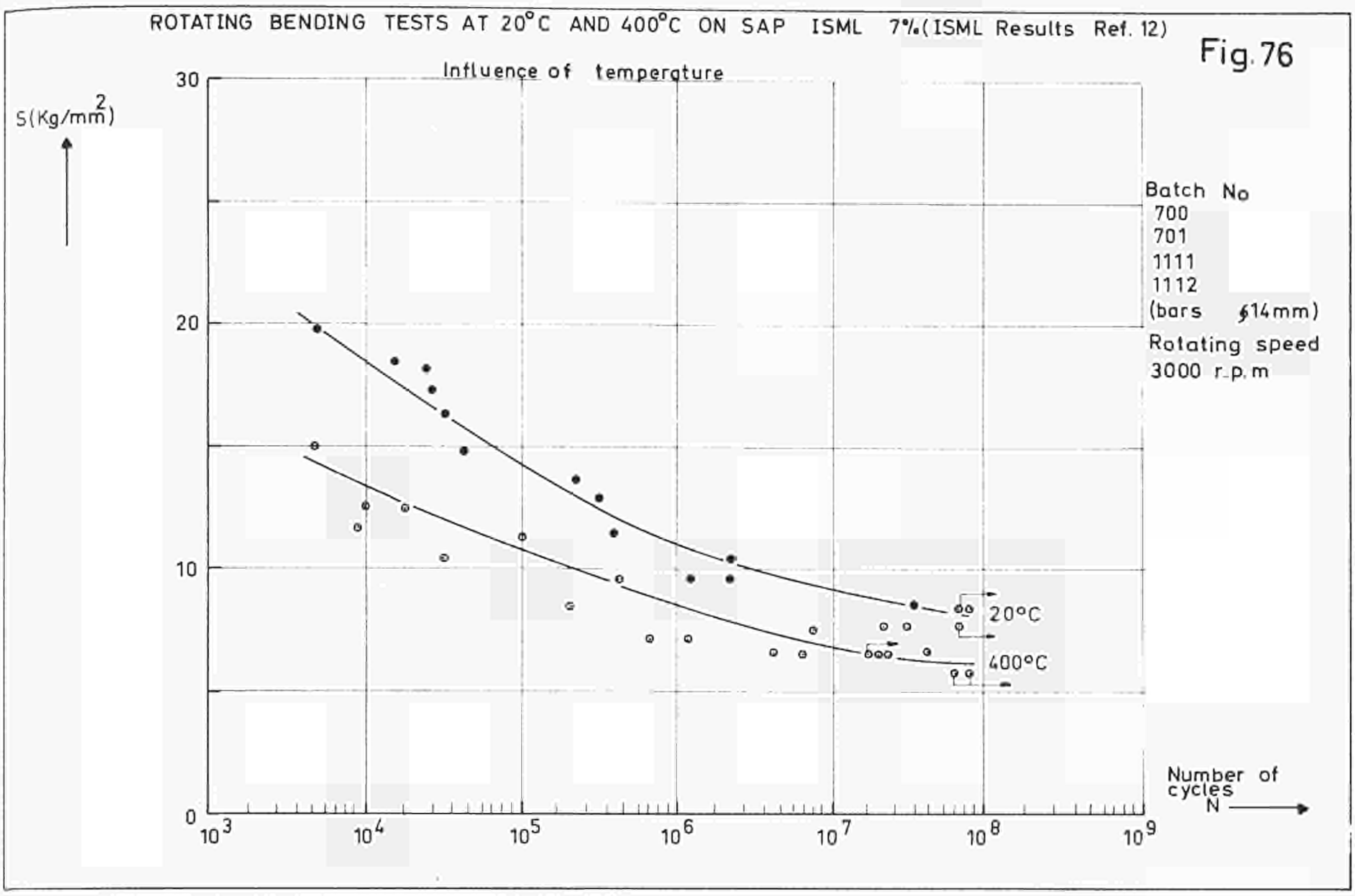
ROTATING BENDING TESTS AT 20°C AND 400°C ON SAP ISML 7%(ISML Results Ref. 12)
Fig. 76
Influence of temperature
S(Kg/mm²)
Batch No
700
701
1111
1112
(bars ∅14mm)
Rotating speed
3000 r.p.m
20°C
400°C
Number of cycles
N
30
20
10
0
10³
10⁴
10⁵
10⁶
10⁷
10⁸
10⁹

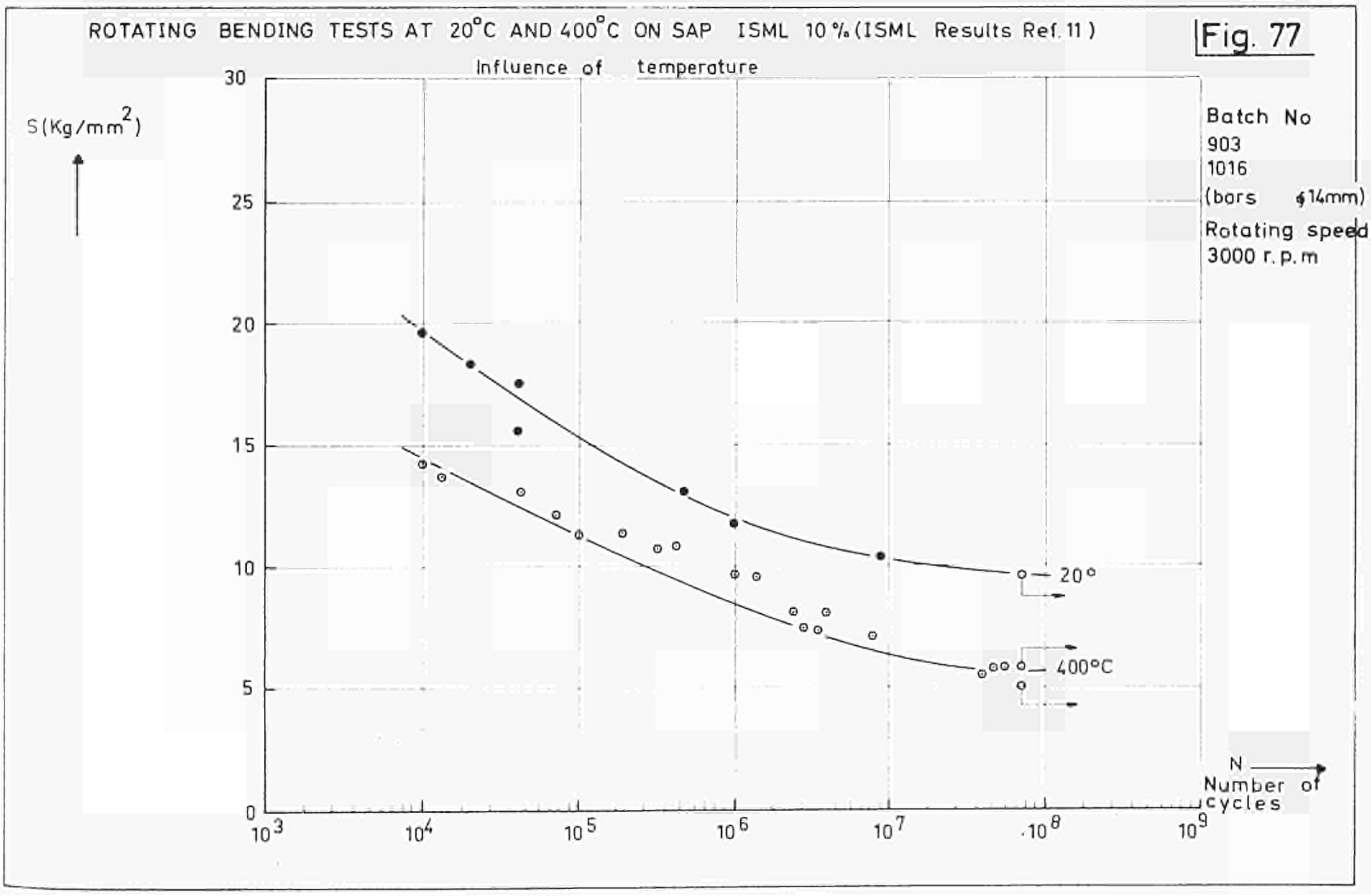
ROTATING BENDING TESTS AT 20°C AND 400°C ON SAP ISML 10%(ISML Results Ref. 11)
Fig. 77
Influence of temperature
S(Kg/mm²)
Batch No
903
1016
(bars ∅14mm)
Rotating speed
3000 r.p.m
20°
400°C
N
Number of cycles
30
25
20
15
10
5
0
10³
10⁴
10⁵
10⁶
10⁷
10⁸
10⁹

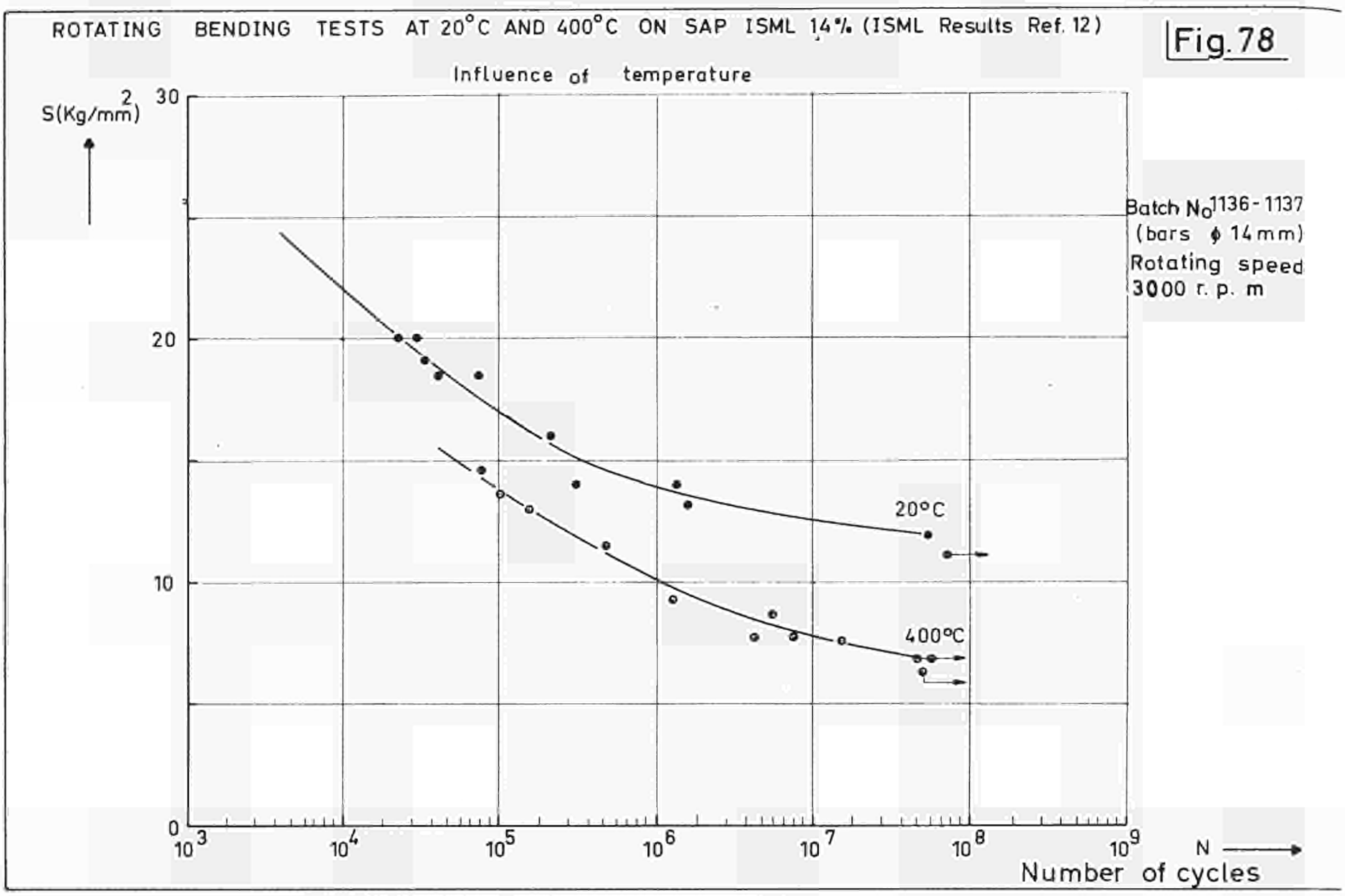
ROTATING BENDING TESTS AT 20°C AND 400°C ON SAP ISML 14% (ISML Results Ref. 12)
Influence of temperature
Fig. 78
S(Kg/mm2)
Batch No 1136-1137
(bars ϕ 14 mm)
Rotating speed
3000 r. p. m
20°C
400°C
N
Number of cycles

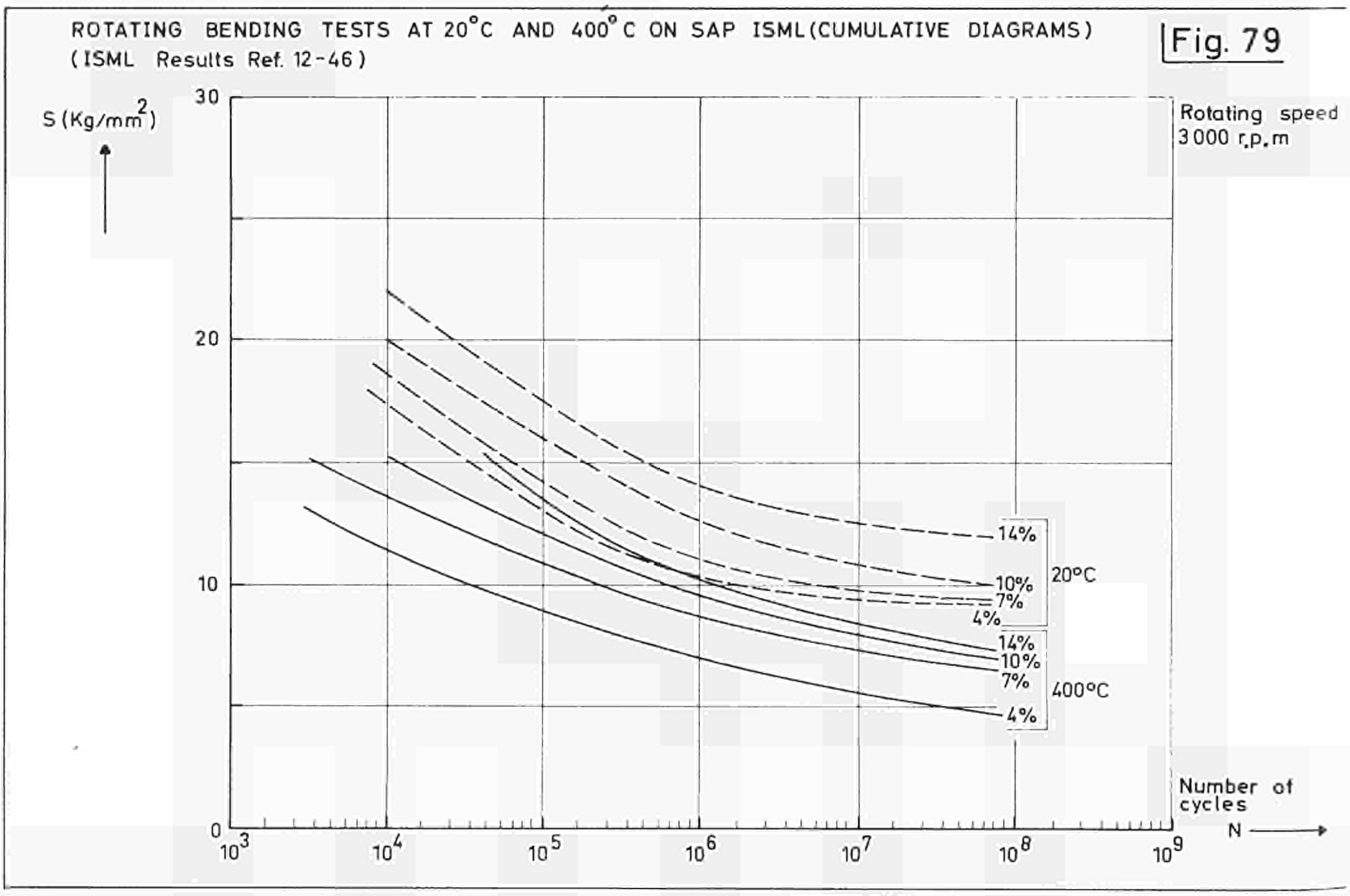
ROTATING BENDING TESTS AT 20°C AND 400°C ON SAP ISML (CUMULATIVE DIAGRAMS)
(ISML Results Ref. 12-46)
Fig. 79
S (Kg/mm2)
Rotating speed
3000 r.p.m
14%
10%
7%
4%
20°C
14%
10%
7%
400°C
4%
Number of cycles
N

ISML NOTCHED SPECIMEN FOR ROTATING BENDING TEST AT 20°C (Ref. 2)

Fig. 80

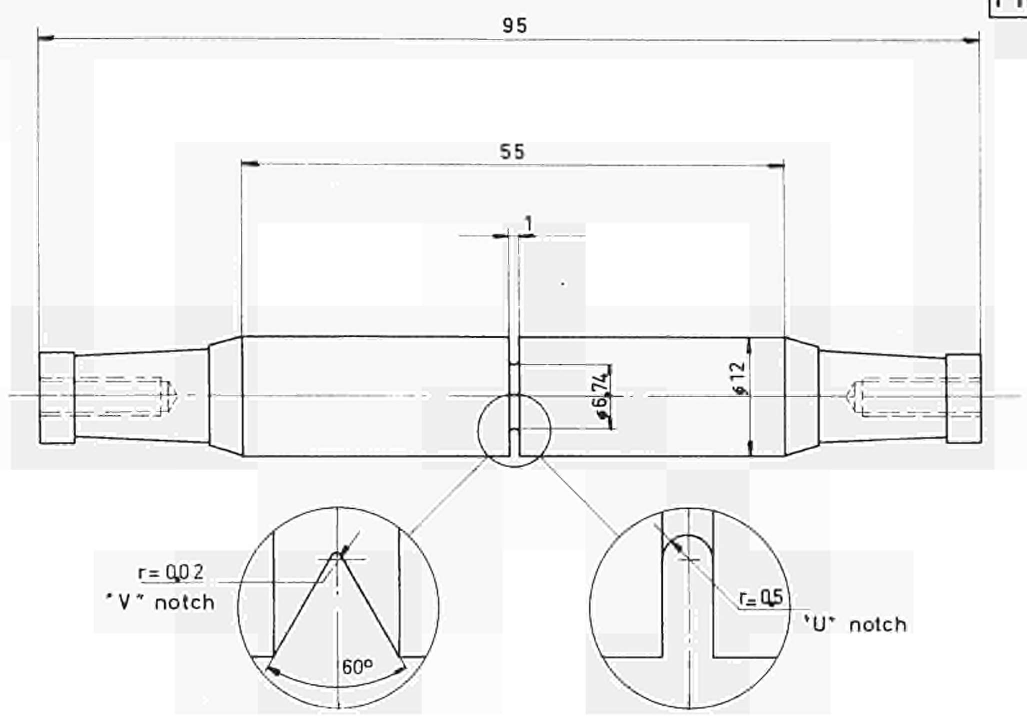

ISML SPECIMEN FOR ROTATING BENDING TESTS AT 20°C (Ref. 2)

Fig. 81

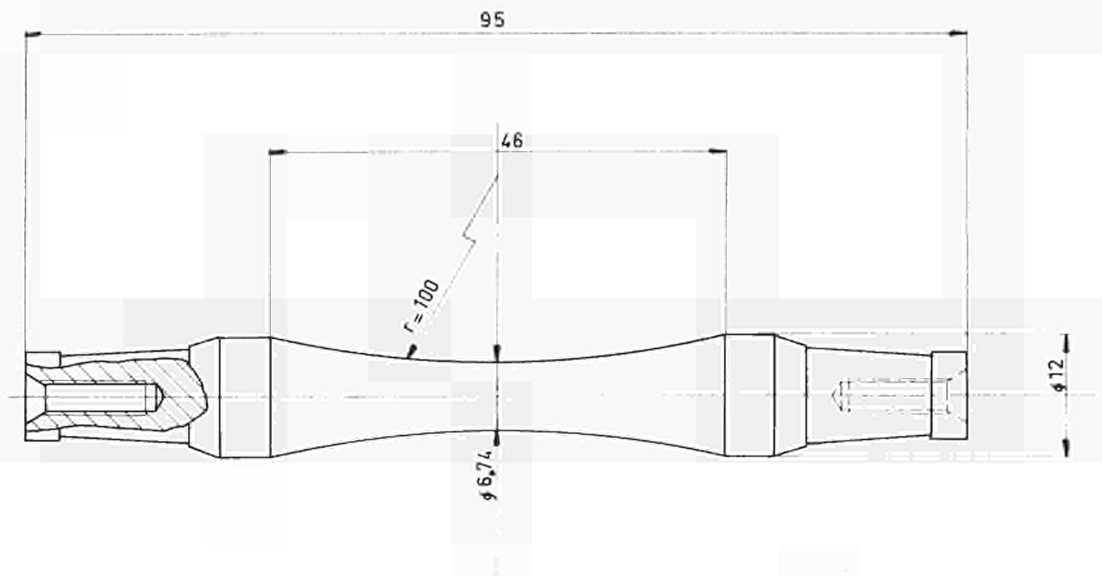

Fig. 82

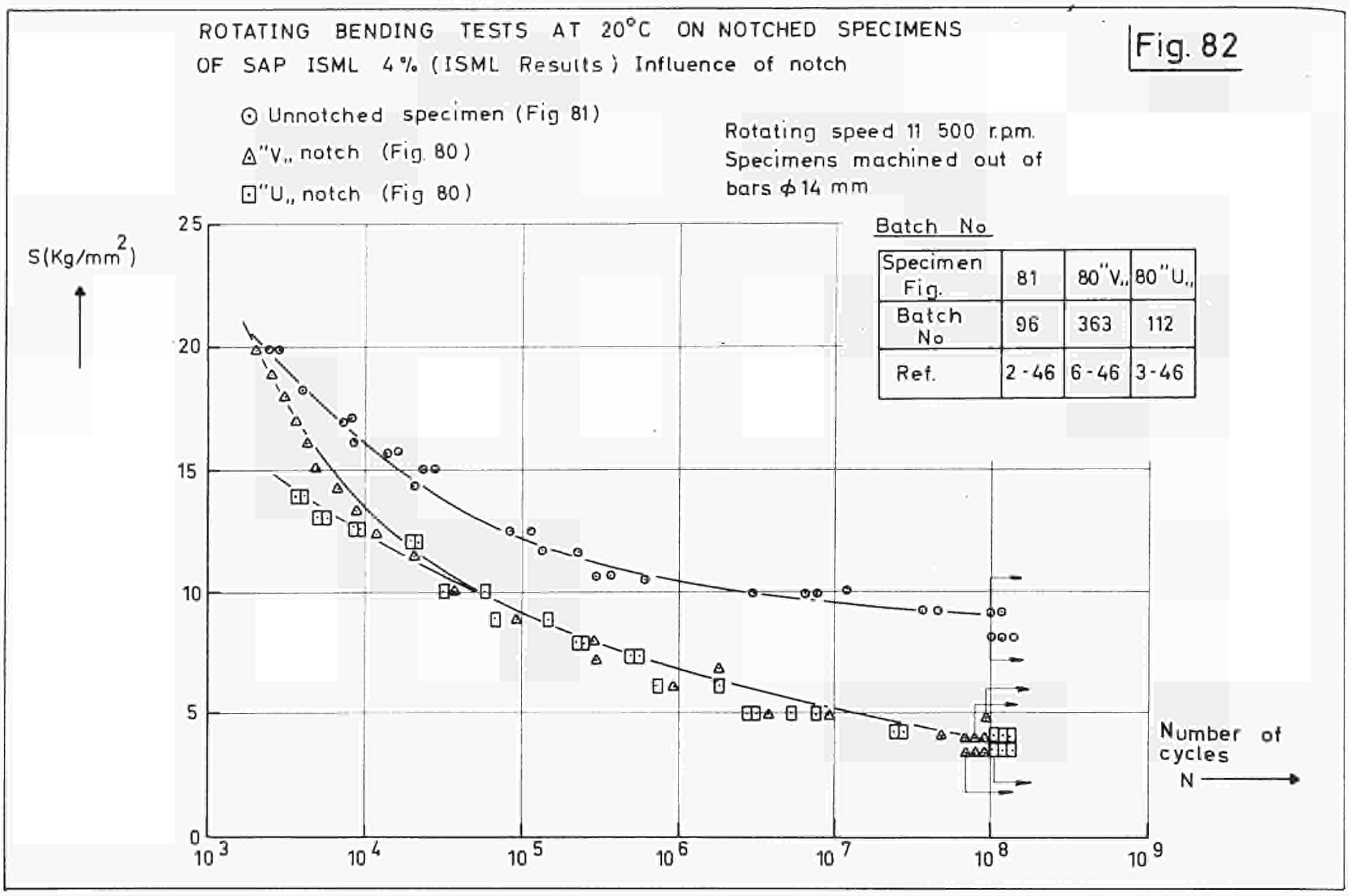
ROTATING BENDING TESTS AT 20°C ON NOTCHED SPECIMENS
OF SAP ISML 4% (ISML Results) Influence of notch
⊙ Unnotched specimen (Fig 81)
△ "V" notch (Fig. 80)
⊡ "U" notch (Fig 80)
Rotating speed 11 500 r.p.m.
Specimens machined out of bars ϕ 14 mm
Batch No
Specimen Fig. | 81 | 80 "V" | 80 "U"
Batch No | 96 | 363 | 112
Ref. | 2-46 | 6-46 | 3-46
S (Kg/mm²)
25
20
15
10
5
0
10³
10⁴
10⁵
10⁶
10⁷
10⁸
10⁹
Number of cycles N

Fig. 83

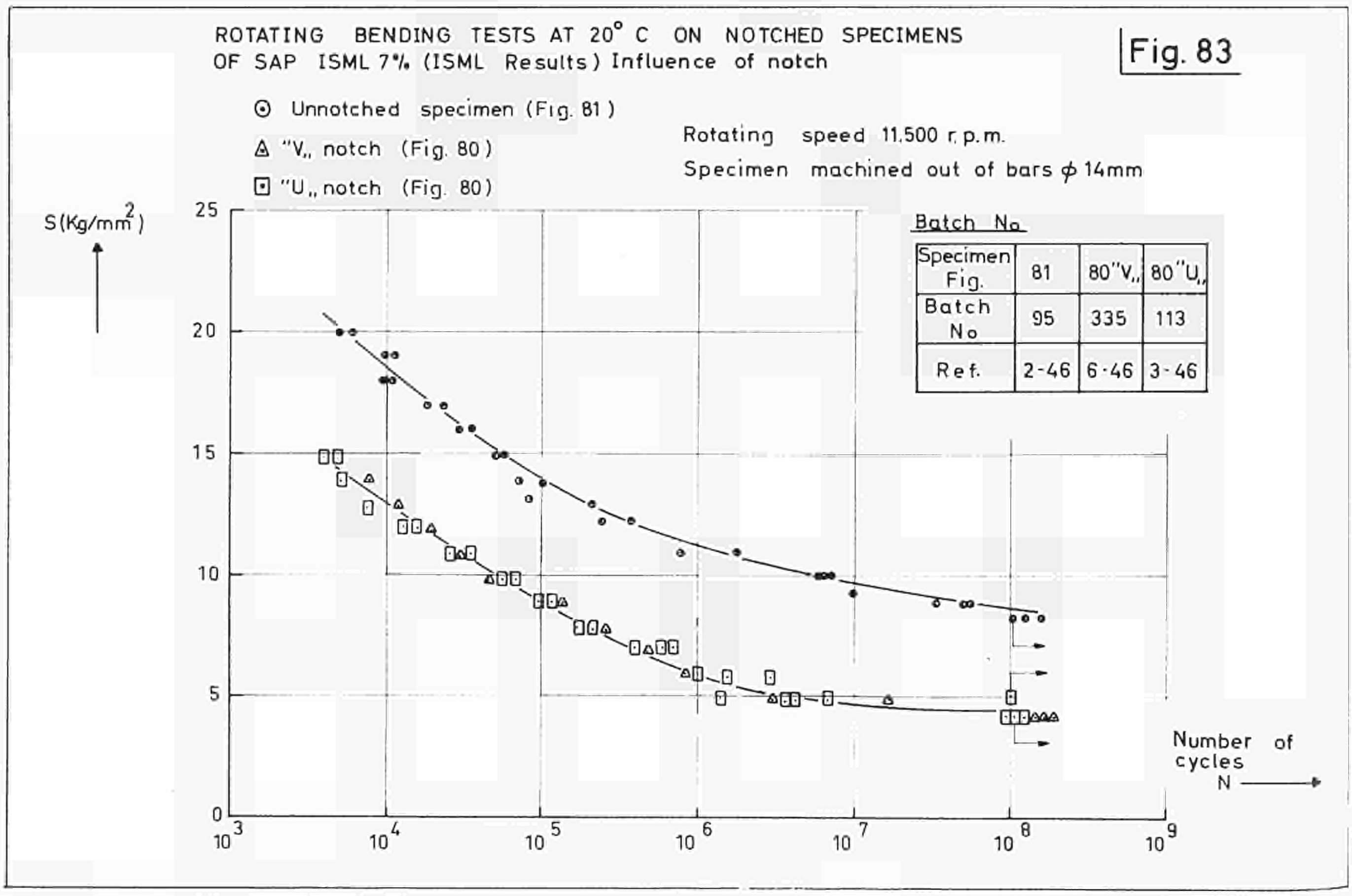
ROTATING BENDING TESTS AT 20° C ON NOTCHED SPECIMENS
OF SAP ISML 7% (ISML Results) Influence of notch
⊙ Unnotched specimen (Fig. 81)
△ "V" notch (Fig. 80)
⊡ "U" notch (Fig. 80)
Rotating speed 11.500 r.p.m.
Specimen machined out of bars ϕ 14mm
Batch No
Specimen Fig. | 81 | 80 "V" | 80 "U"
Batch No | 95 | 335 | 113
Ref. | 2-46 | 6-46 | 3-46
S (Kg/mm²)
25
20
15
10
5
0
10³
10⁴
10⁵
10⁶
10⁷
10⁸
10⁹
Number of cycles N

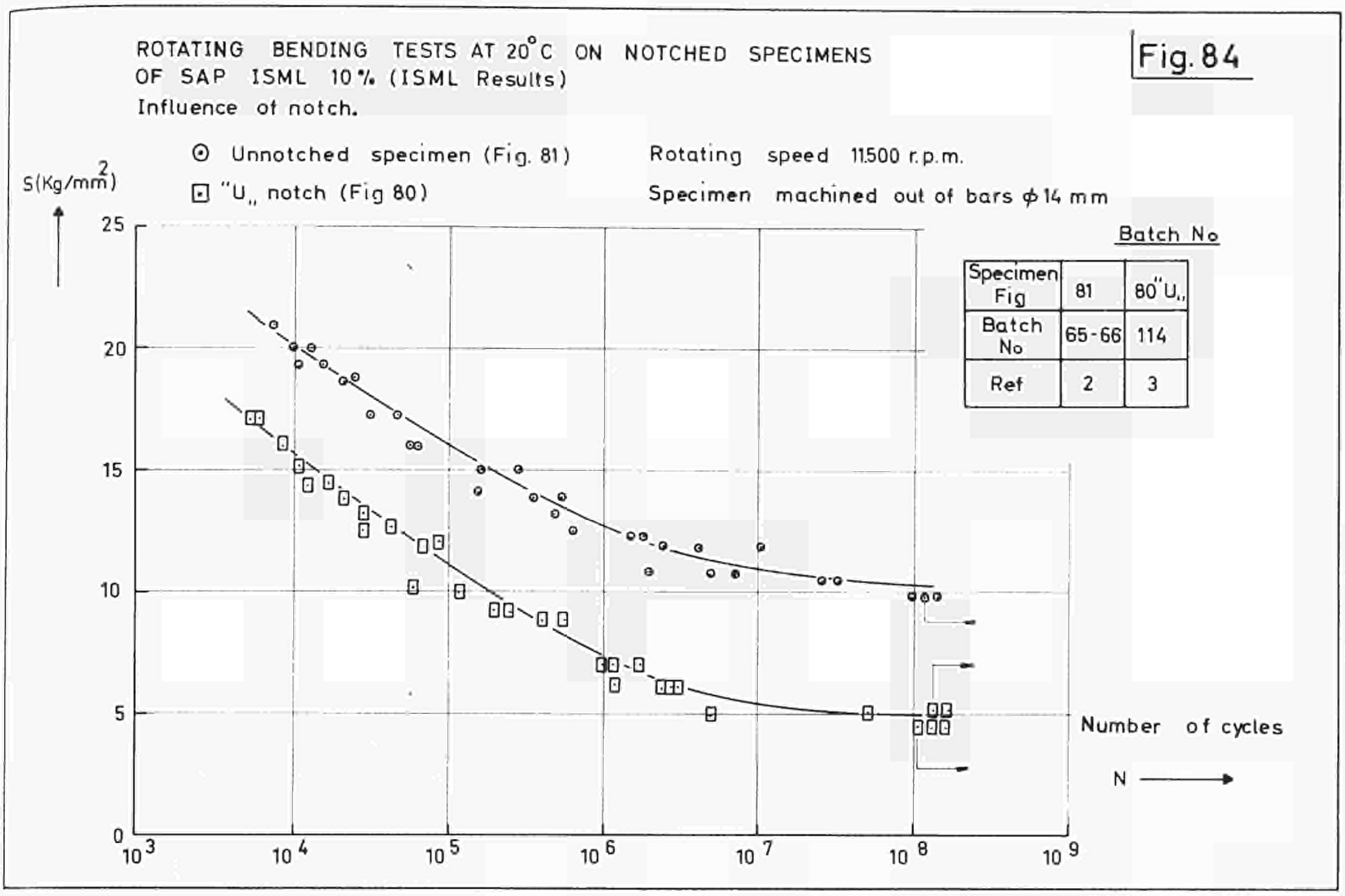
ROTATING BENDING TESTS AT 20°C ON NOTCHED SPECIMENS
OF SAP ISML 10% (ISML Results)
Influence of notch.
Unnotched specimen (Fig. 81)
"U" notch (Fig 80)
Rotating speed 11.500 r.p.m.
Specimen machined out of bars ϕ 14 mm
S (Kg/mm²)
Batch No
Specimen Fig | 81 | 80"U"
Batch No | 65-66 | 114
Ref | 2 | 3
Number of cycles
N

Fig. 84

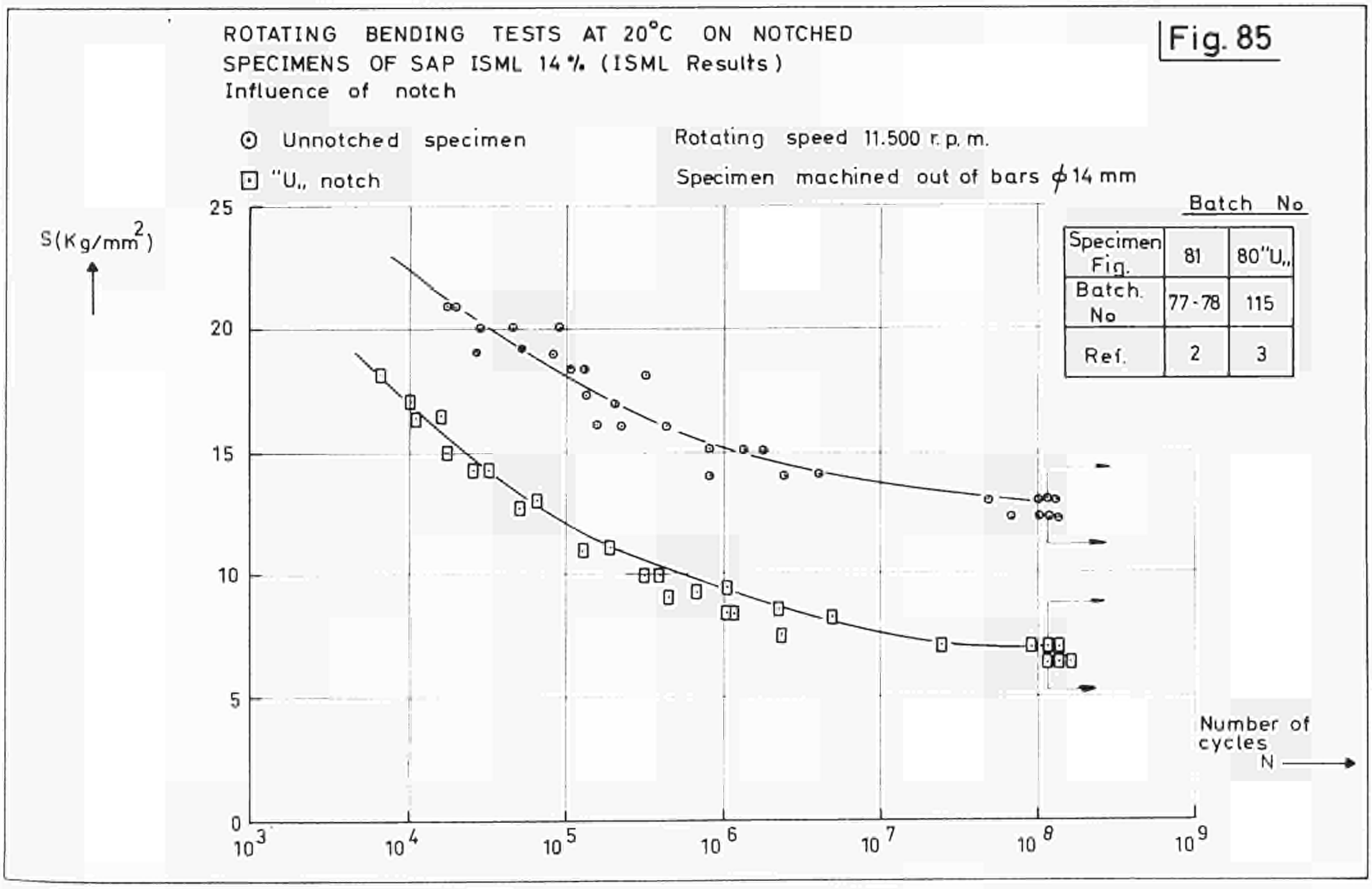
ROTATING BENDING TESTS AT 20°C ON NOTCHED
SPECIMENS OF SAP ISML 14% (ISML Results)
Influence of notch
Unnotched specimen
"U" notch
Rotating speed 11.500 r.p.m.
Specimen machined out of bars ϕ 14 mm
S (Kg/mm²)
Batch No
Specimen Fig. | 81 | 80"U"
Batch. No | 77-78 | 115
Ref. | 2 | 3
Number of cycles
N

Fig. 85

[redacted]I - F[redacted]HED [redacted]S

E[redacted]

HISTOGRAMS OF THE TENSILE PROPERTIES
AT 20°C OF SAP ISML (Different extrusion ratios)
ISML Results (Ref. 11)

FIG. 86

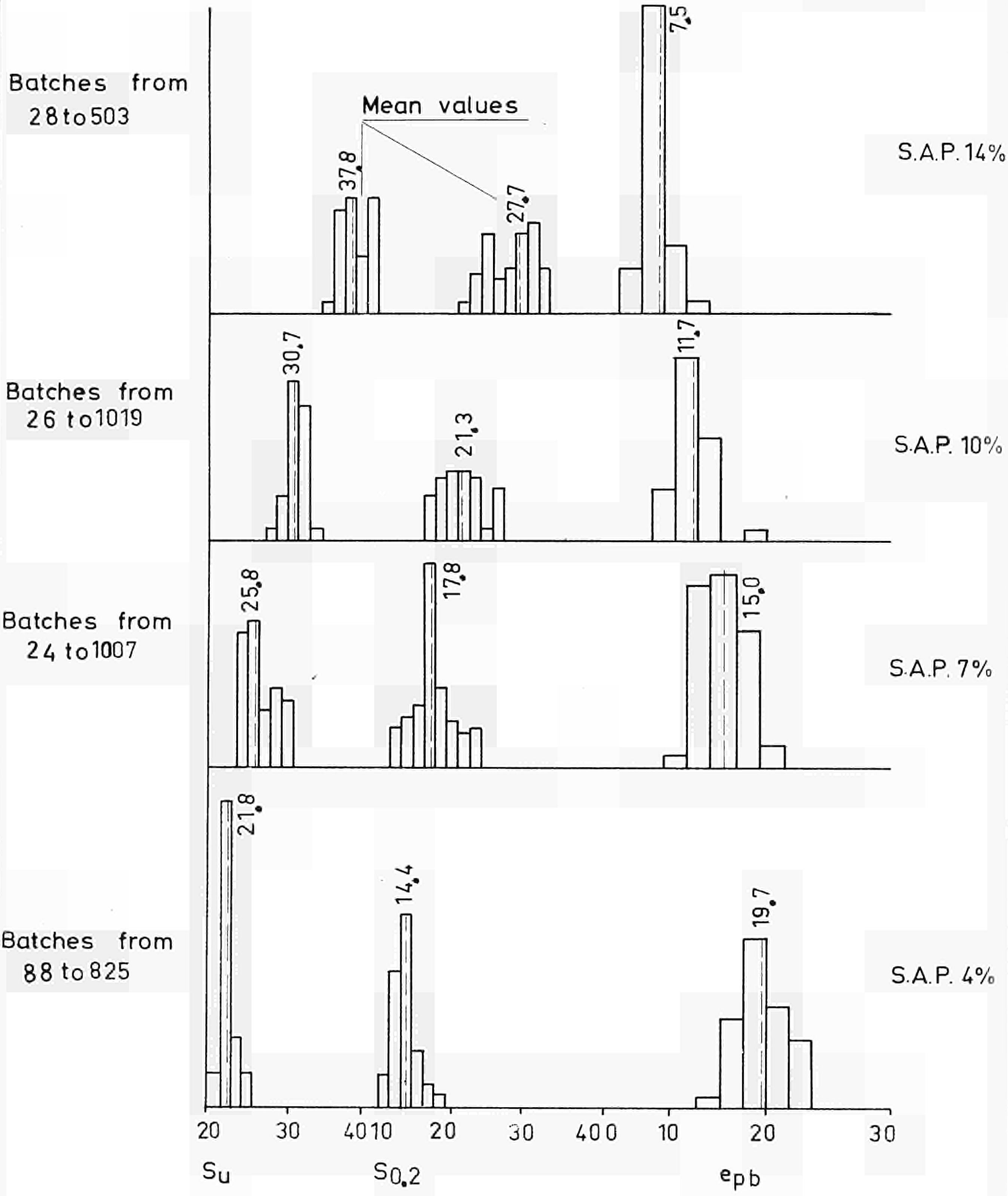

HISTOGRAMS OF THE TENSILE PROPERTIES AT 400°C OF SAP ISML (Different extrusion ratios) ISML Results (Ref 11)

FIG. 87

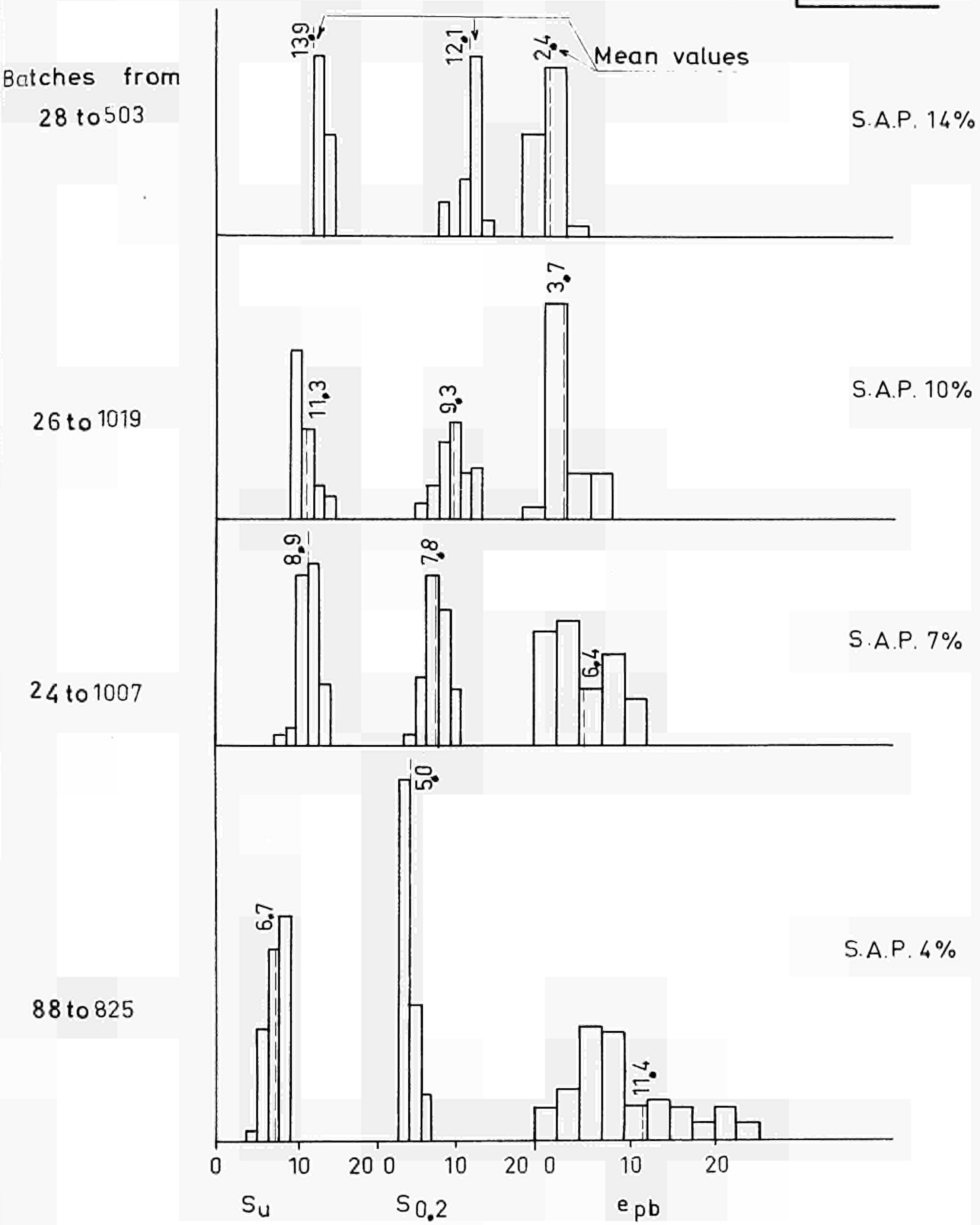

TENSILE TESTS AT 450°C ON BARS OF SAP ISML 7%
(ISML Results Ref. 35 Batch No 1810 to 2623)
Histograms of Maximum Tensile Stress (Su) and plastic strain at breaking point.

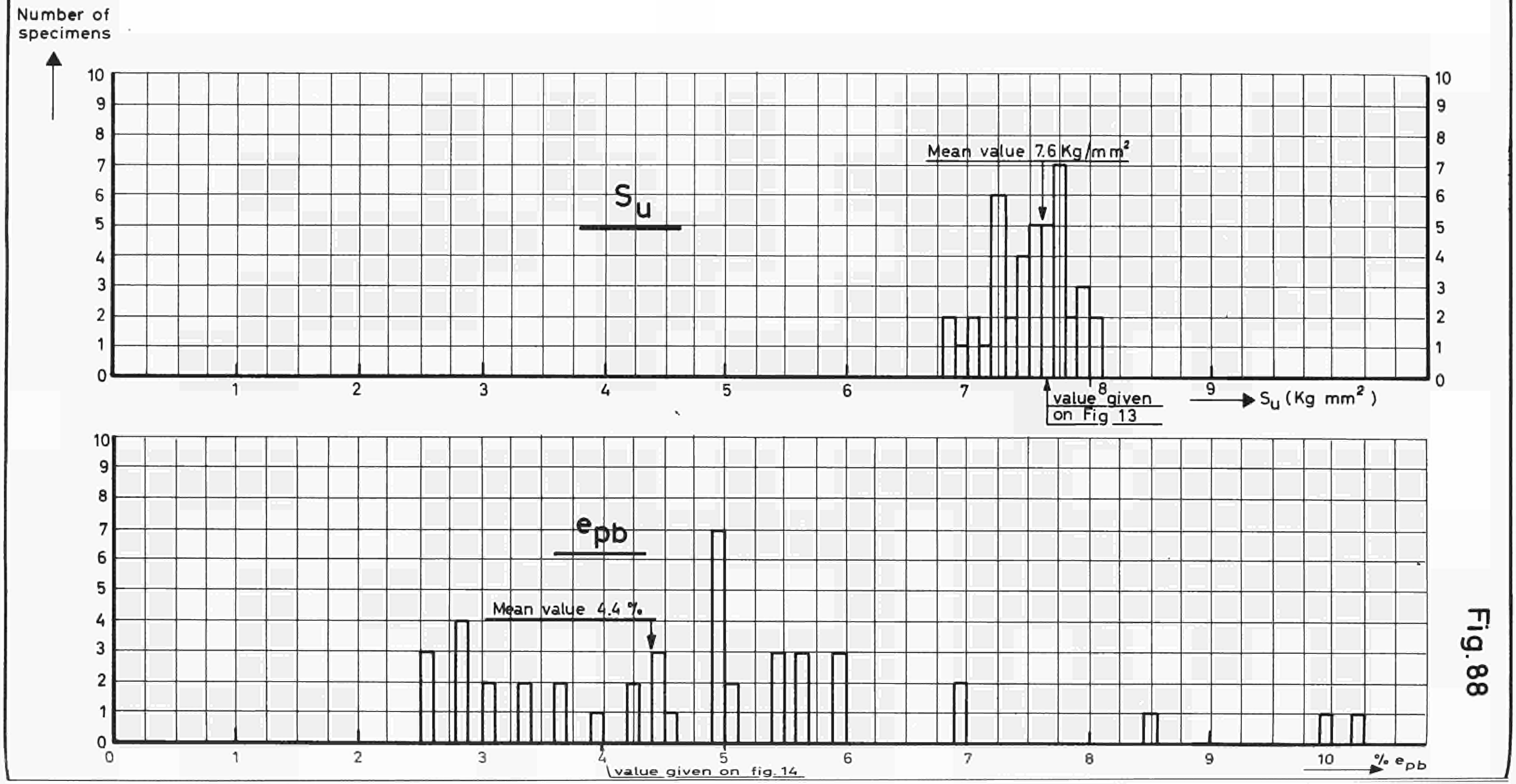

Fig. 88

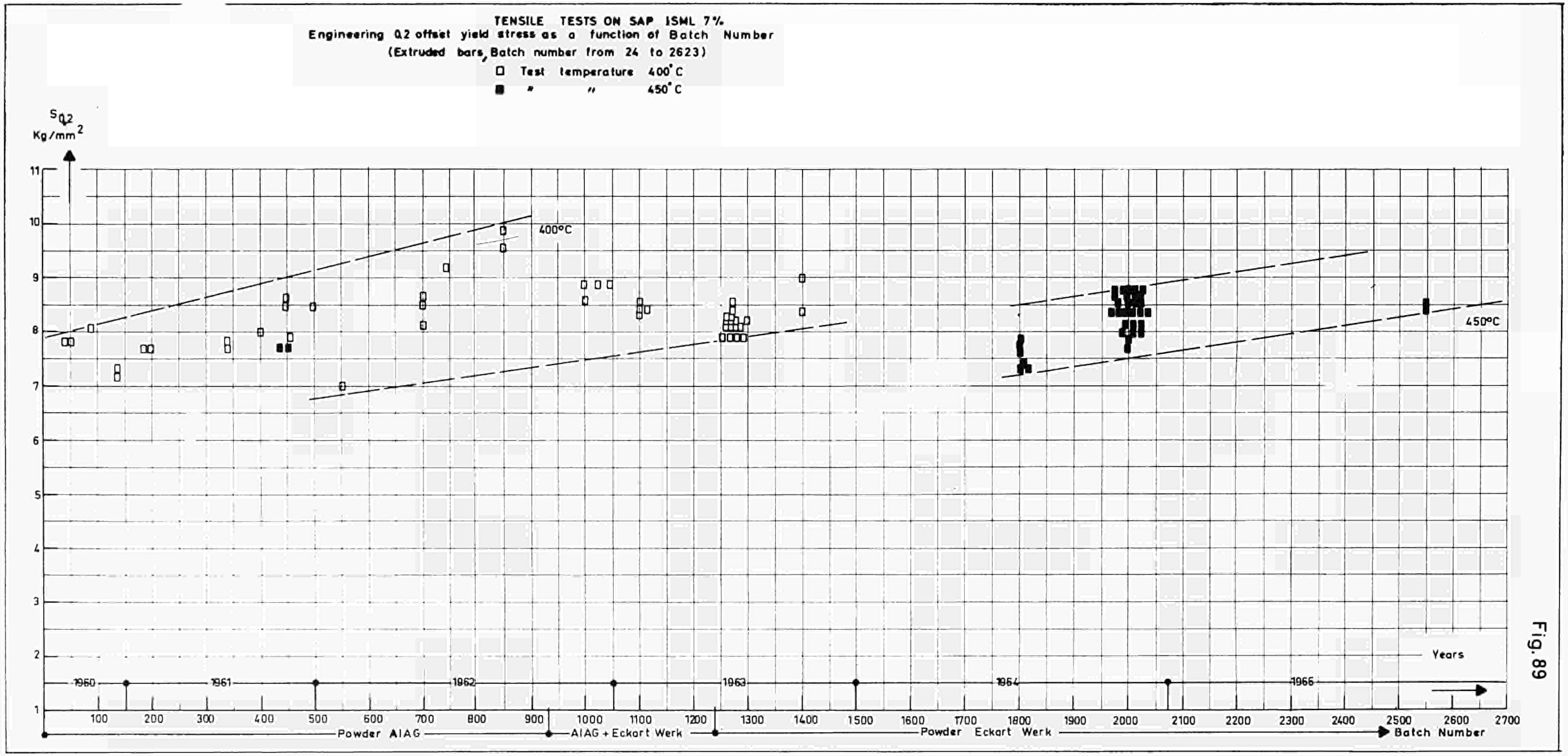
TENSILE TESTS ON SAP ISML 7%
Engineering 0.2 offset yield stress as a function of Batch Number
(Extruded bars, Batch number from 24 to 2623)
Test temperature 400° C
" " 450° C
S0.2 Kg/mm2
400°C
450°C
Years
1960
1961
1962
1963
1964
1966
Powder AIAG
AIAG + Eckart Werk
Powder Eckart Werk
Batch Number

Fig. 89

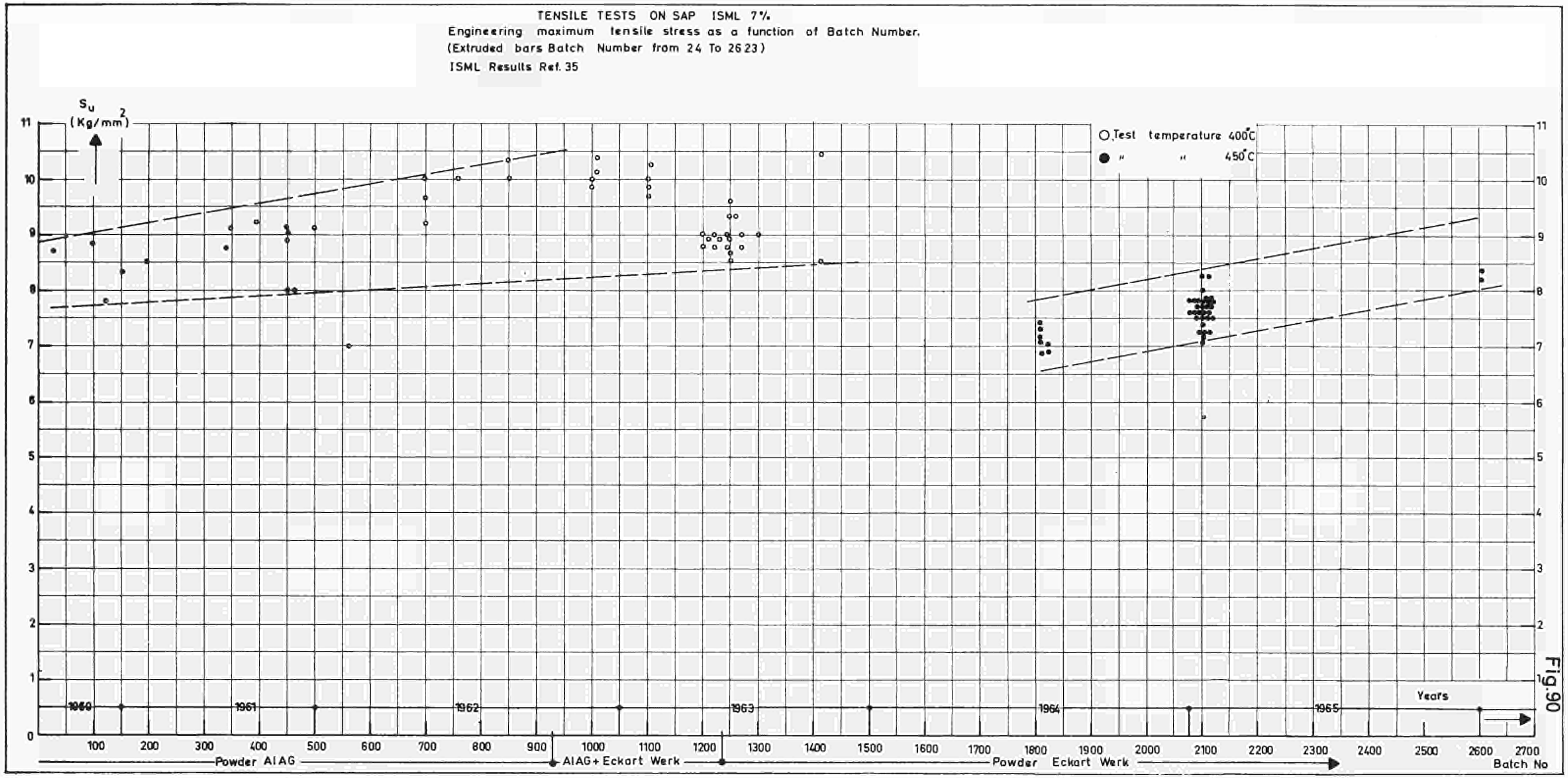
TENSILE TESTS ON SAP ISML 7%
Engineering maximum tensile stress as a function of Batch Number.
(Extruded bars Batch Number from 24 To 2623)
ISML Results Ref. 35
Su (Kg/mm2)
O Test temperature 400°C
● " " 450°C
1960
1961
1962
1963
1964
1965
Years
Powder AIAG
AIAG + Eckart Werk
Powder Eckart Werk
Batch No

Fig.90

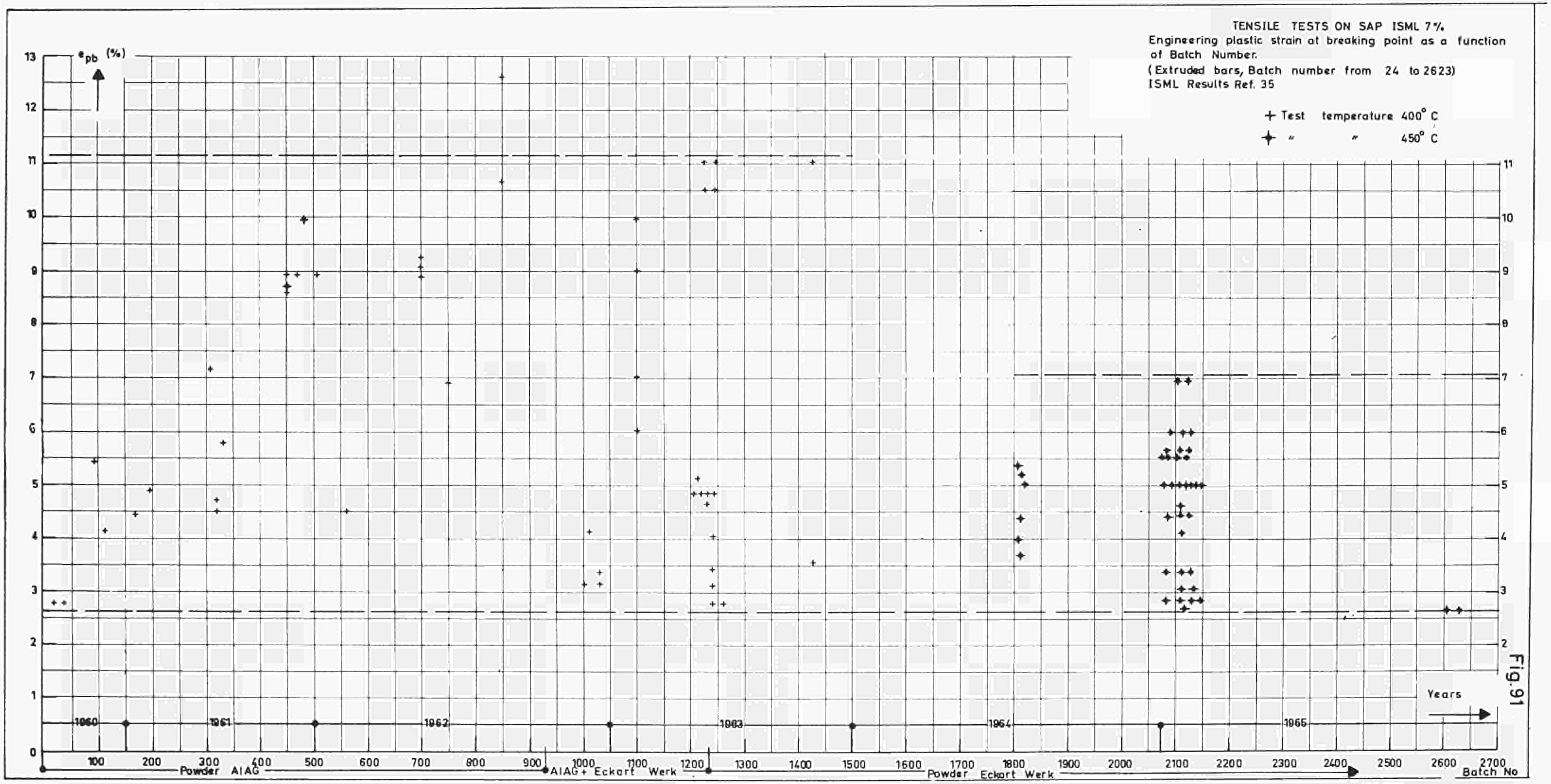
TENSILE TESTS ON SAP ISML 7%
Engineering plastic strain at breaking point as a function of Batch Number.
(Extruded bars, Batch number from 24 to 2623)
ISML Results Ref. 35
+ Test temperature 400° C
" " 450° C
e_{pb} (%)
Years
1960
1961
1962
1963
1964
1965
Powder AIAG
AIAG + Eckart Werk
Powder Eckart Werk
Batch No
Fig. 91

YOUNG'S MODULUS AT 20°C OF SAP ISML VS OXIDE CONTENT

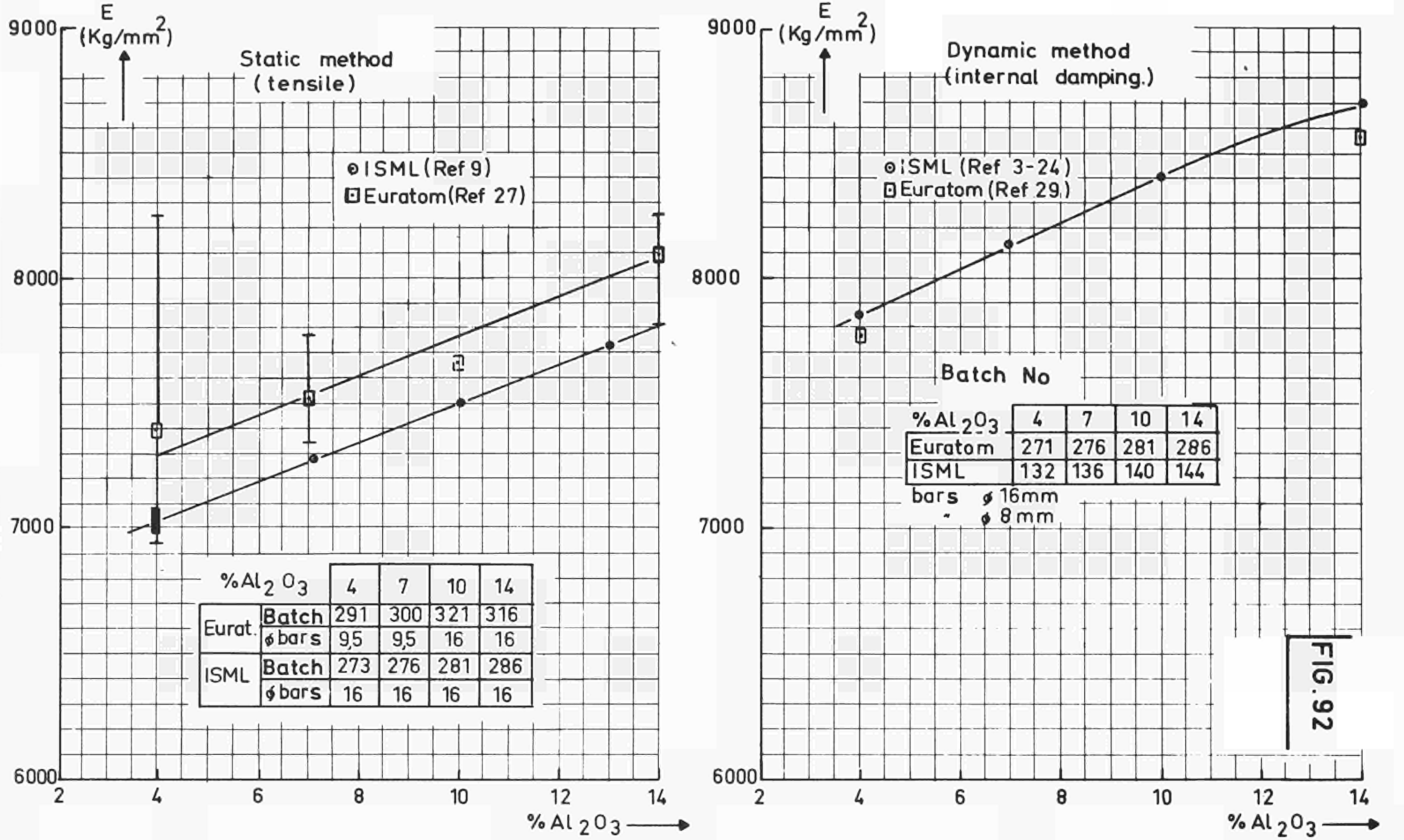

% Al_2O_3		4	7	10	14
Eurat.	Batch	291	300	321	316
	ø bars	9,5	9,5	16	16
ISML	Batch	273	276	281	286
	ø bars	16	16	16	16

Batch No

% Al_2O_3	4	7	10	14
Euratom	271	276	281	286
ISML	132	136	140	144

bars ø 16mm
" ø 8 mm

FIG. 92

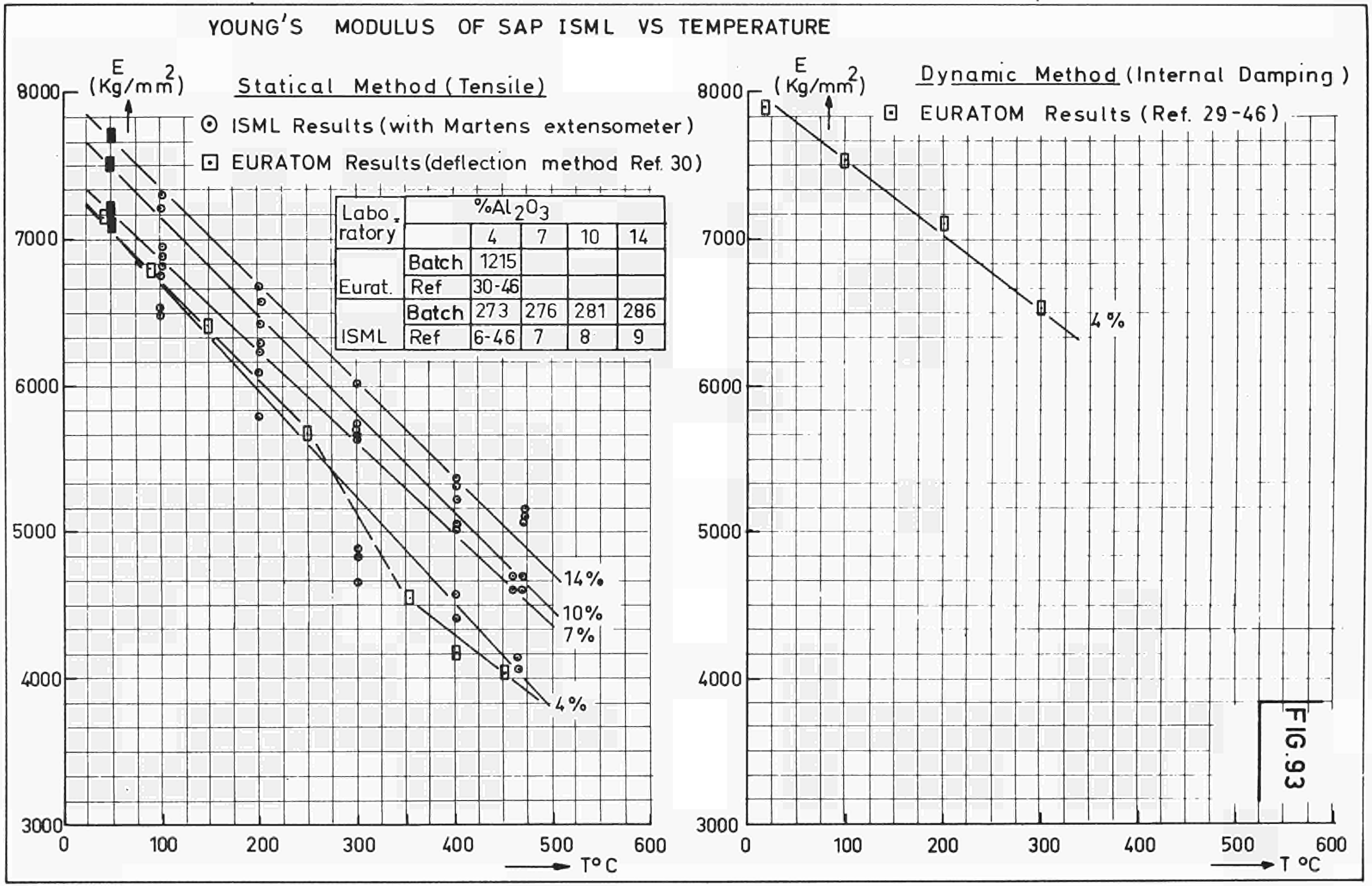
YOUNG'S MODULUS OF SAP ISML VS TEMPERATURE
E (Kg/mm2)
Statical Method (Tensile)
ISML Results (with Martens extensometer)
EURATOM Results (deflection method Ref. 30)
Laboratory
%Al2O3
4 7 10 14
Eurat. Batch 1215
Ref 30-46
ISML Batch 273 276 281 286
Ref 6-46 7 8 9
14%
10%
7%
4%
8000
7000
6000
5000
4000
3000
0 100 200 300 400 500 600
T°C
Dynamic Method (Internal Damping)
EURATOM Results (Ref. 29-46)
4 %
T °C

FIG. 93

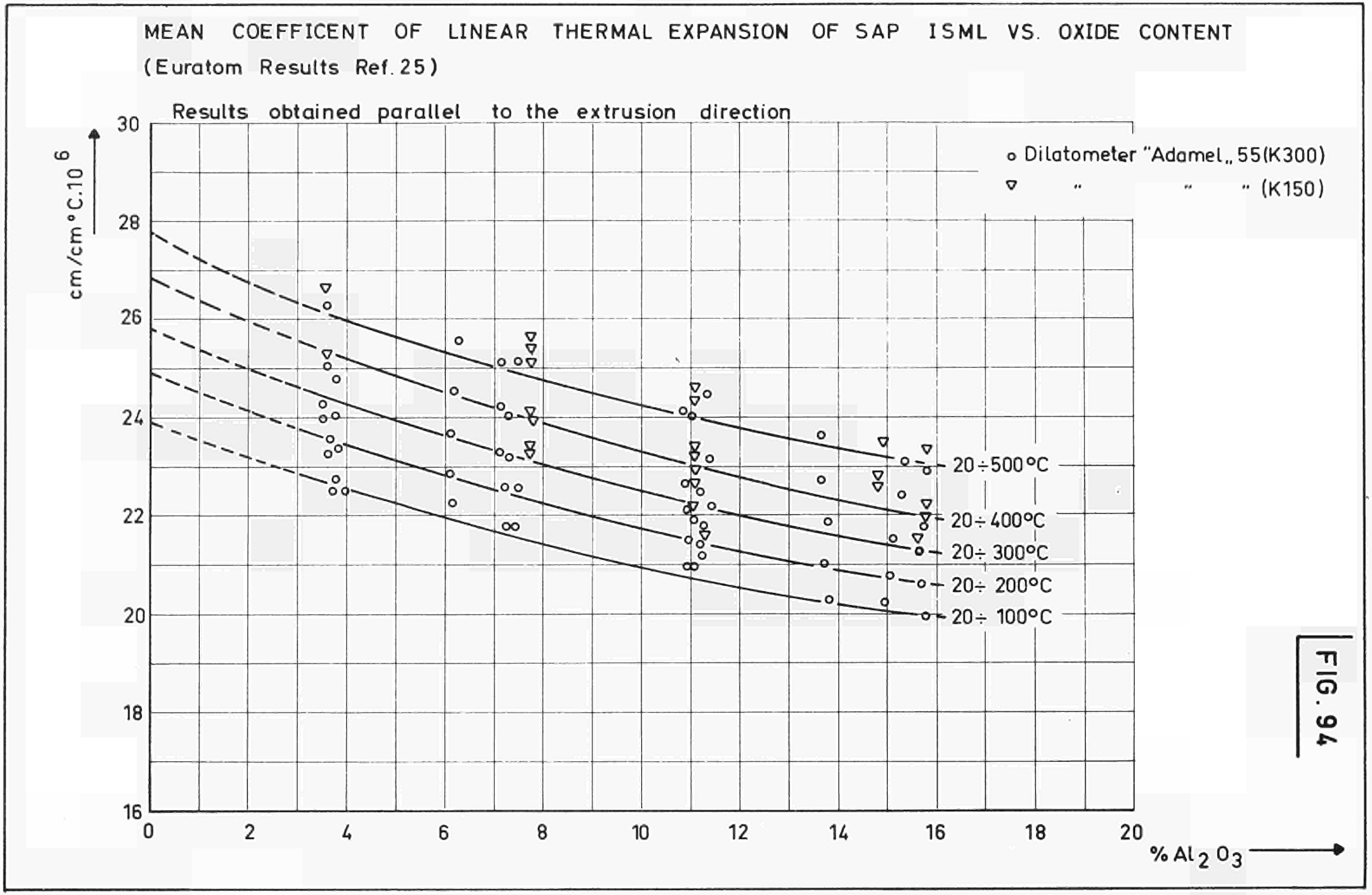

MEAN COEFFICENT OF LINEAR THERMAL EXPANSION OF SAP ISML VS. OXIDE CONTENT
(Euratom Results Ref. 25)
Results obtained parallel to the extrusion direction
cm/cm °C.10 6
o Dilatometer "Adamel„ 55(K300)
▽ " " " (K150)
20÷500°C
20÷400°C
20÷300°C
20÷200°C
20÷100°C
30
28
26
24
22
20
18
16
0
2
4
6
8
10
12
14
16
18
20
% Al 2 O 3

FIG. 94

ELECTRICAL RESISTIVITY AT 20°C OF SAP ISML WITH VARIOUS OXIDE CONTENTS (Euratom and ISML results)

	Conventional signs	Material	Ref. No
Euratom results	○	Aluminium A 5 N	50
	●	SAP(% Al_2O_3 average of 6 analyses)	50
	□	Aluminium 99.99 %	54
	■	SAP (real Al_2O_3 content)	
ISML results	+	Aluminium 99.995 %	9
	×	SAP(% Al_2O_3: nominal value	26

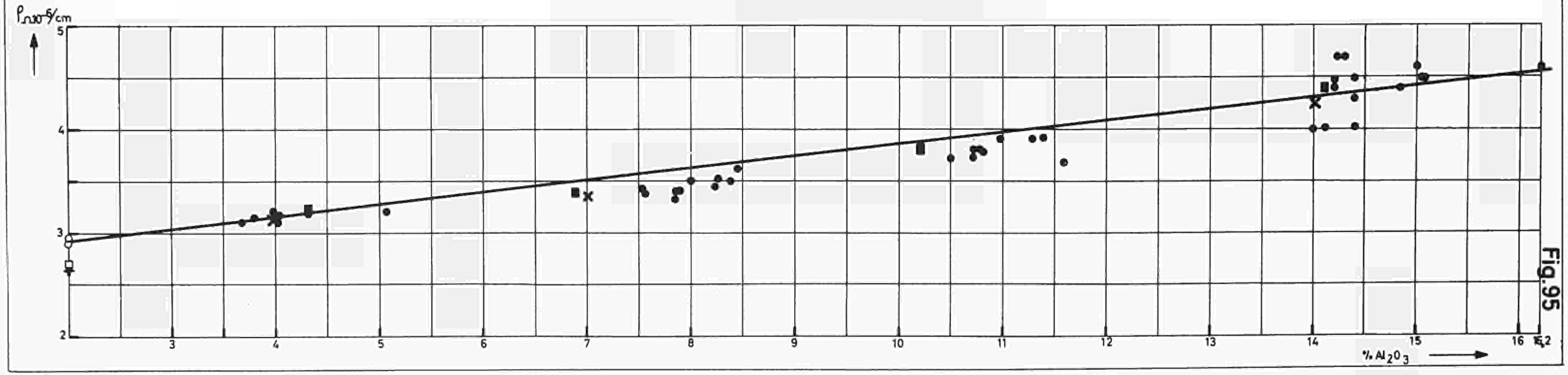

Fig. 95

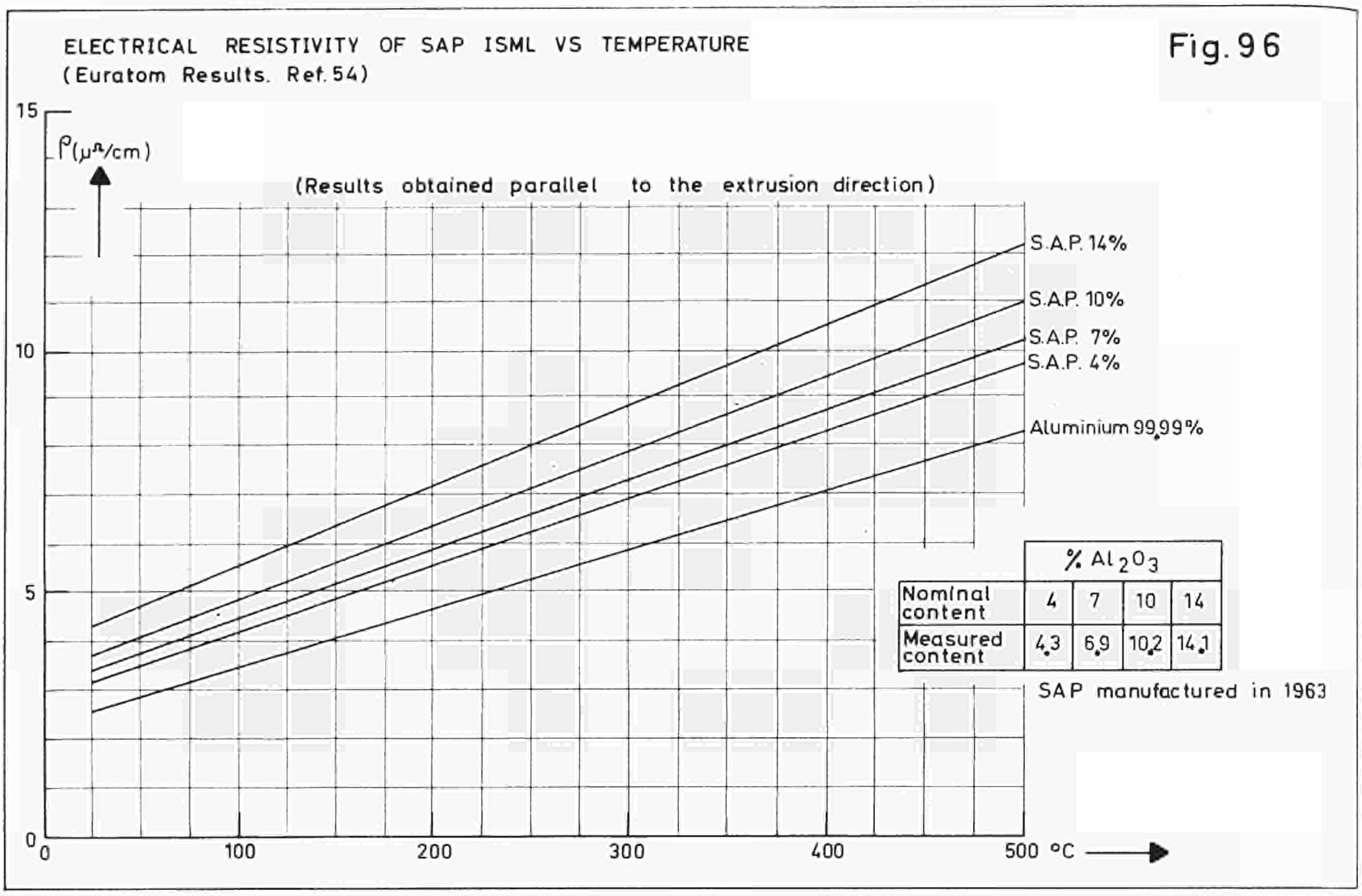
ELECTRICAL RESISTIVITY OF SAP ISML VS TEMPERATURE
(Euratom Results. Ref. 54)
Fig. 96
ρ(μΩ/cm)
(Results obtained parallel to the extrusion direction)
S.A.P. 14%
S.A.P. 10%
S.A.P. 7%
S.A.P. 4%
Aluminium 99.99%
% Al2O3
Nominal content
4
7
10
14
Measured content
4.3
6.9
10.2
14.1
SAP manufactured in 1963
15
10
5
0
0
100
200
300
400
500 °C

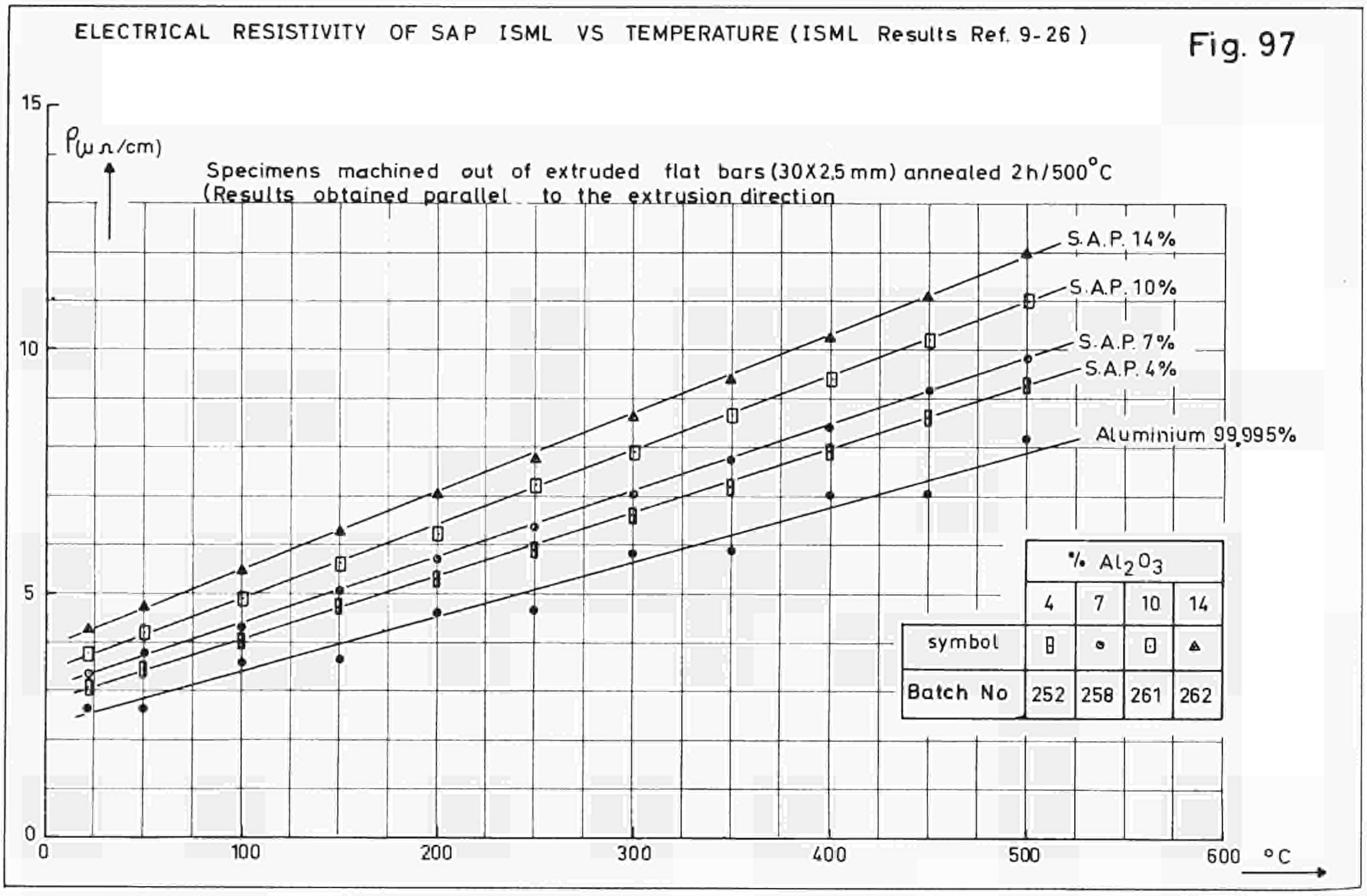
ELECTRICAL RESISTIVITY OF SAP ISML VS TEMPERATURE (ISML Results Ref. 9-26)
Fig. 97
ρ(μΩ/cm)
Specimens machined out of extruded flat bars (30X2.5 mm) annealed 2h/500°C
(Results obtained parallel to the extrusion direction
S.A.P. 14%
S.A.P. 10%
S.A.P. 7%
S.A.P. 4%
Aluminium 99.995%
% Al2O3
4
7
10
14
symbol
Batch No
252
258
261
262
15
10
5
0
0
100
200
300
400
500
600 °C

ELECTRICAL RESISTIVITY AT 100°C AND 500°C OF SAP ISML VS. OXIDE CONTENT
(Euratom Results Ref 54)

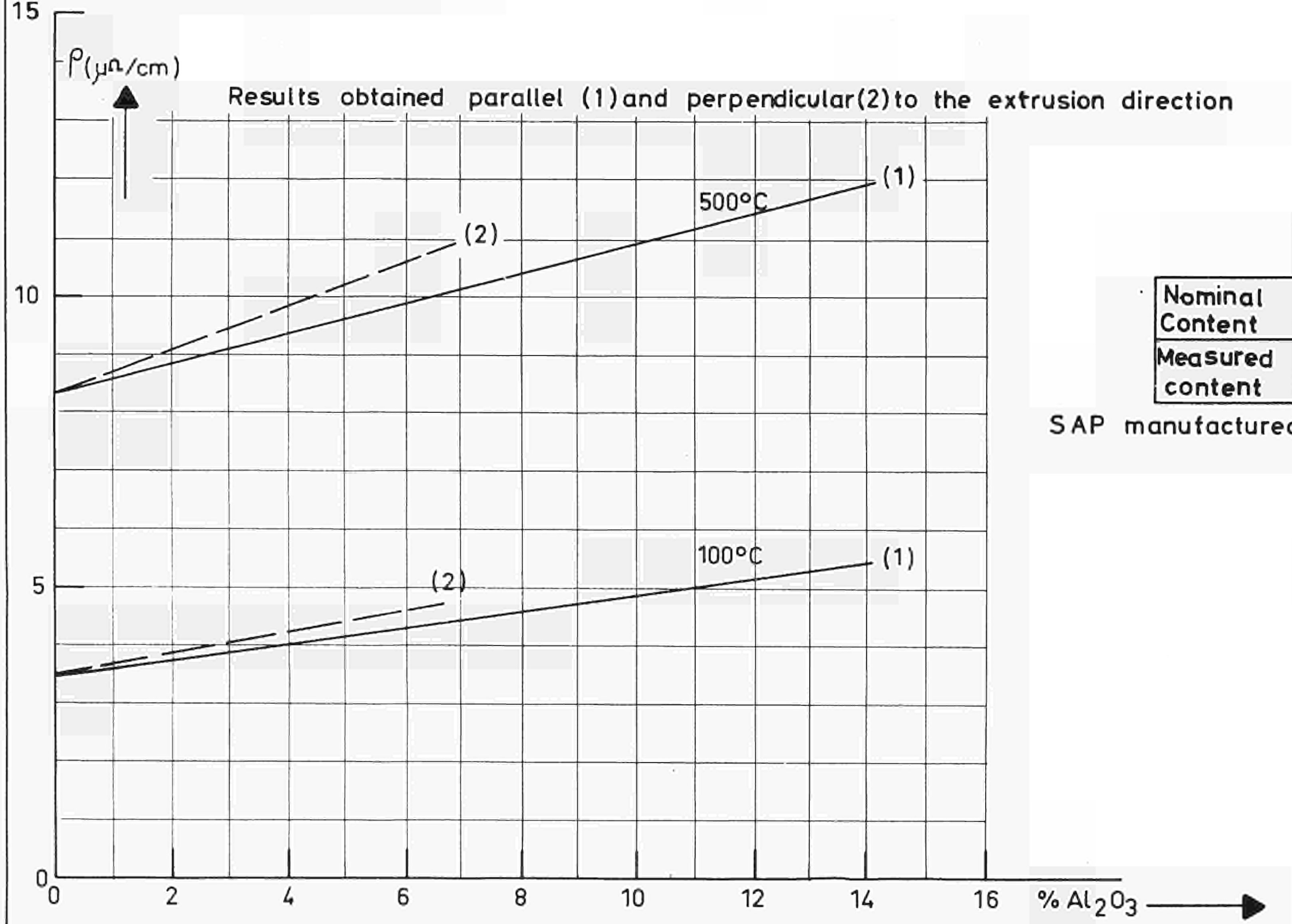

	% Al_2O_3			
Nominal Content	4	7	10	14
Measured content	4.3	6.9	10.7	14.1

SAP manufactured in 1963

FIG. 98

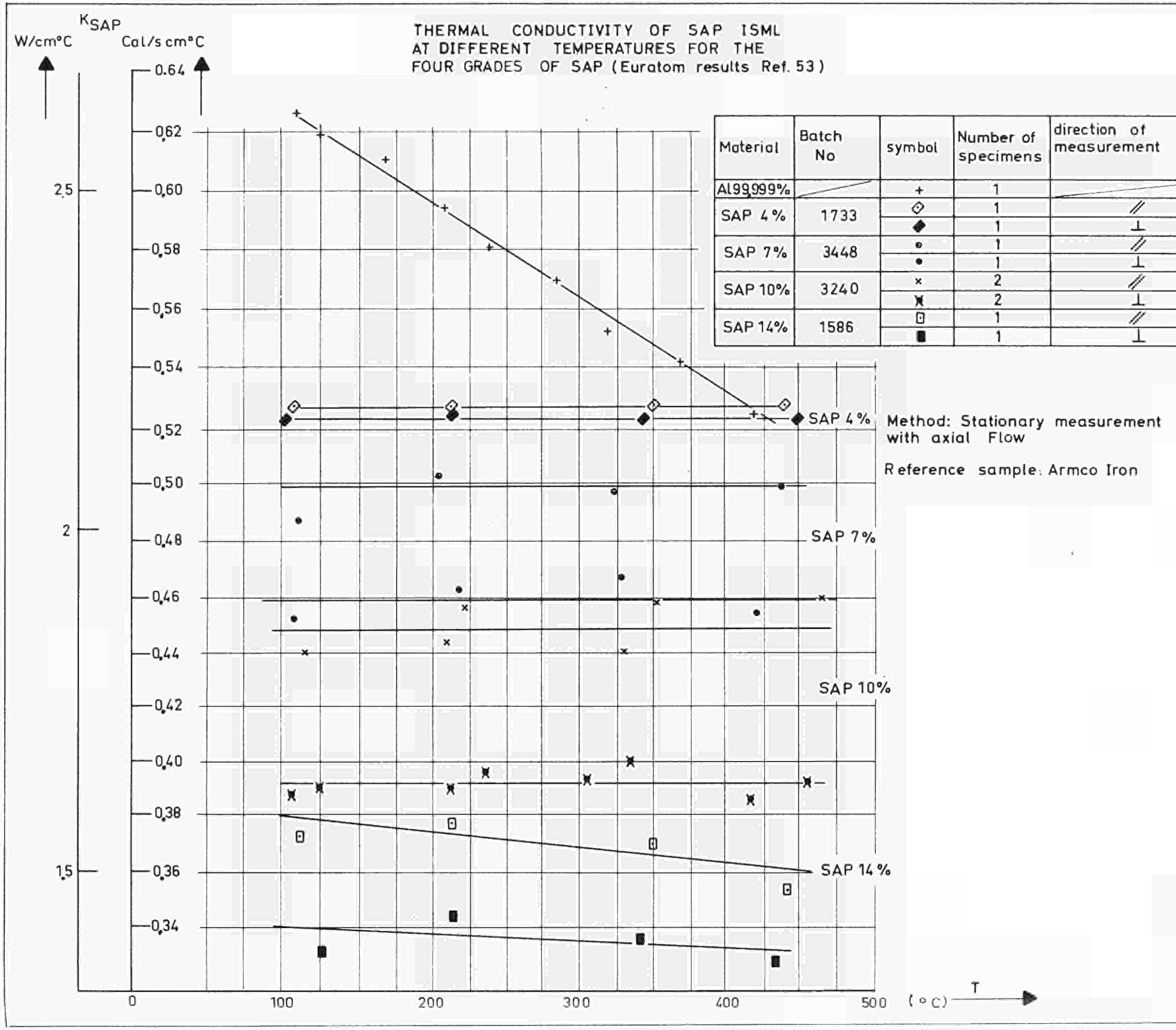
THERMAL CONDUCTIVITY OF SAP ISML
AT DIFFERENT TEMPERATURES FOR THE
FOUR GRADES OF SAP (Euratom results Ref. 53)
W/cm°C
K SAP
Cal/s cm°C
0.64
0,62
0,60
0,58
0,56
0,54
0,52
0,50
0,48
0,46
0,44
0,42
0,40
0,38
0,36
0,34
2,5
2
1,5
0
100
200
300
400
500
(° C)
T
Material
Batch No
symbol
Number of specimens
direction of measurement
Al99,999%
1
SAP 4%
1733
1
1
SAP 7%
3448
1
1
SAP 10%
3240
2
2
SAP 14%
1586
1
1
SAP 4%
SAP 7%
SAP 10%
SAP 14%
Method: Stationary measurement with axial Flow
Reference sample: Armco Iron

Fig.99

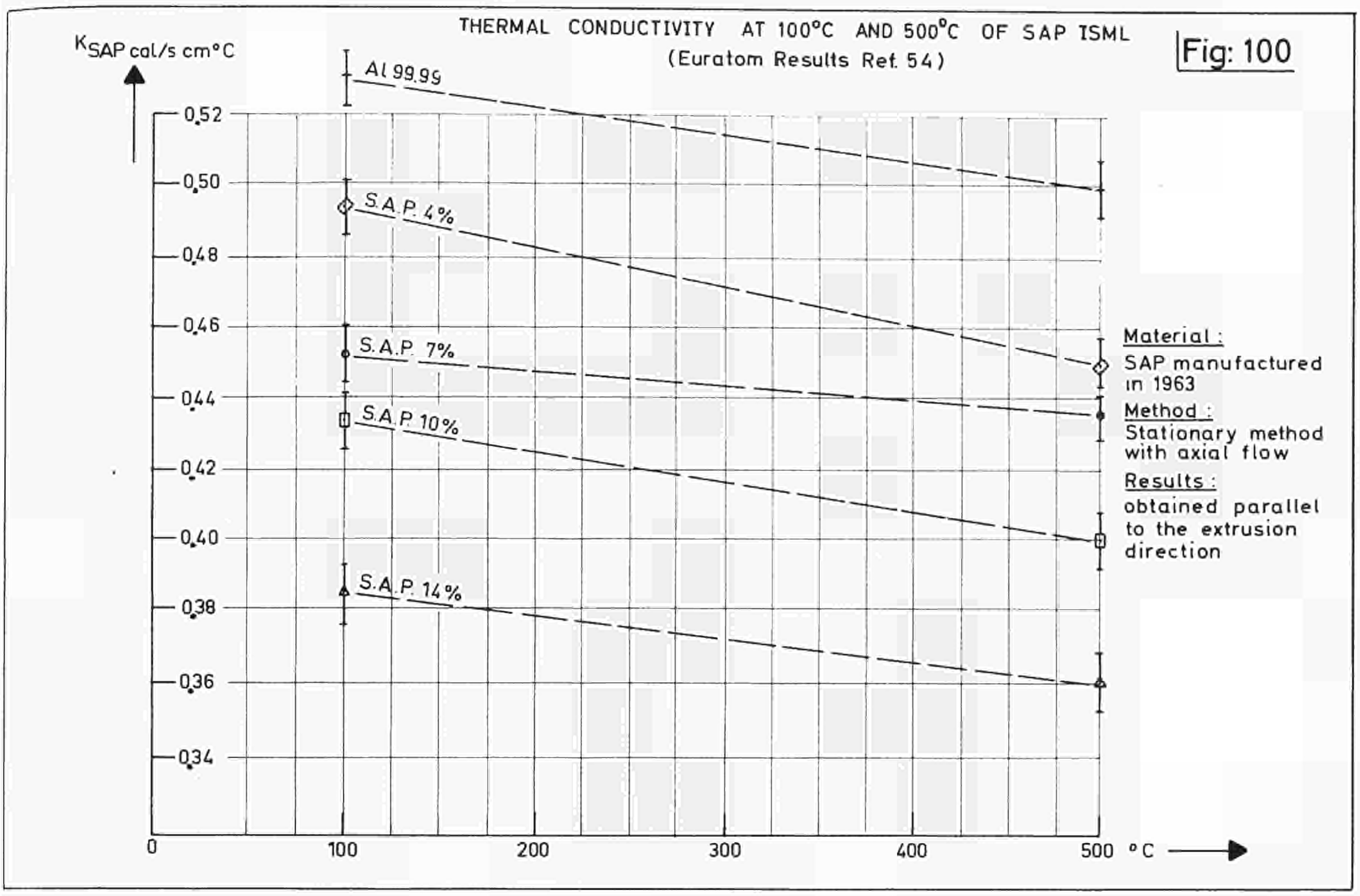

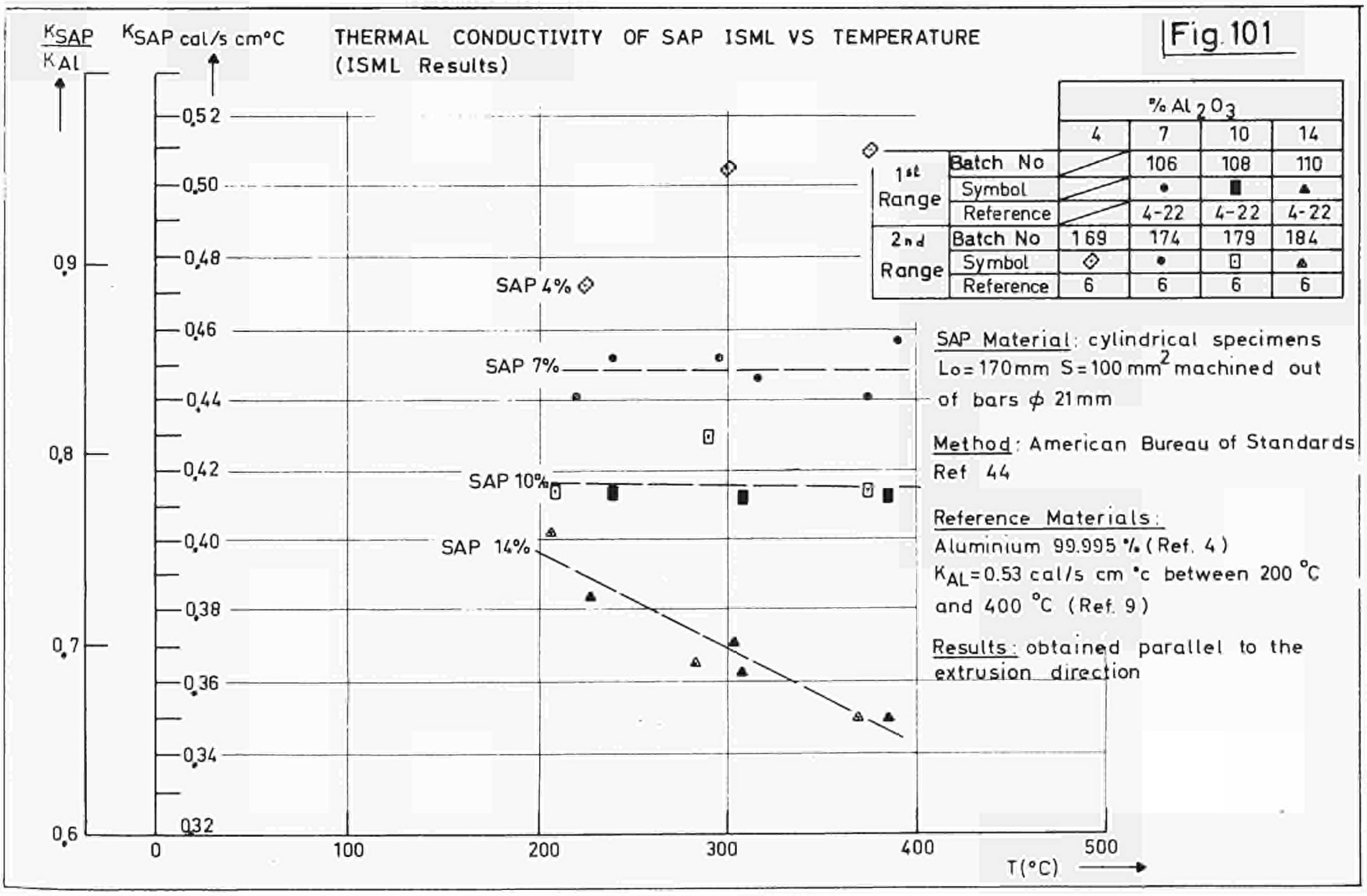

		% Al_2O_3 4	7	10	14
1st Range	Batch No	/	106	108	110
	Symbol	/	•	■	▲
	Reference	/	4-22	4-22	4-22
2nd Range	Batch No	169	174	179	184
	Symbol	◇	•	⊡	▲
	Reference	6	6	6	6

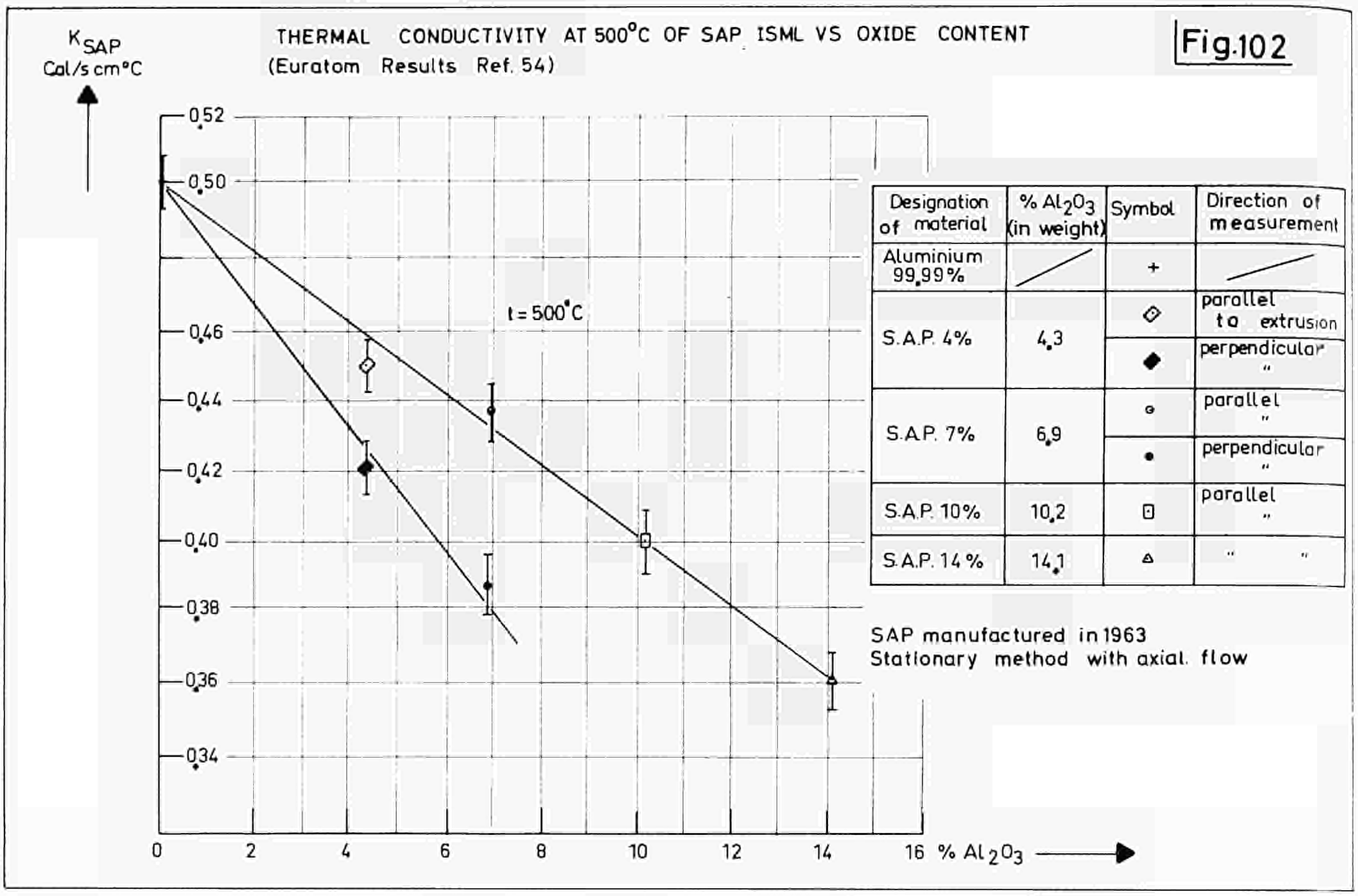

Fig.102

THERMAL CONDUCTIVITY AT 500°C OF SAP ISML VS OXIDE CONTENT (Euratom Results Ref. 54)

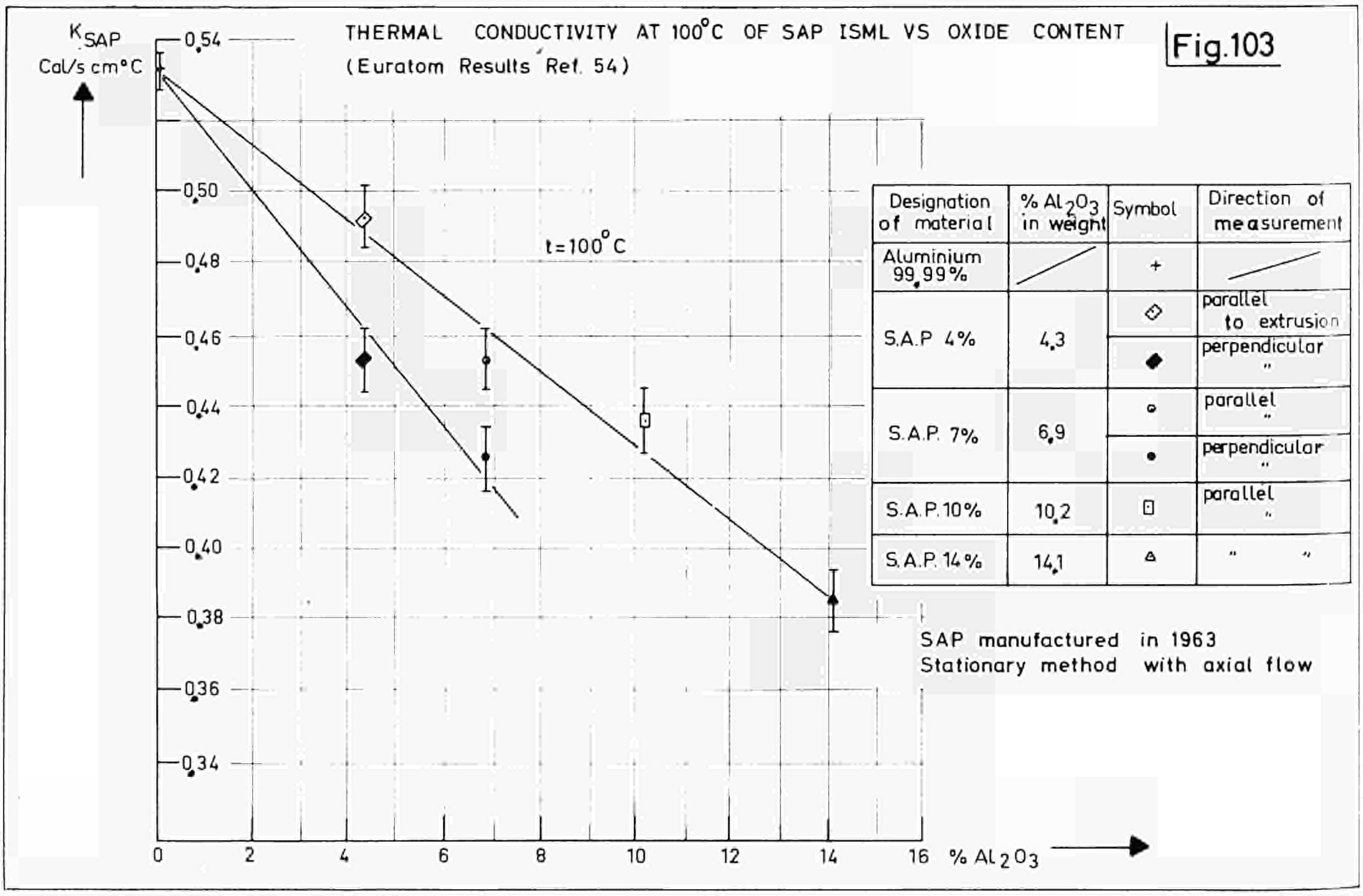

Fig.103

THERMAL CONDUCTIVITY AT 100°C OF SAP ISML VS OXIDE CONTENT (Euratom Results Ref. 54)

DENSITY OF SAP ISML VS NOMINAL GRADES (ISML Results Ref.64)

FIG. 104

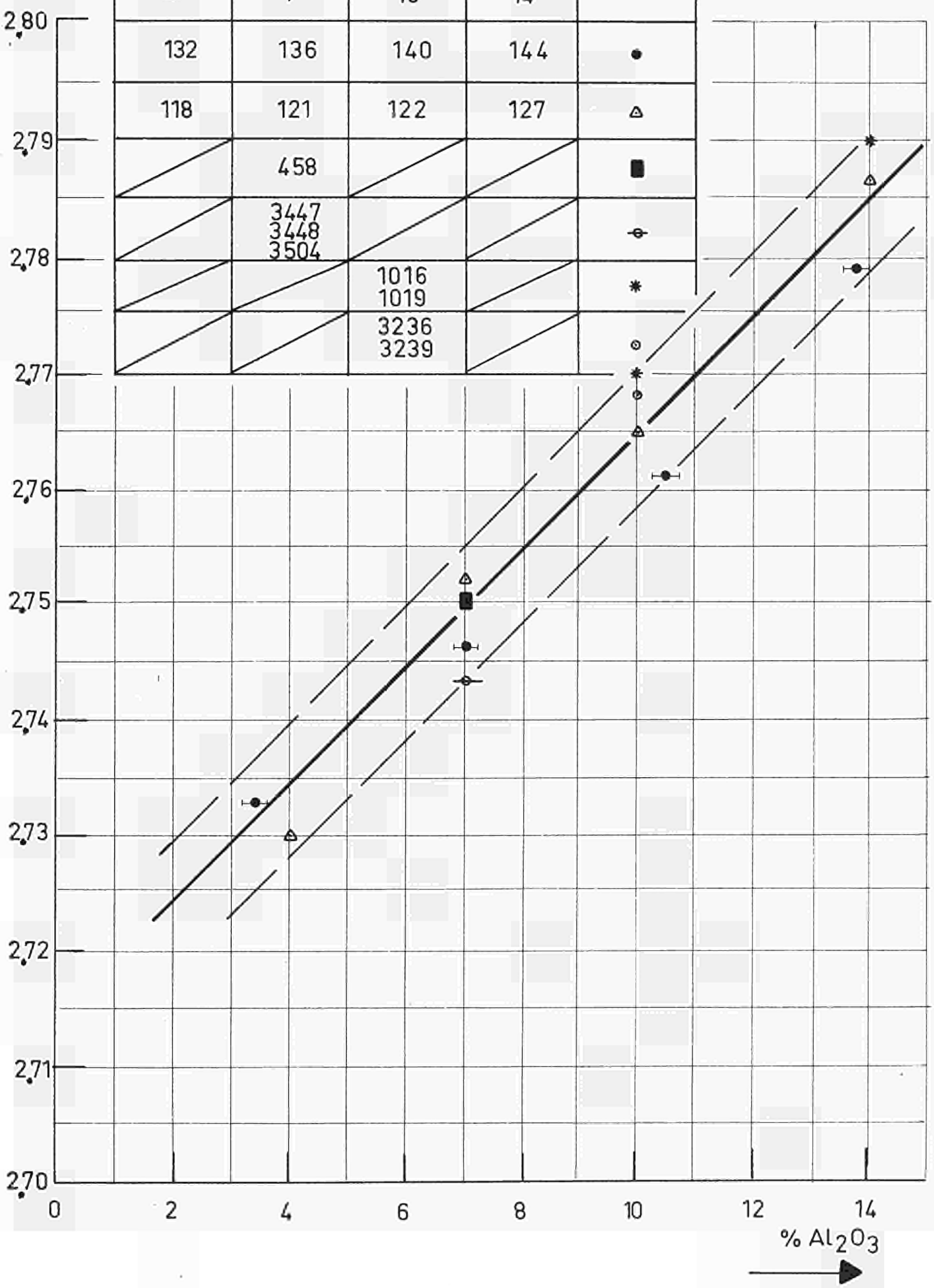

Batch No

% Al_2O_3				Symbol
4	7	10	14	
132	136	140	144	●
118	121	122	127	△
	458			■
	3447 3448 3504			⊖
		1016 1019		*
		3236 3239		○

DENSITY OF SAP ISML VS OXIDE CONTENT
(AEK Risö Results Ref. 99-41)

FIG.104 A

Oxide cont.	3.9	7.1	10,0	14,2	symbol
Batch No	1220	1221	1222	1223	⊙
	from fig 104				— —

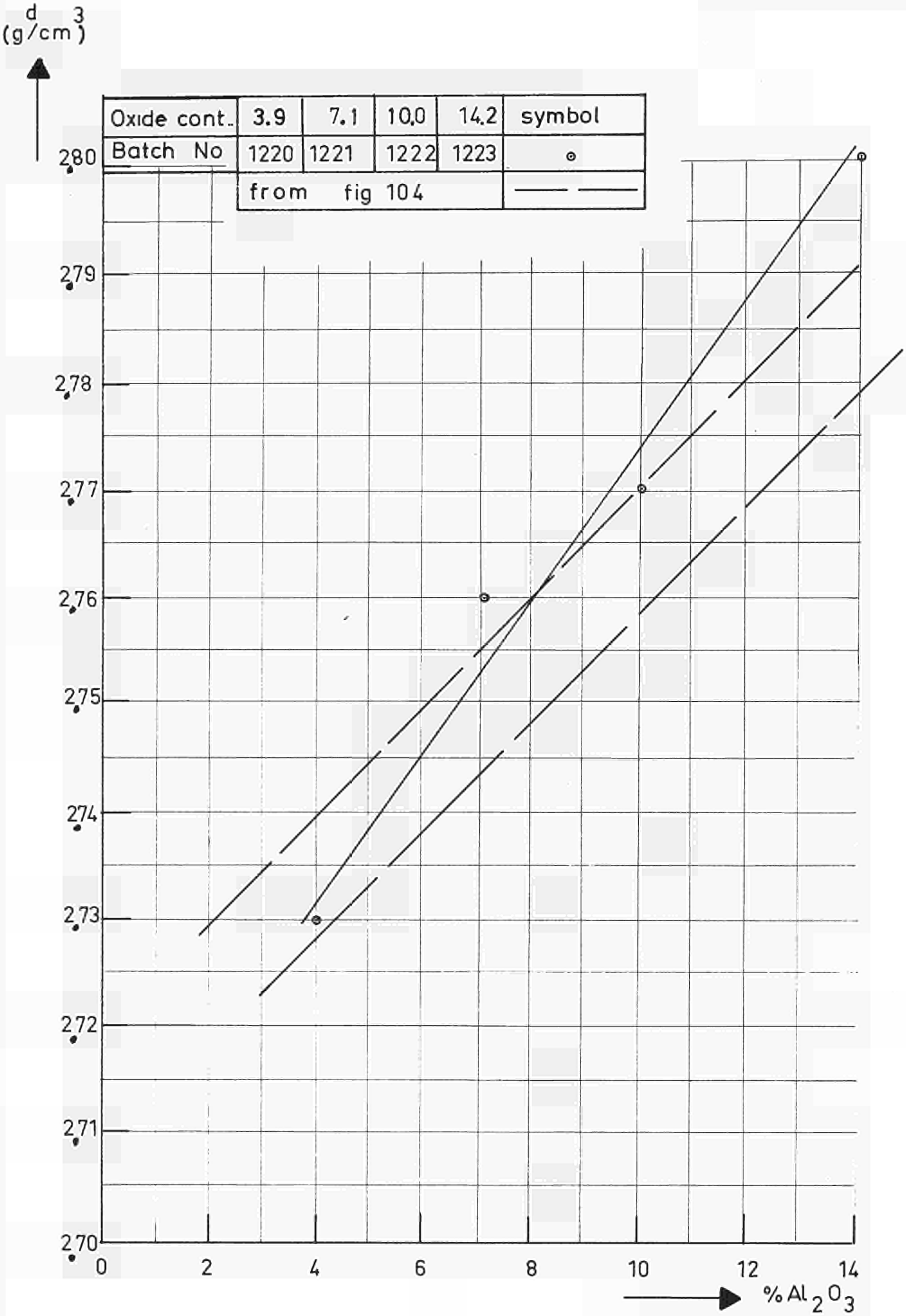

TENSILE TESTS ON SMOOTH TUBES OF SAP ISML (ISML Results Ref. 22-31) Mechanical Properties vs. oxide content.

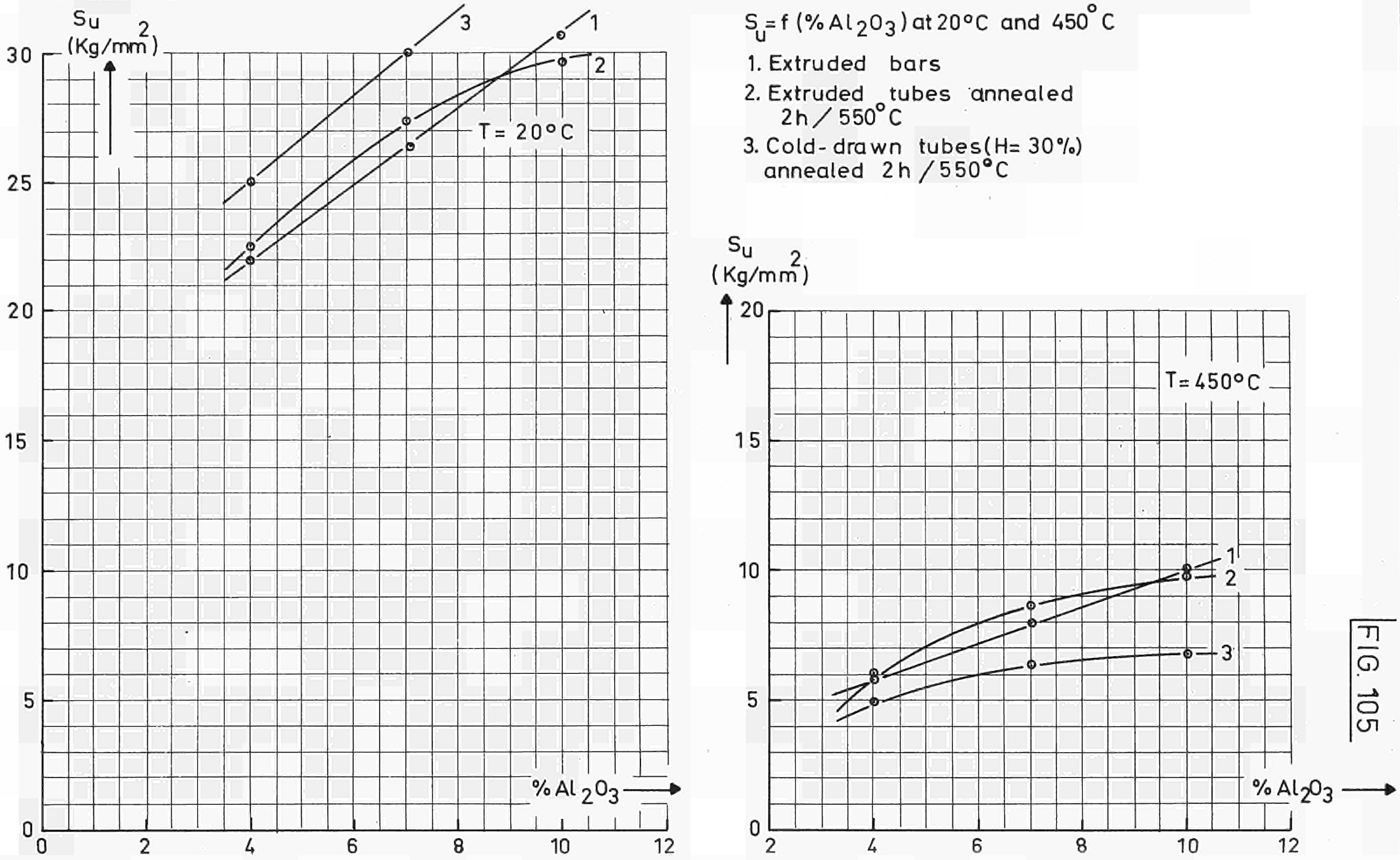

FIG. 105

TENSILE TESTS ON SMOOTH TUBES OF SAP ISML(ISML Results Ref. 22-31)

Mechanical Properties vs oxide content.

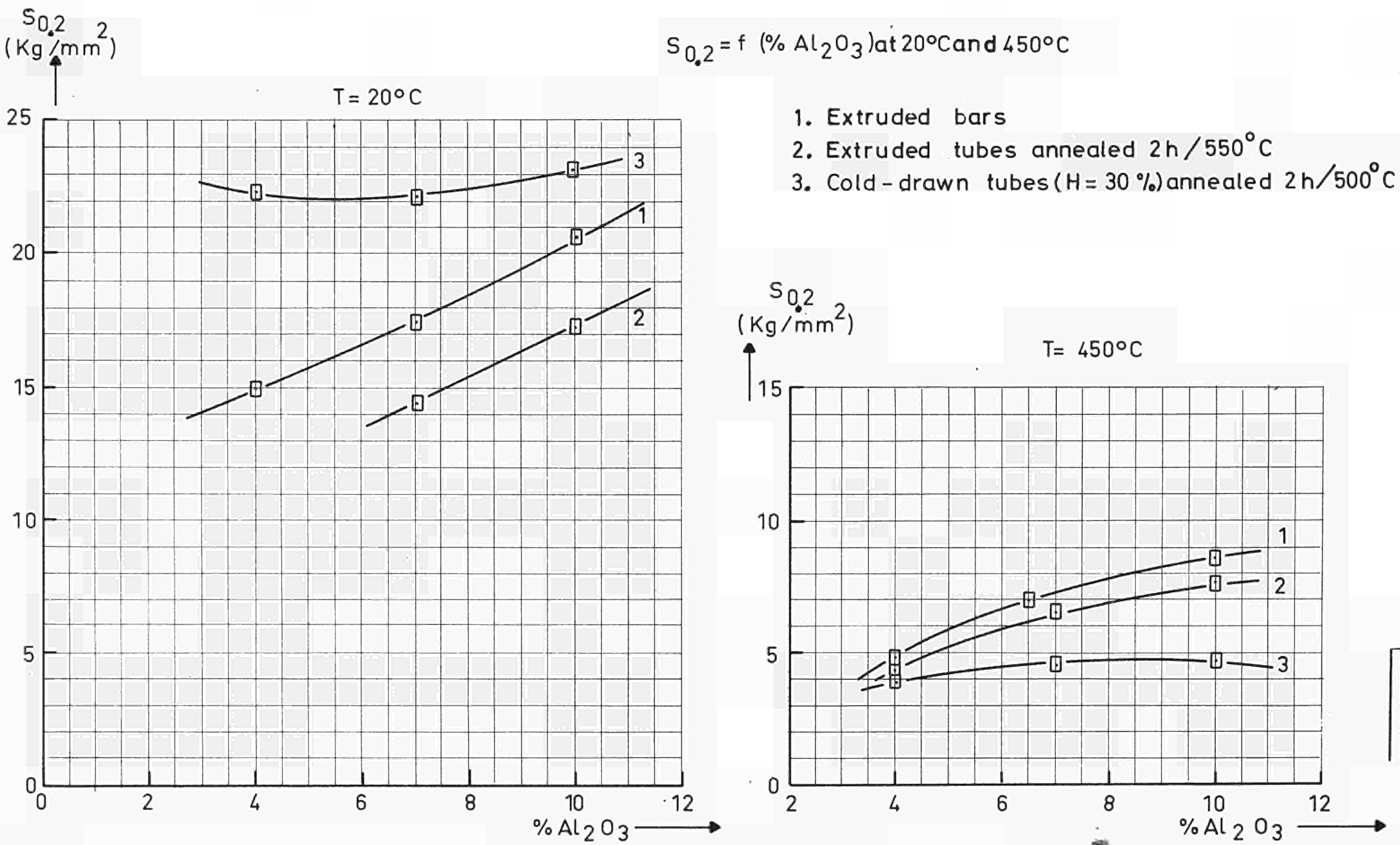

FIG. 106

TENSILE TESTS ON SMOOTH TUBES OF SAP ISML (ISML Results Ref 22-34)
Mechanical Properties vs. oxide content.

$e_{pb} = f(\% Al_2O_3)$ at 20°C and 450°C

1. Extruded bars
2. Extruded tubes annealed 2h/550°C
3. Cold-drawn tubes (H= 30%) annealed 2h/550°C

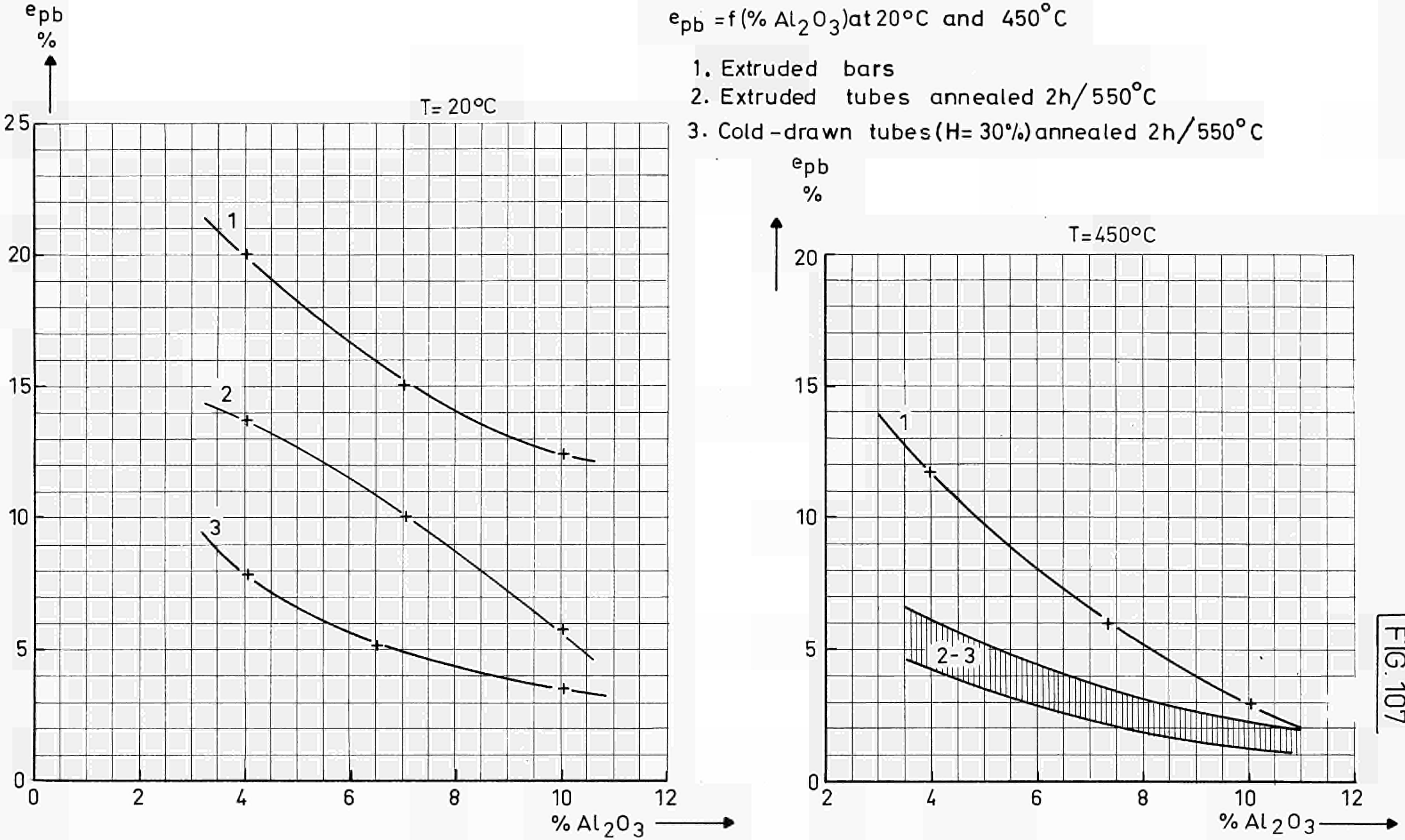

FIG. 107

STRESS RUPTURE TESTS UNDER INTERNAL GAS PRESSURE ON SMOOTH TUBES OF SAP ISML 4% (ISML Results)
Influence of temperature

	Batch No	Reference
400°C Tests	374-375	8
450°C Tests	440	10

P: Burst pressure

σ_t Tangential stress

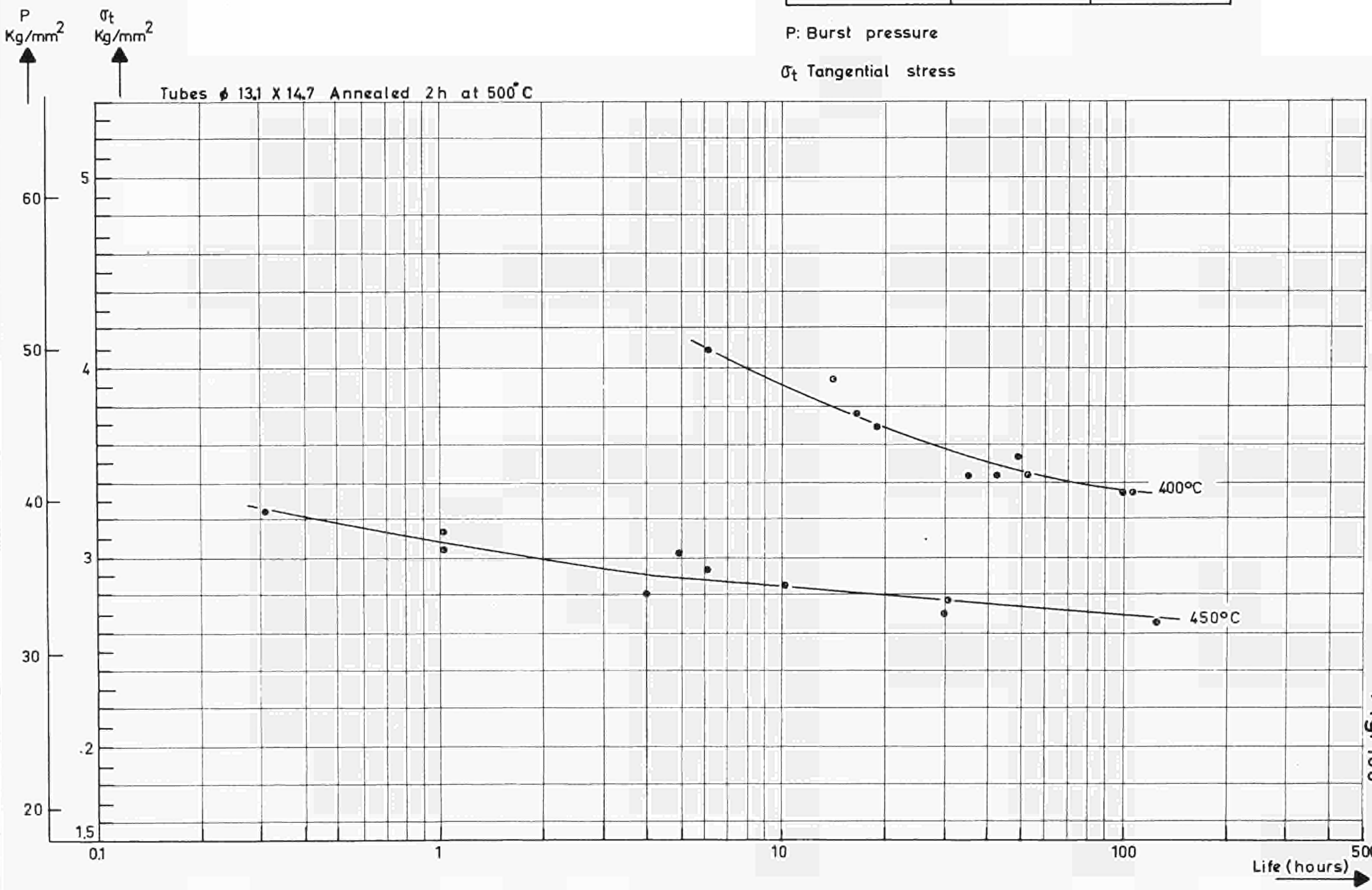

Fig. 108

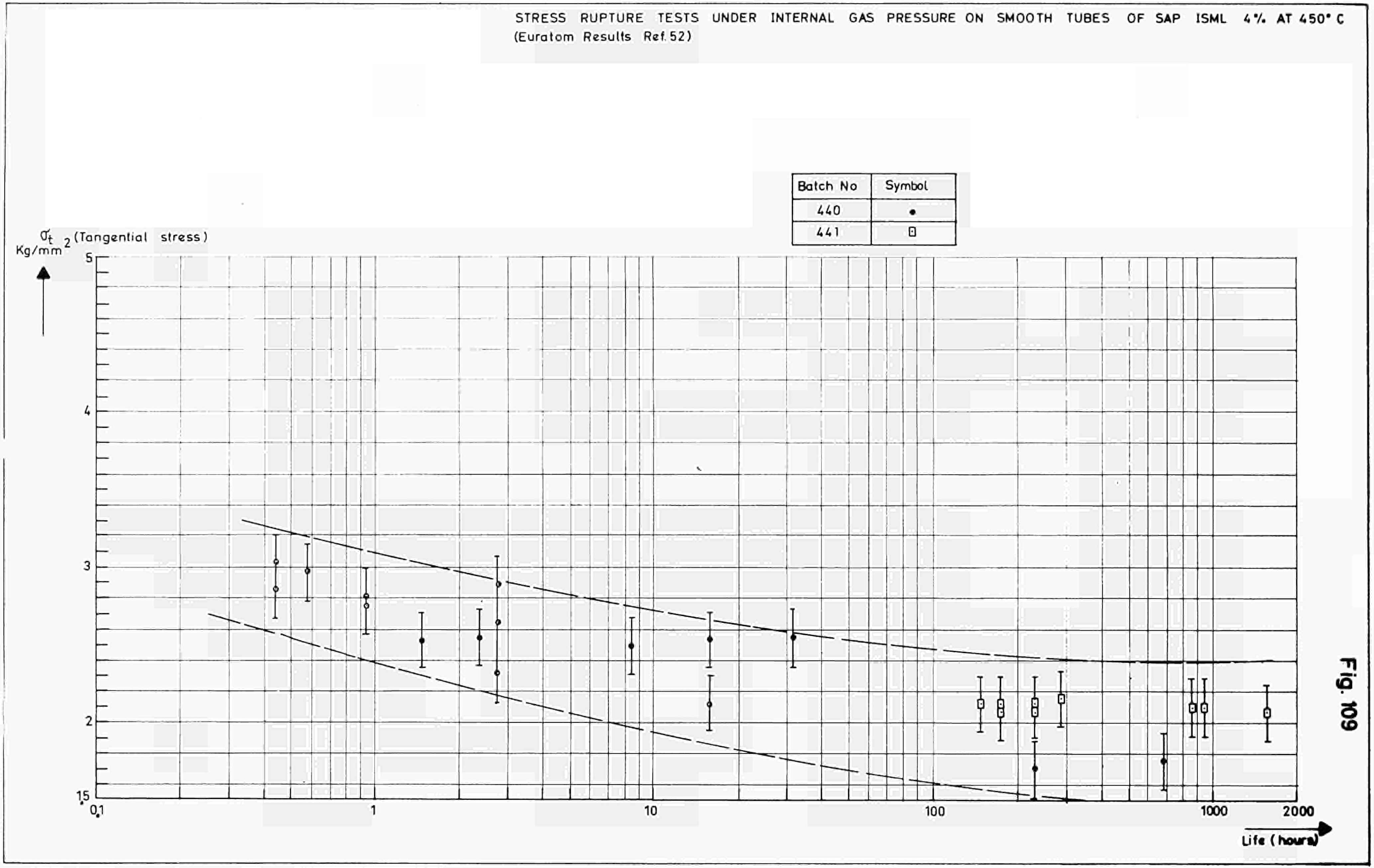

STRESS RUPTURE TESTS UNDER INTERNAL GAS PRESSURE ON SMOOTH TUBES OF SAP ISML 4% AT 450° C
(Euratom Results Ref. 52)
Batch No
Symbol
440
441
σt Kg/mm2 (Tangential stress)
5
4
3
2
1.5
0.1
1
10
100
1000
2000
Life (hours)

Fig. 109

STRESS RUPTURE TESTS UNDER INTERNAL GAS PRESSURE
ON SMOOTH TUBES OF SAP ISML 7%
(ISML Results)

	Batch No	Reference
400°C Tests	448	8
450°C Tests	450	10

P: Burst pressure
σt: Tangential stress

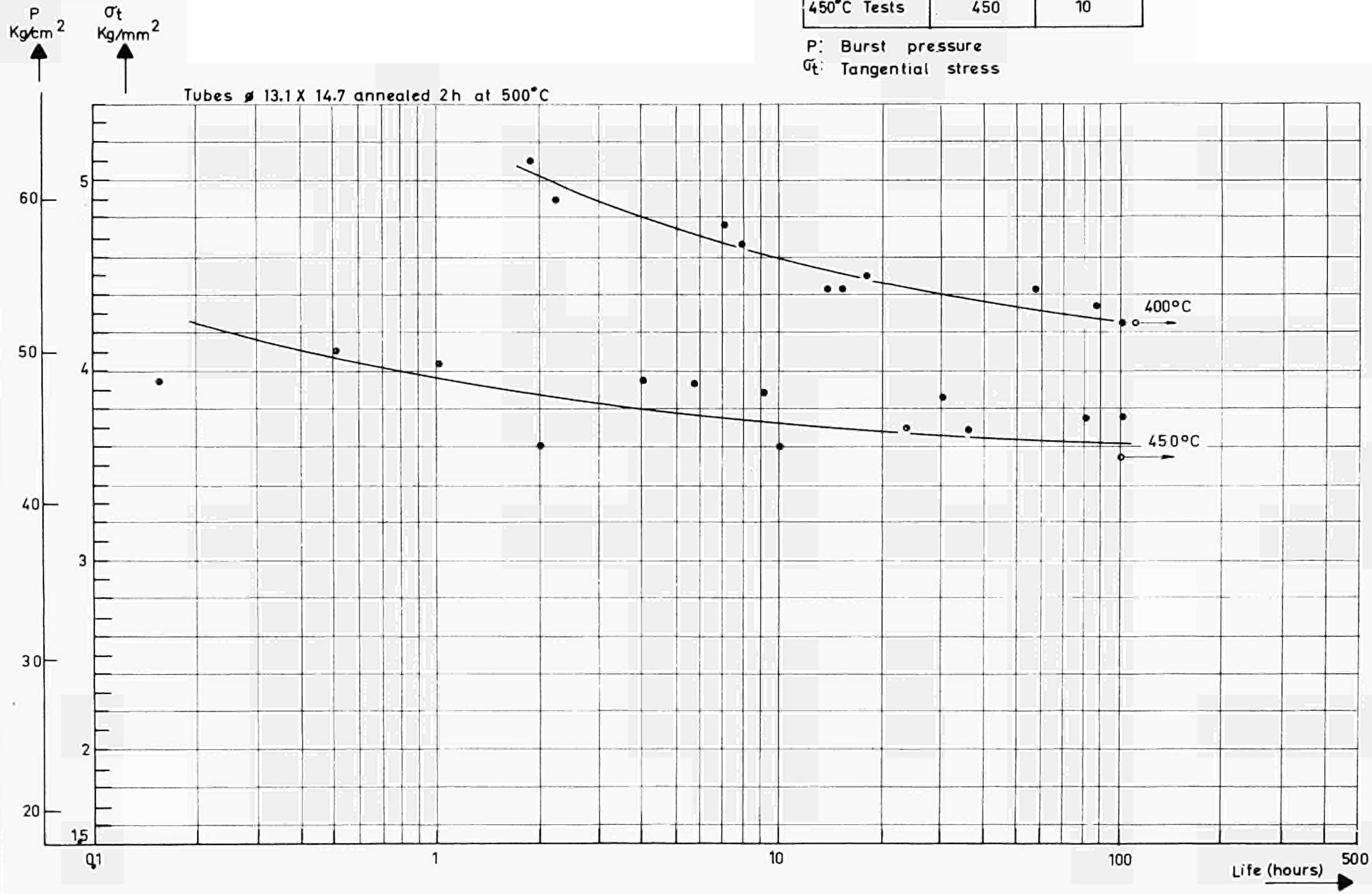

Fig. 110

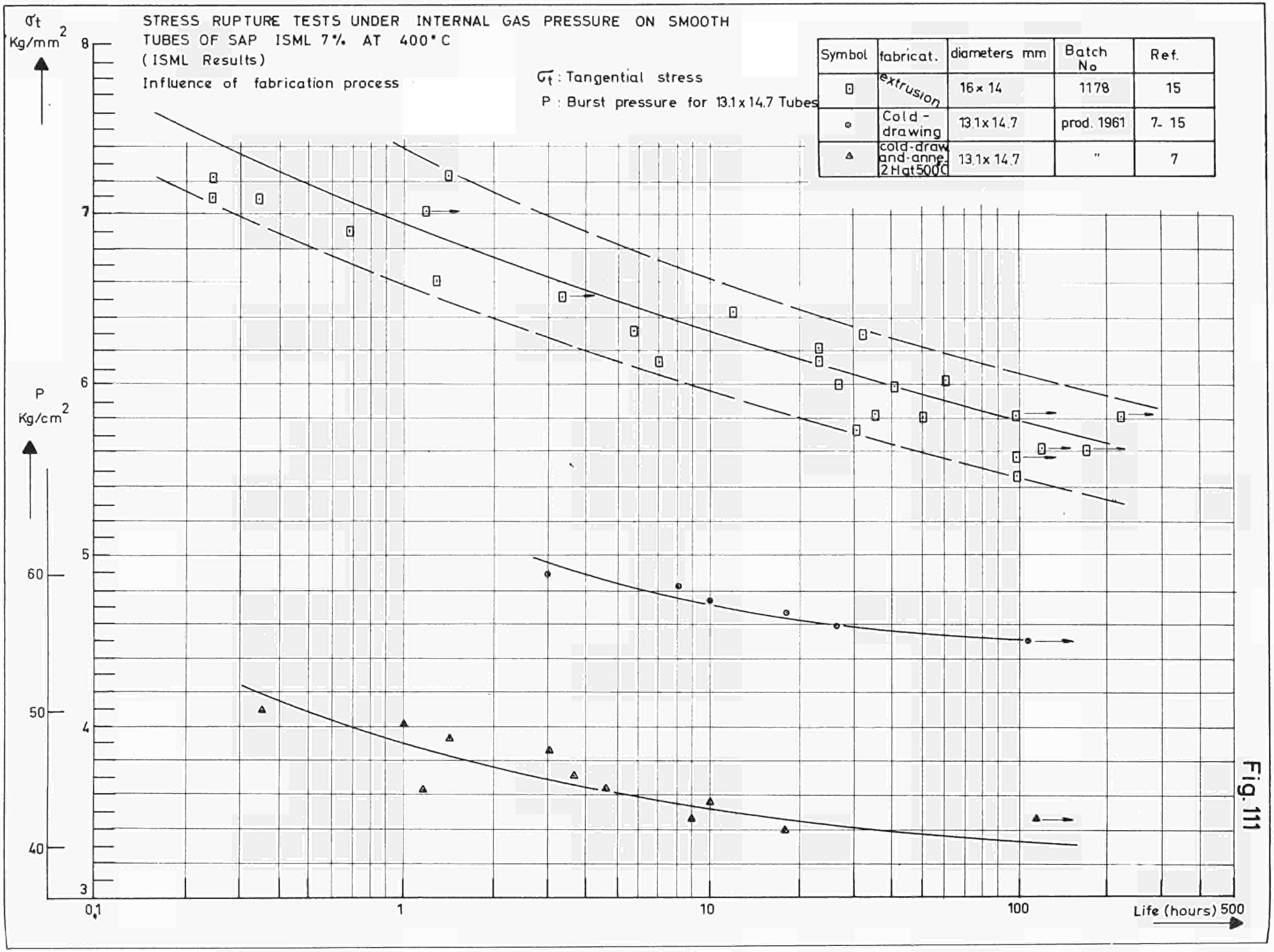
STRESS RUPTURE TESTS UNDER INTERNAL GAS PRESSURE ON SMOOTH TUBES OF SAP ISML 7% AT 400°C
(ISML Results)
Influence of fabrication process
σt : Tangential stress
P : Burst pressure for 13.1 x 14.7 Tubes
Symbol | fabricat. | diameters mm | Batch No | Ref.
extrusion | 16 x 14 | 1178 | 15
Cold-drawing | 13.1 x 14.7 | prod. 1961 | 7-15
cold-draw and anne. 2 H at 500C | 13.1 x 14.7 | " | 7
σt Kg/mm2
P Kg/cm2
Life (hours)
0,1
1
10
100
500
8
7
6
5
4
3
60
50
40

Fig. 111

TENSILE TESTS AT 450°C ON FINNED TUBES OF SAP ISML 7%

(ISML Results on various profiles Ref. 35 Batch N° 2007 to 3570)

Histograms of Maximum Tensile Stress (Su) and plastic strain at breaking point (in black, results concerning the profile ISML 9)

(whole bulk 192 specimens ISML 9 93 specimens)

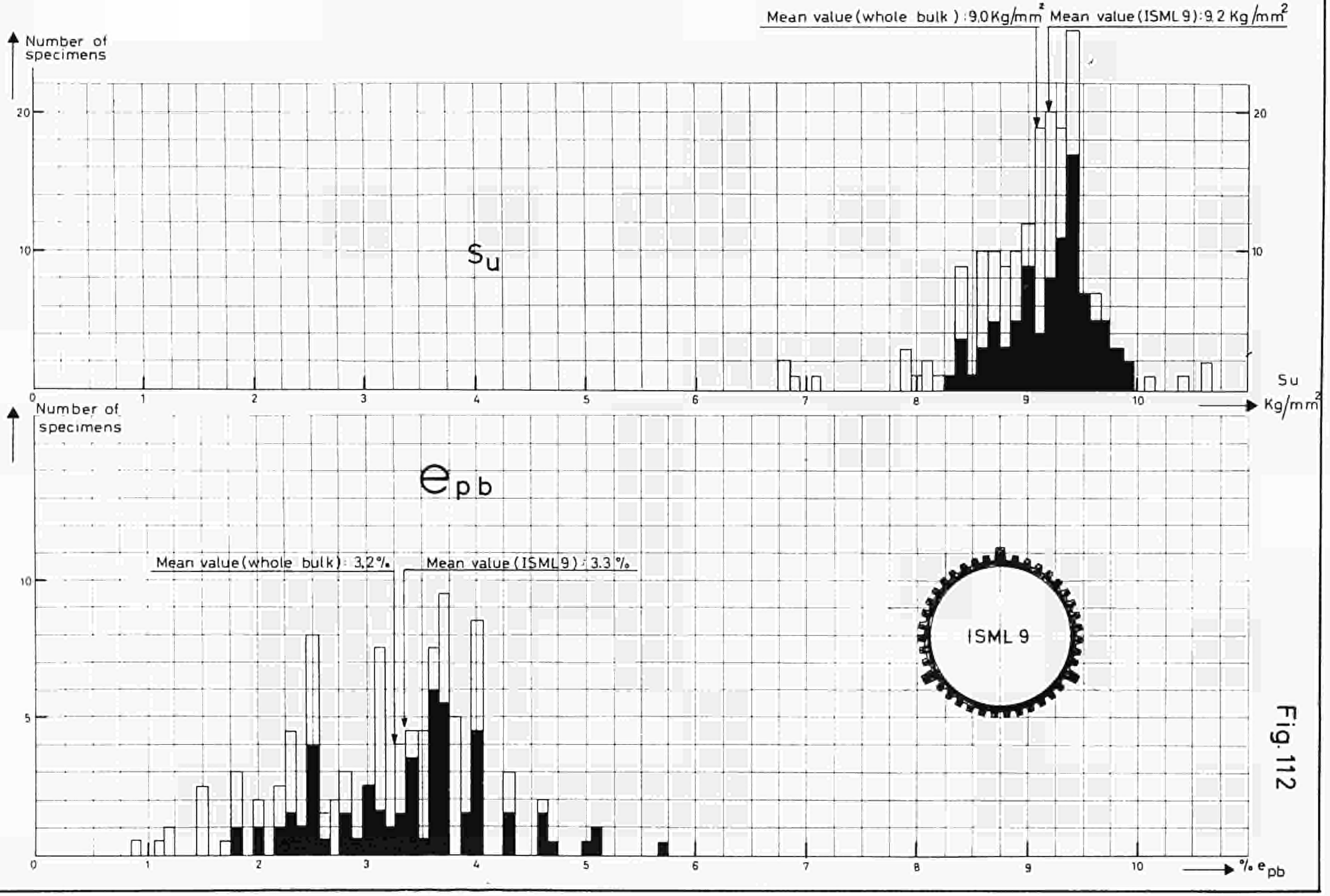

Fig. 112

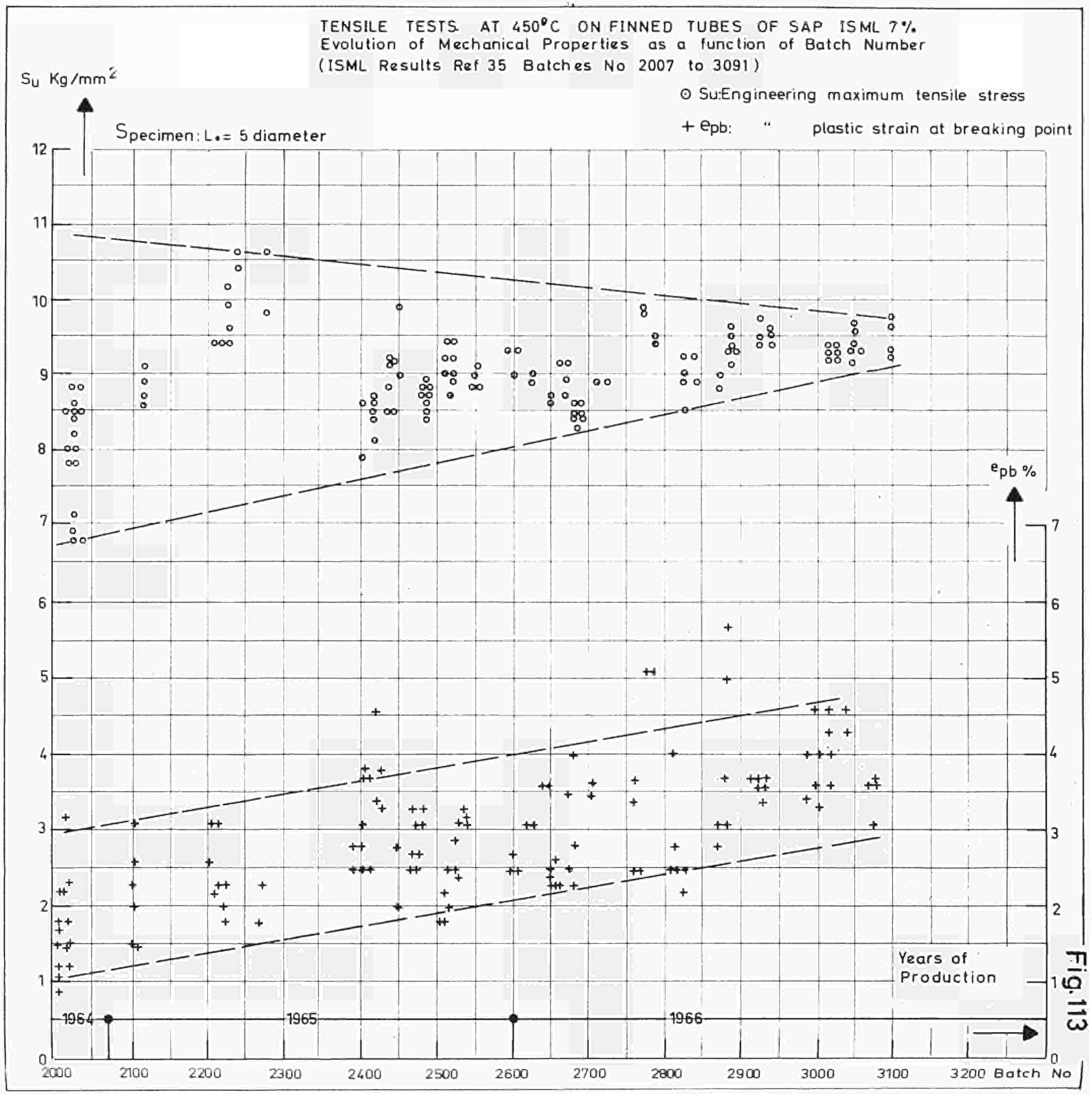

TENSILE TESTS AT 450°C ON FINNED TUBES OF SAP ISML 7%
Evolution of Mechanical Properties as a function of Batch Number
(ISML Results Ref 35 Batches No 2007 to 3091)
Su Kg/mm²
⊙ Su:Engineering maximum tensile stress
+ epb: " plastic strain at breaking point
Specimen: L₀= 5 diameter
epb %
Years of Production
1964
1965
1966
Batch No

Fig.113

FIG.114

TENSILE TESTS AT 450°C ON FINNED TUBES (Profile ISML 9) OF SAP ISML 7%

Evolution of Mechanical Properties as a function of Batch Number

(ISML Results Ref. 35- Batch No 2459 to 3120)

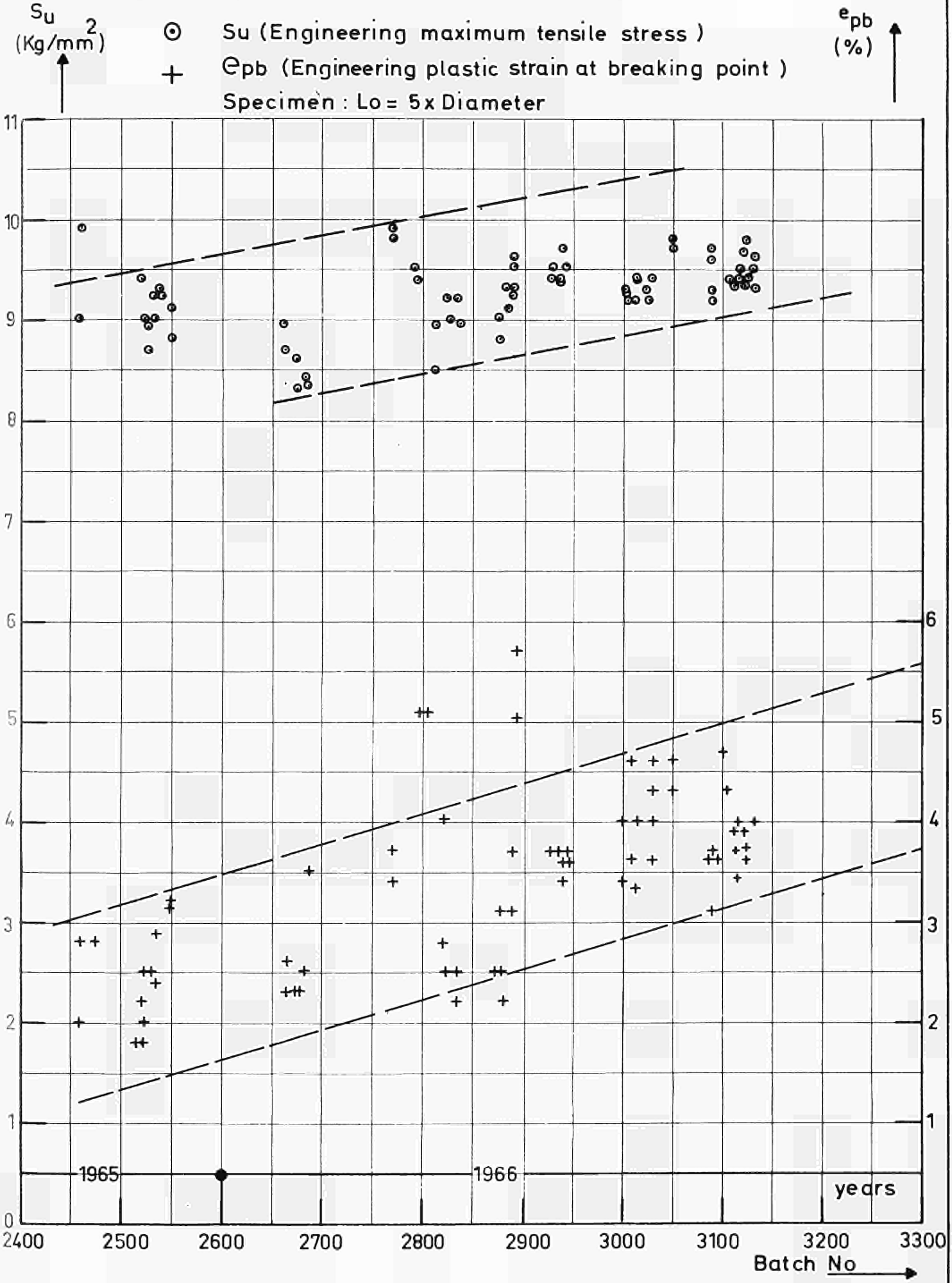

STRESS RUPTURE TESTS ON SAP ISML 4%

(Euratom and ISML Results)

Comparison between bars and tubes

	$\%Al_2O_3$	dimens. mm	Batch No	Test temp.	Type of stress	from Fig:	Symbol
Bars	4	ϕ 9.5	289	460	Tension	40	— — —
SMOOTH TUBES	4	ϕ13.1×14.7	440-441	450	Internal Pressure (Tangential stress)	109	//////
			440	450		108	———

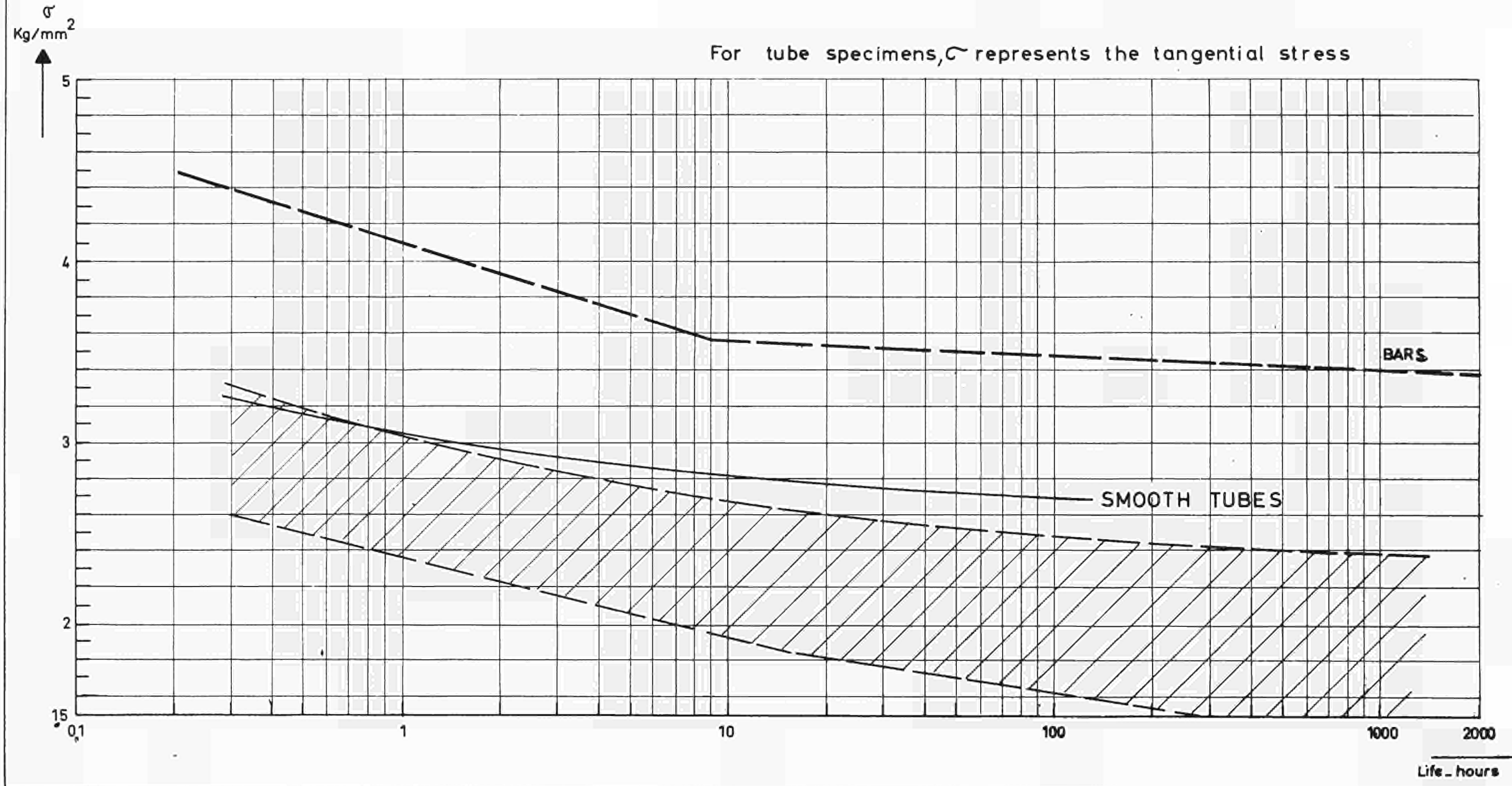

Fig. 115

STRESS RUPTURE TESTS ON SAP ISML 7%
(Euratom and ISML Results)
Comparison between bars and tubes

	% Al_2O_3	dimens. mm	Batch No	Test temp	Type of stress	from Fig:	Symbol
Bars	7	ϕ 9,5	275	460	Tension	41	— — — —
			1722	450	Internal Pressure (tangential stress)	43	//////
Smooth tubes	7	ϕ13.1 × 14,7	450			110	———

For tube specimens, σ represents the hoop stress(tangential stress)

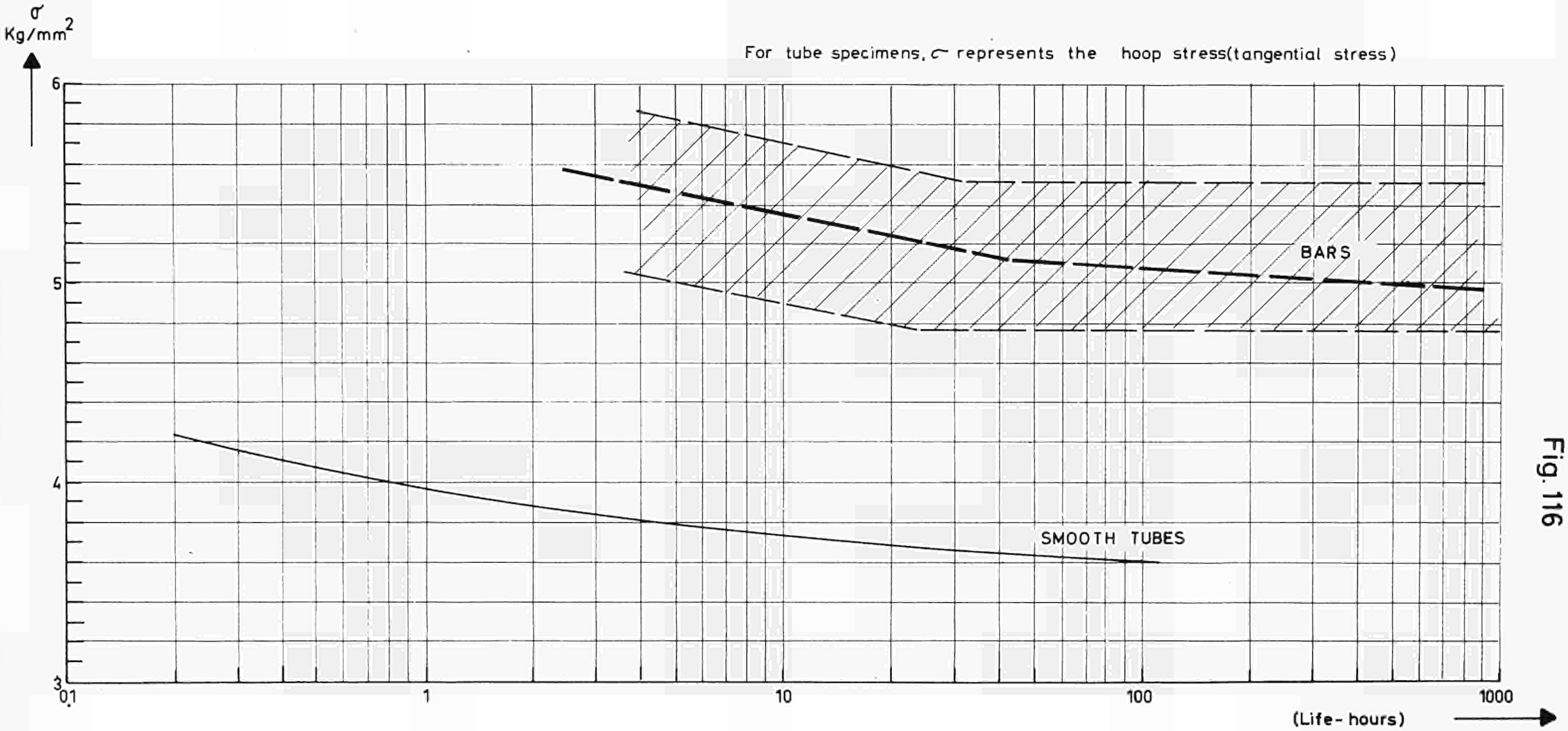

Fig. 116

TENSILE TESTS AT 450°C ON BARS AND FINNED TUBES OF SAP ISML 7 %

Comparison between finished product and base material

	% Al_2O_3	Dimens. mm	Batch. N°	Report histogr. Fig.	Representation
Bar	7	ø 21 x 16 ø 14 x 9.5	from 1810 to 2623	88	(black)
Finned tubes	7	21 < i d < 25 t ≃ 1mm	from 2007 to 3570	112	

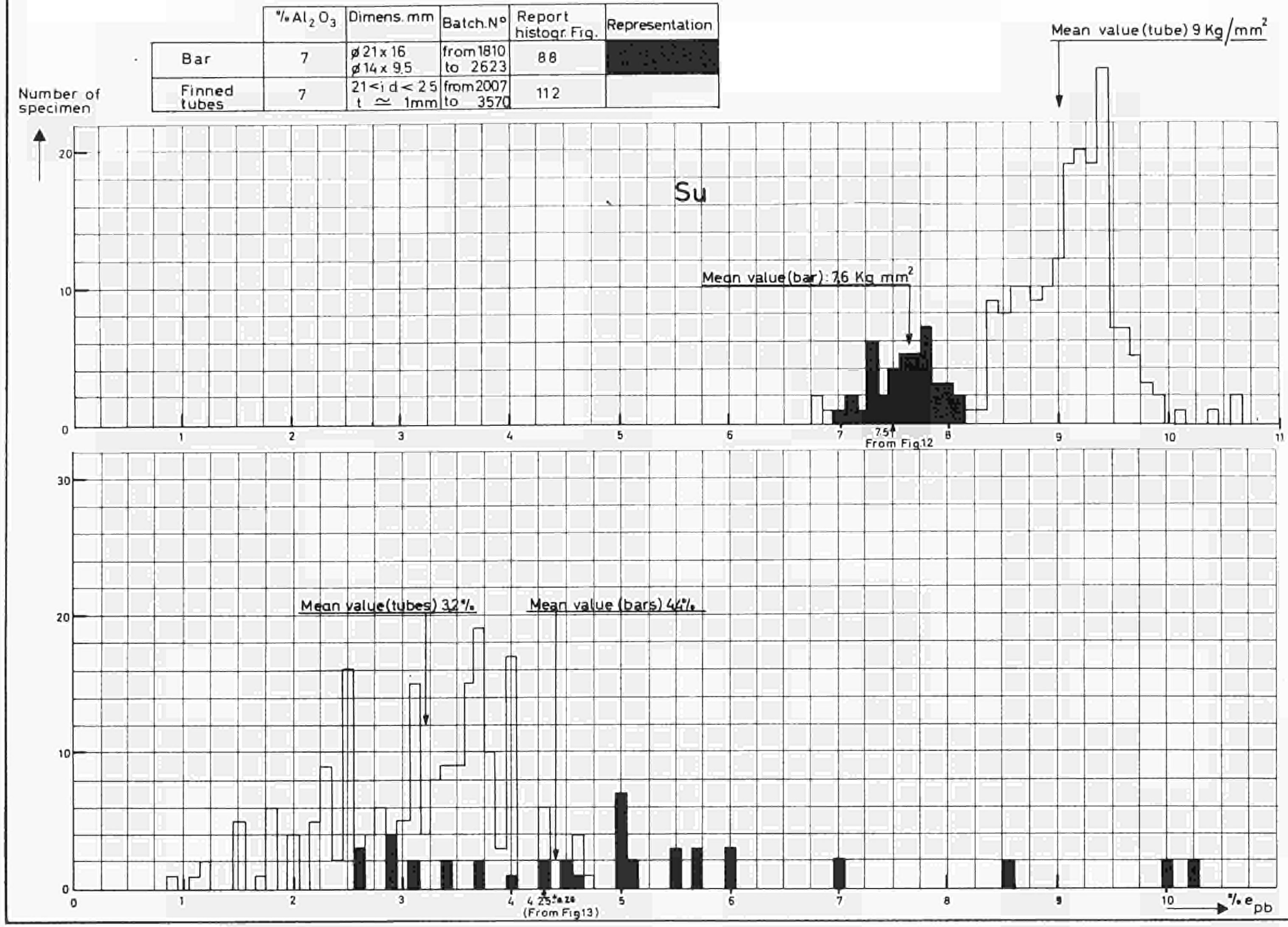

Fig. 117

Burst Tests on finned tubes of SAP ISML 7% at 460°C
Tangential stress at breaking point vs. depth of Defect.
(Euratom Results Ref. 62 bis)

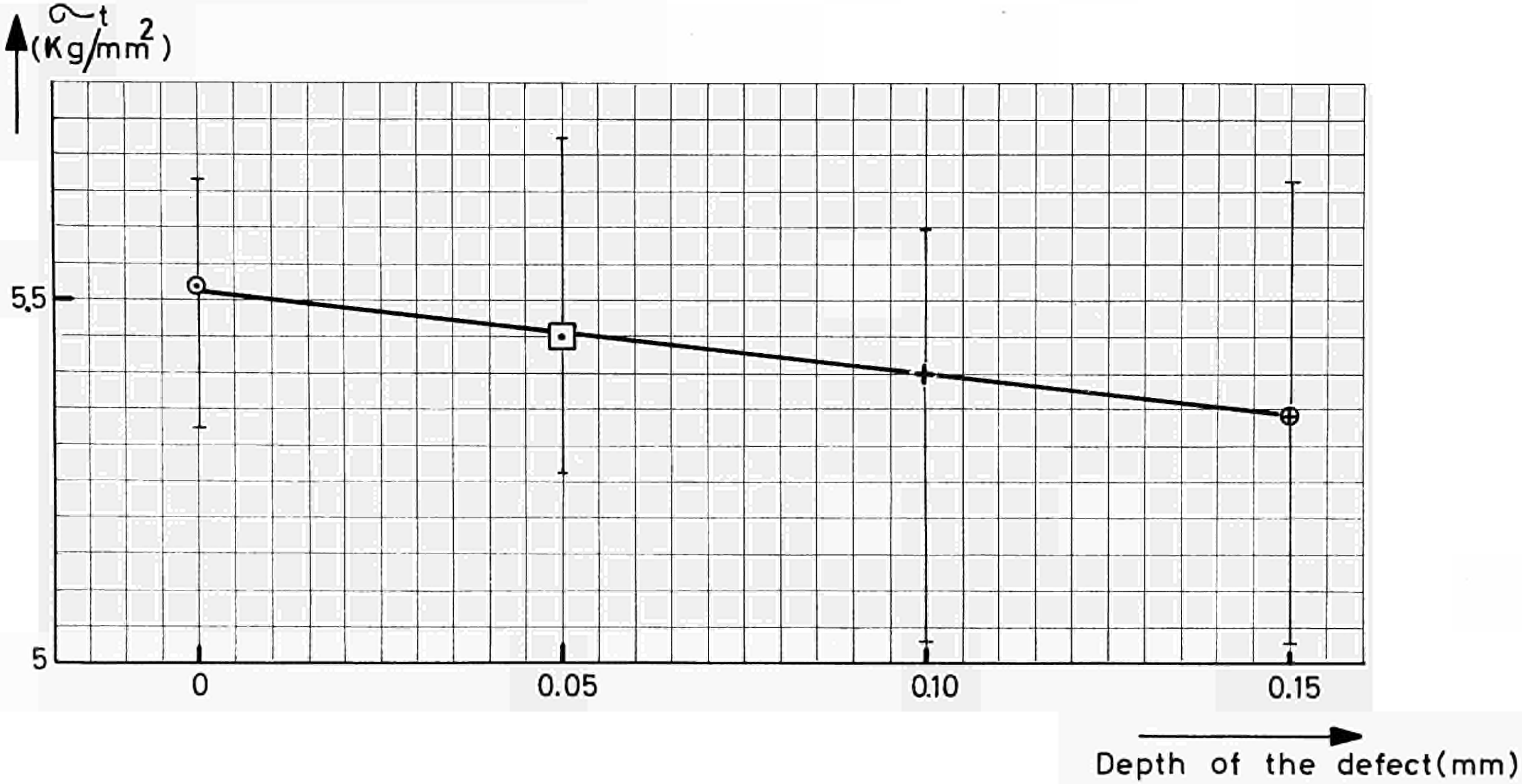

Fig 118

Fig.119

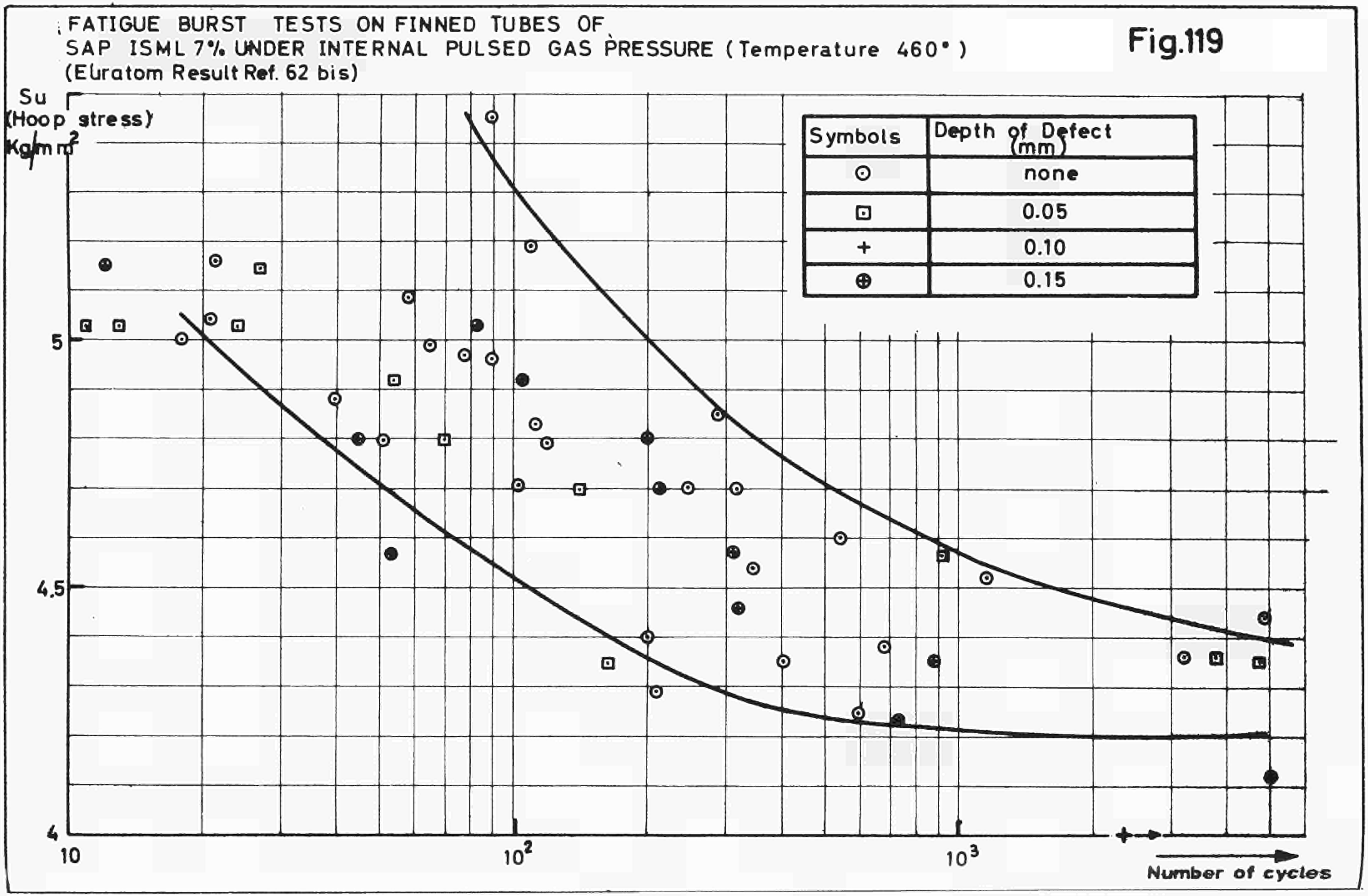

FATIGUE BURST TESTS ON FINNED TUBES OF
SAP ISML 7% UNDER INTERNAL PULSED GAS PRESSURE (Temperature 460°)
(Euratom Result Ref. 62 bis)
Su
(Hoop stress)
Kg/mm²
5
4.5
4
10
10²
10³
Number of cycles
Symbols
Depth of Defect (mm)
none
0.05
+
0.10
0.15

EXPERIMENTAL CONDITIONS
AND
COMPLEMENTARY RESULTS

3. EXPERIMENTAL CONDITIONS AND COMPLEMENTARY RESULTS

3.1 Mechanical Properties of Semi-finished products

3.1.1 Tensile Tests

3.1.1.1 Euratom and ISML Laboratory Tests

3.1.1.1.1 Test conditions

Test specimen

First of all, we can analyze the influence of the relation $x = \frac{\text{length}}{\text{diameter}}$ as related to the specimen, on the elongation value on rupture on SAP ISML 10% for instance. Fig. 1 shows that the elongation decreases with increasing x because the influence of the elongation at necking diminishes with increasing length.

This effect is more clearly visible in Fig. 2, where the elongation values have been related to increasing values of $\frac{1}{x}$.

Fig. 2 also shows the values of $\frac{1}{x}$ for the specimens used by different laboratories (Section 2.1) which studied the SAP ISML, namely:

- Euratom
- ISML
- Risö (Ref. 41)
- AECL (Ref. 33)
- TLH (Ref. 67 to 86 Part II)

The drawings of the specimens used by Euratom and ISML are given in Figs. 3 and 4 respectively (dimensions in mm).

Testing instruments

In the Euratom laboratories we used a universal electric testing machine (Instrom TTCM). The applied load is measured very accurately between 1 g and 5 t by means of a series of load cells, strain gauges being used as transducers. The crosshead speed can be varied very precisely within a range from 0.0005 to 50 cm/min. The influence of the tensile speed on the mechanical properties is presented on diagrams Nos. 6,7,8,9,9A,9B,9C.

In the ISML laboratories a hydraulic testing machine (Amsler) was used. The testing speed varies with the load and cannot be accurately determined. The measurement of the load is obtained directly from the variation of the pressure in the hydraulic system.

Measurement of elongation

In most of the current tests no extensometer was used except for very accurate measurements (as in Fig. 10).

In the ISML laboratories, which are primarily intended for fabrication control purposes, two marks are engraved on the specimen indicating the gauge length. After rupture the two parts are put together again and the new distance between the two engraved marks measured. For determination of Young's modulus extensometers of the Martens type are used.

In the Euratom laboratories the elongations are determined from the diagrams representing the load (P) as a function of the crosshead displacement (ΔL). This latter can be amplified over a wide range; generally, during the elastic part an enlargement of 100 x was used and during the rest of the test 10 x. If we consider the plastic elongation only, then the influence of the frame deflection of the machine is eliminated (Ref. 30).

For special measurements extensometers with inductive transducers or differential methods (specimens of different lengths) are employed.

Determination of the engineering yield stress

The engineering yield stress was always determined with the aid of the P = f(ΔL) diagrams in continuous tests (Δ L was enlarged 100 x). Afterwards a straight line at 0.2% plastic elongation was drawn parallel to the elastic line of proportionality (Ill. 5 & 6). Intermittent tests, causing a plastic elongation of 0.2% after unloading, were therefore not carried out. The diagrams in Fig. 10 give various values for the engineering yield stress, obtained by several methods at 20 and 450°C as a function of the percentage of Al_2O_3 and as a function of temperature for SAP 7%. The engineering yield stress at 0.004% is clearly lower than at 0.2% and is very near the limit of proportionality.

3.1.1.1.2 Results

Feature of the load elongation curves

In Illustration 6 are presented fac-simile of load-elongation curves obtained on the Instron recorder. We have chosen two representative tests (on SAP 7% at 20 and 450°C) in order to give an idea of the tensile behaviour of SAP material at room and at high temperature. Therefore, the two diagrams have been drawn at the same scale.

It can be seen on these curves that at high temperature, the difference between $S_{0.2}$ and S_u is strongly reduced. At the same time, the uniform elongation (e_{pu}) decreases till nearly zero, so that the local necking initiates much earlier. In other words the zone of strain-hardening and the plastic reserve have practically disappeared.

Properties as a function of temperature for several grades of SAP

For each Al_2O_3 percentage a diagram of the tensile stresses ($S_{0.2}$ and S_u) and of the tensile strains (e_{pu} and e_{pb}) is given as a function of the temperature (20 up to 600°C). Each point represents the average of at least three different tests.

Illustration 6

LOAD-ELONGATION CURVES OF SAP ISML 7%

Definition of terms applied

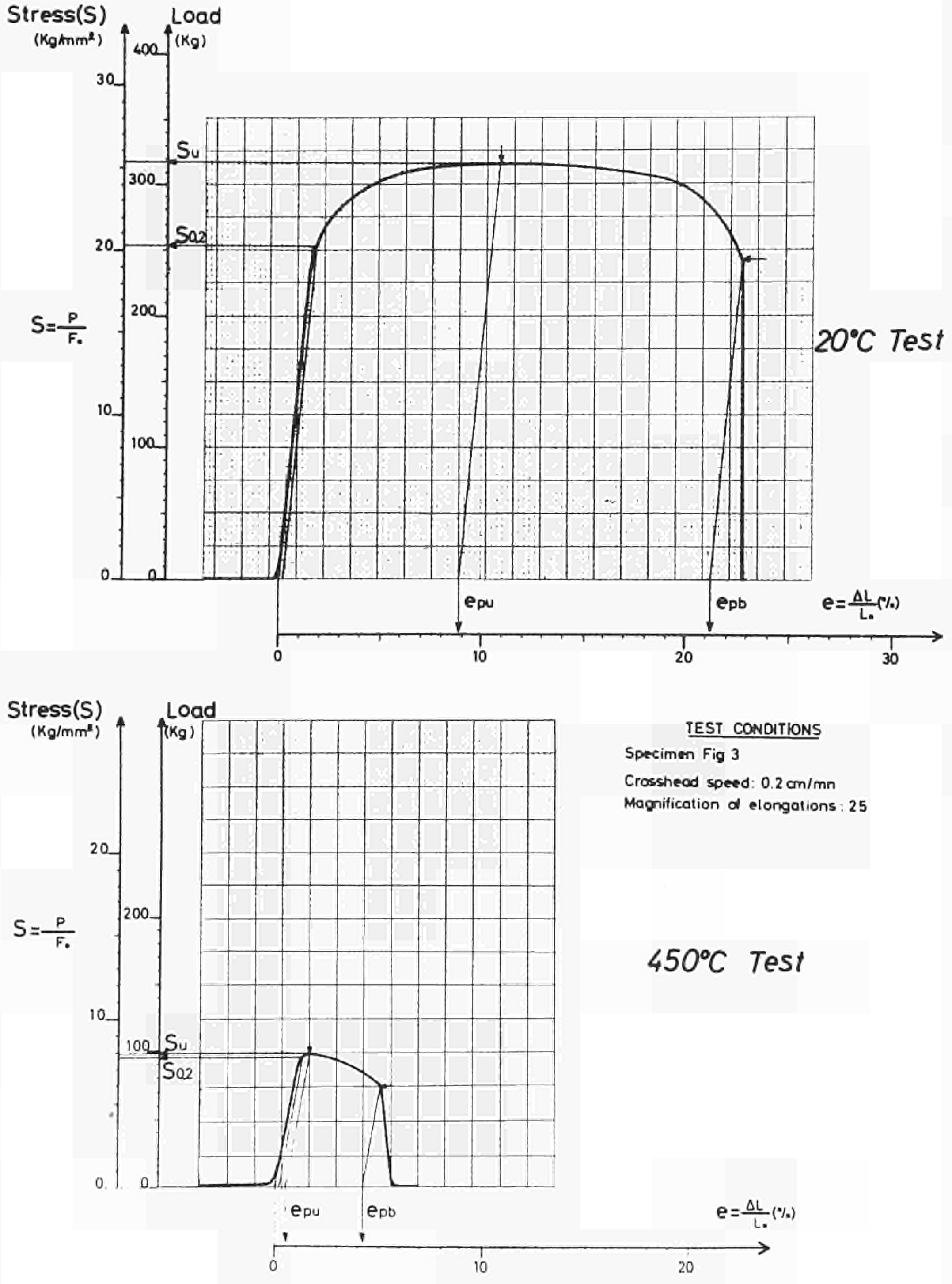

SAP ISML 4%

The properties were determined on two main batches: one old batch (fabrication of May 1961) and one more recent (fabrication of June 1962) Figs. 11 and 12. This latter batch has slightly better mechanical strength (10% at 20°C and 20% at 450°C) and lower elongation at 20°C.

SAP ISML 7% (Figs. 13 and 14)
SAP ISML 10% (Figs. 15 and 16)
SAP ISML 14% (Figs. 17 and 18)

Observation of the curves:

As a general rule, the tensile stresses and the elongation both decrease with increasing temperature. From about 300°C onwards S_u mingles with $S_{0.2}$, and e_{pu} reaches its minimum value which remains nearly constant up to 600°C.

Comparison of the four grades of SAP

For each property all four grades of SAP were compared (other presentation of previous results) on the following diagrams:

Property	Fig. No.	
	Euratom results	ISML results
S_u	19	20
$S_{0.2}$	21	22
e_{pu}	23	--
e_{pb}	24	25

ISML gave averages for the results obtained from production control tests of extruded rods, over a three-year period. The curves are seen to behave similarly for each type of SAP.

Cumulative curves as a function of the percentage of Al_2O_3

- Diagrams of the tensile stresses (Fig. 26) and elongations (Fig. 27) for various temperatures between 20 and 600°C (values derived from the curves shown in Figs. 11 to 18); The tensile stresses increase with increasing oxide contents. However, the elongations decrease with increasing oxide percentages.
- Curves of the tensile stresses and elongations at 20 and 400°C determined by ISML on extruded rods (Fig. 28).

The latter curves were plotted with the aid of average values taken from the histograms (Figs. 86 and 87), representing three years of fabrication.

3.1.1.2 AECL Laboratory Tests (Ref. 33)

Test conditions

The tensile specimens (Fig. 31) were tested on a Hounsfield testing machine and the yield strength determined from the autographic record.

Test results

Only the values for SAP 4% are reported here. Tests have been carried out only at room temperature and above 375°C. The diagram of the stress versus temperature (Fig. 32) shows approximately the same values as Fig. 11. The diagram of the strain versus temperature (Fig. 33) lacks precision between 20 and 350°C but the general form of the 400-500°C range is the same as Fig. 12

3.1.1.3 Risö Laboratory Tests (Ref. 41)

Test conditions

The tensile specimen has a diameter of 4.5 mm and a gauge length of about 45 mm. Either a 10 t Amsler or a 5 t Instron testing machine was used. With the latter (for more precise tests), a crosshead speed of 0.1 mm/min was applied up to $S_{0.2}$, the rest of test being performed at 1 mm/min. The Amsler or Instron furnaces were regulated to within $\pm$ 3°C and the soaking time before testing was about 30 min. At least two specimens were tested for each temperature and SAP grade. The $S_{0.2}$ was always determined continuously with an extensometer.

Test results

Fig. 34 gives the properties at 20 and 400°C as a function of the percentage of Al_2O_3. Compared with the diagrams in Figs. 26 and 27 it will be seen that the tensile stresses agree with the classical values, but the strains are slightly lower, especially at 400°C.

3.1.2 Compression Tests (Euratom results)

3.1.2.1 Experimental Conditions

Shape of the test specimen

We chose the same diameter (4 mm) as for the cylindrical part of the tensile specimen (Fig. 3). After having studied the compression behaviour of specimens from various heights (three times, twice, once the diameter) a cylinder with a height equal to its diameter was taken as a specimen (thus minimizing the effects of parasitic buckling).

Testing machine

For the compression test we used an Instron TTCM universal electrical testing machine. The velocity of the crosshead (1mm/min) was enlarged a hundred times on the load-elongation diagram.

3.1.2.2 Behaviour of the "Engineering Stress-Strain" Diagrams

Construction of the curves (Illustration 5, section "Symbols"

As for the tensile test, we used the "load-elongation" diagrams plotted by the machine. The section of which the tensile stress can be calculated is the original section of the specimen. The strain is calculated on the basis of the original height of the specimen before the test.

Observation of the curves

Ill. 5 shows the behaviour of the diagrams for a tensile test and for a compression test. The symbols used for compression are the same as those for tensile tests (see Table 2), but followed by an apostrophe.

In the elastic region the inclination angles α and α' of the curves are different, since the deflection of the machine is not the same. This difference is eliminated by considering only the plastic strains. The maximum engineering tensile stress (S'_u) is assumed to be the stress which corresponds to point B' where the curve shows a point of inflection, this latter also enabling the value of elongation e'_{pu} to be calculated. This is logical, whereas in a "true stress/true strain" diagram the tensile and compression curves show the same behaviour, since in that case the point B is also a point of inflection.

3.1.2.3 Results: Cumulative curves for tensile and compression stresses and elongations as a function of the temperature for the four grades of SAP ISML

Properties	Results of tensile tests in Fig.	Results of compression tests in Fig.
S'_u	19	35
$S'_{0.2}$	21	36
e'_{pu}	23	37
e'_{pb}	24	--

The engineering 0.2 offset yield stress ($S'_{0.2}$, Fig. 36) under compression is slightly higher than $S_{0.2}$ under tensile stress, especially at 20°C. The maximum engineering compression stress (S'_u, Fig. 35) at 20°C is higher than S_u (about 30%), but at higher temperatures becomes comparable.

The engineering plastic uniform strains (e'_{pu}, Fig. 37) in compression tests are clearly higher than the e_{pu}-values under tensile stress. The minimum values - which were situated around 300°C for e_{pu} - are shifted to about 450°C for e'_{pu}. Thus this behaviour of e'_{pu} looks like that of e_{pb} under tensile stress (Fig. 23).

In conclusion it may be said that both the tensile and the compression test results show a drop in stress and strain for increasing temperature.

3.1.3 Creep Tests

3.1.3.1 Euratom-ISML Tests

3.1.3.1.1 Test conditions:-

- Test specimens:

The test specimens used by the Euratom and ISML laboratories are given in Figs. 38 and 39 respectively. The former were taken from rods with a diameter of 9.5mm, and the latter from rods with a diameter of 21 mm.

- Testing machines:

Euratom tests:
We used Adamel TAC stress-to-rupture machines fitted with a modified electrical accessory permitting magnifications up to 500 times (this magnification value has always been used for tests on SAP because of the low elongation values of this material). The extensometer is fixed above the heads of the test specimens, i.e., at the two ends. The temperature is controlled by two Chromel Alumel thermocouples, and regulation of the furnace keeps the temperature constant to ± 1.5°C.

ISML tests:
The tests quoted in this report were carried out in the laboratories of AIAG/Neuhausen. The extensometer was fixed in two grooves in the heads of the test specimen (Fig. 39). The temperature of the test specimen was maintained at ± 1°C.

3.1.3.1.2 Stress-to-rupture curves

The ISML tests were performed at 400°C and the Euratom tests at 420 and 460°C. The stress-to-rupture tests were drafted in semi-logarithmic scales up to 10,000 hr. Each of these curves shows a sudden change in the slope at a point which varies with each percentage of Al_2O_3. The test specimens show no tertiary creep, and no re-acceleration of the elongation just before rupture of the specimen.

SAP 4%: Fig. 40

SAP 7%: Fig. 41: Results for an old batch (made in May 1961). The results at 460°C show a slight scatter.

Fig. 42: Stress-to-rupture at 420°C. For the same batch as before, the scatter is lower.

Fig. 43: These results refer to more recent batches (1964 and 1966) and show very marked scatter; around a stress of 5 kg/mm^2 the scatter amounts to 0.35 kg, i.e., 7%.

Fig. 44: Uniform elongations. These values were obtained with the aid of the tests described in Fig. 43 and are tabulated in a histogram. The elongations at loading are of the order of 0.5%. At rupture, the average elongation is of the order of 0.8% and the minimum elongation 0.4%.

SAP 10%: Fig. 45

SAP 14%: Fig. 46

3.1.3.1.3 Cumulative diagrams

The previous results were tabulated in cumulative diagrams as a function of various parameters.

Stress-to-rupture curves

- Stress-to-rupture of SAP 7% at 400, 420 and 460°C (Fig.47). The relative position of the curve obtained at 420°C as compared with those at 400 and 460°C does not seem to be very logical when an attempt is made to interpolate linearly for an intermediate temperature.

- Stress-to-rupture at 400°C for the four oxide percentages (ISML results) (Fig. 48). The changing point of the slope for each curve varies somewhat from one oxide percentage to another. The relative curve at 7% seems to be abnormally displaced upwards.
- Stress-to-rupture at 460°C for the four percentages of oxide (Euratom results) (Fig. 49). The curves show rather similar slopes.

Stress to produce creep strain of 0.1% at 400°C (ISML results, Fig. 50)

Because there is considerable scatter of the results of the elongation measurements (see histogram in Fig. 44), this curve can only be regarded as a tendency.

Elongation curves at 400°C for 1,000 hr as a function of the applied stress (ISML results, Fig. 51)

The values given are very low, but the number of observations is very small, so these curves are merely regarded as indicative.

3.1.3.2 Battelle Institute Tests (Frankfurt)

Test conditions

Test specimens (Fig. 54): taken from rods 21 mm in diameter

- Testing machine:

The machines used were designed at the Institute. The knives of the extensometer are fixed to the heads (the two ends) of the test specimen. The elongation was measured with the aid of a microscope. The light-beam passed through a quartz window mounted in the wall of the furnace. The absolute accuracy of the measurement is to within about 3 microns. The temperature of the test specimen is kept constant to ± 3°C.

Stress-to-rupture curves for SAP 4% and 7% at 460°C

Stress-to-rupture curves (Fig. 55):

The results refer to two batches (batch 645 of March 1962 and batch 890 of October 1962). For a given stress-to-rupture time, the scatter of the stress values is of the order of 12%. The values obtained for the more recent batch seem to be lower.

Elongations (Fig. 56):

The results are so scattered that we preferred to present them in the form of histograms.

Minimum elongation at rupture 0.2 to 0.3%.
Average elongation about 0.45%

SAP 7%: The study refers to three batches (December 1961, October 1962, September 1963). Stress-to-rupture (Fig. 57):

The more recent batches seem to be less resistant, especially for long duration.

Elongations (histogram in Fig. 58):
Minimum elongation at rupture 0.2 to 0.3%
Average elongation about 0.5%

These elongations are comparable to those obtained for SAP ISML 4%.

The elongation scatter has dropped in comparison with that in the Euratom results (Fig. 44) and the mean value of the Battelle data is lower (0.5 as opposed to 0.8%).

3.1.3.3 AECL Tests

Test specimen (Fig. 59)

Stress-to-rupture curves of SAP ISML 4, 7 and 10% at 426°C (800°F) (Fig. 60)

The results obtained by AECL at 426°C are as low as those obtained by Euratom at 460°C (see Fig. 49). As far as SAP ISML 7% is concerned, these results are 15% less than those obtained by Euratom at 420°C (Fig. 47).

3.1.3.4 Comparison of Results Obtained by Battelle Institute and Euratom

These two laboratories in fact carried out similar tests on SAP ISML 4% and 7% at 460°C. However, the diameter of the rods from which the test specimen were taken and therefore the extrusion ratio were different, as indicated below:-

	diameter of rods (mm)	extrusion ratio
rods used by Euratom	9.5	74
rods used by Battelle Institute	21	15

The stress-to-rupture curves given previously are compared in one diagram (Fig. 61)

SAP 4%

The Euratom results are situated in the lower part of the scatter range of the Battelle findings.

SAP 7%

The overlapping areas of the results obtained by the two laboratories refer to older batches (No. 551 and 906). The lower values refer to a more recent batch (No. 1300).

3.1.4 Relaxation Tests

3.1.4.1 Test Conditions

Test specimen

Test specimen TR 1 (Fig. 3))
Test specimen of 7 mm diameter (Fig. 63) } Euratom laboratories
Test specimen ISML (Fig. 62))

Testing machines

Electronic relaxation machine (Euratom) (Ref. 62)

This machine was developed by Euratom under contract. The test specimen, which is placed in a closed room under vacuum, is fitted with two extensometer shafts connected to a transducer of capacitive displacement. A dynamometer, also connected to a capacitive transducer, is inserted in the loading system under vacuum. The bridges intended for measuring the load and elongation form a system which is closed in such a way that it is possible to work at constant load (creep test) or at constant elongation (relaxation test), thus eliminating the inherent deformations of the machine frame and the friction forces at the passages into the vacuum chamber. The upper part of the enclosure in which the test specimen is situated is placed in a furnace the temperature of which may be regulated to ± 1.5°C.

Machine for creep test (Adamel TR-3 Euratom) (Ref. 57)

With this apparatus the isothermal viscosity can be tested up to 60 kg/mm^2 and the stress relaxation up to 40 kg/mm^2 on a test specimen 4 mm in diameter. The test specimen is put into a furnace (temperature ± 1°C). The load is applied with the aid of a lever and a spring. The extremities of the two quartz shafts of the extensometer are held in two holes drilled in the axis at the ends of the heads of the specimens. The displacement of the extensometer shafts is mechanically magnified up to 1000 times. The extensometer actuates an electrical contact which starts a motor to change the loading spring.

Relaxation machine of the ISML laboratory (Ref. 21) (Baldwin modified)

Essentially the machine consists of an extensometer which is fixed to the test specimen and sends out the signal for regularization of the load. The variations in the load in time are directly recorded by the machine. The furnace for heating the test specimen is provided with a special regulating system by which the temperature can be kept constant at less than 1°C.

Universal testing machine Instron type TTCM (Euratom Ref. 60)

The first orientation tests carried out by Euratom were made on this machine, according to a method described by the designer (Ref. 61). Essentially it consists in applying a certain load after which the movable crosshead is held rigid and the decrease in the load as a function of the time is accurately measured. The application of this method is rather tricky because the deflection of the machine frame and the temperature variations have to be taken into consideration.

A correction factor for the machine deflection could be established approximately from a short test series in the following way. An extensometer was used (magnification 1000 x and an error of less than 1%); after the desired initial load had been applied, the position of the crosshead was corrected manually in order to maintain the initial elongation of the specimen.

The decrease in the load as a function of the time thus measured was three times as high as the values found earlier by the simpler method. We therefore applied this correction factor, equal to 3, in the following results.

3.1.4.2 Euratom Results

We principally studied the SAP ISML 7% and performed three series of tests, applying initial stresses equal to 1/3, 2/3 and 3/3 of the yield point at 0.2% ($S_{0.2}$).

at 20°C (Refs. 58-60, Fig. 64)

The preliminary results give an idea of the behaviour of the curves. The decrease in the stress expressed as a percentage of the initial stress is indicated in the table below:-

	Decrease in the stress %			
Initial stress	1 hr	5 hr	10 hr	100 hr
1/3 $S_{0.2}$	3	5	-	-
2/3 $S_{0.2}$	5	9	11	-
3/3 $S_{0.2}$	18	23	-	-

at 450°C (Refs. 57, 58 and 60, Fig. 65)

For stresses equal to 2/3 of the yield point, the curves show a change in slope which is especially visible in the region of 1 hr.

For lower stresses, the slope of the curve is less. The slopes of the curves obtained with three different machines are very comparable. The decrease in the stresses is reported in the table below:-

In Fig. 65a only the relaxation curves obtained with the Instron machine are shown. They correspond to initial stresses of 1/3, 2/3 and 3/3 of $S_{0.2}$ at 450°C. The higher the stress, the steeper the slope.

Initial stress	Decrease in the stress %		
	1 hr	10 hr	100 hr
1/3 $S_{0.2}$	16	30	40
2/3 $S_{0.2}$	20	40	70
3/3 $S_{0.2}$	ruptured after 15 min.		

3.1.4.3 <u>ISML Results</u> (Ref. 21, Fig. 66)

The partial results given here are for SAP 7%. Preliminary creep tests have shown that the deformation imposed at the beginning of the test should not subject the material to stresses in excess of 5 kg/mm^2 (i.e., 2/3 of the yield point). The first test specimen underwent a deformation of 0.165%.

The decrease in the stress is reported in the table below:-

Initial stress	Decrease in the stress %		
	1 hr	10 hr	100 hr
0.55 $S_{0.2}$	25	40	45

The behaviour of the curve is very different from that obtained on the various machines used by Euratom. The phenomenon seems to slow down after 10 hr, whereas in the other cases it speeds up.

3.1.5 Impact Strength Tests (Refs. 9 and 10)

3.1.5.1 Test Conditions

The standard Charpy specimen was used (Fig. 67). The specimen was machined from bar stock 10.3 x 10.3 mm square (E = 60) and afterwards annealed for two hours at 500°C. The instrument used was an Amsler machine; the hammer energy applied was 30 mkg. With the same hammer lower energies were applied, as indicated in Fig. 68. For the high-temperature tests every specimen was soaked at its testing temperature for 30 min. Generally five tests were performed for each temperature.

3.1.5.2 Results

The impact strength of SAP ISML 4% and 7% Al_2O_3 versus temperature is shown in Fig. 68. It is clear that the impact strength increases with temperature. The part of the curve shown as a dotted line indicates values which are too low because at these points the specimens did not rupture completely.

The curve for SAP 7% lies below the 4% Al_2O_3 curve, thus indicating a lower ductility, which is in agreement with other types of mechanical tests. There are two individual points (at 20 and 400°C) for SAP 4% which are well below the established SAP 4% curve. These points were obtained for a very old batch made under quite different fabrication conditions (only simple extrusion was applied).

3.1.6 Hardness Tests

3.1.6.1 Macrohardness

Brinell Macrohardness: ISML (Ref. 2-4) measured the Brinell macrohardness at 20°C applying a ball diameter of 2.5 mm, a load of 62.5 kg and a time of 30 secs. Results as a function of oxide contents are given on Fig. 70.

The same laboratory performed tests up to 400°C on SAP 7 and 14% (Ref. 21b). The test conditions were as follows: ball diameter 5 mm, load 125 kg maintained during 3 min. Results are given on Fig. 70b.

Similar tests have been done in Euratom laboratories up to $600^{o}C$ with a machine of Euratom construction. The test conditions were as follows:-

- ball diameter: 2.5 mm
- loading speed: 0.4 mm/s
- load maintained during 3 mins.
- number of indentations for each temperature: 4
- maximum difference of temperature between two indentations: $\pm$ $3^{o}C$.

Results are reported on Fig. 70 a

Vickers Macrohardness: Euratom measured the Macrohardness with a Tukon-Wilson tester by the Vickers method. A load of 1 or 2 kg was used as can be seen in Fig. 69. Five different samples were prepared for each SAP grade and three separate indentations were made on each sample.

3.1.6.2 Vickers Microhardness (Euratom results)

Euratom measured the microhardness at room temperature with a Leitz-Durimet by the Vickers method (load 100 g, time 10 s). The arithmetic mean of ten measurements for each grade of SAP is reported in Fig. 69.

Preliminary results of Vickers Microhardness at high temperature have also been obtained in the Euratom laboratories with a new machine developed under contract (S.E.A.V.O.M./EURATOM)(Ref. 28bis). The maximum difference of temperature between two successive indentations on the same specimen is reported on the table below:-

Test temperature ^{o}C	Maximum temperature difference
1,000	$\pm$ 8
600	$\pm$ 4
400	$\pm$ 2

The indenters are made of diamond. The heating of test specimen is obtained through electron bombardment, the vacuum of the chamber being maintained between 10^{-5} and 10^{-6} Torr.

The test conditions were as follows:

- load: 50 g
- loading duration: 1 s
- load maintained during 20 s
- number of indentations for each temperature: 3 to 4
- number of measurements possible on one specimen: $>$100
- the measurement of indentation is made at the required temperature

The results are given on Fig. 69A.

3.1.7 Fatigue Tests by Rotating Bending (ISML results)

3.1.7.1 Fatigue Life at 20° and 400°C

Test conditions (Ref. 8)

The fatigue test specimen for this series of tests is shown in Fig. 74. The surface finish was held between 0.09 and 0.1 micron and was measured by a Taylor-Hobson roughness meter in the longitudinal direction of the specimen. The rotating bending fatigue machine was a Schenck-Duplex, turning at 3,000 rpm.

Results

The results are shown in Figs. 75-79 for 20 and 400°C. Generally speaking, the 400°C curve is about 50% lower than the 20°C curve. The maximum number of cycles was 10^8, but the curves did not reach the asymptotic value at this point, so the real fatigue limit is not known. Thus we can only speak of a fatigue life at 10^8 cycles.

From the same batch some tensile tests were carried out in order to compare the results of the two tests.

Ratio $\frac{F}{S_{0.2}}$ \ % Al_2O_3	4	7	10	14
at 20°C	0.56	0.48	0.49	0.49
at 400°C	0.92	0.71	0.68	0.60

In the above table the ratio between the fatigue life at 10^8 cycles (F) and the 0.2 offset yield stress is given for four SAP grades at 20 and 400°C.

3.1.7.2 Notch Effect in Fatigue Tests by Rotating Bending at 20°C

Test conditions (Ref. 2)

The unnotched specimen is shown in Fig. 81 and the notched one in Fig. 80. The details of the V- and U-notch are also visible in Fig. 80. The surface finish was held between 0.09 and 0.1 micron, as above. The apparatus was an ISML FRS type turning at 11,500 rpm.

Results

The results are given in Figs. 82-85. Each graph shows the unnotched and notched (U-form) fatigue results up to 10^8 cycles for a given SAP alloy (4,7, 10 or 14% Al_2O_3).

Ratio at 20°C \ % Al_2O_3	4	7	10	14
$\frac{F_n}{F}$	0.42	0.48	0.45	0.55

The ratio of the fatigue life (Fn) up to 10^8 cycles for the notched (U-form) and unnotched specimen (F) is given above. Generally speaking, the notch effect is less severe with increasing Al_2O_3 contents. Besides the U-notch (Neuber coefficient = 2.2), a V-notch (Neuber coefficient = .9) was applied in two test series on SAP 4% and 7%.

From Figs. 82 and 83 it can be seen that the form of the notch has no major influence, except for low cycle values of the SAP 4%.

With different conditions, as in Section 3.1.7.1, we can again determine the ratio $F/S_{0.2}$ at 20°C for the unnotched specimen.

Ratio at 20°C \ % Al_2O_3	4	7	10	14
$\frac{F_n}{S_{0.2}}$	0.60	0.50	0.55	0.45

The ratio between the fatigue life (Fn) at 10^8 cycles and the 0.2 offset tensile yield stress is given in the above table. The same tendency is visible as in Section 3.1.7.1, that is to say, the reduction in the strain (difference $S_{0.2}$ - Fn) is more severe for a high percentage of Al_2O_3.

3.1.8 Gradual Evolution of Batch Quality (ISML Results)

3.1.8.1 Scatter of Results (Refs. 11 and 35)

Histograms of the tensile properties ($S_{0.2}$ - S_u - e_{pb}) of different grades of SAP are given in Figs. 86-87-88.

They originate from:-

a) production controls of the standardized production
b) controls of major changes in the standardized production method
c) verification of batches destined for special laboratory test series (e.g., impact strength, creep, fatigue, hardness, etc.).

In Figs. 86 and 87, which give the results for 20 and 400°C, the data are not complete because the numbers in the ordinates of the histograms are not listed. Furthermore, the results in Figs. 86 and 87 are for very old batches produced before the end of 1962.

The more recent results on complete histograms are given in Fig. 88, which contains 43 test results for SAP 7% at 450°C.

These 43 tensile tests were selected from batches which were fabricated under standard conditions. For the histograms of Fig. 88 the scatter can be roughly defined as:

for the stresses $\frac{8.1 - 6.8}{7.57} = 17\%$

for the strains $\frac{6 - 2.5}{4.38} = 80\%$

3.1.8.2 Properties as a Function of Batch Number (Ref. 35)

Figs. 89-91 showed the curves of the mechanical properties ($S_{0.2}$ - S_u - e_{pb}).

The tensile test results were selected in order to represent only batches made under standard fabrication conditions.

The method of manufacturing the base material (the starting powder) was unchanged until the end of 1962 (batch No. 1,000). Furthermore, the tensile testing temperature was changed from 400 to 450°C.

The three diagrams give an idea of the evolution. There is instantaneous scatter - in the vertical sense, as for batch numbers which are close to one another - and long-term scatter - in the horizontal sense, as with the time axis. These two types of scatter are difficult to express in figures owing to the lack of results.

The existence of this "scatter range" also has an effect on the 85 preceding diagrams. These are results relating to a certain batch number and thus these data are not representative for SAP as a whole.

If the results of the previous 85 diagrams are to be used, it will be necessary to apply a safety margin, which is related to the width of the "scatter range".

3.2 Influence of the Mechanical and Thermal Treatments on the Extruded Product.

The extruded product is only the base material for the preparation of the finished products. It has already been stated (Section 1.7) that in certain cases (thin-walled tubes, plates, foils) it is necessary to use cold-deformation (rolling or cold-drawing). The evolution of the mechanical properties after cold-deformation as compared with the properties of the extruded product was therefore studied. Furthermore, it is nearly always necessary to include an annealing treatment and often the operating temperature of the final product is quite high, so the evolution of the properties of the material as a function of the annealing temperature was examined.

The main results obtained are given here and the reader is referred to the specific paragraphs of each type of test for details of the general experimental conditions.

3.2.1 Influence of Cold-Deformation

3.2.1.1 Tensile Tests (Refs. 27 and 46, Figs. 28 and 29)

The study was carried out on SAP ISML 4% extruded (E = 2.5) and then rolled (H = 92%). At room temperature the rupture strength of the rolled product (Fig. 28) is higher than that of the extruded material. At 20°C, as expected, the plastic strain (Fig. 29) is lower after cold-deformation. The high-temperature tensile tests (heating time + time at temperature 1 hour, so annealing effect cannot be avoided) demonstrate lower strength and higher ductility in the 300-500°C range for the cold-deformed samples. Near 600°C, however, the differences become negligible.

3.2.1.2 Vickers hardness tests (Ref. 56)

The Vickers hardness versus the degree of deformation for aluminium and the four SAP ISML alloys is plotted in Fig. 71. For the same degree of deformation the absolute increase in the Vickers hardness rises with the Al_2O_3 content.

3.2.2 Influence of Heat Treatment After Rolling

3.2.2.1 Tensile Test (Refs. 27 and 46, Figs. 28 and 29)

The tests were performed on SAP ISML 4% only. With a treatment of 3 hr at 620°C an attempt was made to recrystallize the rolled material, or at least to recover it.

In diagrams (Figs. 28 and 29) this recrystallization effect is clearly noted for tensile tests at 20°C, that is to say, for increasing ductility and decreasing strength values.

Some strange phenomenon occurs at 300 and 400°C. At 300°C, the ductility of the recrystallized material has the same ductility values as the extruded material. At 400°C the strength of the recrystallized material lies between the rolled and the extruded strengths.

3.2.2.2 Vickers Hardness (Ref. 56)

In Fig. 72 the recovery of Vickers hardness from H_V 75 to H_V 52 is plotted versus the annealing temperature for SAP ISML 4%. All the specimens were annealed together for one hour at the temperatures given in the figures. The specimens were alternately heat-treated, then measured, etc., right through the whole temperature range from 20 to 660°C. This figure shows that for an alloy which has undergone only 22% deformation complete recovery is obtained only at extremely high annealing temperatures. With increasing deformation, the recovery temperature is shifted to a slightly lower temperature. Fig. 73 shows the change in the recovery temperature of different alloys for a deformation of 95%. A shift in the recovery temperature to higher values for increasing Al_2O_3 contents is clearly visible. In conclusion, it may be said that the SAP structure is stable, recovery and in particular recrystallization being obtained only by thermomechanical treatment which lay completely outside the field of industrial practice.

3.2.3 Influence of the Heat Treatment on SAP 4% at 460°C (Ref. 48)

Creep tests were carried out on test specimens which were taken from the same batch and had undergone heat treatment at extremely high temperature (540°C; melting point of Al = 660°C) for periods of between several hours and 3,000 hr. The results are given in Fig. 52. It can be seen that treatment at high temperature of very long duration considerably lowers the properties of the material.

3.2.4 Influence of Thermal Cycling During Creep Test (Ref.49, Fig.53)

Thermal cycling of the specimen was effected in the course of a creep test at 460°C by switching off the heating furnace four times in 24 hr until the temperature reached 340°C. No influence on the stress-to-rupture curve was observed.

3.2.5 Influence of previous creep test on tensile properties

3.2.5.1 Euratom results

In order to see if the elongation of the specimen in creep test (at 460°C) does reduce the amount of elongation obtainable in tensile tests (at 450°C) we performed tensile tests on specimens which had remained unbroken after creep tests at a stress level of 0.6 Su. The test conditions, both for creep and tensile tests were the standard ones (see Sections 3.1.1.1 and 3.1.3.1) but naturally the creep specimen (Fig. 38) was also used for tensile tests.

Tests have been done on an old Batch (No. 275) and a more recent one (No. 1720-1722). The final results are given on the table below.

Evolution of tensile properties after creep
of SAP ISML 7% related to tensile properties
without previous creep

Material: SAP 7%		Evolution of tensile properties			
Batch No.	Origin of powder	$\Delta S_{0.2}$ (kg/mm²)	ΔS_u (kg/mm²)	Δe_{pu} %	Δe_{pb} %
275	AIAG	- 3%	- 2.7%	-27.3%	-13.5%
1720 1722	Eckart-Werke	+4.2%	+ 3.2%	-40%	-45.3%

The behaviour of the two batches are opposite in strength. However for both batches, the elongation shows a tremendous decrease.

3.2.5.2 ISML results (Ref. 14)

Tests have been done at 400°C on old batches of SAP ISML 4, 10 and 14%. The test specimens (Fig. 39) machined from bars Ø 21 mm have been submitted to creep tests up to 5,000 hours at a stress level of 0.66 S_u, without rupture. Tensile specimens (Fig. 4) were machined out of creep specimens and then tested. As for Euratom results, we give on the table below the evolution of tensile properties.

Material		Evolution of tensile properties		
Batch No.	Origin of powder	Al_2O_3	$\Delta\ S_u$ (kg/mm^2)	$\Delta\ e_{pb}$ (kg/mm^2)
381	AIAG	4%	+5.7%	-30%
409	"	10%	-6.0%	-57%
416	"	14%	-5.0%	-56%

As a comparison basis, we have chosen the values of tensile properties obtained on bars Ø 16 mm according to Fig. 27. We had previously shown (Fig. 24) that there was no large increase in the values of e_{pb} from a bar Ø 16 and a bar Ø 21 mm.

We see that the decrease of elongation is in good agreement with Euratom conclusions.

3.3. Mechanical properties of finished products

3.3.1 Smooth Tubes

3.3.1.1 Tensile Tests (ISML Results, Ref. 22)

Figs. 105 to 107 contain some tensile properties ($S_{0.2}$-S_u-e_{pb}) as a function of the percentage of Al_2O_3 for:-

- simple extruded smooth tubes (position 2)
- extruded smooth tubes, afterwards cold-drawn (position 3)
  Other test conditions are not known.

As was already known in the case of bar material, it will be seen that an increase in the Al_2O_3 content is accompanied by increasing stress and decreasing strain. If we compare positions 2 and 3 in Figs. 105, 107 and 108, the influence of the cold deformation can clearly be seen:

- at 20°C higher stresses and lower strains
- at 450°C lower stresses (especially for SAP 10%) and no significant differences in strain.

3.3.1.2 Burst Tests (Euratom Results)

The tubes were tested in a furnace at 460°C under internal gas-pressure (Nitrogen) up to rupture. The test specimens were 300 mm long and a thermocouple was set inside the test specimen. They were closed by two plugs consisting of an internal aluminium ring pressed on to the tube wall by two cones. The rate of pressure increase was about 10 kg/cm^2 per minute, so the test duration was comprised between 4 and 7 minutes.

The smooth tubes were extruded and then cold-drawn but not annealed. They were left in furnace 1 1/2 hours for temperature equilibration. The resulting transverse stresses (hoop-stress) (in kg/mm^2) are listed in the following table.

Test specimen	% Al_2O_3	4	7
	Batch No.	Production early 1962	2265 to 2273
	diameters (mm)	13.1 14.7	25.5 27.5
Test conditions	Duration (min)	7	4
	Number of tests	5	18
Results (tangential rupture stress in kg/mm^2)	Maximum	4.3	5.9
	Average	4.0	5.2
	Minimum	3.5	4.1
Scatter %		20%	35%

Referring to tensile tests on smooth tubes (Fig. 105), we find:

SAP 4% $S_u = 5 \ kg/mm^2$

SAP 7% $S_u = 6.3 \ kg/mm^2$

so the ratio for transverse stress (S tr) and longitudinal stress (S lo) becomes

for SAP 4% $S_{lo} / S_{tr} = \frac{5.0}{4.0} = 1.25$

for SAP 7% $S_{lo} / S_{tr} = \frac{6.3}{5.2} = 1.2$

However, the thermal treatment applied to burst test specimens and to tensile test specimens are not the same, so, the difference in transversal and longitudinal rupture stresses would be somewhat higher.

3.3.1.3 Stress-rupture Tests Under Internal Gas Pressure (Euratom and ISML results) Refs. 8 and 52.

Both laboratories used the same principle as described above in Section 3.3.1.2, but for these creep tests it was necessary to maintain a certain constant gas pressure and to record the time-to-rupture.

Stress rupture curves up to 100 hours are given for SAP 4% and 7% and 400 and 450^{o}C in Figs. 108 and 110. The influence of the temperature and Al_2O_3 percentage are quite normal. A more complete curve up to about 1,500 hours based on two different batches of SAP 4% is given in Fig. 109.

A comparison between two different laboratories (and different batches) is made in Fig. 115. The Euratom results at 100 hours are about 25% lower than those of ISML.

The creep properties of three different production processes are compared in Fig. 111. The creep properties of the extruded tube are largely superior to the tubes which are afterwards cold-drawn and the stresses drop again when the tubes are annealed afterwards (maximum difference about 50%).

3.3.2 Finned Tubes

ISML fabricated different types of finned tubes necessary for the different solutions of neutron - and heat-transfer - calculations. The general features of the tube profiles are given in the table below.

Description \ Profile number	3	6	7	8	9	10	11	12
No. of thermal fins	36	36	36	32	36	36	36	28
No. of spacers	3	3	6	2	3	3	3	-
type of fins straight S helical H	H	H	S	H	H	H	S	H
internal diameter (mm)	25.5	25.5	25.5	21.15	25.4	24.9	24.9	14.6
wall-thickness (mm) tolerances + 0.2 - 0	1.0	1.0	1.0	1.0	1.0	1.0	1.0	0.9
external diameter of thermal fins	29.9	29.5	29.5	24.95	29.8	28.9	28.9	18.4
external diameter of spacers	33.5	30.5	30.5	27.55	32.1	29.9	29.9	-

3.3.2.1 Tensile Tests

Many tensile tests were performed for production control purposes. Two properties (S_u and e_{pb}) are shown in histograms in Fig. 112 in order to give an idea of the scatter. Two types of histograms are superimposed, one for the results for all the tubes, and the other for profile No. 9. As usual, the elongations are measured after rupture by putting the two parts of the tube together. The new distance between two marks is then determined. However, from this value must be subtracted the maximum clearance which remains when the two halves are put together.

The arithmetical mean values of profile No. 9 are about 2% higher than the values for all the tubes, so this single profile seems to be really representative of the whole bulk.

Comparison between extruded finned tubes and smooth tubes shows good agreement.

properties at 450°C for 7% SAP / types of specimen	S_u (Kg/mm^2)	e_{pb} (%)
smooth tubes (annealed 2 hr/500°C: Fig. 105 Ref. 22-31)	8.6	2.3 to 3.7
finned tubes (non-annealed)	8.9	2.9
finned tubes profile No. 9 (non-annealed) Fig. 112, Ref. 35	9.2	3.3

3.3.2.2 Compression tests

Experimental conditions

As for cylindrical specimens, an Instron TTCML testing machine was used and the tests carried out at 450°C. The test specimens consisted of pieces of tube carefully cut perpendicular to their axis. Their length was approximately equal to the greater external diameter of the tube.

Results

The rupture stresses are the ratio of the rupture load and of the cross-area (S) of the tube. The "maximum engineering stress", the "engineering 0.2 offset yield stress" and the "plastic uniform strain" are defined as for cylindrical specimens (see Illustration 5). Here, the values of e_{pb} have no sense, because the breaking point is not reached, as it is in tension tests. The main results are listed on the following table (mean value, max. and min. value).

Characteristics of the Specimen				Results		
Profile of the tube	Height (mm)	Cross area (mm^2)	Number of tests	S'u (kg/mm^2)	S'0.2 (kg/mm^2)	e'pu %
ISML 9	30	146	18	7.26 7.15 to 7.39	5.34 4.93 to 5.61	0.32 0.20 to 0.39
ISML 12	18	72	12	6.90 6.86 to 7.0	5.44 5.0 to 5.83	0.20 0.16 to 0.26

A rough estimation of the scatter (as in Section 3.9.1) for tensile and compression tests is given in the following table.

Profile of the tube	Type of Test			
	Tension (ISML)		Compression (Euratom)	
	S_u	e_{pb}	S'_u	e'_{pu}
ISML 9	17%	118%	3%	60%
ISML 12			2%	50%
All finned tubes	43%	166%		

We notice that the scatter is always lower in compression. Moreover this last type of test is easier to perform for production control and allows the values of elongation to be obtained more precisely, which lowers the scatter.

3.3.2.3 Burst tests

Burst tests as production control (Euratom results)

Sixty burst tests have been done on two main profiles in SAP 7%. The test conditions are similar to those for smooth tubes (see Section 3.3.1.2). For the calculation of tangential stress, the thin-wall formula $\sigma_t = \frac{P.Di}{2.t}$ was consistently used, "t" representing the minimum wall thickness (i.e. without fins) of the tube considering a medium tolerance. The results are assembled on the following table (mean value, max. and min. value).

Specimen		Results		
Profile of the tube	Number of specimens	Burst pressure kg/cm^2	Tangential rupture stress σ.t(kg/mm^2)	scatter %
ISML 9	30	48 (44 to 50.5)	5.55 (5.1 to 5.8)	12.5
ISML 12	30	69 (64 to 74)	5.6 (5.2 to 6.0)	14

Most ruptures occurred at the bottom and along one of the higher spacer fins. The comparison between smooth extruded and cold drawn tubes and finned extruded tubes of SAP 7% is reported in the table below.

Profile of the tube	Number of specimens	Tangential rupture stress σ_t (kg/mm^2)	Scatter %
Smooth tube	18	5.2	35%
ISML 9	30	5.55	12.5%
ISML 12	30	5.6	14%

The values of rupture stresses for finned tubes are about 7% higher and the scatter is only the half.

The ratio between tangential and longitudinal stresses in finned tubes as compared with smooth tubes is given below.

Type of tube	Tension test	Burst test	Ratio
Smooth	6.3	5.2	1.2
Finned	9	5.6	1.6

This result shows that in finned tubes the difference in mechanical strength in the two directions is higher than in smooth tubes.

3.3.2.4 Influence of internal artificial defects on the transverse mechanical properties of finned tubes.

Preliminary studies have been carried out at 450°C on finned tubes (ISML 9) with internal artificial defects machined with a constant profile tool (Ref. 62 bis). All tubes were first ultrasonic tested to ensure that they were free from any natural defect and their thickness between every fin carefully measured. The form and dimension of the defects are shown on Illustration 7. Its location is represented on Position 3. A macrography shows on Illustration 8 the real profile obtained. Ten specimens have

INTERNAL DEFECTS
MACHINED IN FINNED TUBES

Shape and dimensions of the defect

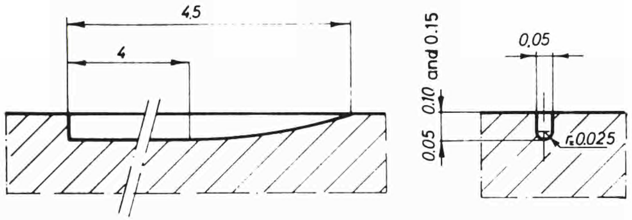

Position of the defect

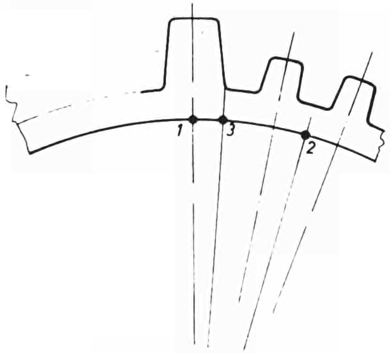

Illustration 7

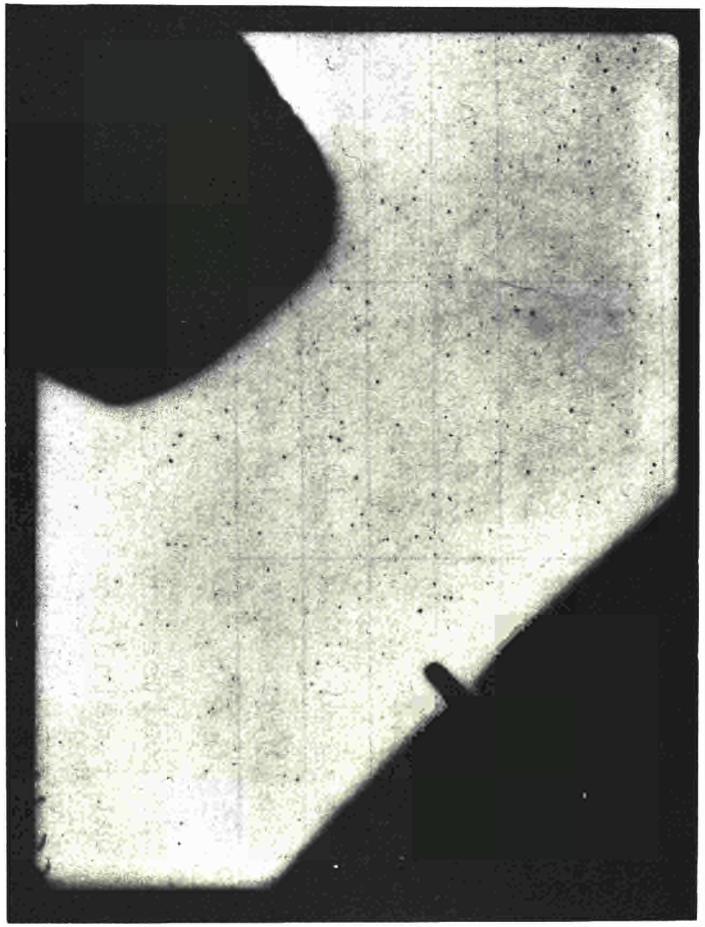

Illustration 8 Artificial defect 0.15 mm depth machined on finned tubes (magnification 50)

been tested for each type of defect. The results are summarized in the table below. The tangential stress is calculated using the wall thickness measured on the ruptured generatrix: most ruptures occur along and at the bottom of a spacer fin; only 30% of all the tubes ruptured on the defect.

Depth of defect (mm)	Mean value of tangential stress (kg/mm^2)	Scatter (%)	Decrease of strength (%)
0	5.52	6.5%	0
0.05	5.45	8.5%	1.3%
0.10	5.40	10.5%	2.4%
0.15	5.34	12 %	3.3%

We notice that the scatter increases with increasing the depth of the defect, but remains lower than in production control tests. The mean values of the rupture stresses show a slight decrease of only 3.3% which is of no real significance due to the large scatter.

3.3.2.5 Fatigue tests under internal gas pressure

Experimental conditions

The test arrangement is similar to the one used for smooth tubes (see Section 5.1.2). Experiments have been carried out on test specimens 300 mm length of finned tubes profile ISML 9 free from natural defects (U.S. controlled) but having artificial internal defects as described in the previous section. The pressure rose from 1 kg/cm^2 up to the preselected value in approximately 1 minute and was decreased to the initial value nearly instantaneously.

Results

As previously, the tangential rupture stress is calculated with the classical $\sigma_t = \frac{P.Di}{2.t}$ formula, "t" being the thickness along the line of rupture. As a matter of fact, 66% of all the tubes ruptured outside the zone of the artificial defects. Most ruptures occurred at the bottom and along one of the three spacer fins. The results are reported on the diagram Fig. 119. We see clearly that the rupture stresses of tubes with defects of 0.05 and 0.10 mm and the most part of those of 0.15 are contained in the dispersion band of the values for tubes without defects. Such short longitudinal defects affecting 10% of the wall thickness do not seem to be very critical even in fatigue testing.

3.3.2.6 Creep tests in compression (Euratom results)

Test conditions

We used the Adamel TAC stress to rupture machines (as in Section 3.4.1.1) fitted with a cage system allowing work in compression. The test temperature was 460°C. Specimens were pieces of ISML 7 finned tubes of 40 mm length (cross section 138 mm^2).

Results: The number of specimens tested at each stress is as follows

3.8 kg/mm^2	3 tests
4.0 kg/mm^2	3 tests
5.0 kg/mm^2	6 tests

In these conditions only three specimens at 5.0 kg ruptured after 21, 817 and 2,089 hours respectively, all the others remaining unbroken after more than 4,000 hours. Similar experiments made on cylinders have not ruptured even under a stress of 5.0 kg/mm^2.

3.3.2.7 Gradual Evolution of Batch Quality

As for the bar production (see Figs. 89-91) we have plotted the tensile properties as a function of the batch number.

Fig. 113 concerns all the tubes as a whole and Fig. 114 profile No. 9 only.

A scatter range is clearly visible in all cases. However, over a long period there is a general tendency for the properties to increase.

3.3.3 Pressure Tubes

The main results obtained are given in Ref. 55.

3.4 Comparison Between Rods and Tubes

3.4.1 Smooth Tubes

Creep tests

The creep properties of SAP 4% and 7% are compared in Figs. 115 and 116 respectively. The critical stresses act in two different directions, relative to the fibrous Al_2O_3 structure.

Thus, for rod material it is a longitudinal stress and for tube material (creep test with internal gas pressure) transverse. The following table for smooth tubes and rods can be drawn up for the ratio between these two stresses after 100 hr creep-rupture.

ratio / $\%Al_2O_3$	Slow testing (creep)	Fast testing (tensile & burst tests) (Section 5.1.2 and 5.2.3)
4	S_{lo}/S_{tr} = 1.3 to 2.1	S_{lo}/S_{tr} = 1.25
7	S_{lo}/S_{tr} = 1.35	S_{lo}/S_{tr} = 1.2

This ratio is compared to the fast testing ratio. It will be seen that the difference between the transverse and longitudinal strengths is greater during slow testing.

Tension tests

In Figs. 105-107 the properties of smooth tubes and extruded rods (position 1). are compared.

Generally speaking, it may be said that for smooth tubes the strains are lower for 20 and 450°C and the stresses also for the 450°C tests.

3.4.2 Finned tubes

Histograms of tensile tests of tubes and rods of SAP ISML 7% at 450°C are given in Fig. 117.

Specimen	Properties at 450°C	
	S_u (kg/mm^2)	e_{pb} %
rod	7.6	4.4
tube	9.0	3.2

Note the higher strength (18%) and lower ductility (a decrease of 27%) of the tubes.

3.5 Physical Properties

Since the aim of this report is mainly to describe the mechanical properties, a complete description of the physical properties will not be given. We shall limit ourselves to those which could be of immediate interest to the designer.

3.5.1 Young's Modulus

3.5.1.1 Experimental devices

3.5.1.1.1 Static methods

Euratom tests:

All these tests were carried out on a universal electrical Instron machine.

Tests at 20°C (Ref. 27, Fig. 92).

Test specimen diameter 4 mm, gauge length 25.4 mm, drawn from bars of 9.5 mm, extrusion ratio E = 76.

Elongation measured with the aid of a Wideman-Baldwin inductive extensometer type PSH 8 MS (magnification 500 x). The results were taken from diagrams plotted by the xy recorder of the Instron machine (load as a function of specimen elongation).

High temperature tests (Ref. 30, Fig. 93)

Test specimens: 1st test specimen (Fig. 3) diameter 4 mm, length 30 mm.
2nd test specimen diameter 4 mm, length 5 mm.

We used a differential method involving the use of two test specimens of different lengths so as to eliminate the effects due to the deflection of the frame of the machine. The furnace kept the temperature constant at ± 1°C.

ISML tests (Ref. 6).

This laboratory used test specimens 10 mm in diameter and 100 mm long drawn from bars 16 mm in diameter (extrusion ratio E = 26.6). The testing machine was an Amsler hydraulic machine. The elongations were measured with the aid of a Martens-type extensometer (magnification 500 x). The furnace was set to ± 2°C.

3.5.1.1.2 <u>Dynamic methods</u>

Euratom tests (Ref. 29, Fig. 92)

These were performed by internal damping on a Bordoni-type machine (Ref. 24) designed by Euratom.

ISML tests (Ref. 3, Fig. 92)

The apparatus used was of the Bordoni type (Ref. 24) with electrostatic excitation. The test specimens were cylinders 8 mm in diameter and 160 mm long obtained by double extrusion (extrusion ratio E = 107). The measurements were made under a vacuum of 1.5 mm Hg. The damping of the oscillations was observed with the aid of an oscilloscope.

3.5.1.2 <u>Results</u>

3.5.1.2.1 <u>Young's modulus at 20°C as a function of the oxide content</u> (Fig. 92)

Young's modulus increases with the oxide content.

<u>Static method</u>:

- Euratom tests

Each point represents an average of five measurements.
The average scatter is of the order of ± 7%.

- ISML tests

Each point represents the average of two tests. The scatter is much smaller.

- Comparison of the two results:

The values obtained by Euratom are higher by about 4% than those of ISML over the whole range of Al_2O_3 contents.

Dynamic method:

As foreseen, the dynamic Young's modulus is higher than the static Young's modulus (about 12%).

3.5.1.2.2 Variations in Young's modulus with the temperature for four SAP ISML contents.

Static method:

For the SAP 4%, the Euratom results show a discontinuity between 250 and 350°C. The lack of agreement with the ISML results is of the order of 3%.

Dynamic method:

The dynamic Young's modulus was only determined on SAP 4%, and is about 20% higher than the static modulus.

3.5.2 Linear Thermal Expansion

3.5.2.1 Test conditions

- Apparatus : A Chevenard-type dilatometer with photographic recording was used. It was a special Adamel Type 55 equipped to operate under vacuum or in controlled atmosphere.
- Test specimen : A 50 cm long specimen was used for measuring the expansion in the extruded direction and a 25 cm specimen for the perpendicular direction.
- Experiment : This was conducted in argon atmosphere with an increasing temperature of 60°C/hr. The magnification K was 150 or 300 times.

3.5.2.2 Experimental results

The results obtained perpendicular or parallel to the extrusion direction were practically identical. The results for the latter direction are given in **Fig. 94**. The values for the linear thermal expansion are plotted as a function of the oxide content for several temperature ranges between 20 and 500°C.

It was possible to establish the equation below expressing the length of SAP samples of different grades as a function of the temperature:

SAP ISML 4% $l_t = l_o (1 + 21.32 \cdot 10^{-6}t + 9.10^{-9} t^2)$

SAP ISML 7% $l_t = l_o (1 + 20.38 \cdot 10^{-6}t + 9.10^{-9} t^2)$

SAP ISML 10% $l_t = l_o (1 + 19.73 \cdot 10^{-6}t + 9.10^{-9} t^2)$

SAP ISML 14% $l_t = l_o (1 + 18.93 \cdot 10^{-6}t + 9.10^{-9} t^2)$

It can again be seen from these formulae that the thermal expansion drops as the oxide content increases.

3.5.3 Electrical Resistivity

3.5.3.1 Test conditions

Euratom laboratory (Ref. 50)

The tests described were performed with a double Thompson bridge. The electrical resistance of the bridges was verified to an accuracy of better than $2 \cdot 10^{-4}$. The test specimen is a cylinder 6 mm in diameter and 80 mm long. The sample holder was designed specially in order to increase the relative precision of the gauge length up to 0.1%. Under the above conditions, the relative error in the determination of the resistivity $\frac{(\Delta R)}{R}$ is less than 0.5%.

Euratom laboratory (Ref. 54)

The electrical resistivity was measured by the d.c. potentiometric method. The samples were mounted in series with a standard resistance, immersed in a thermostatic bath and the current flow then measured with a potentiometer. The limit accuracy in the determination of the current was that of the standard, i.e., $2 \cdot 10^{-4}$. The samples were immersed in a thermostatic bath kept at 25 ± 0.05°C and the potential drop between two knife edges measured with a five dial potentiometer. Care was taken to eliminate thermoelectric emf by reversing the current.

The samples were cylinders 4 mm in diameter and 50 mm long. The error affecting the dimensions can be estimated at <1%. All the samples had been annealed for two hours at 550°C in a high-vacuum furnace.

The resistivity at high temperature up to 500°C was measured by determining the ratio between the resistances at the given temperature and at 25°C. The resistivity data at high temperature were corrected for the effect of thermal expansion.

As a coefficient of thermal expansion of SAP, a value of 24.10^{-6} cm/°C was taken which is independent of the orientation (Ref. 25).

The samples were heated in a high-vacuum furnace stabilized to ± 0.5°C, standardized thermocouples being used. The reproducibility of the electrical resistivity data was to within 2.10^{-3} and it can be assumed that the error affecting these values is $\leqslant$ 1%.

ISML Laboratory (Ref. 9).

The classical d.c. potentiometric method was used, the testing specimen being connected in series with a calibrated resistance. The testing specimen is machined from an extruded plate (30 x 2.5 mm) and annealed for 24 hr at 500°C. The tests were conducted up to 550° in a furnace with a temperature determination of ± 1°C. The accuracy of the readings of the potentiometer was 10^{-7}. The relative scatter in the results observed in several tests in the same conditions did not exceed 3.10^{-4} . The ratio $\frac{R_t}{R_{20}}$ was determined for every temperature and the absolute value of R_{20} for every percentage of Al_2O_3.

3.5.3.2 Results

- Resistivity as a function of the oxide content at 20°C
  (Ref. 50, Euratom, Fig. 95)

On this diagram we have also plotted the values determined by other laboratories. This diagram clearly shows that the absolute resistivity increases with the oxide content. Every test specimen was chemically analyzed, and there is a relatively high scatter in the oxide content.

The mean scatter of the resistivity is in the range of ± 3.5%. The values obtained in other laboratories for other batches are in the normal scatter range.

- Resistivity as a function of the test temperature for different grades of SAP ISML (Refs. 9, 26 and 54, Figs. 96 and 97, Euratom and ISML results)

The electrical resistivity increased with temperature and the results obtained in the two laboratories are in good agreement.

- Resistivity parallel and perpendicular to the direction of extrusion as a function of the oxide content at 100°C and 500°C

Euratom result (Ref. 54, Fig. 98)

The resistivity values increase with the oxide content, as seen above (Fig. 95). Moreover, the transverse resistivity is higher than the longitudinal one.

3.5.4 Thermal conductivity

3.5.4.1 Experimental procedure

Euratom laboratory (Ref. 53)

The apparatus is Euratom-built. The method is a stationary one, conducted with axial flow along a cylindrical sample. Armco iron was selected as the reference sample.

Euratom laboratory (Ref. 54)

For this present study, use was made of a new transient flow method developed to meet the specific requirements of our research. This method enables both the thermal diffusivity and the conductivity in a given direction to be determined and offers the advantage of using a known thermal capacity as a reference. Because the specific heat is a property known with much greater accuracy than the thermal conductivity, the method seems more reliable than those based on comparison with a standard thermal resistance.

Comparative determination on high purity nickel and aluminium samples with conventional steady state techniques and the methods described above resulted in close agreement, the difference being in all cases less than 6%.

ISML laboratory (Ref. 3)

The relative method employed by the US Bureau of Standards (Ref. 44) for use up to 600°C was adopted. The method consists in measuring the thermal gradient along two cylindrical samples, one of them being the material to be tested and the other one a reference sample (in this case lead). The two samples are welded together at the end and placed in a metallic tube. A complete description of this apparatus is given in Ref. 66.

3.5.4.2 Results

- Thermal conductivity plotted as a function of the temperature (Figs. 99, 100 and 101).

The ISML laboratory expressed the thermal conductivity of SAP ISML as a proportion of that of aluminium (Raffinal 99.995%).

The apparatus used by the Euratom laboratory (Ref. 53) was tested on 99.999% aluminium and the values obtained plotted in Fig. 99 are in good agreement with the literature.

From Figs. 99, 101, it can be seen that the conductivity falls compared with that of aluminium as the oxide content increases.

In conclusion, it may be said that the conductivity seems to drop as the temperature rises but the results obtained by the three laboratories do not seem to be in good agreement.

- Thermal conductivity, longitudinal and transverse at 100°C and 500°C versus the oxide content (Ref. 54, Figs. 102 and 103)

The transverse conductivity is always lower than the longitudinal one. The difference increases as the oxide content rises, but is fairly constant for the temperature related.

- Thermal conductivity, longitudinal and transverse, of SAP ISML 10% versus the temperature (Ref. 53, Fig. 99)

The transverse conductivity is 25% lower than the longitudinal one and this difference decreases slightly as the temperature rises.

3.5.5 Density

The values for the density versus the percentage of Al_2O_3 are plotted in Fig. 104.

These results concern batches of SAP ISML which are representative of the production from 1960 to 1966. The scatter of the results does not exceed ± 0.2%. It can be seen that the density is proportional to the percentage of Al_2O_3. Fig. 104a shows results obtained at Risö Institute (Ref. 41). The density of the materials was determined according to Ref. 39. The data are averages of 3-6 measurements.

References

Progress reports concerning Montecatini/ISML research contracts Nos. 003.60.5 ORGI, 26.61.7 ORGI, 092.63.4 ORGI and 065.64.7 TEO 1.

1. SAP Technology for Nuclear Applications: Technical Report Concerning the First Quarter May-July 1960.

2. Tecnologia del SAP per applicazioni nucleari: relazione tecnica trimestriale, 1 August-31 October 1960, Report No. 6011. 063/9798.

3. Tecnologia del SAP per applicazioni nucleari: relazione tecnica trimestriale, 1 November-15 February 1961, Report No. 10.129/6103.042.

4. SAP Technology for Nuclear Applications: Technical Report Concerning the Period 16 February through 15 May 1961.

5. Ricerca SAP per conto Euratom - Relazione relativa al periodo 16 Maggio 1961 - 31 Luglio 1961, Report No. 10.644/6109.059.

6. Ricerca SAP per conto Euratom - Relazione relativa al periodo 1 Agòsto - 30 Novembre 1961, Report No. 10.913/6112.071.

7. Ricerca SAP per conto Euratom - Relazione relativa al periodo 1 Dicembre 1961 - 28 Febbraio 1962, Report No. 11.167/6203.069.

8. Ricerca SAP per conto Euratom - Relazione relativa al periodo 1 Marzo 1962 - 31 Maggio 1962, Report No. 11.430/6206.075.

9. Ricerca SAP per conto Euratom - Relazione relativa al periodo 1 Giugno 1962 - 30 Settembre 1962, Report No. 11.802/6211.061.

10. Ricerca SAP per conto Euratom - Relazione relativa al periodo 1 Ottobre - 31 Dicembre 1962, Report No. 12.039/6301.103.

11. Ricerca SAP per conto Euratom - Relazione relativa al periodo 1 Gennaio 1963 - 30 Aprile 1963, Report No. 12.488/6306.070.

12. Ricerca SAP per conto Euratom - Relazione relativa al periodo 1 Maggio - 31 Agosto 1963, Report No. 12.773/6309.116.

13. Ricerca SAP per conto Euratom - Relazione relativa al periodo 1 Settembre 1963 - 31 Dicembre 1963, Report No. 13.183/6401.110

14. Ricerca SAP per conto Euratom - Relazione relativa al periodo 1 Gennaio - 30 Giugno 1964, Report No. 13.686/6407.036.

15. Ricerca SAP per conto Euratom - Relazione relativa al periodo 1 Luglio 1964 - 31 Ottobre 1964, Report No. 14.060/6411.049.

16. Ricerca SAP per conto Euratom - Relazione relativa al periodo 1 Novembre - 31 Dicembre 1964, Report No. 14.262/6501.049.

17. Ricerca SAP per conto Euratom - Relazione relativa al periodo 1 Gennaio 1965 - 30 Aprile 1965, Report No. 14.654/6505.052.

18. Ricerca SAP per conto Euratom - Relazione relativa al periodo 1 Maggio - 31 Agosto 1965, Report No. 15.057/6509.103.

19. Ricerca SAP per conto Euratom - Relazione relativa al periodo 1 Settembre 1965 - 31 Dicembre 1965, Report No. 15.470/6601.092.

20. Ricerca SAP per conto Euratom - Relazione relativa al periodo 1 Gennaio 1966 - 30 Aprile 1966, Report No. 15.826/6605.059.

21. Ricerca SAP per conto Euratom - Relazione relativa al periodo 1 Maggio - 31 Agosto 1966, Report No. 16.185/6610.007.

21a. Ricerca SAP per conto Euratom - 3° Relazione quadrimestriale 1 Settembre 1966 - 31 Dicembre 1966, Report No. 16.542/6701.066.

21b. Ricerca SAP per conto Euratom - 1° Relazione quadrimestriale 1967, 1 Gennaio - 30 Aprile 1967, Report No. 16.296/6705.078.

21c. Ricerca SAP per conto Euratom - 2° Relazione quadrimestriale 1967, 1 Maggio - 31 Agosto 1967, Report No. 17.295/6710.045.

22. D. GUALANDI and P Jehenson, "Contribution to the Study of the Technology of Al-Al_2O_3 Composites with a View to their Nuclear Applications", Third Geneva Conference, May 1964.

23. C. BELVEDERE, "Sulla lavorazione plastica del SAP-ISML con particolare riferimenti all'estrusione e trafilatura dei tubi a parete sottile", Euratom Report EUR-4281 and "Alluminio - Nuova Metallurgia", 33, 185, 1964.

24. D. GELLI and T. FEDERIGHI, "Risultati di misure della dissipazione interna e del modulo elastico dinamico sul SAP-ISML", Alluminio - Nuova Metallurgia, 33, 371, 1963.

25. G. BEGHI, G. PIATTI and D. QUATAERT, "Analisi dilatometrica del SAP a differenti tenori di ossido", Euratom Report EUR-1613i, 1964.

26. R. O. SIMMONS and R.W. BALLUFFI, "Measurements of the High-Temperature Electrical Resistance of Aluminium: Resistivity of Lattice Vacancies", Phys. Rev. 1960, Vol. 117/1, pp 62-68.

27. M. DESLOIRE, "Influence de divers facteurs métallurgiques sur la fragilité du matériau composite aluminium alumine", Euratom Report EUR-1846f, 1964.

28. M. PIAT, "Rapport de stage", EUR/C-IS/1332/63f, 1963. (Not available).

28bis P. BONNET et M. GRIN (Euratom), D. GRUNSPAN (S.E.A.V.O.M.) "Machine de microdureté à haute temperature sous vide". (Congrès international sur les Applications des Techniques du Vide à la Métallurgie, Strasbourg 13-17 Novembre 1967).

29. A.M. SCHNEIDERS, "Internal Friction and Young's Modulus, Measurement on SAP", EUR - 1275e, 1965, reprinted from Alluminio - Nuova Metallurgia, 11, 1964.

30. D. J. BOERMAN, "The Influence of the Deflection of an Electromechanically Operated Tensile Machine on the Stress-Strain Diagram", Materialprüfung, Vol. 7, No. 5, 1965, pp.159-164.

30 bis. H. KELLERER, W. WÖRNER, "Die Messung der Hochtemperatur - Brinellhärte von SAP" Internal Euratom Report, October 1967, (Not available).

31. B. HUBER, Internal Euratom Report, ORGEL Project. (Not available).

32. D. J. BOERMAN, "Compression and Tension Tests of SAP at Different Temperatures", Internal Report (Not available).

33. D. G. BOXALL and J.W. STANDISH, "Mechanical Properties of Dispersion-Strengthened Aluminium Alloys", AECL Report, No. 1532, June 1962.

34. J.W.STANDISH, "Further Mechanical Properties of Dispersion-Strengthened Aluminium Alloys", Report No. DF 63 CAP 13, 11 March 1963.

35. Archives of mechanical tests 1960-1966, ISML Novara.

36. N. HANSEN, E. ADOLPH and J. CHRISTENSEN, "Sintered Aluminium Powder for Reactor Applications", Danish Atomic Energy Commission, Risö Report, 13, May 1960.

37. N. HANSEN and H. LILHOLT, "Bibliography on Dispersion-Strengthened Materials", Risö Report 48, 1962; Supplement I, 1963; Supplement II, 1964; Supplement III 1965.

38. "Second Progress Report for the DOR Design Studies", Risö Report 49, 1962.

39. N. HANSEN, and K.W. JONES, "High-temperature Stability of Sintered Aluminium Products Examined by Density Measurements". Risö Report 58, March 1963.

40. "Annual Progress Report", Risö Report 90, 1964.

41. N. HANSEN, "Tensile Properties at Room Temperature and at 400°C of Commercial Sintered Aluminium Products", Risö Report 96, December 1964.

42. "Annual Progress Report for the Period Ending March 31, 1965, Risö Report 110, July 1965.

43. N. HANSEN, P. KNUDSEN, A.C. WINTHER and E. ADOLPH, "Sintered Aluminium Products for Organic Reactor Applications", Third Geneva Conference, 1964.

44. M.S. VAN DUSEN and S.M. SHELTON, "Apparatus for Measuring Thermal Conductivity of Metals up to 600°C, J. Res. N.B.S., XII, pp. 429-440, 1934.

45. P. BONNET and M. GRIN, "Contribution à l'étude de la fragilité à chaud du produit composite aluminium - alumine", Mémoires Scientifiques de la Revue de Métallurgie, LX, No. 10, 1963.

46. "Euratom's Scientific Activities - ORGEL Program Experimental Studies", EUR-1830e, 1964.

47. Research Contract No. 065-62-3 ORG D Battelle Institut, Frankfurt, "Standversuche an Sinteraluminium" July 1967.

48. G. BEGHI, M. GRIN and G. PIATTI, "Influence des traitements thermiques de longue durée sur les propriétés des composites $Al-Al_2O_3$", "Les Mémoires Scientifiques de la Revue de Métallurgie". Vol. 64, No. 4, 1967, 385-392.

49. "Influence du cyclage thermique sur la durée de vie du SAP ISML", G. MATHEY, unpublished internal data, 1963.

50. R. DEBEIR, "Résistivité électrique du SAP ISML à température ambiante en fonction du pourcentage d'oxyde", unpublished data, internal report, 1963.

51. P. BONNET, M. GRIN and G. MATHEY "Comportement du SAP ISML en fluage", Euratom report EUR 3566i 1967.

51 bis. P. BONNET, H. KELLERER, G. PIATTI, H.W.SCHLEICHER, "The creep behaviour of $Al-Al_2O_3$ alloys" (SAP) Presented at the Symposium sur la métallurgie des poudres", Stuttgart 7-10/5/1968.

51 ter. P. BONNET, D. BOERMAN, G. MATHEY, "Données complémentaires sur des problèmes concernant le fluage du SAP". Internal report to be published.

52. J. P. LECOQ, " Essais de fluage en pression interne sur tubes de gaine", unpublished internal data, 1962.

53. S. GIULIANI, "Misura della conducibilità termica di materiali di interesse nucleare entro 100 e 500°C" EUR 3644 i.

54. D. NOBILI and M.A. DE BACCI, "Experimental Investigations on the Thermal and Electrical Conductivity of SAP", unpublished internal data, 1964.

55. M. MONTAGNANI, "Le proprieta e i metodi di prova dei materiali di struttura in relazione al modo di impiego nei reattori", report given at XII Convegno AIM Bari, 5-9 November, 1966.

56. M. SCHÜLE and G. FIORITO, "Recovery of Work-Hardening of SAP alloys", Proceedings of the Third Chemistry Department Symposium JRC Euratom, Ispra, July 1966, internal report (Not available).

57. A.M.SCHNEIDERS, "Essais de relaxation sur SAP ISML", Physical Chemistry Department, internal data, 1966.

58. M. GRIN and G. MATHEY, "Essais de relaxation sur SAP ISML", Metallurgy Department, internal data, 1966.

59. E.A.BLOCK, "Dispersion-Strengthened Aluminium Alloys", Metallurgical Reviews 6, 193, 1961.

60. D.J. BOERMAN, "Premiers résultats sur la relaxation du SAP", internal data, November 1965.

61. G.C. KARAS, "Short-term stress relaxation studies at low initial strain rates", British Plastics, September 1961, pp. 485-490.

62. P. BONNET, M. GRIN and R. MARGUERY, "Une machine électronique de fluage-relaxation sous vide", Euratom report in Preparation, 1968.

62 bis. P. BONNET, J. JANSEN, M. VEAUX, "Notch/ sensitivity in finned tubes of SAP ISML under internal gas pressure, Euratom report in preparation 1968. Results to be presented at the 12° Colloque de métallurgie-Saclay (France), 24-26 juin 1968.

63. P.G.BORDONI, "Metodo elettroacustico per ricerche sperimentali sulla elasticità", Nuovo Cimento, IV, pp. 177-200, 1947.

64. D. GELLI, "Densité du SAP ISML en fonction du pourcentage d'oxyde", private report, ISML, 1966.

65. D.J. BOERMAN, "Computer analysis of tensile tests (Part I), EUR 2514e, 1965. Part II in preparation (1968).

66. "Le transfert de chaleur par conduction dans les solides. Sa mesure principalement dans le cas des matériaux réfractaires". Parts I, II and III. Report of the Commissariat à l'énergie atomique, Centre d'Etudes de Saclay, No. DM/812, June 1960.

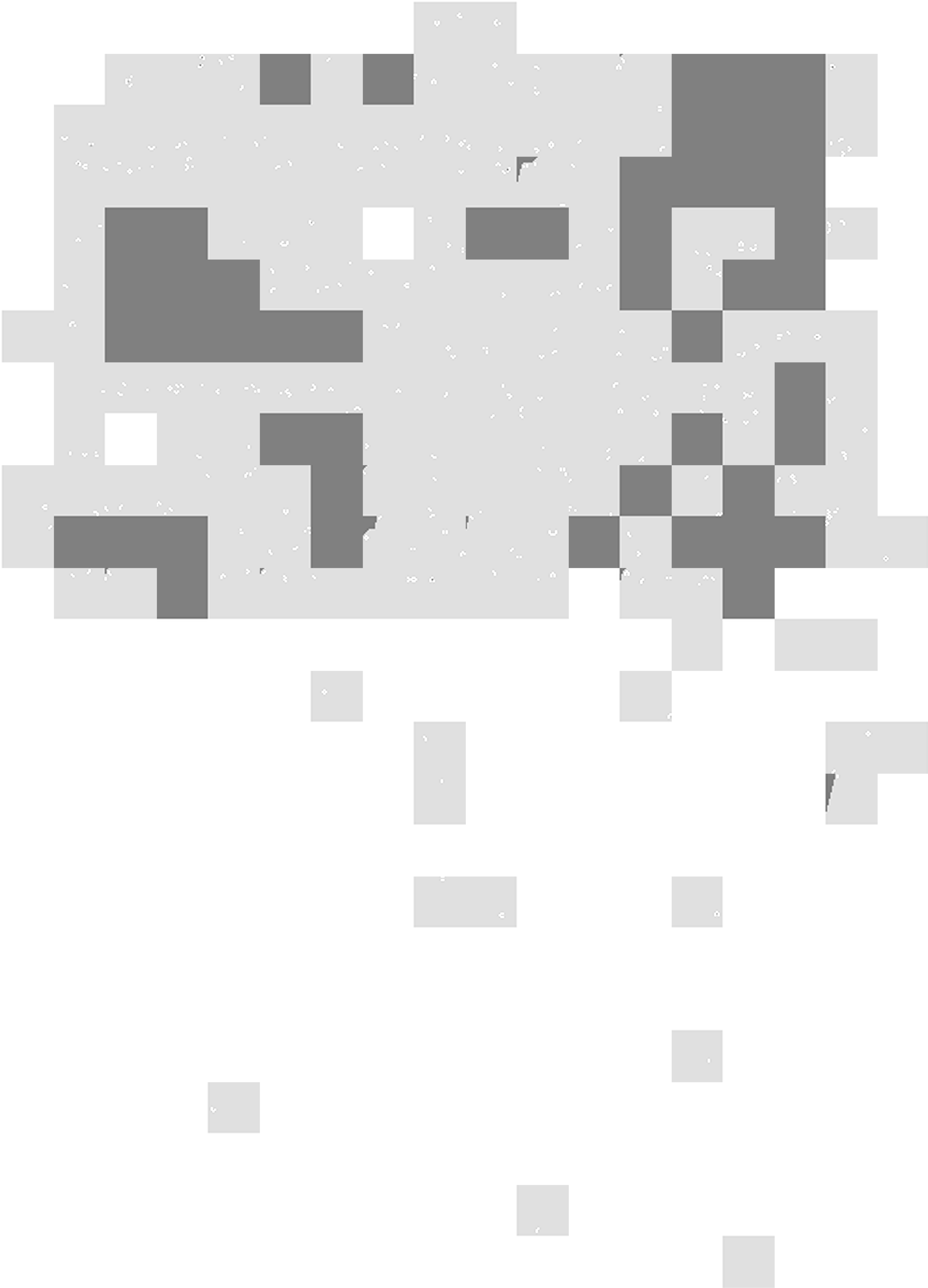

NOTICE TO THE READER

All Euratom reports are announced, as and when they are issued, in the monthly periodical **EURATOM INFORMATION,** edited by the Centre for Information and Documentation (CID). For subscription (1 year : US$ 15, £ 6.5) or free specimen copies please write to :

Handelsblatt GmbH
"Euratom Information"
Postfach 1102
D-4 Düsseldorf (Germany)

or

Centrale de vente des publications
des Communautés européennes
37, rue Glesener
Luxembourg

To disseminate knowledge is to disseminate prosperity — I mean general prosperity and not individual riches — and with prosperity disappears the greater part of the evil which is our heritage from darker times.

Alfred Nobel

SALES OFFICES

All Euratom reports are on sale at the offices listed below, at the prices given on the back of the front cover (when ordering, specify clearly the EUR number and the title of the report, which are shown on the front cover).

CENTRALE DE VENTE DES PUBLICATIONS
DES COMMUNAUTES EUROPEENNES
37, rue Glesener, Luxembourg (Compte chèque postal N° 191-90)

BELGIQUE — BELGIË
MONITEUR BELGE
40-42, rue de Louvain - Bruxelles
BELGISCH STAATSBLAD
Leuvenseweg 40-42 - Brussel

DEUTSCHLAND
BUNDESANZEIGER
Postfach - Köln 1

FRANCE
SERVICE DE VENTE EN FRANCE
DES PUBLICATIONS DES
COMMUNAUTES EUROPEENNES
26, rue Desaix - Paris 15e

ITALIA
LIBRERIA DELLO STATO
Piazza G. Verdi, 10 - Roma

LUXEMBOURG
CENTRALE DE VENTE
DES PUBLICATIONS DES
COMMUNAUTES EUROPEENNES
37, rue Glesener - Luxembourg

NEDERLAND
STAATSDRUKKERIJ
Christoffel Plantijnstraat - Den Haag

UNITED KINGDOM
H. M. STATIONERY OFFICE
P. O. Box 569 - London S.E.1

EURATOM — C.I.D.
29, rue Aldringer
Luxembourg